CHEMICAL REVIEWS

pubs.acs.org/CR

Review

Electrochemical Methods for Water Purification, Ion Separations, and Energy Conversion

Mohammad A. Alkhadra, Xiao Su, Matthew E. Suss, Huanhuan Tian, Eric N. Guyes, Amit N. Shocron, Kameron M. Conforti, J. Pedro de Souza, Nayeong Kim, Michele Tedesco, Khoiruddin Khoiruddin, I Gede Wenten, Juan G. Santiago, T. Alan Hatton, and Martin Z. Bazant*

Cite This: *Chem. Rev.* 2022, 122, 13547−13635

Read Online

ACCESS | Metrics & More | Article Recommendations

ABSTRACT: Agricultural development, extensive industrialization, and rapid growth of the global population have inadvertently been accompanied by environmental pollution. Water pollution is exacerbated by the decreasing ability of traditional treatment methods to comply with tightening environmental standards. This review provides a comprehensive description of the principles and applications of electrochemical methods for water purification, ion separations, and energy conversion. Electrochemical methods have attractive features such as compact size, chemical selectivity, broad applicability, and reduced generation of secondary waste. Perhaps the greatest advantage of electrochemical methods, however, is that they remove contaminants directly from the water, while other technologies extract the water from the contaminants, which enables efficient removal of trace pollutants. The review begins with an overview of conventional electrochemical methods, which drive chemical or physical transformations via Faradaic reactions at electrodes, and proceeds to a detailed examination of the two primary mechanisms by which contaminants are separated in nondestructive electrochemical processes, namely electrokinetics and electrosorption. In these sections, special attention is given to emerging methods, such as shock electrodialysis and Faradaic electrosorption. Given the importance of generating clean, renewable energy, which may sometimes be combined with water purification, the review also discusses inverse methods of electrochemical energy conversion based on reverse electrosorption, electrowetting, and electrokinetic phenomena. The review concludes with a discussion of technology comparisons, remaining challenges, and potential innovations for the field such as process intensification and technoeconomic optimization.

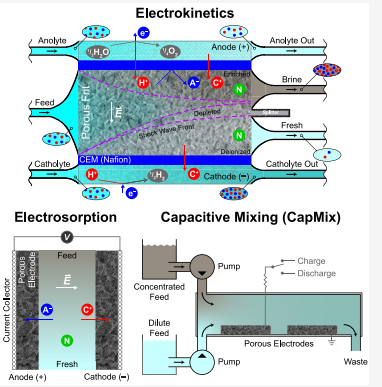

CONTENTS

Received: May 6, 2021
Published: July 29, 2022

https://doi.org/10.1021/acs.chemrev.1c00396
Chem. Rev. 2022, 122, 13547−13635

1. INTRODUCTION

1.1. Conventional Methods of Water Purification

It is estimated that four billion people live in localities which are, for at least one month of the year, under conditions of severe water scarcity.[1,2] One increasingly common method used to secure supplies of potable water is desalination, and so the development of desalination systems that are energy and infrastructure efficient is a critical technological challenge.[3] In the most general sense, desalination is a process that is used to remove ions, colloidal particles, chemical compounds, and organic matter, referred to hereafter by the single term contaminants, from saline water. Existing methods for desalination can be broadly categorized into physical methods and chemical methods.[3]

Physical methods include distillation,[4−6] freezing (or freeze−thaw) desalination,[7,8] (liquid-phase) solvent extraction,[9] membrane processes,[10−12] solar desalination,[13−15] and wave-powered desalination.[16] Distillation, a process which appears to have been used by early experimentalists of the classical era such as Aristotle,[17] involves separation of water from contaminants across the interface between a gas and a liquid by selective boiling and condensation. Modern implementations of this method include multi-stage flash distillation, multiple effect distillation, vapor compression, and humidification dehumidification, all of which are in essence a sequence of countercurrent heat exchangers.[5,18−24] In a similar way to distillation, freezing desalination also uses a phase change (freezing and melting) to separate water from contaminants.[25,26] Solvent extraction is used to separate contaminants based on their relative solubilities in two immiscible liquids, normally water (polar) and an organic solvent (nonpolar), where transport is driven by gradients in the chemical potential of the contaminants.[27] Membrane processes are diverse in that the kind of (semipermeable) membrane used can be tuned based on the target contaminant from which the water is to be removed. These processes include microfiltration, ultrafiltration, nanofiltration, reverse osmosis (RO), and forward osmosis (FO), and they are distinct primarily in the pore sizes of the corresponding membrane.[11,28−38] During operation, water is driven across a membrane by an input of mechanical work (or by a gradient in osmotic pressure in the case of FO) to retain the contaminants in a concentrated brine. Like distillation, solar desalination is said to have been employed by humans for thousands of years, originally by Greek mariners and Persian alchemists.[39,40] The basis of this technology is not distinct from distillation or membrane processes; it is simply a means to generate the energy that these methods require: that is, heat for distillation or electricity for membrane processes. Wave-powered desalination is similar in principle to solar desalination methods in that it generates electricity (by the motion of submerged buoys in this case) to run a desalination process based on RO.[16] Although these technologies are mature and are cost-effective

https://doi.org/10.1021/acs.chemrev.1c00396
Chem. Rev. 2022, 122, 13547−13635

for the desalination of seawater (as well as other concentrated solutions), they are inherently inefficient and energy intensive when used to treat dilute feeds or to selectively remove target contaminants from a concentrated feed, as explained in the following section. It is in these situations that selectively removing trace amounts of a desired species is preferable to indiscriminately concentrating all dissolved species in a brine.

Chemical methods, which tend to be selective in molecular separations, can be classified into two major types: the first, discussed in this section, involves no electrochemistry (i.e., the established chemical methods), and the second, introduced in sections 1.3 and 2, is based on electrokinetic and electrochemical phenomena. Established chemical methods include precipitation,[41] coagulation flocculation,[42] adsorption,[43,44] ultraviolet, ozone, and chlorine disinfection,[45] aeration,[46] and ion exchange.[47,48] Precipitation involves the creation of a solid (the precipitate) from a solution using a chemical referred to as the precipitant.[49,50] Similarly, coagulation flocculation involves the addition of compounds (typically metallic salts) that promote the clumping of fines into larger floc, which can be readily separated from water by sedimentation, filtration, or flotation.[51,52] Adsorption is a physicochemical phenomenon that is used to remove contaminants by binding them to the surfaces of an adsorbent material.[44,53] Disinfection technologies in general are used to kill bacteria, viruses, and other disease-causing pathogens present in water. The most common disinfection treatments are based on ultraviolet radiation, chlorination, and ozonation, all of which inactivate the waterborne pathogen by disrupting its cellular functions.[45] Aeration of water is achieved by passing air through the liquid and is typically used to remove iron or organic matter, dispel certain dissolved gases, or oxidize dissolved or suspended compounds.[54,55] Ion exchange represents a broad class of processes where ions are exchanged between an electrolyte solution and a solid ion exchanger, such as polymeric resin, chelating agents, zeolites, clay, and montmorillonite.[47,48,56−62] Ion exchange is in general a reversible process, where the ion exchanger is regenerated using a wash solution. Altogether, these traditional chemical methods are based on either chemical reactivity (precipitation, adsorption, and chelation), affinity for charged or functionalized surfaces (coagulation flocculation and ion exchange), or susceptibility to oxidative degradation (disinfection and aeration) of the contaminants.

In practice, a water treatment process often combines several of the methods described above to improve the quality of water and make it suitable for a specific end use. Figure 1 shows the process diagram of a representative municipal water treatment facility, in which the water treated contains high levels of hardness and iron.[63] As described in ref 63, raw water is taken from wells and sent to an aerator, where contact with air removes volatile solutes (e.g., H_2S, CO_2, CH_4) and odorous substances (e.g., CH_3SH, bacterial metabolites). Contact with oxygen further promotes iron removal by oxidizing soluble Fe(II) to insoluble Fe(III). After aeration, lime is added (as CaO or $Ca(OH)_2$) to raise the pH and cause the precipitation of Ca^{2+} and Mg^{2+}. Precipitates of these hardness ions settle from the water in the primary basin, and much of the remaining solid material is suspended and requires the addition of coagulants (e.g., Fe(III), $Al_2(SO_4)_3$) to settle. Activated silica or synthetic polyelectrolytes (e.g., poly(sodium styrenesulfonate), poly(acrylic acid)) may also be added to induce coagulation or flocculation. Settling of colloidal particles occurs in the secondary basin after the addition of carbon dioxide to lower the pH. Sludge from both basins is then pumped to a lagoon, and the water is finally chlorinated, filtered, and pumped to the water mains.

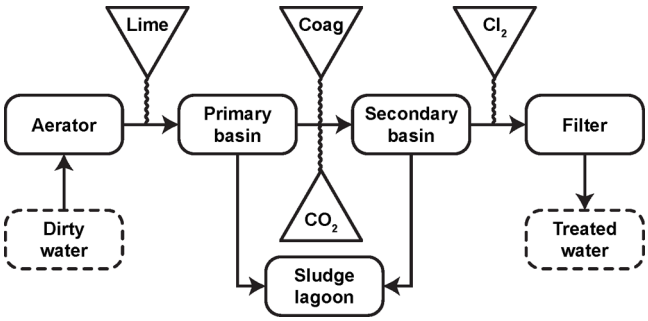

Figure 1. Process diagram of a representative municipal water treatment facility. This process combines several of the methods described in section 1.1 to improve the quality of water and make it suitable for domestic use. Adapted with permission from ref 63. Copyright 2001 CRC.

1.2. Limitations of Conventional Methods

Almost all of the methods introduced in section 1.1 have seen commercial success for a range of applications across numerous industries. Each of these methods, however, has applications and operating constraints outside of which the use of an alternative process would be more practical. For example, thermal distillation has historically been the dominant means of seawater desalination, but the most prevalent technology used today in large-scale desalination plants is RO because of its high energy efficiency and small footprint.[33,64] This technology works by pumping the feed at pressures above the osmotic pressure of the solution through a membrane permeable only to water molecules (3−5 MPa for seawater).[12] RO has been optimized over several decades of development for the desalination of concentrated feeds like seawater,[38,65] and modern seawater RO (SWRO) plants currently require under 3 kW h m^{-3} of energy when including all pre- and post-treatment steps.[66−69] While RO is the best available solution for city-scale seawater desalination, RO systems demonstrate poor scaling of energy demand with decreasing feed concentration, as demonstrated in Figure 2.[70] For example, brackish water RO (BWRO) plants require nearly the same energy input as SWRO plants (1−3 kW h m^{-3}), despite the fact that brackish water is less concentrated than seawater by about an order of magnitude.[71] According to the van't Hoff equation, osmotic pressure is linearly proportional to concentration for dilute solutions, which suggests that the energy demand for BWRO should be about an order of magnitude lower than for SWRO. Friction losses in RO systems, however, do not scale with salt concentration, but rather with the amount of water transported across the membrane. This intrinsic feature of RO explains the relatively high losses and poor energy efficiency of BWRO compared to SWRO.[72] Because desalination of brackish water is a promising solution for water scarcity, and because removal of trace contaminants from dilute feeds is an important capability, technologies whose energy demand scales with feed concentration would be more desirable than RO for these applications.

Another notable drawback of RO plants is that they require large capital expenditures and mature infrastructure, which limits their utility for small-scale applications or in remote

https://doi.org/10.1021/acs.chemrev.1c00396
Chem. Rev. 2022, 122, 13547−13635

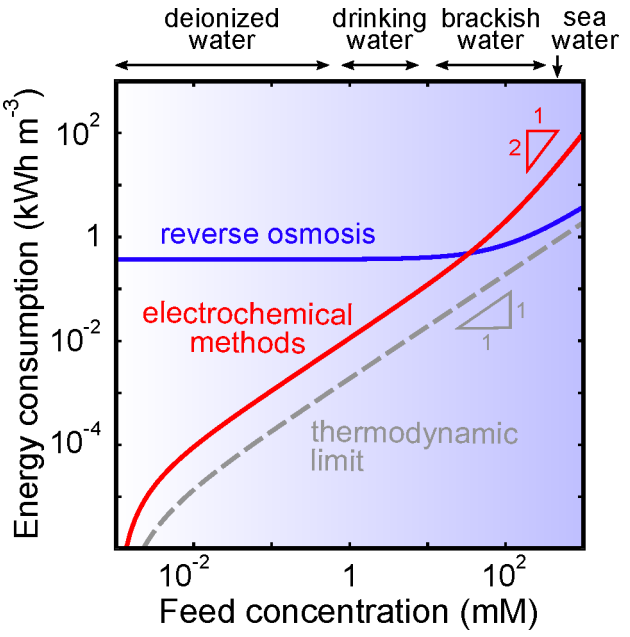

Figure 2. Estimates of the volumetric energy consumed by RO and a generic electrochemical process based on the analysis in section 6.1, specifically eqs 17 and 18. These estimates assume that the feed is desalinated to a final concentration of 1 μM; here, γ = 0.5 (water recovery, defined as the fraction of the feed recovered as permeate) and $\mathcal{P}$= 10 L h^{-1} m^{-2} (productivity). Energies are compared to the thermodynamic limit, represented by the dashed curve, and are reported in units of kW h m^{-3} of diluate.

locations.[66] Moreover, it is difficult to downscale RO systems because high-pressure pumps and resilient plumbing are required at any scale to pressurize the feed in excess of the osmotic pressure. Facile downscaling to smaller, less-expensive plants that can be introduced into small residential areas and communities would help water treatment technologies further penetrate the market. Inexpensive, small-scale plants may in fact be the most appropriate solution for developing and off-grid locations, where water scarcity is severe and commonplace, and where infrastructure may be underdeveloped or nonexistent. Small-scale portable desalination units are also in demand by industrial facilities, by mobile military units and vessels, in recreational spaces, and in the travel industry.[73,74] To meet these growing and diverse needs for purified water, the technological focus should extend beyond RO by including scalable systems with lower energy demands and more flexible infrastructure requirements for treatment of brackish water and dilute feeds.

Many of the drawbacks of RO, particularly when used to treat dilute feeds, can be overcome by using the physicochemical methods introduced in section 1.1. These methods, however, have their own limitations and often require nonreusable chemicals. Solvent extraction can be both efficient and cost-effective in separating hazardous contaminants from benign feeds, but this process requires large volumes of organic extractants and sometimes toxic solvents, and the entrainment of phases yields low-quality effluents.[75,76] Precipitation is another simple and cost-effective process that is commonly used to remove toxic heavy metals from water, but it produces large amounts of sediment and sludge that is often difficult and expensive to dispose of. Precipitation is also ineffective at removing ions that are present at low concentration, and its utility may be limited when the water is contaminated with multiple metals.[76,77] Coagulation flocculation is often employed after precipitation to remove solid particulates from water, and this method could also be used to capture larger particles and inactivate biological agents.[78,79] The applicability of this method is limited, however, because it requires nonreusable inorganic coagulants which are usually toxic.[76,80] Ion exchange, on the other hand, offers a wider range

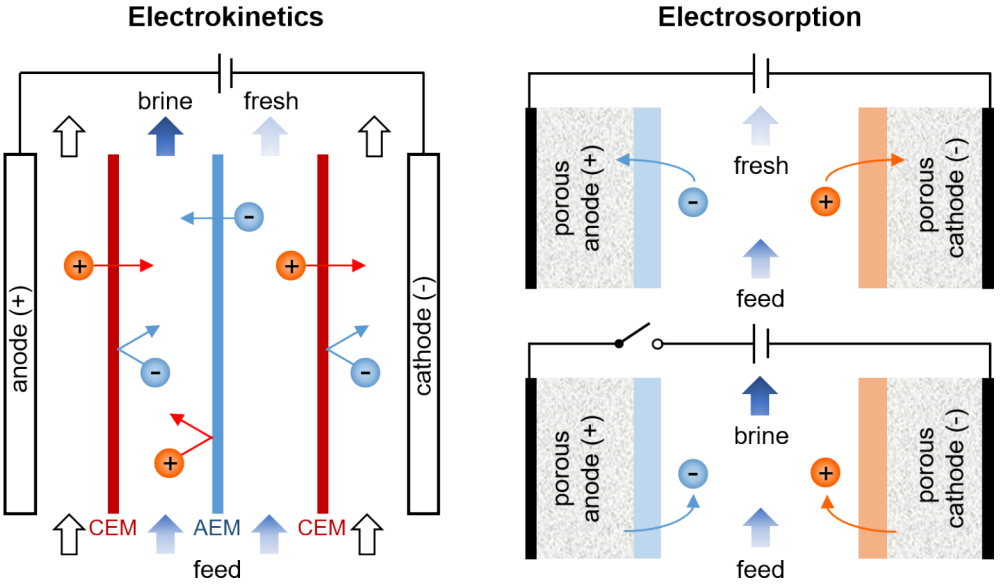

Figure 3. Electrokinetics and electrosorption are the two main mechanisms by which contaminants are separated in any nondestructive electrochemical process. Electrokinetic processes, which are typically continuous, involve transport of charged or uncharged but dielectric[119,120] species in an electrolyte in response to an applied electric field, and so removal of contaminants relies on effective mass transfer. Electrokinetic methods like EDI and shock ED use porous materials in the feed channels to increase ion removal and improve energy efficiency when the feed is dilute. Electrosorption processes are cyclic and encompass all phenomena in which the binding of contaminants is aided by an applied electric field. In addition to effective transport, electrosorption relies on favorable reaction kinetics and thermodynamics.

https://doi.org/10.1021/acs.chemrev.1c00396
Chem. Rev. 2022, 122, 13547−13635

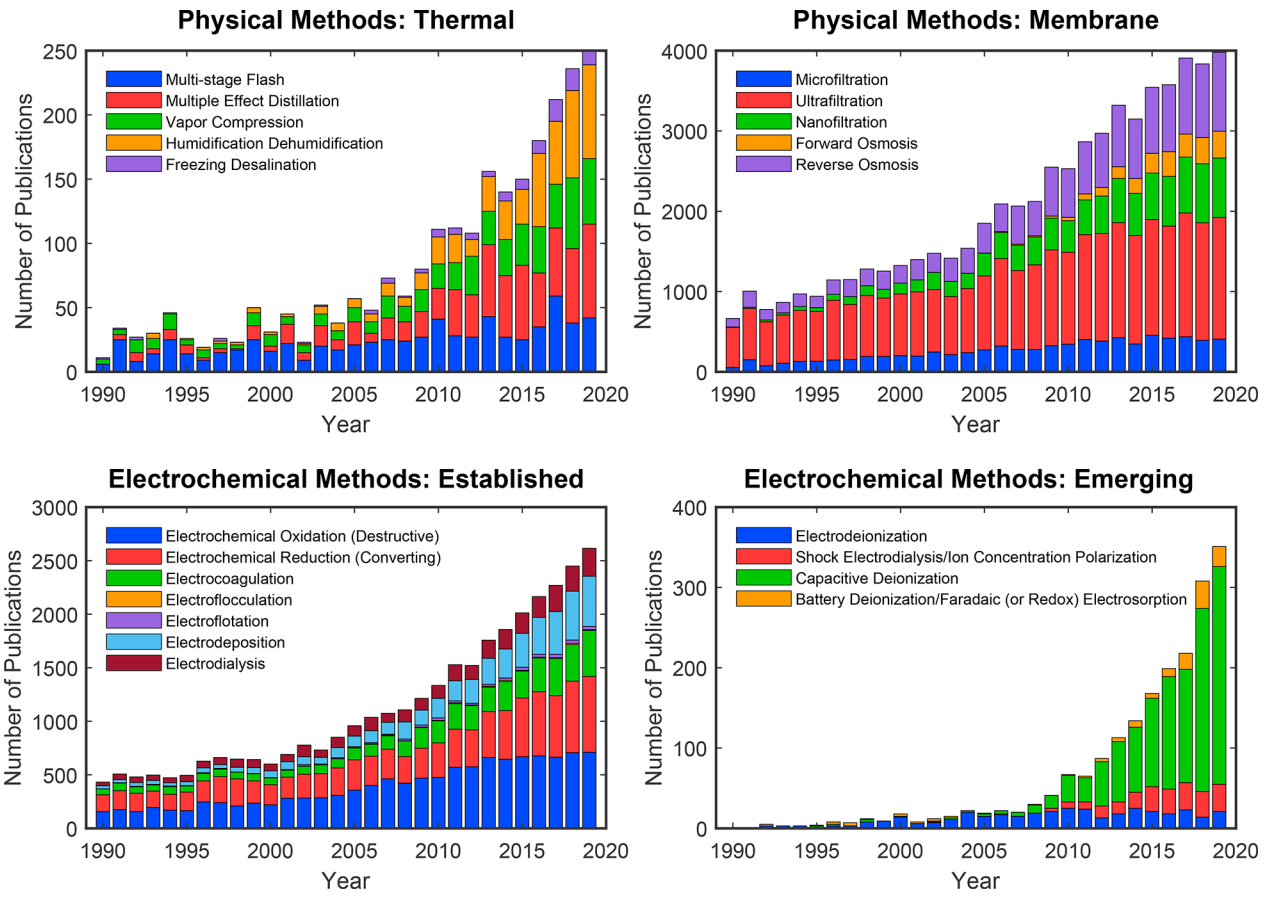

Figure 4. Number of publications per year for various methods used for water purification or ion separations. The technologies considered here are broadly classified as either physical (top row) or electrochemical (bottom row). This review focuses on electrochemical methods, and special attention is given to the emerging methods, including shock ED, CDI, and Faradaic electrosorption. The literature search was performed using Elsevier's Scopus database with the search field TITLE-ABS(···).

of simple and well-established commercial products, many of which can be regenerated for repeated use.[76,77,81] The performance of ion exchange resins and chelating agents, however, is sensitive to variations in pH, and some of these agents react with dissolved metal ions to form soluble metal complexes that lead to secondary pollution.[76,77,82]

1.3. Emerging Electrochemical Methods

A variety of innovative techniques based either on electrokinetics or electrosorption have been proposed for water purification and ion separations, and these techniques have given rise to emerging electrochemical methods.[83−91] The recent discovery of deionization shock waves in microchannels[92,93] and porous media,[87,94,95] for instance, inspired a new area of research in electrokinetic methods for deionization. Parallel developments in materials science have uncovered a wealth of novel electrode chemistries, where the electrosorption of ions is promoted by Faradaic reactions, to replace carbon, conventionally the material of choice in capacitive systems.[86,96] These innovations have not only enhanced deionization capacity but have also imparted molecular selectivity to the electrodes. Recent examples of Faradaic platforms for water purification are based on electrochemical reduction of target contaminants,[97,98] electrochemical switching of ion exchange,[99−101] and molecularly selective removal of ions,[86,96,102] uncharged compounds,[103,104] and biomolecules (e.g., proteins).[105] Many of these advances have relied on Faradaic compounds with immobilized surfaces to achieve superior electrochemical performance and chemical specificity. By modulating the binding interactions at the surfaces, the affinity of the electrodes can be tuned specifically for minority components in a feed, which in practice may be either highly valuable or seriously toxic.

Emerging electrochemical methods include electrodeionization (EDI, sometimes called hybrid ion exchange ED),[61,106−108] shock electrodialysis (shock ED),[87,109] capacitive deionization (CDI),[110,111] battery deionization (BDI),[112,113] and Faradaic electrosorption.[86,96] These technologies are unique from all of the others discussed so far in that removal of contaminants is based on their response to electric fields in solution or electrochemical reactions at electrodes. Electrochemical systems use applied electrical currents to remove contaminants from the feed by either driving separations in bulk electrolytes,[61,114] electrochemically trapping them in electric double layers (EDLs),[90,110,115] or intercalating them in solid electrodes (e.g., materials composed of two-dimensional, layered structures).[116−118] The first of these mechanisms is governed by electrokinetics, and the second and third are forms of electrosorption, as explained in Figure 3. The primary input of energy to these systems is an applied electric potential, which makes these processes scalable without the need to be operated at extreme temperatures or pressures. Energy dissipation in electrochemical systems, however, arises from three general sources:[358,1180] (i) ohmic resistance, due to hydrodynamic drag acting on moving ions in

https://doi.org/10.1021/acs.chemrev.1c00396
Chem. Rev. 2022, 122, 13547−13635

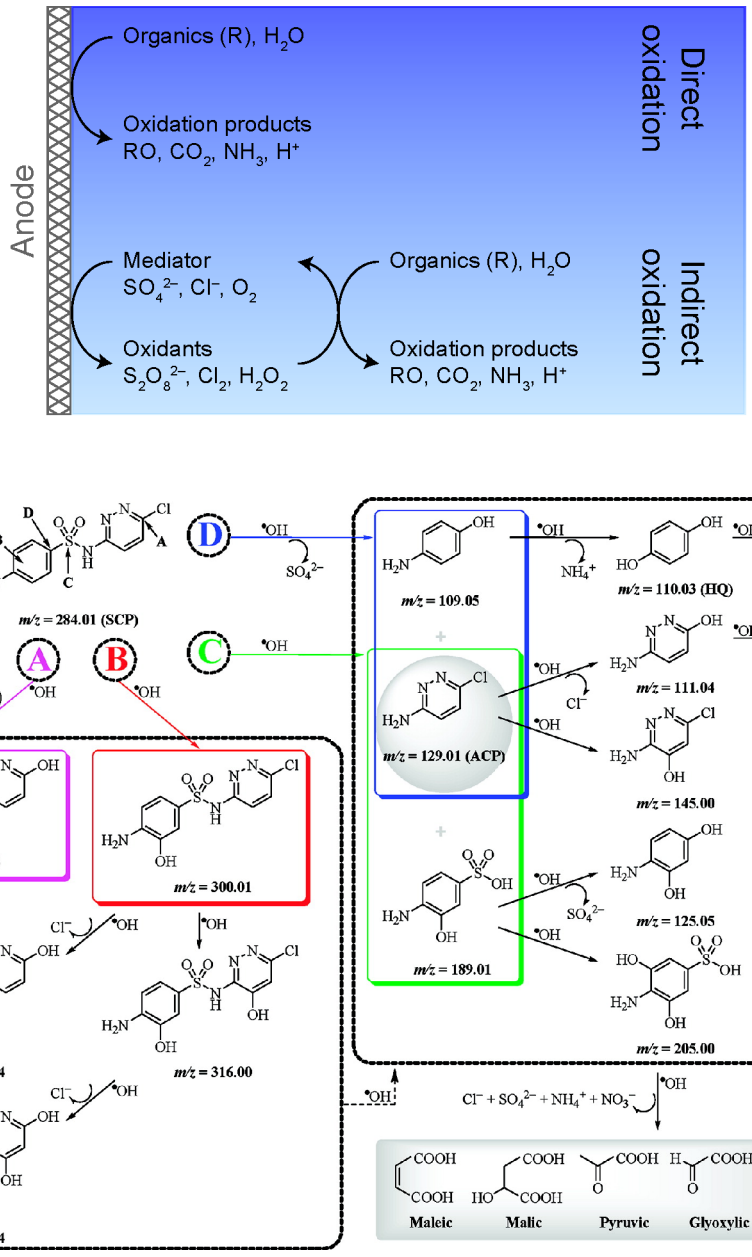

Figure 5. Electrochemical oxidation is an established destructive, nonelectrosorptive method that is used to degrade most organic contaminants and certain inorganic compounds. (top) The method involves formation of reactive oxidizers that interact with contaminants either at the anode surface (direct oxidation) or in the bulk (indirect, or mediated, oxidation).[123] Reproduced with permission from ref 191. Copyright 2017 Royal Society of Chemistry. (bottom) Complex organic compounds, such as the sulfonamide antibiotic sulfachloropyridazine, are degraded and mineralized by the attack of reactive oxidizers at key reaction sites (designated by the letters A–D). In this example, hydroxyl radicals can attack four unique sites on sulfachloropyridazine to yield different primary cyclic byproducts, all of which are eventually transformed into CO_2. Reproduced with permission from ref 192. Copyright 2012 American Chemical Society.

electrolytes or membranes,[72] as well as electronic resistance in porous electrodes and current collectors; (ii) Faradaic reaction resistance at electrode–electrolyte interfaces, leading to activation overpotential; and (iii) concentration polarization, associated with limitations in ion diffusion. These losses all scale with the number of ions removed rather than the amount of solution process, as shown in Figure 2. These systems therefore tend to be more energy efficient compared to physical methods (and are molecularly selective) when used to treat brackish water and dilute feeds.

Among the existing electrochemical methods, electrodialysis (ED) has been studied and used for water desalination for decades, and several ED desalination plants for treatment of brackish water are currently operational in the U.S.[114,121−125] The past decade, however, has seen the emergence of several novel electrochemical systems for water purification with unique functionalities and working principles compared to ED, and these are EDI,[126] shock ED,[87] CDI,[115,127,128] and Faradaic electrosorption.[86] This review summarizes the development of these novel technologies to form the basis for the emerging field of electrochemical systems for water purification and ion separations. For completeness, we also briefly discuss related microfluidic technologies, which have been reviewed in detail elsewhere.[129,130] Microfluidic systems, which are driven by

https://doi.org/10.1021/acs.chemrev.1c00396
Chem. Rev. 2022, 122, 13547−13635

electrical energy, have throughputs at the scale of nanoliters and may be difficult to scale up to the volumes needed for deployment for human consumption, agriculture, or industry. Electrochemical systems instead are based on cells and stacks made of components like ion exchange membranes (IEMs), porous dielectric separators, and porous electrodes that can be produced in large areas as flat sheets or films, and thus these systems naturally have clearer pathways for scale up.

1.4. Outline of This Review

Conventional electrochemical methods, which exploit Faradaic electron transfer reactions at electrodes to drive chemical or physical transformations, have been previously reviewed, particularly in their use for removal of organic matter,[131] organic compounds,[132−137] inorganic contaminants,[138−142] and microorganisms[143−145] as well as for degradation of various contaminants and micropollutants.[123,146−149] The technologies on which many of these publications focus are well established and currently used in industry. We begin the review by introducing these established electrochemical transformation methods and the broad range of applications for which they are used (section 2). We then build on the existing literature and related reviews[68,105,115,118,123,126,150−155] by emphasizing the principles and applications of emerging electrochemical methods for desalination, water purification, and ion separations (sections 3 and 4). As shown in Figure 4, several of these emerging methods have developed only in the last 10 years and have been reviewed either briefly or independently of other methods. To provide a foundation for our discussion, we examine recent developments in electrokinetic phenomena and electrosorption for water purification and selective ion separations. See refs 76 and 118 for tables that summarize the advantages and disadvantages of techniques used for water purification, including many of the emerging methods discussed here.

In section 3, we explain (nondestructive) methods based on electrokinetics, which may either include or exclude membranes. Two methods in the class of membrane-based systems are ED and EDI, where the membrane plays a critical role in the removal of charged species. Ions can be separated from the bulk fluid directly, however, by virtue of the electrokinetic phenomena, without much contribution from the membrane itself. Key developments have also been made in the class of "semimembraneless" systems (i.e., systems in which the feed is partitioned into fresh and brine streams across a deionization shock wave that functions as a virtual interface), which include microfluidic (or nanofluidic) concentration polarization and shock ED. These methods are both based on the phenomenon of concentration polarization, which arises due to extreme gradients in the concentration of ions in solution. In section 4, we describe electrosorption, the phenomenon that is responsible for sorption in electrochemical systems, and how this process is used for desalination and molecular separations. (These separations are often nondestructive, but in certain cases, they may involve electrochemical conversion or degradation of the contaminants.) This explanation is followed by an overview of CDI techniques as well as recent innovations in Faradaic (or redox-active) materials and their broad use in chemical and environmental processes. With these methods explained, we introduce inverse methods of energy conversion that convert gradients in salinity to energy (section 5). We conclude by discussing the energetics, thermodynamic and technological challenges, and prospects of electrochemical methods for water purification and ion separations (sections 6 and 7).

2. ELECTROCHEMICAL TRANSFORMATIONS

In the general areas of water purification and wastewater treatment, a variety of electrochemical processes have been developed to remove contaminants ranging from ions to colloidal particles. For example, chemical coagulation flocculation, flotation, precipitation, and redox (reduction and oxidation) can be improved by applying electric fields.[156−158] In this section, we discuss nonelectrosorptive electrochemical methods that are well established and reviewed extensively in the literature, namely electrochemical oxidation, electrochemical reduction, electrocoagulation, electroflotation, and electrodeposition.[98,146,156−160] These processes involve Faradaic reactions at electrodes to drive chemical or physical transformations of ionic or molecular solutes. For example, electrochemical redox reactions are used primarily when the objective is to degrade or convert nonbiodegradable organic contaminants and certain inorganic compounds (e.g., cyanides, thiocyanates, sulfides) and disinfect water. In section 3, we examine both traditional and emerging electrokinetic methods based on ED, which rely on coupled transport phenomena in electrolyte solutions. We then discuss in section 4 electrosorption systems (both capacitive and Faradaic) for selective ion removal based on various functional materials, including porous carbon, inorganic crystals, and polymers.[90,115]

2.1. Electrochemical Oxidation

Electrochemical oxidation is a chemical reaction involving the loss of one or more electrons by an atom or a molecule at the anode when an electrical current is passed through the system.[146,161,162] In the context of water treatment, electrochemical oxidation generates reactive oxidizing agents called free radicals that interact with the contaminants and degrade them, as explained in Figure 5.[123] Superoxide ($O_2^{\bullet-}$), hydroperoxyl ($HO_2^{\bullet}$), hydroxyl ($HO^{\bullet}$), and sulfate ($SO_4^{\bullet-}$) radicals are examples of reactive agents that can degrade organic and organometallic contaminants by initiating a radical oxidation chain (see refs 123, 146, and 163−167 for lists of common reaction pathways by which these radicals are formed).[136,168−170] Superoxide and hydroxyl are two of the most important radicals in free-radical chemistry, and they are both believed to be key species in oxidative processes.[163,164,171] While superoxide is normally a nucleophile and reducing agent,[164,172] it exists in equilibrium with the hydroperoxyl radical, which can behave as an oxidizing agent in various biological and chemical reactions.[173−177] (In general, superoxide is a weak reducing agent, but in the presence of solids or cosolvents that are less polar than water (e.g., H_2O_2), superoxide becomes reactive and can degrade halogenated aliphatic compounds,[178,179] including perfluorocarboxylic acids,[180,181] via nucleophilic attacks.[182]) The hydroxyl radical oxidizes both organic and inorganic compounds with high reaction rates, such that its action occurs only in the region where it is produced.[183] The degradation process begins with formation of the reactive oxidizer, followed by initial attacks on target molecules and their breakdown into biodegradable intermediates. Subsequent attacks on these intermediates by the oxidizer can lead to their mineralization (i.e., production of water, carbon dioxide, and inorganic salts), as shown in Figure 5.[123,146] Another class of oxidizers is obtained by the oxidation of chloride ions to generate active chlorine (Cl_2), which may

https://doi.org/10.1021/acs.chemrev.1c00396
Chem. Rev. 2022, 122, 13547−13635

disproportionate to hypochloric acid (HClO) or hypochlorite (ClO^-) depending on the pH. Although these species can effectively oxidize various contaminants in real wastewaters (e.g., landfill leachates, textile effluents, olive oil wastewater, tannery wastewater),[97] this approach has the drawback of producing chlorinated organic compounds during the electrolysis, which is the main limitation of electrochemical oxidation.[97,184] These chlorinated byproducts increase the toxicity of the effluent because they tend to be much more persistent than what is initially present in the feed.[185−187] In the absence of chloride electrolytes, however, electrochemical oxidation can be reliably used for disinfection, wastewater treatment, groundwater treatment, soil remediation, wastewater sludge conditioning, and odor and taste removal.[146,188−190]

In the 1990s, researchers became increasingly aware that the anode material is an especially important consideration in the design and optimization of electrochemical oxidation processes.[193−196] (The cathodes are usually stainless steel plates, platinum meshes, or carbon felt electrodes.) The results obtained by several groups indeed demonstrated that the choice of anode influences the selectivity and efficiency of organic compound oxidation.[165,197] According to a model proposed by Comninellis,[194] anode materials are divided into active anodes (e.g., carbon, platinum, iridium oxides, ruthenium oxides) and nonactive anodes (e.g., antimony-doped tin oxide, lead dioxide, boron-doped diamond).[97] Active anodes have low oxygen evolution overpotential and are good electrocatalysts for oxygen evolution, while nonactive anodes have high oxygen evolution overpotential and are poor electrocatalysts for oxygen evolution. Anodes based on boron-doped diamond (BDD) have received considerable attention due to their chemical stability, high electrical conductivity, resistance to corrosion even in harsh environments, and wide window of electric potential.[198] As a result, BDD is generally viewed as one of the most effective and energy efficient anodes for mineralization of organic contaminants, although its use in practice is limited due to high manufacturing costs.[198] Moreover, BDD (as well as other anodes) promotes the oxidation of chloride to chlorate (ClO_3^-) and perchlorate (ClO_4^-), which are water-soluble disinfection byproducts that are exceedingly mobile in aqueous solutions and are highly persistent under typical water conditions.[97,146] Because disinfection byproducts in drinking water are usually regulated, their concentrations should be monitored and controlled when performing in-line electrolysis.

Other prominent anodes include dimensionally stable anodes (DSAs, also called mixed metal oxide electrodes) and substoichiometric titanium oxide anodes.[97,199,200] DSAs are fabricated by coating a substrate such as titanium with several kinds of metal oxides, including RuO_2, IrO_2, and PtO_2. These anodes exhibit high conductivity and corrosion resistance, and recent studies showed that doping DSAs with metal and nonmetal elements can further improve their performance.[201−204] Moreover, the use of nanotechnology has gained traction in the field of electrode fabrication to increase the porosity and active surface area of the anodes.[205,206] Anodes based on substoichiometric titanium oxide (Ti_nO_{2n-1}) also display high conductivity and corrosion resistance, and their many advantages and long service life have led to their broad use in fuel cells, lead-acid batteries, and, most recently, wastewater treatment.[207−210] Ganiyu et al. prepared a Magnéli-phase Ti_4O_7 electrode by plasma deposition and compared it to DSA and BDD anodes for the degradation of the beta-blocker propranolol[211] and the analgesic paracetamol.[212] These studies showed that the Ti_4O_7 electrode can achieve similar or better removal of organic carbon compared to DSAs and BDD. Several methods have been reported in the literature to improve the performance of substoichiometric titanium oxide electrodes, and these methods include plasma spraying,[213] which produces doped functional coatings, and high-temperature sintering, which produces an electrode with extensively interconnected macropores.[210]

Most anodes used in electrochemical oxidation produce highly active hydroxyl radicals on their surfaces,[214] and treatment of wastewater with these materials requires adequate flow of the contaminants toward them. When the concentration of pollutants near the anode is low, the process rate is limited by mass transfer of these species to the surface of the electrode.[97] Common methods to overcome this limitation include gas sparging,[215] incorporation of turbulence promoters,[97] and use of nanoengineered materials.[216−218] Most importantly, the efficiency of electrochemical oxidation can be improved with the indirect (or mediated) oxidation method, which avoids the production of oxygen by generating precursors that are transformed to active oxidizers. Persulfate ($S_2O_8^{2-}$), percarbonate ($C_2O_6^{2-}$), and hydrogen peroxide (H_2O_2) are examples of precursors that can be produced using BDD anodes.[219−221] These species are relatively stable at ambient conditions and generate highly active inorganic radicals that enable mediated oxidation of organic contaminants.[97] Michaud et al. experimentally tested the production of precursors using BDD and observed that persulfate is produced with high current efficiency when the electrolyte is concentrated in sulfate (SO_4^{2-}) and the process temperature is low.[219] The persulfate precursor is activated to generate sulfate radicals, and this step requires a transition metal catalyst or sufficient energy.[222] Activated persulfate can then oxidize organic compounds, and this approach has been used to treat groundwater and soils contaminated with biorefractory organic species.[97]

In recent years, there have been significant advances in the design, synthesis, and use of nanostructured electrodes for electrochemical oxidation.[218] Nanoengineered materials exhibit new and improved properties, such as an increase in the number of active sites and an improvement in electrical conductivity, and these materials can promote heterogeneous catalysis at electrode surfaces.[218] According to Du et al., a wide range of nanostructured cathodes have been reported in literature, and they can be divided into four categories: cathodes based on carbon nanomaterials such as carbon nanotubes (CNTs) and graphene,[223,224] carbon cathodes doped with heteroatoms such as fluorine and nitrogen,[225,226] metals or metal oxides deposited on carbon,[227−229] and metal oxide cathodes.[230,231] In most studies, these electrodes are used for electrosynthesis of H_2O_2 via oxygen reduction, and the structural morphology and composition of functional groups largely affect cathode performance.[224,232,233] Du et al. also explain that there exists a large variety of nanostructured anodes, which can be divided into four categories similar to those of the nanostructured cathodes: anodes based on carbon nanomaterials such as CNTs and nanostructured BDD,[234−237] anodes doped with heteroatoms such as fluorine and boron,[238,239] metals or metal oxides deposited on carbon,[240−242] and metal or metal oxide anodes.[243−246] Most articles published on nanostructured electrodes report

https://doi.org/10.1021/acs.chemrev.1c00396
Chem. Rev. 2022, 122, 13547−13635

improvements in the kinetics of $HO^{\bullet}$ production and pollutant oxidation due to the synergistic effects of greater stability, electrical conductivity, electrochemical reactivity, and active-site exposure.[218] Even though nanoengineering has enabled major advances in improving electrode stability, more efforts are needed to demonstrate stability for long-term use, and standard protocols must be established to assess the lifetime and reliability of these systems.[218]

Over the past two decades, scale up of anode systems has gained attention, where the focus has been on increasing the throughput of laboratory-scale systems while retaining performance and reliability.[247,248] At the same time, electrochemical advanced oxidation processes have been developed to improve the efficacy and applicability of conventional electrochemical oxidation.[146,249−251] These specialized variants of electrochemical oxidation introduce Fenton's reaction chemistry,[192,252,253] photoelectrocatalysis,[254] sonoelectrolysis,[146] and aerobic or anaerobic digestion (using microbial electrochemical technologies)[255−258] to the standard process.[259] In conventional electrochemical oxidation, the reactive oxidizers are often (but not always) produced at the anode surface; the advanced variants facilitate additional generation of oxidizers in the bulk.[146,197] Although these oxidative processes are more widely studied and used (because they usually lead to mineralization of the contaminants), treatments based on electrochemical reduction have been gaining interest because they enable partial recovery of chemicals as well as production of value-added substances.[97]

2.2. Electrochemical Reduction

Electrochemical reduction, the complementary process to electrochemical oxidation, is a chemical reaction involving the gain of one or more electrons by an atom or a molecule at the cathode when an electrical current is passed through the system.[123] Similar to electrochemical oxidation, electrochemical reduction can occur either directly on the surface of the cathode or indirectly in the bulk by the action of a reducing agent generated at one of the electrodes.[98] This process is typically used to treat water contaminated with heavy metal ions (see section 2.5 also),[123,260] inorganic anions (e.g., bromate, perchlorate),[261,262] or halogenated organic compounds (e.g., organic volatile halides, chlorofluorocarbons, polychlorohydrocarbons, polyhalophenols)[97,98] by converting these species into more benign products. As shown in Figure 6, the mechanism of this conversion usually involves the removal of halogen atoms or the reduction of aldehydes and ketones to produces less toxic species.[97,123]

Among the major parameters that determine the efficiency of electrochemical reduction are catalyst loading, cathode potential, and water quality.[98] Generally, an increase in catalyst loading improves reduction activity, though only up to a limit beyond which activity either steadies or even decreases as the distance for electron transfer increases.[263] In the case of nanosized catalysts such as palladium, the particles can aggregate at higher loading, which results in excessive local evolution of hydrogen bubbles that restrict access of the contaminants to the catalyst.[264] As is the case for catalyst loading, a reaction will have an optimal operating cathode potential above which the abundance of hydrogen bubbles produced could inhibit adsorption of contaminants.[265,266] Electrochemical reduction is also sensitive to the quality and characteristics of the feed, which influence performance and electrode lifetime.[98] Performance typically improves at lower

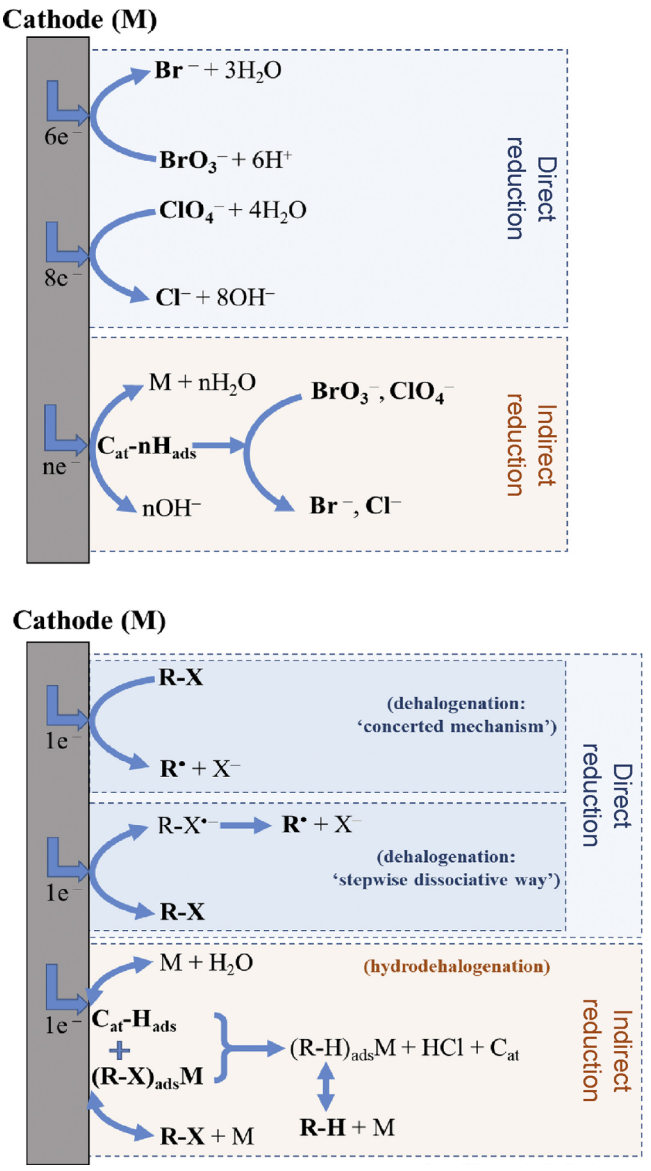

Figure 6. Electrochemical reduction is an established conversion method that is used to treat oxidized contaminants, such as (top) inorganic and (bottom) organic halides (R-X). The method involves formation of high energy electrons or reactive species that interact with contaminants either at the cathode surface (direct reduction) or in the bulk (indirect reduction). M refers to the cathode material (i.e., the catalyst, C_{at}); C_{at}-H_{ads}, $(R\text{-}X)_{ads}M$, and $(R\text{-}H)_{ads}M$ are the hydrogen atom, organic halide, and dehalogenated organic compound (R-H), respectively, adsorbed on the cathode. Reproduced with permission from ref 98. Copyright 2020 Elsevier.

pH (due to increased formation of adsorbed hydrogen),[267,268] at higher ionic strength (due to smaller EDLs),[98] and in the absence of certain species (e.g., organic matter, electrocatalyst poisons, competing ions).[264,269]

The choice of electrode is another critical design parameter that influences the mechanism of electrochemical reduction, as it impacts the reaction pathway, selectivity, and energy consumption.[97,98] An effective catalyst enables strong bonding on the surface of the substrate.[98] From among the many materials investigated to date, electrodes based on silver, nickel, and carbon hold prominent positions due to their high electrocatalytic activity, robustness, and inexpensiveness with

https://doi.org/10.1021/acs.chemrev.1c00396
Chem. Rev. 2022, 122, 13547−13635

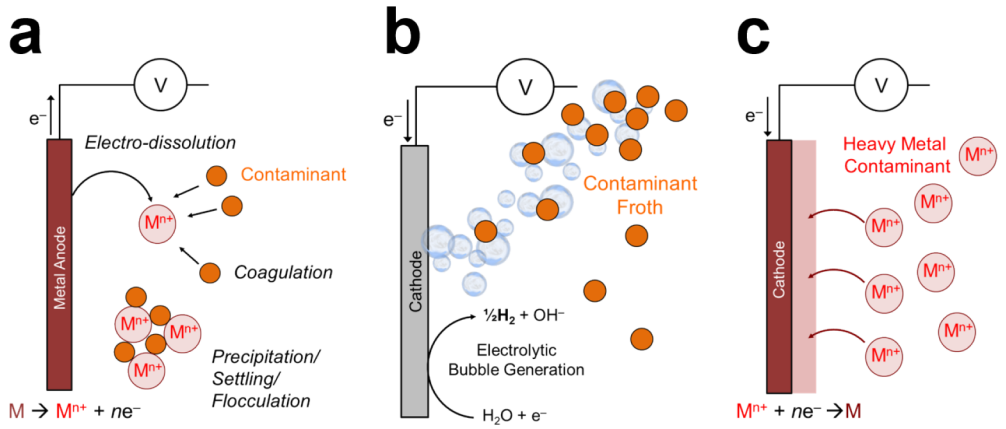

Figure 7. Established nondestructive, nonelectrosorptive methods of water purification. (a) Electrocoagulation and electroflocculation is a two-step process by which metal anodes are dissolved to induce formation of flocs that trap contaminants for removal by settling, sedimentation, precipitation, or flotation. (b) Electroflotation produces bubbles by water redox to transport lighter contaminants or flocs by flotation. (c) Electrodeposition is based on the electrochemical deposition of metal ions in solution onto an electrode.

respect to conversion of halogenated contaminants.[97,98] Noble metals such as palladium, platinum, and ruthenium are also effective materials for electrocatalytic hydrodehalogenation,[263] especially when combined with other elements to produce bimetallic catalysts.[270−272] These bimetallic catalysts can even be modified by adding nanosized or anchored materials to further improve their electrocatalytic efficiency.[263,273,274] The main limitation of metallic catalysts, however, is their high cost, which makes the use of carbon-based materials an attractive alternative.[98,275] Some of the most effective carbon-based catalysts involve nanostructured polymer coatings that selectively adsorb halogenated compounds,[276,277] but the electrocatalytic activity of modified carbon materials in general is low.[278] Activity can be improved by combining nanostructured carbons such as reduced graphene oxide (RGO) with metallic electrodes.[264]

In general, electrochemical reduction is an effective method not only for treatment of pollutants, such as volatile organic halides and chlorofluorocarbons, but also for their transformation into value-added products.[97] This capability can be achieved by selective removal of halogens as well as by carboxylation or carbonylation of the organic compounds. The combination of electrochemical reduction and electrosynthesis is another way by which wastewater can be treated and upgraded for synthesis of value-added organic products.[279,280] Moving forward, it will be important to assess and improve the stability and lifetime of electrocatalytic materials for use in practical applications.

2.3. Electrocoagulation and Electroflocculation

The two-step process of electrocoagulation and electroflocculation relies on the dissolution of metal anodes to induce the formation of flocs, which trap contaminants and enable their removal by settling, sedimentation, precipitation, or flotation.[156,281−285] This method was patented in 1906 by Dieterich for treatment of sewage in London and bilge water from ships using iron and aluminum as sacrificial anodes.[286,287] As shown in Figure 7, the crucial electrochemically mediated step relies on in situ oxidation of the appropriate metal surfaces (often aluminum or iron)[288] to produce metal ions which then form flocs that facilitate the removal of solids, organic species, and inorganic compounds.[158] What follows is essentially ordinary coagulation: the (typically negative) surface charge of the contaminants is neutralized, which destabilizes them and causes them to form aggregates that can be removed by settling, sedimentation, precipitation, or flotation.[289] Electrocoagulation is regularly used in industrial applications, such as removal of heavy metals, remediation of wastewater, and treatment of produced water.[290,291,292] To improve the performance of electrocoagulation for wastewater treatment, numerous studies have sought to integrate this technology with other processes, such as peroxidation or a more specialized biological process, both of which facilitate the removal of organic matter.[293]

Electrocoagulation has been extensively studied, often using iron electrodes, for specialty separations and wastewater treatment, particularly to remove light organic pollutants such as oils, dyes, and humic particles.[294] In addition, electrocoagulation can be used with aluminum electrodes to remove heavy metal ions, including Ag^{+}, Zn^{2+}, Cu^{2+}, Ni^{2+}, and Cr^{6+},[295−297] as well as halide ions.[298] Compared to classical coagulation, electrocoagulation has several advantages that lower its operating cost. For example, the cationic coagulant is generated in situ by a chemical reaction on the sacrificial electrode, and this feature limits the introduction of counterions from chemical reactants that contribute to the formation of sludge.[299] Electrocoagulation thus requires no separation of unreacted counterions from the chemical coagulant in solution, which are usually removed to meet discharge standards.[300] The reduced formation of sludge also lowers expenses associated with handling and disposal of this waste. Another advantage of electrocoagulation is that the electrochemical reactions that drive this process produce OH^{-}, which eliminates the need for external chemical agents to regulate pH.[301] These reactions also produce gaseous H_2, which could be captured and used subsequently as a fuel.[302]

In contrast to classical flocculation, which requires the input of large amounts of chemicals, electroflocculation relies on Faradaic (anodic) dissolution to dose the system with the coagulant, a property that enables finer control and easier handling of the process. Complexation of the released metal ions, such as Al^{3+} or Fe^{3+}, with hydroxides produces monomeric ($Al(OH)_2^{+}$ and $Al(OH)^{2+}$) or polymeric species ($Al_{13}(OH)_{34}^{5+}$) that then flocculate with organic compounds (e.g., dyes) and further promotes precipitation by either sedimentation or flotation.[303] Despite their advantages,

https://doi.org/10.1021/acs.chemrev.1c00396
Chem. Rev. 2022, 122, 13547−13635

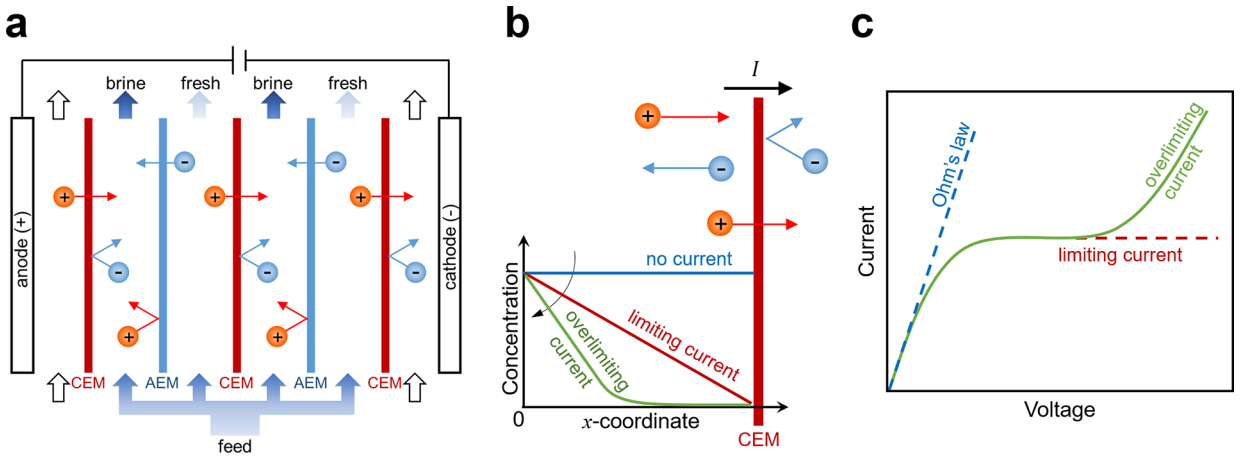

Figure 8. Operating principles and underlying physics of ED. (a) The feed flows through a stack of channels separated by alternating CEMs and AEMs, across which a current is applied. These channels are filled with spacer material that physically separates the membranes, promotes turbulent mixing, and inhibits ICP and the formation of laminar boundary layers near the membranes.[350,351] The concentration profiles of the ions exhibit axial growth of boundary layers of depletion and enrichment in the diluate and concentrate channels, respectively. Adapted with permission from ref 347. Copyright 1968 Elsevier. (b) Ion fluxes near a CEM and the associated convection−diffusion boundary layers, which become more strongly depleted with increasing current until the diffusion limit is reached. (c) The current−voltage relationship reaches a plateau at the limiting current, while overlimiting current, which results in an extended zone of ion depletion, is observed at higher voltages.

however, electrocoagulation and electroflocculation exhibit operational challenges, such as electrode passivation, sludge deposition on the electrode, nonuniform dissolution of the anode, and inconsistent production of the coagulant, all of which undermine performance under long-term, continuous operation.[304] The sacrificial anode is also consumed over time, which necessitates periodic replacement of the electrode, and the high concentration of residual (metal) ions requires a post-treatment step prior to discharge.[305] But because of their operational simplicity, low cost, and versatility, electrocoagulation and electroflocculation remain active areas of research.[306]

2.4. Electroflotation

Electroflotation is often used in conjunction with electrocoagulation and electroflocculation for electrochemical−physical separations.[307−310] Electroflotation relies on the electrolytic process of water redox, in which bubbles are formed to transport lighter contaminants or flocs by flotation. The key driving Faradaic reaction for electroflotation is the electrolysis of water at both electrodes (O_2 evolves at the anode and H_2 at the cathode). The first proposed use of electroflotation is attributed to Elmore in a patent from 1905 for mining separations,[311] and this process has since been expanded to handle a range of contaminants such as oils and low-density suspended particles in mining water and groundwater, among others.[307] The primary limitation of electroflotation is the difficulty of controlling the uniformity of bubble evolution.[158,312] Careful optimization of current densities and voltage windows is therefore crucial for effective performance.[139,282,309,313]

Electroflotation has several features that are attractive for applications in water treatment. For example, this process can be used to recover valuable components from wastewater without the need for chemical reagents.[314] The reason is that electroflotation generates gaseous O_2 and H_2, which are more active than the gases used in conventional flotation (e.g., natural gas, air, N_2). Electroflotation can also produce bubbles with diameters of 1−30 μm, which leads to better dispersion, finer distribution, and longer residence times of the bubbles in solution.[315−317] This feature facilitates the flotation of fine particles in a way that is difficult to achieve by classical flotation. Finally, the energy consumption of electroflotation is in the range of 0.1−0.5 kW h m^{-3}, and it decreases as the electrical conductivity of the solution increases.[315]

2.5. Electrodeposition

The process of electrodeposition is synonymous with electroplating and is one of the earliest applications of electrochemistry, especially in metallurgical processing.[139,318−320] While many of these plating methods are major sources of heavy metal pollution, the same electrochemical principles have been used to treat industrial wastewater and sometimes even to recover and reuse discharged materials. As an example, copper electrodeposition is commonly used to print circuit boards and manufacture electronics. Recovery of copper from spent parts, however, has also been an application of electrochemical methods that combine leaching, ED, and electrodeposition from wastewater.[321,322]

Electrodeposition involves the application of cathodic overpotentials to induce the electrochemical deposition (or reduction) of metal ions in solution onto an electrode. In other words, this process is direct electrochemical reduction of metal ions adsorbed on an electrode surface. Electrodeposition can effectively handle both copper and arsenic wastes, often with the production of pure elemental copper depending on the electrochemical parameters.[323,324] This method has also been used for secondary recovery of residual copper from low-content tailings derived from waste electrical cable.[325] These applications of electrodeposition rely on the same principle of removing metal ions from aqueous solutions that is used to charge aqueous metal flow batteries, such as zinc−air,[326] zinc−bromine,[327] zinc−iron,[328] and lithium−air batteries.[329]

2.6. Challenges and Limitations

Established nonelectrosorptive processes exhibit irreversible side reactions that consume significant amounts of energy and reduce current efficiency.[287] Depending on the complexity of the electrochemical matrix, a number of byproducts can be produced, some of which passivate the electrodes and further

https://doi.org/10.1021/acs.chemrev.1c00396
Chem. Rev. 2022, 122, 13547−13635

diminish performance.[282,287,330] For example, even though there were attempts as early as the late 1800s to implement electrocoagulation and electroflotation at scale, these processes never evolved into mainstream technologies because of their prohibitively high operating costs.[282] Electrocoagulation and electroflotation have also lacked systematic studies aimed at scaling up the processes and optimizing their operating parameters.[282,306] These methods, however, remain promising for localized and small-scale applications, and they continue to offer interesting avenues for scientific research in interfacial science, electrochemical engineering, and reactor design.

3. ELECTROKINETIC SEPARATIONS

When current is applied across a pair of electrodes, ions and larger particles in solution are transported by electromigration and electrokinetic phenomena,[91,331−333] such as surface conduction, electroosmosis, and electrophoresis. Water purification by electrokinetics is based on the transport of contaminants in an electrolyte, and methods of this kind can be used to remove both organic[159,334−336] and inorganic[68,115,153,337] ions from water. Electrokinetic methods such as ED, EDI, and shock ED are continuous and involve an electric field that is perpendicular to the direction of fluid flow. These methods also include IEMs to fractionate the feed into diluate and concentrate streams. EDI and shock ED are similar in that a porous material (e.g., ion exchange resin beads, ceramics, clays, porous glass) is used to enhance mass transfer across the liquid to the solid phase. This unique feature of EDI and shock ED allows for currents beyond the ideal diffusion-limited current and makes these methods well suited to remove trace contaminants from dilute feeds. In this section, we briefly discuss the operating principles and basic physics of ED and EDI. We then focus on the emerging method known as shock ED, which is being reviewed for the first time. Our discussion of shock ED is preceded by an examination of the key developments in microfluidics and electrokinetic modeling that inspired the invention of shock ED as a method for water purification and ion separations. We conclude this section with a discussion of fouling phenomena and methods to overcome them in electrokinetic systems.

3.1. Electrodialysis

3.1.1. Basic Principles of Electrodialysis. ED is a membrane-based electrochemical method that was developed in the 1950s[114,338] for desalination of brackish water and for ion separations.[339−344] The operating principles and underlying physics of this method are summarized in Figure 8 (see refs 152 and 153 for detailed reviews of membrane phenomena in ED). The process begins by passage of the feed through a stack of parallel, nonporous cation and anion exchange membranes (CEMs and AEMs; see refs 345 and 346 for detailed reviews of IEMs and the state of their development). At the same time, direct current (DC) is applied across the stack, perpendicular to the direction of flow to separate ions in alternating channels of fresh water (diluate) and brine (concentrate). In the sections where diluate is produced, cations pass through CEMs and anions through AEMs on the opposite side, which lowers the concentration of uncharged salt in a boundary layer that grows into the channel downstream. In the sections where concentrate is produced, anions are retained by CEMs and cations by AEMs, which results in boundary layers of increasing salt concentration.[339,347,348] Once the boundary layers span the entirety of the channels, a condition termed "fully developed" forced convection,[349] the dissolved salts have been effectively transported from diluate channels into neighboring concentrate channels for discharge.

Depletion and enrichment of salt in unsupported electrolytes lead to self-generated diffusional electric fields that impede the transport of active ionic species through the phenomenon of ion concentration polarization (ICP). These electric fields arise to maintain electroneutrality via redistribution of the inactive (typically oppositely charged) ionic species. The additional internal voltage drop associated with variations in salt concentration relative to that of electrical conduction in a uniform bulk electrolyte (Ohm's law) is termed the concentration overpotential. When the salt concentration tends to zero, the concentration overpotential diverges and leads to a diffusion-limited current, as long as the transport is dominated by electrodiffusion in a neutral unsupported electrolyte without the creation of any additional ions.[332,352,353] For example, the mobilities of cations and anions in an electrolyte are comparable but may differ considerably in an IEM or a nanochannel with charged surfaces.[354] Salt depletion dramatically increases the electrical resistivity of the solution, which leads to significant departures from Ohm's law as shown in Figure 8, and limits the achievable rate of ion removal by ED.[339−342,355] The current−voltage relationship for ICP in a symmetric (z:z) binary electrolyte resembles that of an ideal diode:

$$I = I_{\mathrm{lim}}\left[1 - \exp\left(\frac{-zFV}{RT}\right)\right] \tag{1}$$

where I is current, I_{lim} is the diffusion-limited current (or limiting current),[95] z is charge, V is voltage, F is Faraday's constant, R is the universal gas constant, and T is temperature. The maximum diffusion-limited current, I_{lim}, is approached when a large potential difference (relative to the thermal voltage, $RT/F \approx 26$ mV at room temperature), V, is applied to the system and as the salt concentration in the diluate sections approaches zero.

The theory of ED was pioneered by Peers,[356] after which it was extended for arbitrary transference numbers by Rosenberg and Tirell[357] as well as for fully developed convection by Sonin and Probstein.[347] A useful approximation for the limiting current is given by the Peers equation,

$$I_{\mathrm{lim}} = \frac{FDc_0}{\delta(\tau_\alpha - \tau_\beta)} \tag{2}$$

where c_0 is the bulk salt concentration, D is the effective salt diffusivity for coupled diffusion and electromigration (usually taken to be the ambipolar diffusivity in a dilute, binary electrolyte,[358,359] although concentration dependent corrections can be significant[360]), τ_α is an effective transference number for counterions that selectively cross the solution−membrane interface ($\tau_\alpha = 1$ for an ideal membrane or electrode),[340−342] τ_β is the transference number for counterions in the solution, and δ is the effective boundary layer thickness. This thickness scales as $\delta/H \sim \mathrm{Pe}^{-1/3}$ in the Lévêque approximation,[339,347,349,361] where $\mathrm{Pe} = UH/D$ is the Péclet number, defined by the channel spacing, H, and characteristic fluid velocity, U. This theory is based on a boundary layer analysis of the steady convection−diffusion equation for an uncharged binary electrolyte,[339,349] where the flow is assumed to be fully developed and unidirectional and axial diffusion is

https://doi.org/10.1021/acs.chemrev.1c00396
Chem. Rev. 2022, 122, 13547−13635

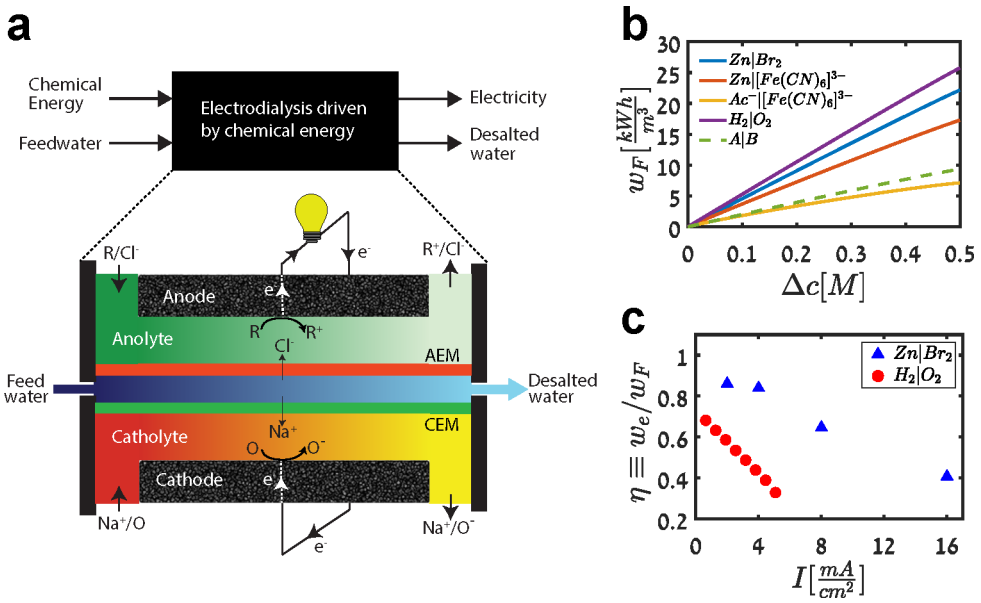

Figure 9. Operating principles of chemical energy ED. (a) Schematic of an ED cell driven by chemical energy, where a reductant R and oxidant O are used to drive desalination and generate electricity. Adapted with permission from ref 442. Copyright 2019 Elsevier. (b) Calculations of the maximum available energy from an ED cell driven by chemical energy for various redox couples. (c) Measured thermodynamic efficiency of ED cells driven by hydrogen−oxygen and zinc−bromine redox couples. Reproduced with permission from ref 448. Copyright 2020 The Electrochemical Society.

neglected, as is usual for forced convection in straight pipes and channels.[349,362] Similar boundary layer approximations can be derived for membraneless flow batteries with forced convection over (selective) redox electrodes instead of IEMs.[363] Extensions for turbulent flow,[364] including effects of screen spacers to promote turbulent mixing,[365] were incorporated in a general equivalent circuit model of ED by Belfort and Guter.[366] Theoretical models were also used to calculate the pH profile[367] and analyze ion selectivity (e.g., K^+ versus Ca^{2+},[348] NO_3^- versus Cl^-[368]) in ED.

In practical systems, the ideal diffusion-limited current is always exceeded when the applied voltage is sufficiently high, and possible mechanisms of this "overlimiting current" have been extensively studied in membrane science.[153,369] In bulk liquid electrolytes, there are two main kinds of mechanisms responsible for overlimiting current: electrochemical and electrokinetic.[370] Electrochemical mechanisms involve charge regulation[371−377] and self-ionization of water molecules,[72,356,378] both of which may lead to current induced membrane discharge[379] (i.e., loss of ion selectivity) and in turn passage of co-ions that would otherwise be repelled by the membrane. Electrokinetic mechanisms are based on the Rubinstein−Zaltzman electroconvective instability, where the EDL (either in[380] or out of equilibrium[381,382]) between the depleted solution and the membrane becomes hydrodynamically unstable to electroosmosis and in turn drives bulk vortices that transport ions to the membrane faster than by diffusion.[383−388] In ED, electroconvective mixing can enable overlimiting current and improve the transport of ions,[389] although at the expense of greater energy consumption compared to operating below the limiting current. These observations led the scientific community to develop ways to control electroconvection, including the use of topological heterogeneity, for example by patterning the surface of an IEM,[388,390−393] and pulsed electric fields.[394−398] Phenomena resembling electroconvection also arise in metal electrodeposition, and they strongly influence the formation of patterns.[399,400] Understanding and controlling these instabilities in bulk electrolytes is a grand challenge, the solution to which could lead to novel electrochemical systems that benefit from operating in the exotic regime of overlimiting current despite the higher energy demand.

The efficiency of ED depends on device structure (e.g., spacer thickness and geometry, number of cell pairs in the stack), membrane properties (e.g., material chemistry, concentration of the fixed ionic moiety),[365,401−405] electrode design (e.g., capacitive flow or membrane electrode, electrode redox couple),[406] operating conditions (e.g., electric potential, current density, hydrodynamics, temperature), and feed composition.[114,407] On the basis of their structure, commercial IEMs are classified as either homogeneous or heterogeneous.[408] A homogeneous IEM generally displays higher conductivity and permselectivity compared to a heterogeneous membrane because the latter comprises a larger insulating phase in its matrix as a result of the fabrication method.[409,410] A heterogeneous IEM, on the other hand, often has greater mechanical strength and is less expensive to manufacture.[411] The heterogeneous structure of such a membrane also promotes electroconvection and mass transfer by localizing the migration of ions through the conductive parts of the membrane.[388,412−416] Because a commercial ED stack may contain 300−500 cell pairs,[417] the conductivity of the membrane will largely determine the overall conductivity of the stack, which in turn influences the energy consumption of the process. Another critical feature of IEMs is their resistance to the formation of deposits (e.g., organic fouling, inorganic scaling), which degrade the performance of the membranes and negatively affect the quality of the water produced.[418,419] Much research has therefore been devoted to developing IEMs that have improved antifouling properties,[420−423] as discussed in section 3.6.

https://doi.org/10.1021/acs.chemrev.1c00396
Chem. Rev. 2022, 122, 13547−13635

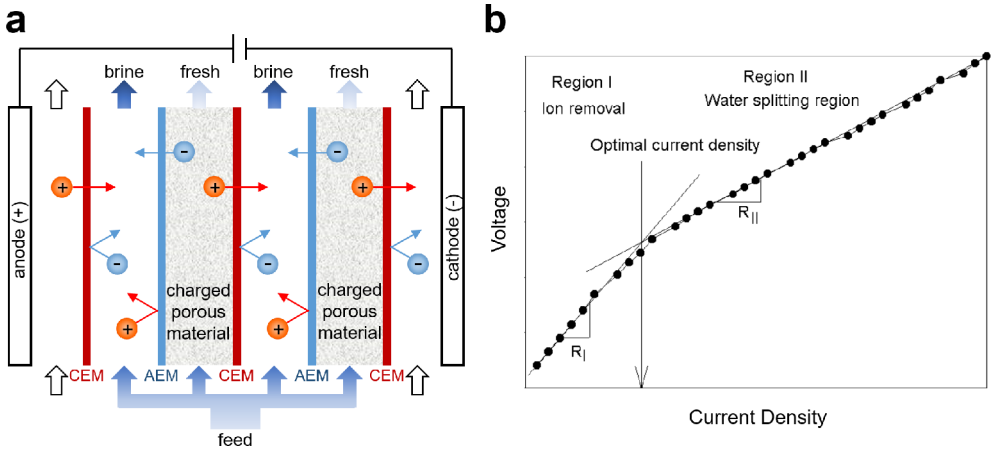

Figure 10. Design and operating principles of EDI. (a) As in ED, ions are depleted in the diluate compartments of an EDI stack and are concentrated in the adjacent (concentrate) compartments due to the permselective properties of the IEMs. In EDI, however, the use of a charged porous material (usually ion exchange resin) enables extreme deionization by boosting the conductivity of the electrolyte in the diluate compartments. (b) Typical current–voltage relationship in EDI, which reveals the existence of two regions with distinct resistivities (characterized by the slope of the graph). Reproduced with permission from ref 462. Copyright 2005 Springer.

3.1.2. Electrodialysis With Bipolar Membranes. One class of ED systems that remains an active area of research is based on bipolar membranes, which facilitate water dissociation without the need for chemicals.[114,345,424−426] Bipolar membranes are fabricated by combining a CEM and an AEM, with a hydrophilic contact region separating the two IEMs. It is at this contact region where water is split into H^+ and OH^-, which migrate into acid and base compartments, respectively, when an electric potential is applied. The primary benefits of using bipolar membranes with ED are that they catalyze the production of H^+ and OH^- at voltages lower than what is needed for standard electrolysis at an electrode, reduce the amount of concentrate generated, and increase the recyclability of the waste by recovering ions from the feed as acids and bases.[58,427,428] The use of a bipolar membrane, however, also introduces an electrical resistance to the system that lowers the current efficiency. This decrease in efficiency is overcome by lowering layer resistance and incorporating weak ion exchange groups in the membrane.[429] As a result, the energy required to produce H^+ and OH^- with commercially available bipolar membranes is nearly equal to the theoretical minimum value[429] (the theory of bipolar membranes is discussed extensively in refs 426, 429−433).

ED systems with bipolar membranes have several applications, one of which is the recovery of acids and bases from salts produced by chemical reactions or neutralization.[434−437] Because ions must first be separated to produce these acids and bases (e.g., Li^+ for LiOH, Na^+ for NaOH, SO_4^{2-} for H_2SO_4), this process desalinates a concentrated feed in the same way as conventional ED.[435,438−440] The first industrial process to employ ED with bipolar membranes was developed by Aqualytics to recover HF and HNO_3 from pickling baths in the steel industry.[435,441] Although commercial use of this technology remains limited due to the high cost, low permselectivity, and short lifetime of existing bipolar membranes,[114,435] novel applications are rapidly emerging, such as pH control, carbon capture, production and recovery of ammonia, and energy storage.[426]

3.1.3. Electrodialysis Driven by Chemical Energy. Recently, chemical energy was used in ED to simultaneously drive separations and generate electricity (Figure 9a).[442−445] Inspired by microbial desalination cells,[446,447] these ED systems are driven by inorganic redox couples, but they do not actually employ microbes because the use of microorganisms can limit electricity production and salt removal rates.[448] ED cells driven by chemical energy can simultaneously produce clean water and generate electricity by performing a combined reaction–separation process that is thermodynamically spontaneous. Atlas et al. calculated the maximum available energy from this combined process, as shown in Figure 9b, and quantified the thermodynamic efficiency of cells driven by chemical energy, as shown in Figure 9c.[448] The authors also found that, for certain chemistries, up to 25 kW h m^{-3} of electricity can be produced. This technology can thus generate significant excess electricity, well above what is that needed for pre- and post-treatment of the feed, which is approximately 1 kW h m^{-3} for seawater.[68]

The concept of chemical energy ED was tested with a variety of redox chemistries, including zinc–bromine,[442] zinc–air,[154] aluminum–air,[444] hydrogen–oxygen,[448−452] and acid–base[453] couples. In particular, the hydrogen–oxygen couple is promising, as it relies on relatively inexpensive gas-phase reactants, and the product of the chemical reaction is simply water (Figure 9a); cells that use the hydrogen–oxygen chemistry are termed "desalination fuel cells."[445,448] Other chemistries that rely on liquid-phase reactants or that produce a waste product complicate disposal of the brine.[442,444] The hydrogen–oxygen chemistry, however, exhibits relatively low thermodynamic efficiency relative to other chemistries, such as zinc–bromine, mainly due to losses at electrodes attributed to (platinum) catalyst poisoning by halide ions in the brine (Figure 9c).[448,454] Therefore, a crucial area of research is the design and development of inexpensive catalyst materials tailored to long-term operation in desalination fuel cells. Asokan et al. demonstrated the use of chloride-tolerant, iron-based catalysts for oxygen reduction in a desalination fuel cell, which opens the field of nonplatinum group metal catalysts for these systems.[455]

3.2. Electrodeionization

EDI, shown in Figure 10a, is typically used to generate highly pure products by processing feeds with low levels of dissolved solids (e.g., RO permeate).[126,456−460] This method originated

https://doi.org/10.1021/acs.chemrev.1c00396
Chem. Rev. 2022, 122, 13547−13635

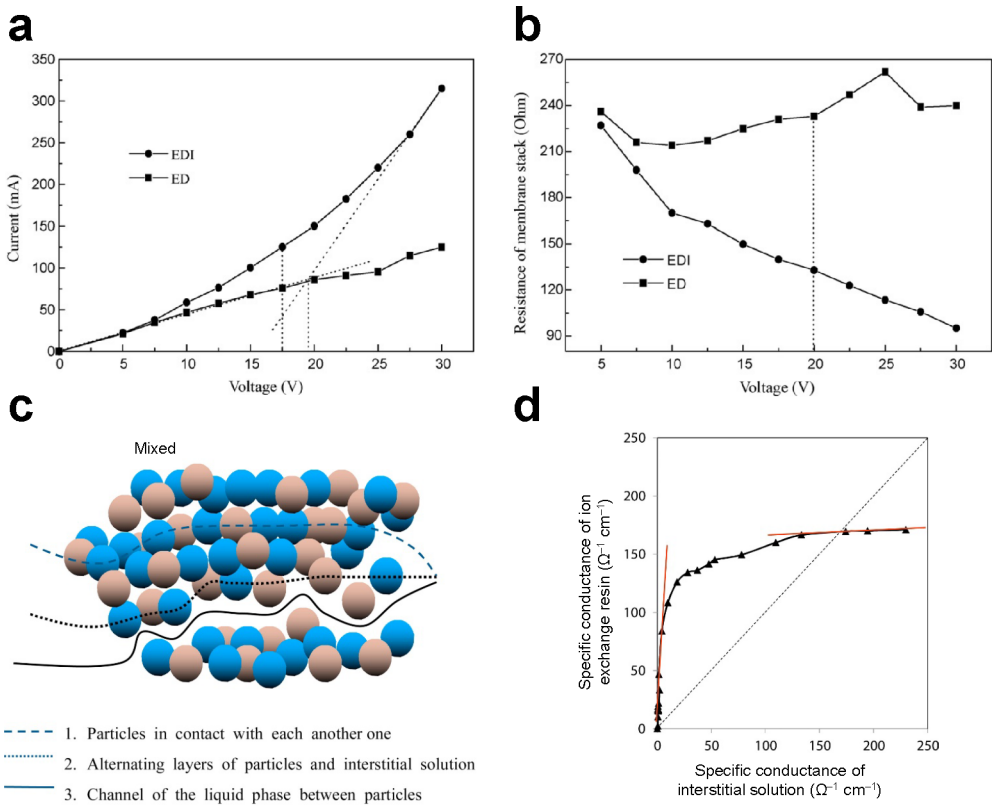

Figure 11. Role of ion-exchange resin in EDI. Comparison of (a) current−voltage and (b) resistance−voltage relationships in ED and EDI. Reproduced with permission from ref 465. Copyright 2009 Elsevier. (c) Schematic of the three pathways for charge transport in a mixed bed. (d) Specific conductance of the ion exchange resin versus that of the interstitial solution. Reproduced with permission from ref 470. Copyright 2015 Elsevier.

in the late 1950s with the intent of enabling extreme deionization of contaminated feeds by packing the channels of an ED stack with charged porous media or conductive ion exchange resin beads.[61,106] The purpose of these conductive materials is to reduce the ICP observed in ED by enhancing transport of ions via electrokinetic phenomena (see Figure 11c and Figure 13). As in ED, ions are depleted in the diluate compartments of an EDI stack and are concentrated in the adjacent (concentrate) compartments because of the permselective properties of the IEMs. To deionize the electrolyte while maintaining reasonable conductivity across the stack, however, a conductive material such as ion exchange resin is needed to lower the resistivity of the electrolyte in the diluate compartments.[61,461] As shown in Figure 10b, there is an optimal current density that is believed to coincide with the limiting current introduced in section 3.1.[462] Another, more subtle reason ion exchange resin is used in the diluate compartments in EDI is to regulate the pH of the product streams by exploiting the relationship between the applied electrical current and the equilibrium concentrations of H^+ and OH^- in solution.[463]

As illustrated in Figure 8c, a typical ED cell exhibits a dramatic increase in electrical resistivity when salt is depleted from the diluate compartments. Because the concentration of ions in these compartments is smaller near the membranes than it is in the bulk, water dissociation occurs and reduces current efficiency.[464,465] The use of ion exchange resin (whether as loose beads or as a wafer[83,466,467]) in EDI mitigates this effect by promoting transport in a conductive medium, which functions as a bridge for ions between membrane pairs. The current−voltage curves in Figure 11a,b show that EDI maintains increasingly higher conductivity (or lower resistivity) than ED as a function of applied voltage.[126] Pathways of charge transfer in the ion exchange bed of an EDI cell are often studied using the porous plug model[468−470] introduced by Wyllie and co-workers.[471] The overall conductivity of the ion exchange bed is the sum of the conductivities of the ion exchange resin and interstitial solution. These conductivities are sustained via three different pathways, namely the resin (solid), the interstitial solution (liquid), or both (solid−liquid), as shown in Figure 11c. Alvarado et al. studied these pathways using an EDI cell as a mixed bed to treat a synthetic solution containing chromium at concentrations up to 250 mg L^{-1}.[470] In this system, nearly 82.9% of the electric charge was transported by the combined solid−liquid pathway, whereas only 0.6% was transported by the interstitial solution alone. In total, the ion exchange resin, alone or in combination with the interstitial solution, contributed to approximately 94% of ion transport, which underscores the crucial role of ion exchange in driving charge transfer in EDI (Figure 11d).

In addition to facilitating the migration of ions, ion exchange resin enables operation beyond the limiting current, at which diffusion of ions becomes the rate-limiting step in electrochemical separations.[472] Operating in the regime of overlimiting current leads to water dissociation and exotic electrokinetic phenomena like the electroconvective instability,[369,473,474] as was microscopically visualized by Park and Kwak as well as Stockmeier et al.[475,476] In EDI, water dissociates due to the presence of bipolar zones formed at

https://doi.org/10.1021/acs.chemrev.1c00396
Chem. Rev. 2022, 122, 13547−13635

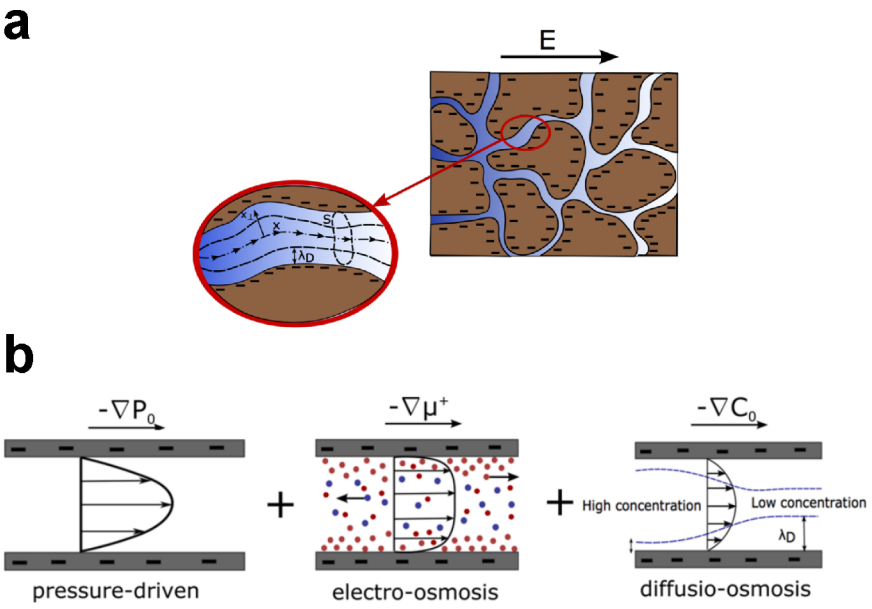

Figure 12. Electrokinetic transport in charged porous media. (a) Schematic of a charged porous medium with solid (brown) and porous (blue) domains. Ion and fluid transport occur along the center axes of pores. The thickness of the EDLs and the amount of surface charge influence the electrokinetic coupling. (b) Fluid can flow due to gradients in pressure, electric field, or electrolyte concentration. Ion separations use these modes of transport to impart selectivity based on electric charge. Reproduced with permission from ref 508. Copyright 2017 American Chemical Society.

points of contact between resin particles and either other resin particles or IEMs.[26,466] As the ion exchange resin traps ions, H^+ and OH^- produced by water dissociation act as charge carriers and regenerate the resin through the process of electroregeneration.[106] Water dissociation is also important when complete removal of weakly ionized species, such as silicon and boron, is needed to produce ultrapure water. The OH^- generated by this dissociation reacts with silicon and boron as follows:[477]

$$SiO_2 + OH^- \rightarrow HSiO_3^- \quad (3a)$$

$$HSiO_3^- + OH^- \rightarrow SiO_3^{2-} + H_2O \quad (3b)$$

$$H_3BO_3 + OH^- \rightarrow B(OH)_4^- \quad (3c)$$

Once the neutral species SiO_2 and H_3BO_3 become ionized, they are readily transported into the concentrate compartment and discharged.

Another useful function of the ion exchange resin in EDI is that, as a selective medium, it preferentially removes ions based on their affinity to the resin.[57] Selective separation of ions with similar charge and size can be achieved by controlling the mobility of these ions with a complexing agent.[478,479] For example, Taghdirian et al. used a complexing agent made of ethylenediaminetetraacetic acid (EDTA) to separate Ni^{2+} from Co^{2+}.[479] This complexing agent formed a strong bond with Ni^{2+}, which produced a negatively charged complex whose mobility was inhibited in the bed of cation exchange resin. On the other hand, Co^{2+} remained a free cation that could readily enter the gel phase of the resin. By removing Co^{2+}, the molar ratio of Ni^{2+} to Co^{2+} in the solution was increased from 3 to over 150.[479]

Although the microscopic mechanisms of EDI have received much less attention compared to those of ED, there have been several efforts to mathematically model[107,460,480−483] and numerically simulate[484−487] the process of EDI. Early descriptions of EDI proposed that the removal of ions occurs in two steps.[488] First, ions diffuse from the bulk to the liquid−solid (resin) interface, where counterions are exchanged with mobile ions on the resin. Second, the adsorbed counterions are transported toward and across the corresponding IEM, where they are released into the concentrate compartments. Removal of ions is controlled by the rate of diffusion from the aqueous phase to the surface of the solid.[126,488] This rate is determined by the properties of the solid surface, the thickness of the liquid layer through which ions diffuse, and the concentration gradient between the two phases. When a current is applied beyond what is needed for the electromigration of ions to the surfaces of the resin, water molecules dissociate into H^+ and OH^-, which replace the ions that have adsorbed on the resin.[126]

3.3. Electrokinetics in Nanochannels and Membranes

While nanofabricated devices are difficult to manufacture at scale, the scalable polymeric IEMs used in ED, EDI, and shock ED are essentially made of a network of nanoscale pores with high charge densities, as shown in Figure 12a.[338,345,489,490] This nanoscale structure promotes selectivity based on the charge of an ion and on chemical interactions between the ion and the pore walls.[491] IEMs are an integral component of many electrochemical methods of ion separations, and this fact underpins the development of membrane properties like conductivity and selectivity.[338,345,492,493] There also exist exciting opportunities for enhanced separations as well as reduction in fluidic resistance using engineered nanoscale conduits like CNTs[494−497] and graphene,[498−500] but the success of these technologies in practice requires a high density of channels and a scalable and controlled fabrication process.

A membrane or surface in contact with an electrolyte solution either already has or will acquire a net charge, and under most circumstances, this surface charge is balanced (or screened) in the liquid by a diffuse layer of oppositely charged ions.[332,333] This concept of an "electric double layer" was originally proposed by Helmholtz,[501] later refined by Gouy and

https://doi.org/10.1021/acs.chemrev.1c00396
Chem. Rev. 2022, 122, 13547−13635

Chapman[502,503] and revised once more by Stern.[504] The local diffuse charge leads to electroosmosis and diffusio-osmosis in response to an electric field and concentration gradient, respectively.[91] The equations that govern transport in charged nanoporous media are therefore coupled, such that gradients in pressure, concentration, or electric potential (Figure 12b) lead to combined fluxes in fluid flow, salt transport, and electrical current.[505] Gross and Osterle described the set of coupled transport phenomena by the Poisson−Nernst−Planck−Stokes (PNPS) equations, with assumptions of local equilibrium and electroneutrality in the cross sections of pores.[506] This approach presents a unified theoretical framework to describe ion and fluid transport in charged porous media down to the nanoscale, and it can be used to model ED, EDI, and shock ED. Recent work extended these results to numerically solve the PNPS equations[507] and describe nanofluidic transport in nanopores.[505] Systems modeled in this way include homogeneous networks with pores connected in series or in parallel as well as heterogeneous networks with pores of varying cross section.[508−510] The homogenization of the PNPS equations to heterogeneous porous media revealed complex flow patterns and vortices due to parallel connectivity in these materials.[511] Other models incorporated chemical interactions, mismatch in the diffusion coefficients,[512] multicomponent electrolytes,[513−515] electroviscous effects,[516] nonionic solutes,[512] salts with asymmetric valences,[517,518] reactions of fixed charges,[519,520] temperature gradients,[521] electron conducting[522] or polarizable nanopores,[523] and dielectric effects[513,514,524−526] to describe the distribution of ions and solvent molecules in the pores. Analytical approximations to the nonlinear transport equations are valid when the surface potentials are small[527] or when the EDLs are overlapping.[505]

Perhaps the most fundamental principle of nanofluidic transport is electroneutrality, which is an implicit assumption embedded in the models previously discussed that dictates that the charge within a pore must balance the charge on the pore walls. Indeed, in deionization processes such as EDI and shock ED, the strong tendency toward electroneutrality in charged nanopores allows for residual conductivity, even as the concentration of ions in the bulk goes to zero, because counterions screening the surface charge are always present at a concentration determined by this charge.[94,354,528,529] Levy et al., however, recently showed that one-dimensional confinement of ions to an isolated nanochannel in a dielectric matrix can lead to breakdown of cross-sectional electroneutrality, as the screening length diverges exponentially with decreasing ion concentration.[530] Under these conditions, which are typical of biological ion channels,[531] the role of ion-specific chemical interactions becomes more significant than that of electroneutrality, although this order of importance is reversed in membranes where the distance between parallel channels becomes smaller than their lengths.[532] In addition to energy barriers to enter a pore, intrapore energy barriers can govern ion transport in one-dimensional pores, where ions are confined to the molecular scale.[533]

Other open questions exist about the structure and dynamics of ions and solvent molecules in the EDL, particularly at high ionic strength[534,535] or in the case of extreme confinement.[491] Discrepancies between molecular dynamics (MD) simulations and continuum electrokinetics predictions occur for channels with widths of ∼1 nm.[491,536] As another example, overscreening of surface charge at high concentration can lead to reversal of electroosmotic flow,[537,538] and a high surface charge density can cause electric charge to crowd an interface.[535,539,540] A theoretical explanation of these phenomena requires consideration of electrostatic correlations in the EDL that go beyond the mean-field electrostatic potential.[537,541,542] Transport models of dense ionic solutions can account for these correlations as well as coupled transport modes due to friction between pairs of species. For example, transport equations based on the Stefan−Maxwell model have been used to describe the coupled fluxes of ions and solvent molecules passing through nanoporous membranes.[543−546] Regardless of the model, fixed surface charge influences the distribution of ions in a nanopore and in turn the observed transport properties. The regulation of surface charge via chemical reactions also affects transport dynamics.[373,376,547−550] While the surface charge is usually assumed to be in equilibrium, nonequilibrium reactions can participate in electrokinetic transport.[551,552]

3.4. Ion Concentration Polarization in Microfluidics

The physical phenomenon that enables shock ED, the deionization shock wave, was first discovered and studied in the seemingly distinct context of ICP in microfluidic devices.[92,93,354,553−559] What we now understand to be stationary deionization shock waves were observed by Wang et al. as early as 2005 in a microchannel near a nanochannel junction and used to trap and concentrate biomolecules in cross-flow, though without a theoretical explanation of the mechanism.[560] In 2010, Kim et al. reported a microfluidic system that used ICP to desalinate seawater by applying current in the direction of flow and across a nanochannel junction,[557] albeit at very low efficiency and in nanoliter volumes.[558] A sharp, stationary depletion region was observed behind the nanojunction, and the deionized fluid below the shock was separated from the enriched brine into different microchannels. Separation of all charged solutes into the brine channel was also claimed,[561] although this would appear to contradict the theory of electrodiffusiophoresis,[562] which predicts the dominance of electrophoresis (motion in the direction of the Coulomb force) over diffusiophoresis (climbing salt concentration gradients, regardless of the charge sign) and suggests that fast-moving, positively charged particles in the deionized channel may not have been detected in the experiments.

The breakthrough in understanding microfluidic ICP that paved the way for shock ED occurred in 2009, when Mani, Zangle, and Santiago theoretically modeled[92] and experimentally observed[93] propagating ion concentration shock waves for the first time in a microchannel−nanochannel device with negatively charged surfaces. Two microchannels were filled with a stagnant electrolyte and were separated by a nanochannel with thick, overlapping EDLs, which behaved like a CEM to induce ICP and initiate a shock wave of salt depletion in one direction and salt enrichment in the other. Mathematical modeling revealed how the nonlinear drift arising from electromigration (competing with electrodiffusion) can create breaking waves of salt concentration and propagating shocks,[92] analogous to the shock waves that arise in isotachophoresis[563,564] and capillary electrophoresis.[565,566]

3.5. Shock Electrodialysis

3.5.1. Deionization Shock Waves in Microstructures.

While developments in microfluidics have been critical to advancing the scientific understanding of ICP under strong confinement, microfabricated lab-on-a-chip devices are neither

https://doi.org/10.1021/acs.chemrev.1c00396
Chem. Rev. 2022, 122, 13547−13635

scalable nor efficient for macroscopic ion separations and water treatment. To produce any meaningful volume of water, a prohibitively large number of channels or devices would need to be fabricated and operated in parallel. Porous media, on the other hand, represent much more compact systems of interconnected microchannels in parallel that can be manufactured at scale, and these include ion exchange resin beads, ceramics, clays, and porous glass. Moreover, theoretical and experimental work have demonstrated that overlimiting current can in fact be sustained in charged porous media.[94,95,568−571]

In 2011, Mani and Bazant demonstrated the propagation of deionization shock waves in porous microstructures by theory and simulation.[94] At the same time, Dydek et al. described the transport processes that enable overlimiting current in a charged microchannel, as shown in Figure 13.[528] This work

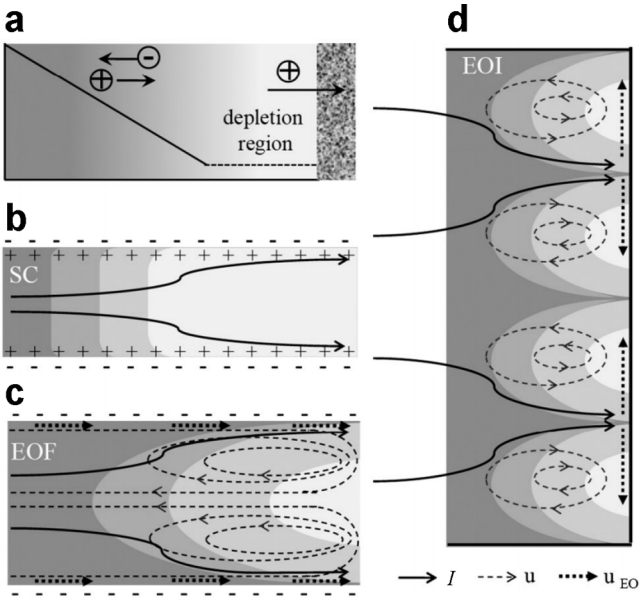

Figure 13. Schematic representations of common mechanisms to sustain overlimiting current in a microchannel between a reservoir on the left and a CEM on the right. The volume average conductivity in (a) exhibits classical linear diffusion (continuous line) up to a region of depletion (dashed line), where charge carriers are transported by (b) surface conduction, (c) electroosmosis, or (d) electroconvection (visualized experimentally by Gu et al.[567]). The relative contributions of these effects depend on the width of the channel, such that surface conduction dominates in narrow channels and electroconvection in wide ones. Reproduced with permission from ref 528. Copyright 2011 American Physical Society.

explained that electroosmosis dominates the transport of ions when an electrolyte is confined to small pores (~100 μm). When the pores are even smaller (~1 μm), surface conduction becomes the dominant mechanism of overlimiting current. Experimental visualizations by Nam et al. later confirmed the theoretical predictions of the regimes in which surface conduction and electroosmosis sustain overlimiting current in a microchannel.[559,572] These observations and discoveries served as the foundation for developing a novel technology that can separate ions by deionization shock waves in porous media. Deionization shocks have also proven useful in controlling the high-rate electrodeposition of metals in charged nanopores,[570] where shock electrodeposition can suppress dendritic growth[573] and enable resistive switching memory[574] and rechargeable metal batteries.[575]

In 2013, Deng et al. reported experimental evidence for overlimiting current, sustained by surface conduction and electroosmosis, and deionization shock waves in a charged porous material.[95] This study was the first to observe these phenomena in porous media, and it demonstrated the feasibility of shock ED as a new platform to desalinate water and perform electrochemical separations.[95,576] The basic design of the original shock ED system used a silica glass frit (weakly charged porous material) sandwiched between two electrodes (which can be thought of as strongly charged porous material; recall the microchannel−nanochannel geometry of Mani et al.[92]), as shown in Figure 14. (Note that the porous material and the IEM must have surface charges of the same sign. This condition ensures the propagation of depleted and enriched regions.[93]) Because overlimiting current is sustained in shock ED to form a deionization shock wave near the cathodic CEM, as shown in Figure 14c, it is possible to deionize the feed to concentrations well below what could be achieved by standard ED. The experimental work by Deng et al. indeed demonstrated that shock ED can produce deionized water with concentrations of ~10 μM (see Figure 14d).[95] In the same year, the nonlinear dynamics of ICP in porous media were mathematically described by Dydek et al. using a homogenized model (which assumes that the EDLs are thin relative to the nominal pore size), with emphasis on water treatment by shock ED.[529] These two publications also proposed a scalable shock ED system that would be operated continuously.

The original shock ED system by Deng et al. was a radially symmetric button cell that had to be operated in batch mode.[95] This geometry made it difficult to scale up the system, and it was clear to the authors at the time that a continuous process was more desirable. The second generation of shock ED devices, built by Schlumpberger et al. then improved by Conforti and Alkhadra, had a rectangular geometry and was shown to remove more than 99.9% of the salt present in solution.[87,577] This new system used a silica frit sandwiched between two CEMs and included a splitter at the outlet between the two membranes to partition the flow into a diluate and a concentrate, as shown in Figures 15 and 16a. In the range of concentrations tested using binary electrolytes of monovalent ions, Schlumpberger et al. showed that desalination was a function of only dimensionless current:

$$\tilde{I} = \frac{I}{I_{\lim}} \quad \text{with} \quad I_{\lim} = z_+ c_+ F Q \tag{4}$$

where z_+ and c_+ correspond to the charge and concentration of the cation and Q is the volumetric flow rate of the feed. This definition of $I_{\lim}$ can be interpreted as the rate of advection of positive charge across the device; it is assumed that the flux of anions is zero across ideal CEMs. The authors also described the effect of electroosmosis on the fraction of liquid recovered as desalinated water from the contaminated feed, often referred to in the literature as the water recovery. Because the zeta potential of the glass frit is negative, the applied electric field induces electroosmosis in the same direction[349,578] (i.e., toward the depleted region near the cathode) and as a result increases water recovery (to above 80% at high current[87]). This effect resembles the function of an electroosmotic pump originally used in microfluidic devices[579,580] and later studied in relation to ICP in microchannels.[581]

https://doi.org/10.1021/acs.chemrev.1c00396
Chem. Rev. 2022, 122, 13547−13635

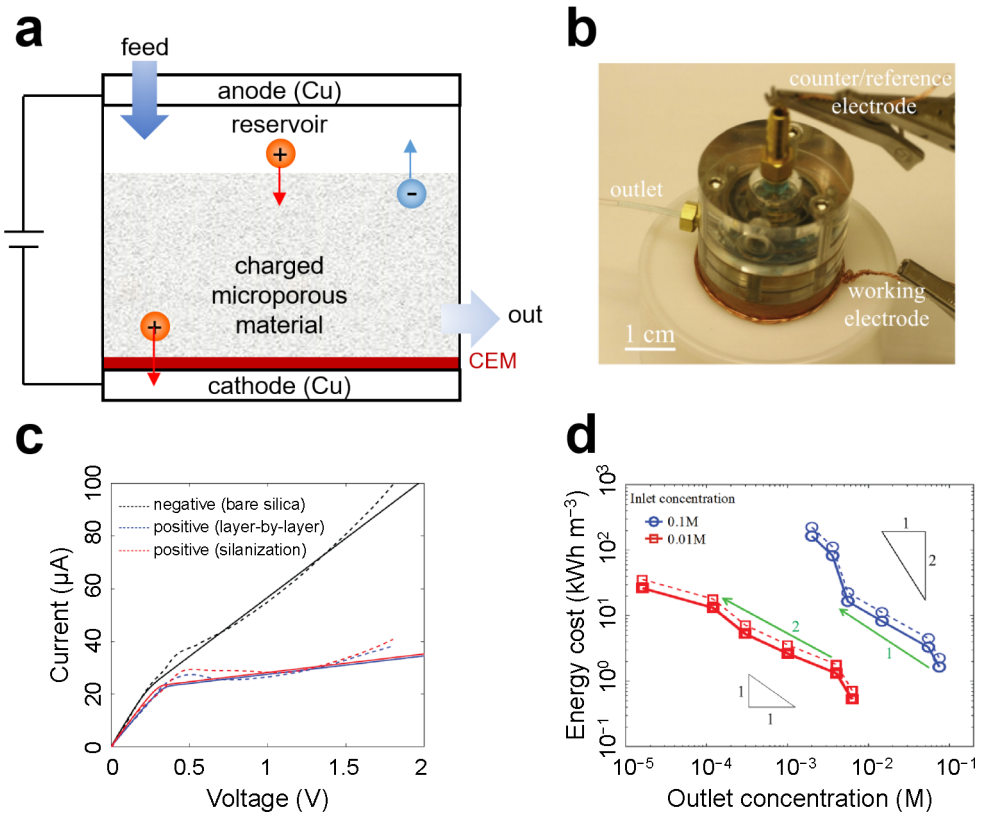

Figure 14. Prototype "button cell" used for shock ED. (a) Rectangular cross section and (b) photograph of the button cell prototype. This device is a cylindrical macroporous material submerged in an electrolyte and placed between copper electrodes. Electrical current is driven by the electrodeposition of copper onto the bottom electrode. (c) Current−voltage relationship in shock ED with 1 mM aqueous $CuSO_4$ as the electrolyte; the effect of the sign of surface charge is also shown. Dashed lines represent experimental data, and solid lines represent the fit to a theoretical model. (d) Energy cost per unit volume of deionized water with (dashed lines) and without (solid lines) the series resistances due to the reservoir and electrodes. Reproduced with permission from ref 95. Copyright 2013 American Chemical Society.

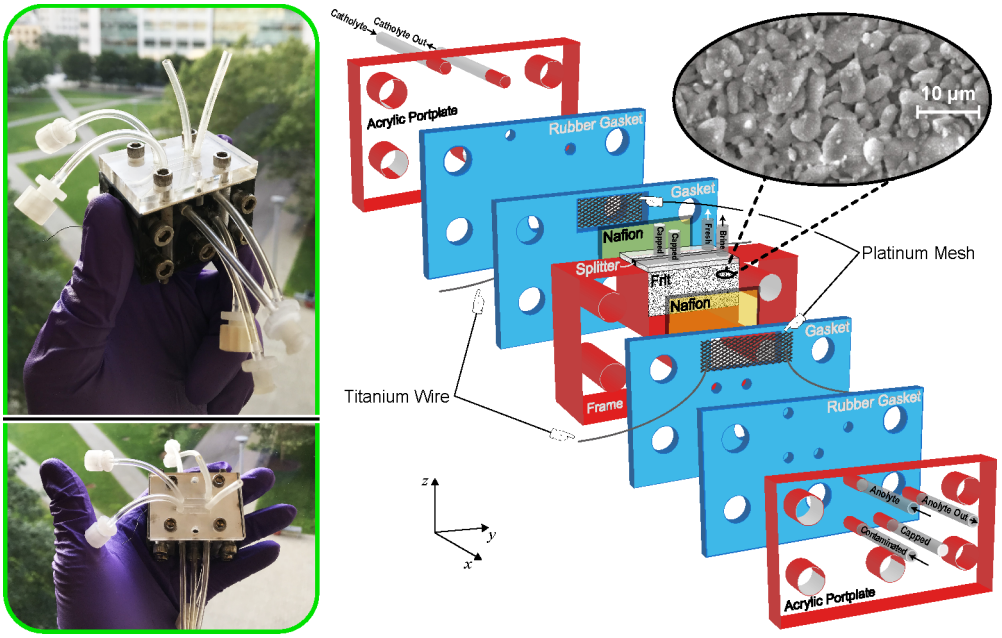

Figure 15. Shock ED as a continuous process. (left) Photographs and (right) illustration of the device that shows assembly: a working device consists of electrodes, wire, and a porous material sandwiched between identical IEMs. Inlet (outlet) streams are labeled contaminated, anolyte (anolyte out), and catholyte (catholyte out); fluid leaving the top edge of the porous material is split into fresh and brine streams. Reproduced with permission from ref 577. Copyright 2019 American Chemical Society.

https://doi.org/10.1021/acs.chemrev.1c00396
Chem. Rev. 2022, 122, 13547−13635

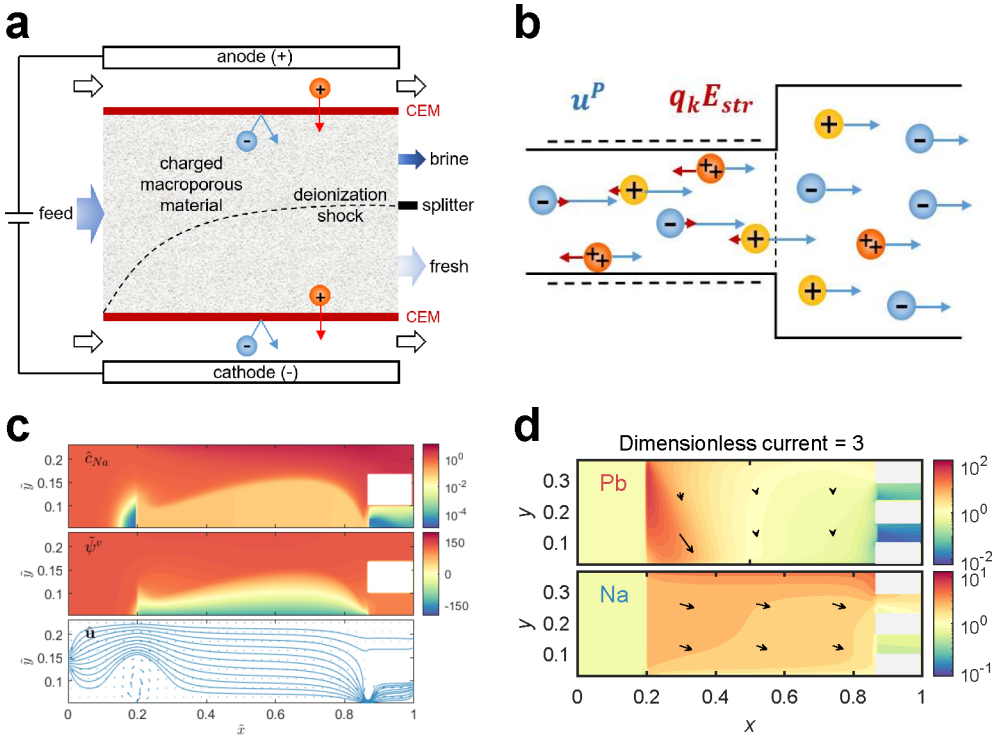

Figure 16. Operating principles and representative simulation results of shock ED. (a) Ions are transported by an electric field perpendicular to the flow, and the electrical current is driven by water redox at the electrodes. (b) Schematic to illustrate ion transport by advection (blue arrows) and streaming potential (red arrows) at the interface between a charged channel and the outlet. u^P is the hydrodynamic flow velocity, and $q_k E_{str}$ is an electrostatic force generated by the streaming potential, where q_k is electric charge and E_{str} is electric field. Reproduced with permission from ref 584. Copyright 2021 American Chemical Society. (c) Steady-state profiles of concentration, c, electric potential, ψ, and velocity, $\mathbf{u}$, at a dimensionless current of five. The velocity profile shows distortion of the depletion zone by electroosmotic vortices. The feed to all channels is 10 mM NaCl aqueous solution at a pH of seven. Reproduced with permission from ref 583. Copyright 2021 Elsevier. (d) Contour plots of dimensionless, depth-averaged concentration and flux vectors for Na^+ and Pb^{2+} at six sample locations in the porous material. Reproduced with permission from ref 584. Copyright 2021 American Chemical Society.

To improve the mathematical model developed by Dydek et al. following these modifications,[529] Schlumpberger et al. considered the role of linear electroosmotic flow and captured some aspects of deionization and water recovery observed experimentally.[582] The model, however, significantly overestimates the extent of deionization and underestimates the overlimiting conductance. Recently, Tian et al. developed a more comprehensive model of shock ED that is valid for multicomponent electrolytes (irrespective of EDL thickness), captures the phenomena of electroosmosis, diffusioosmosis, and water dissociation, and incorporates more realistic boundary conditions.[583] This model also describes the role of electroosmotic vortices at the inlet and outlet of the system, and it considers the effect of hydronium transport. Figure 16c shows the profiles of concentration, electric potential, and velocity obtained from numerical simulations, which have enabled quantitative predictions of deionization and overlimiting conductance that agree with the experimental data in ref 87.

3.5.2. Selective Separations by Shock Electrodialysis. The design introduced by Schlumpberger et al. was the first example of a scalable device that could be used for shock ED.[87] Recent work by Čížek et al. upgraded this design by using a multistack device with AEMs and various porous materials to remove Na^+.[585] In both studies, however, only binary electrolytes of monovalent ions were considered, which encouraged examination of selective removal of multivalent ions. This research began with a systematic study in which Mg^{2+} was selectively removed from an aqueous mixture of NaCl and $MgCl_2$.[109,586] For a feed with Na^+ and Mg^{2+} in molar proportions of nine to one, more than 99% of the Mg^{2+} was removed, even though the total desalination was only 68%. This outcome implied that the divalent ion was selectively removed in the presence of a competing monovalent ion. The results of this work inspired further research into the kinds of contaminants that can be targeted by shock ED in the presence of competing ions. The first of these studies used shock ED in two passes to desalinate artificial seawater (3.5 wt %), from which 99.8% of the salt fed was rejected and more than 99.99% of the Mg^{2+} was removed, as shown in Figure 17a.[587] These results also revealed selectivity toward Mg^{2+}, which was preferentially removed relative to all other species by at least one (Mg^{2+}:K^+) and up to nearly two orders of magnitude (Mg^{2+}:Ca^{2+}). Scaled (retention) selectivity in the fresh stream was calculated as a function of dimensionless current between each pair of unique species i and j using the equation[109]

$$S_{j:i} \equiv j:i = \frac{c_{i_{out}}/c_{j_{out}}}{c_{i_{in}}/c_{j_{in}}} = \frac{c_{i_{out}}/c_{i_{in}}}{c_{j_{out}}/c_{j_{in}}} \quad (5)$$

For example, if $S_{j:i}$ was greater than one, then species j was selectively removed relative to species i. Despite the high rejection of salt and extreme selectivity toward Mg^{2+}, desalination of seawater by shock ED was energy intensive. It was therefore concluded that a more suitable application of this technology would be to target trace contaminants in dilute

https://doi.org/10.1021/acs.chemrev.1c00396
Chem. Rev. 2022, 122, 13547−13635

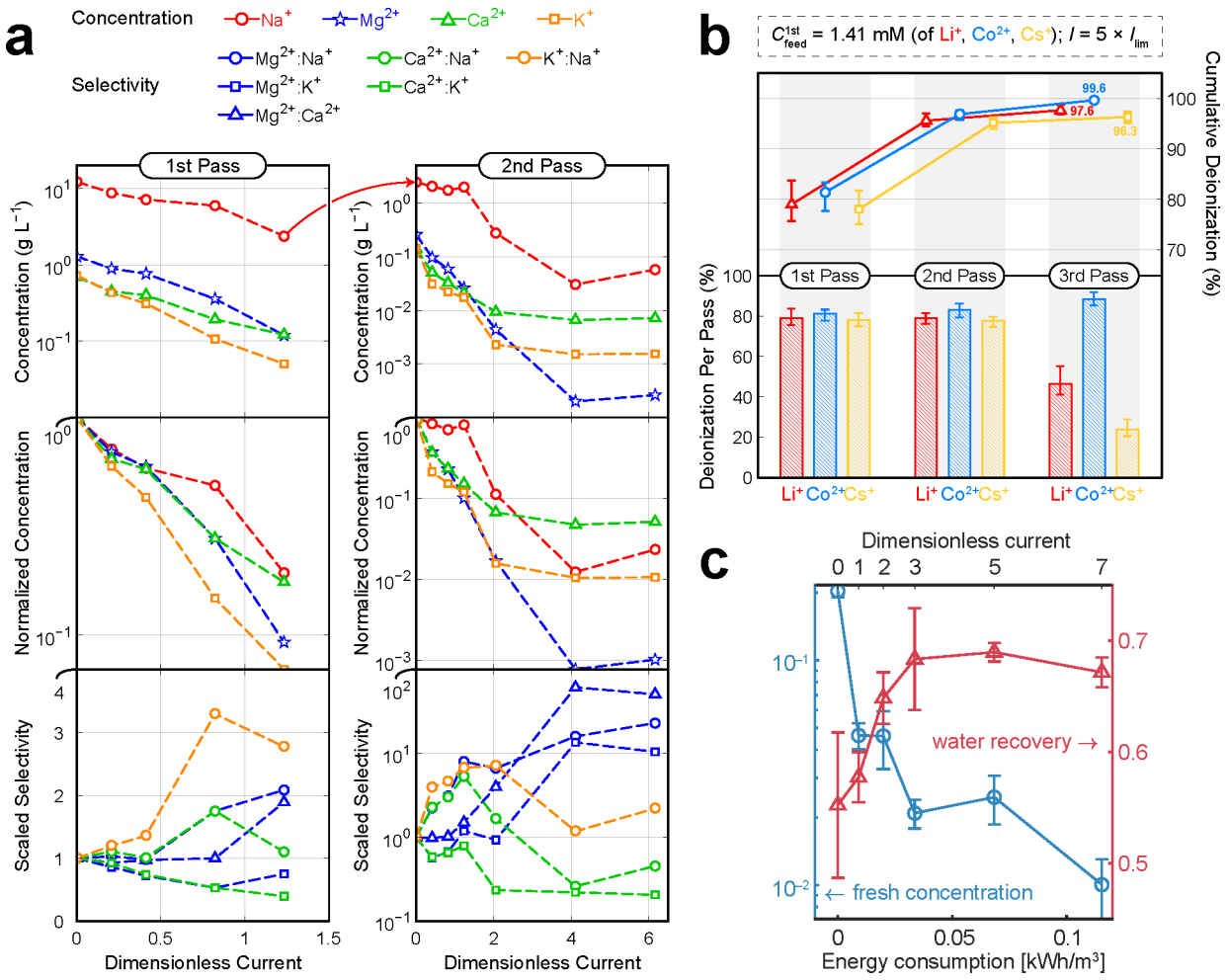

Figure 17. Representative results for selective ion separations by shock ED. (a) Concentration per pass (top and middle) and scaled selectivity (bottom) as functions of dimensionless current for the most abundant cations in seawater. Reproduced with permission from ref 587. Copyright 2020 Elsevier. (b) Deionization per pass (bottom) and cumulative deionization (top) at a dimensionless current of five for three cations normally present in the process water of light-water nuclear reactors. Reproduced with permission from ref 577. Copyright 2019 American Chemical Society. (c) Normalized concentration of Pb^{2+} and water recovery as functions of dimensionless current for removal of Pb^{2+} from water in the presence of excess competing Na^{+}. Reproduced with permission from ref 584. Copyright 2021 American Chemical Society.

feeds, such as toxic heavy metals in drinking water or radioactive ions in the process water of a nuclear reactor (i.e., water used in the boiler or for cooling).

Nuclear fission is a common method to produce energy, although this process leads to contamination of the process water with several dissolved species, some of which are radioactive.[588,589] It is often desirable to selectively accumulate the radionuclides to reduce the volume of nuclear waste and facilitate its containment or disposal.[590−592] Shock ED was thus used to selectively and continuously remove cobalt and cesium from a feed of dissolved lithium, cobalt, cesium, and boric acid.[577] This formulation modeled the contaminated water normally found in light-water nuclear reactors and in other nuclear processes.[593−596] Figure 17b shows deionization per pass and cumulative deionization for each species (with the exception of boron, which was present predominantly as the electrically neutral boric acid) in three passes. In each of the first two passes, all three species were removed in nearly equal proportions, but in the third pass, Co^{2+} was preferentially removed. Overall, the three-step process led to a high cumulative deionization for each species, ranging from 96.3% for Cs^{+} to 99.6% for Co^{2+}. On the basis of these results, a clear and consistent trade-off was observed between the extent of purification (as well as water recovery) and the energy demand of the process. In general, however, the energy demand of this process (which has not yet been optimized) was low, ranging between 1.8 and 4.8 kW h m^{-3}, because only charged species were targeted and essentially no energy was expended, removing boric acid, the most abundant species in the mixture.

Similar to radioactive species, heavy metals can damage normal functions of the human body and lead to heavy metal poisoning. Affordable and effective removal of toxic heavy metals from water, especially in the presence of excess competing ions, has been a longstanding goal in environmental science and engineering.[597] Tian et al. recently demonstrated low-cost, continuous, and selective removal of Pb^{2+} from simulated drinking water using shock ED.[584] As shown in Figure 17c, this process removed over 98% of Pb^{2+} (to safe levels[598] below 1 ppb) with a water recovery of 70% and at an energy cost of 0.1 kW h m^{-3}. At the same time, only 40% of Na^{+} was removed, which maintained electrolyte conductivity and lowered the energy demand of the process relative to nonselective methods.

https://doi.org/10.1021/acs.chemrev.1c00396
Chem. Rev. 2022, 122, 13547−13635

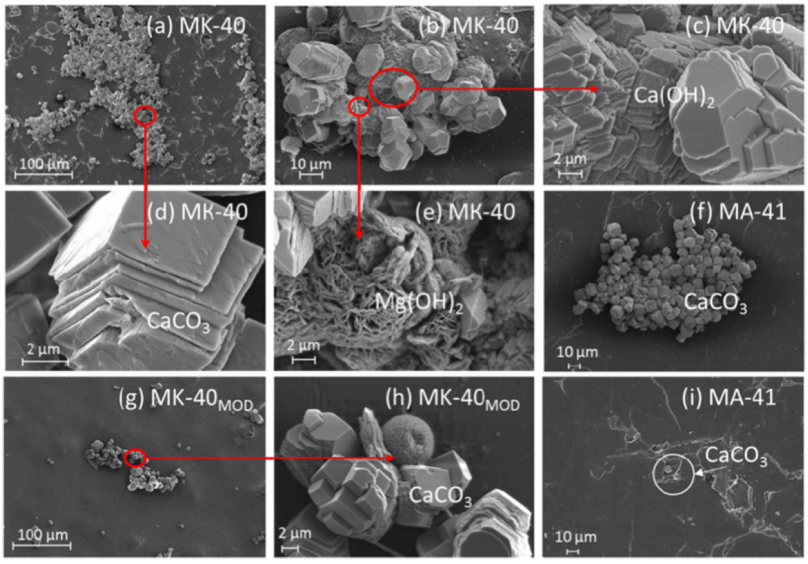

Figure 18. SEM images of deposits of $CaCO_3$, $Ca(OH)_2$, and $Mg(OH)_2$ on the surfaces of three IEMs (MK-40 and MK-40MOD are CEMs; MA-41 is an AEM). Reproduced with permission from ref 604. Copyright 2018 Elsevier.

Although these selective separations have been successfully demonstrated in practice, the basic physical mechanisms of selective ion removal by shock ED are still under investigation. Using the mathematical model of shock ED in ref 583, Tian et al. proposed several possible mechanisms for selective removal of multivalent cations. These mechanisms include greater separation of multivalent cations by the deionization shock wave, their high affinity to the negatively charged surfaces of the porous medium where transport is slow (due to the condition of no slip at solid surfaces), and a strong resistance to their emergence in the fresh product due to streaming potentials.[599] The last two of these mechanisms are shown schematically in Figure 16b. Tian et al. also used this model to explain the selective removal of Mg^{2+} relative to Na^+ observed in refs 109 and 587. A recent publication adapted this model to simulate and interpret selective removal of Pb^{2+} in the presence of excess competing Na^+ (see Figure 17c).[584] Figure 16d shows representative simulation results of concentration profiles and ion fluxes for both Pb^{2+} and Na^+. Indeed, the greater flux of Pb^{2+} relative to Na^+ out of the feed and into the cathode stream (see Figure 16b) underpins the selective removal of Pb^{2+} by shock ED.

3.6. Fouling in Electrokinetic Systems

Fouling is the accumulation of unwanted material (known as foulant), such as mineral scale, organic compounds, colloids, and biomass, on solid surfaces. In electrokinetic systems, fouling typically occurs on the surfaces of membranes[418] and porous media (e.g., ion exchange resin),[600,601] which diminishes performance and increases electrical resistance. If left uncontrolled, fouling may introduce additional problems, such as increased pressure drop, flow blockages and instabilities, material fatigue, and premature system failure. In this section, we discuss how fouling occurs in electrokinetic systems as well as common methods used to prevent and control it.

Mineral scale is deposited on membrane surfaces (or within the membrane itself) when ions such as Ca^{2+}, Mg^{2+}, HCO_3^-, and SO_4^{2-} precipitate (or sometimes crystallize) from solution as solid salts.[418,602] Figure 18 shows scanning electron microscopy (SEM) images of deposits of substrates on both CEM and AEM surfaces, particularly on the faces in contact with the concentrate.[603,604] In the concentrate compartments of ED and EDI cells, the concentration of an ion can approach or even exceed its saturation point, which leads to precipitation of the ion. Turek et al. developed a model to predict the formation of mineral scale by computing the saturation level of divalent cations in the concentrate compartment of an ED cell.[605] Precipitation of minerals also depends on the pH and temperature of the electrolyte.[418,604,606,607] For example, a basic electrolyte is concentrated in OH^-, which reacts with Ca^{2+} and Mg^{2+} as follows:[418]

$$Mg^{2+}(aq) + 2OH^-(aq) \rightleftharpoons Mg(OH)_2(s) \quad (6a)$$

$$Ca^{2+}(aq) + 2OH^-(aq) \rightleftharpoons Ca(OH)_2(s) \quad (6b)$$

As shown in Figure 19, these reactions may occur via several pathways, many of which begin with the dissociation of water into H^+ and OH^- in the boundary layers of the diluate compartment.[369,608] (see ref 609 for a more detailed explanation of the reaction pathways in Figure 19). Cifuentes-Araya et al. demonstrated that scaling of the CEM can be reduced by using a modified cell configuration and pulsed electric fields to control water dissociation.[609−611]

Colloids, which are nondissolved suspended solids (e.g., silt granules, clay minerals, colloidal silica, metal nanoparticles, organic colloids), represent another common source of membrane fouling.[418] The key property of colloids that makes them potential foulants is their charged surfaces, which can lead to electrostatic interactions with oppositely charged IEMs.[612−614] For example, Lee et al.[612] and Mondor et al.[614] reported that colloidal silica deposits irreversibly on the surfaces of AEMs and forms so-called "cake" layers that cannot be removed by chemical cleaning.[615] Similar to colloids, organic compounds (e.g., humic substances, proteins, carbohydrates, organic acids) exhibit electrostatic interactions with the fixed charge of an IEM that can cause organic fouling.[616−620] Unlike colloidal fouling, however, organic fouling may also occur via hydrophobic interactions between the foulant and membrane.[418,621−623]

https://doi.org/10.1021/acs.chemrev.1c00396
Chem. Rev. 2022, 122, 13547−13635

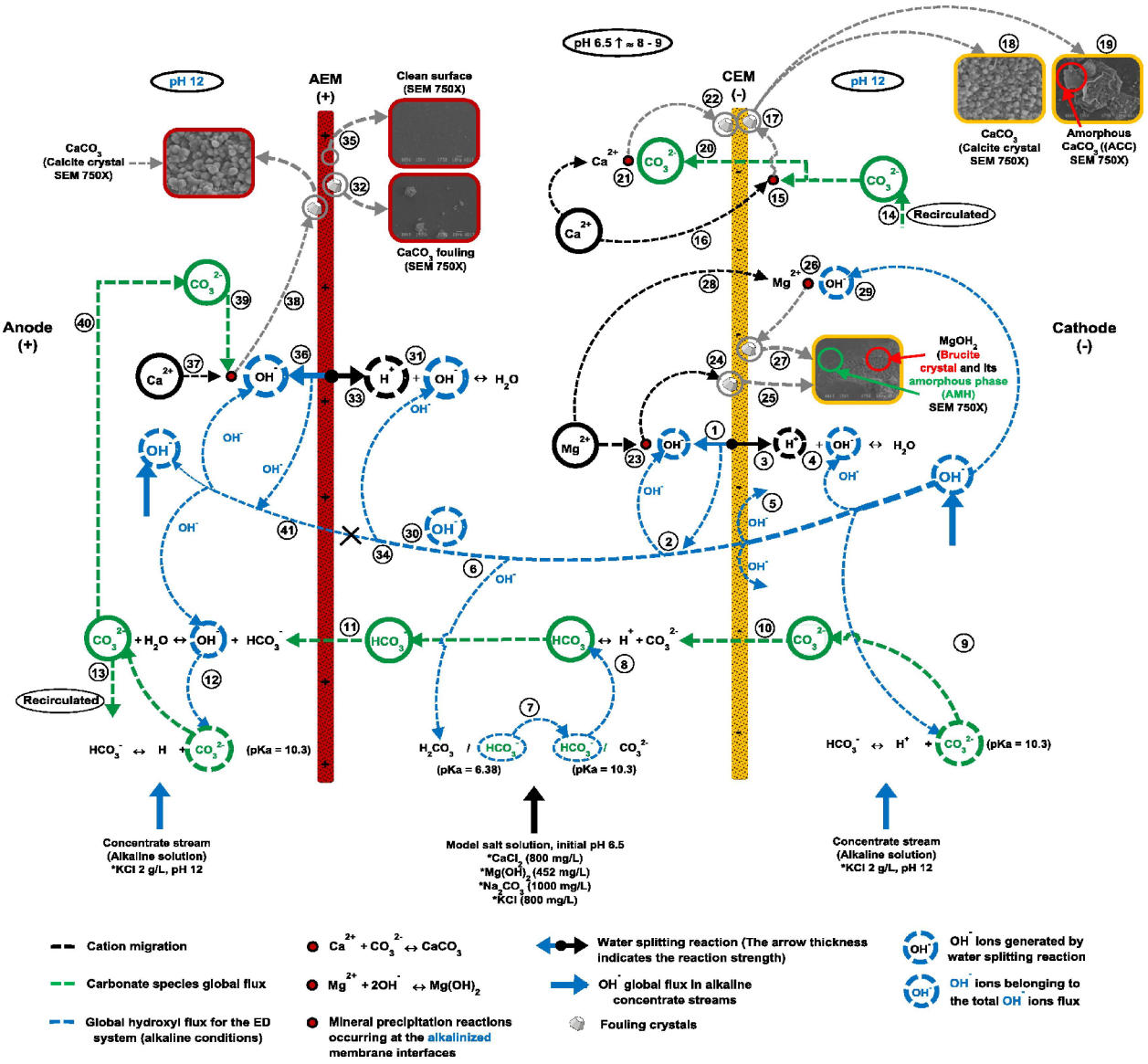

Figure 19. Pathways of mineral scaling on CEMs and AEMs in ED, many of which are initiated by water dissociation in the boundary layers of the diluate compartment. Reproduced with permission from ref 609. Copyright 2014 Elsevier.

Although chemical and mechanical procedures can be used to remove foulants from membrane surfaces,[619] cleaning protocols increase operating costs and user intervention. Frequent cleaning may also damage the membrane and shorten its lifetime. Several strategies have thus been developed to reduce the amount of cleaning and maintenance required, the earliest of which was to periodically reverse the electrical polarity in ED (electrodialysis reversal) and EDI (electrodeionization reversal) systems.[419,459,624−626] Membranes with intrinsic antifouling properties have also been explored as a means to reduce cleaning requirements.[420−423,627] Engineering membranes that are resistant to fouling requires careful design of chemical composition, surface hydrophobicity and roughness, and the surface charge of functional groups.[418] For instance, increasing the hydrophilicity of IEMs by modifying their surfaces with sulfonyl groups reduces the formation of mineral scale.[628] Similarly, the introduction of polyelectrolyte layers inhibits organic fouling by electrostatic repulsion.[629] Other methods to make membranes hydrophilic involve the use of additives such as inorganic particles,[420,421,628,630] some of which could even be placed inside the membrane to modify its entire matrix. Membrane surfaces can also be made homogeneous to improve their resistance to fouling. For example, heterogeneous IEMs exhibit a dramatic reduction in scale deposition after being coated with a homogeneous layer of (hydrophobic) Nafion.[604] The improved resistance to scaling was attributed to enhanced electroconvective mixing, suppressed water dissociation, and decreased crystal growth at the membrane surfaces.[604,631]

4. ELECTROSORPTIVE SEPARATIONS

Electrosorption refers to the adsorption of dissolved species from a solvent onto the surfaces or into the bulk of a charged electrode and is driven by an applied voltage. The ability to cyclically trap and release ions without the need for chemical additives or swings in temperature and pressure is a major advantage of this process. The performance of devices that employ electrosorption depends on both effective transport of species to the electrode and adequate storage capacity by the electrode. When subjected to an electric potential, the surface

https://doi.org/10.1021/acs.chemrev.1c00396
Chem. Rev. 2022, 122, 13547−13635

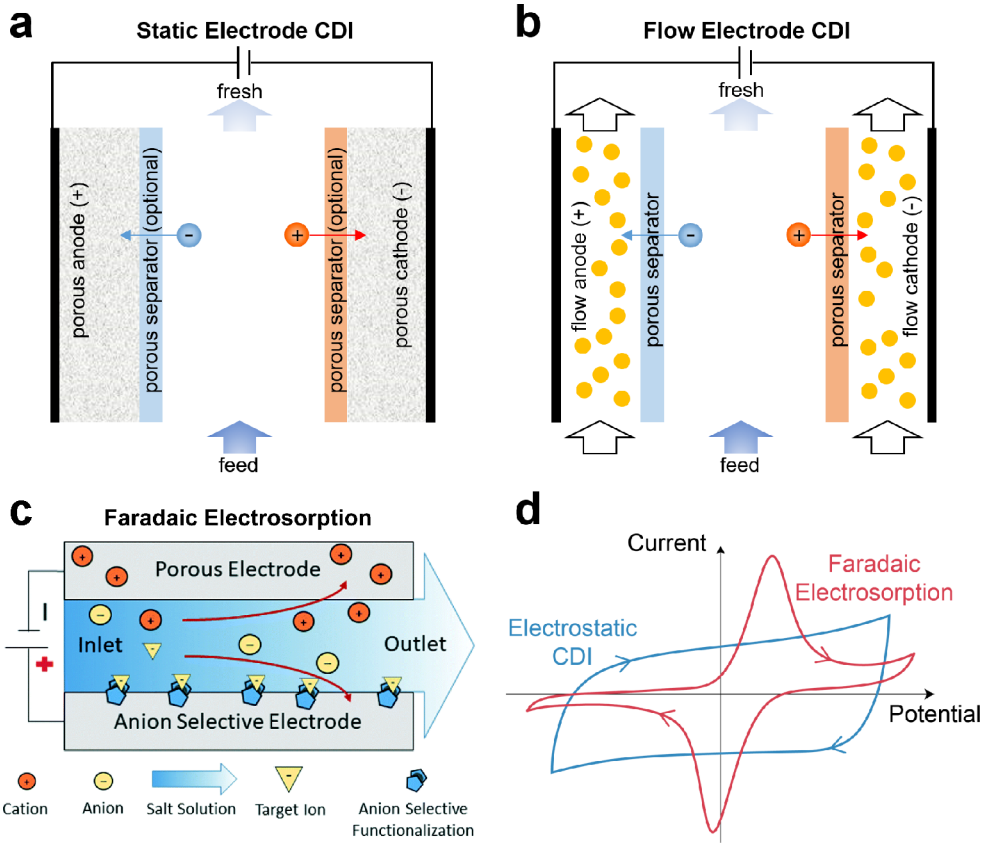

Figure 20. Schematics of various electrosorption processes. (a) Static electrode CDI has electrodes that are rigid solids, such as porous carbon and intercalation materials, whereas (b) flow electrode CDI has electrodes that are made of a suspension (or slurry) of carbon beads in an electrolyte. When oriented vertically, FCDI is often referred to as fluidized bed CDI, in which the flow of suspended carbon is impeded by gravity to establish a densely packed fluidized bed. (c) Faradaic electrosorption comprises redox-active electrodes that can selectively remove target ions. Reproduced with permission from ref 649. Copyright 2020 Royal Society of Chemistry. (d) Typical cyclic voltammograms for electrostatic electrosorption, where double-layer charging is associated with relatively constant capacitance over a wide range of potentials, versus Faradaic electrosorption (or electrochemical adsorption), where redox reactions that transfer electrons between certain ions and the electrode yield peaks in the voltammogram at specific potentials.

of an electrode becomes polarized, and the mechanism by which electrosorption occurs depends on both the identity of the dissolved species and the electrode properties. For instance, ions in an electrolyte can be electrosorbed within the EDL that forms on a polarized surface, and they can be released by either attenuating or reversing the applied electric field. This mechanism is the basis of CDI with porous carbon electrodes, as shown in Figure 20a.[632] A number of emerging applications use CDI for water purification, including desalination of brackish water and selective electrosorption of target ions.[115,150,633−635] While electrosorption is generally limited to removal of charged species, porous carbons have the well-known ability to adsorb organic compounds, which can enable simultaneous removal of salt and uncharged organic contaminants by CDI.[636] Many novel designs and cell architectures have been invented and characterized, such as membrane CDI (MCDI, see Figure 33)[70,637−640] and flow electrode CDI (FCDI, Figure 20b).[641−645] MCDI can improve cell cycle life and energy efficiency, and FCDI enables continuous desalination using a single CDI cell. Moreover, the structure of CDI cells can be categorized as either flow-between (FB) or flow-through electrode (FTE), depending on the direction of the feed. In FB cells, the feed flows between the two porous electrodes, while in FTE cells, the feed flows directly through the electrodes..[646−648]

Selective ion electrosorption is an emerging and promising application of electrosorption technologies.[154,635,645] Compared to other methods such as RO and ED, standard CDI is membraneless and its active elements are the electrodes. These properties enable unique functionalities and mechanisms of selectivity not accessible to membrane-based systems. For example, the selectivity of inexpensive and widely available activated porous carbon electrodes in CDI can be tuned by various parameters such as electrode voltage, chemical charge, pore size, and cell charging time.[650−654] Through design and selection of functional materials, technologies for selective electrosorption are now well developed and can be used to separate both charged and neutral species from water.

Faradaic electrosorption, in particular, relies on the transfer of electrons to a distinct redox-active species bound to the electrode, which changes the oxidation state of that electrode and enables tunable binding of ions based on chemical affinity.[96,655,656] Systems for Faradaic electrosorption include crystalline intercalation materials, which operate on the same principles as lithium-ion batteries for charge storage, and redox-active polymers, which selectively interact with species through single-site binding. By changing the molecular structure of the functional material, the mechanism of binding can be adapted to a specific class of ions. In this section, we describe the general principles of electrosorption in CDI and

https://doi.org/10.1021/acs.chemrev.1c00396
Chem. Rev. 2022, 122, 13547−13635

provide a review of porous carbon, intercalation, and emerging redox-active electrodes for desalination and selective separations.

4.1. Capacitive Deionization With Porous Carbon Electrodes

4.1.1. Electrostatic Electrosorption in Electric Double Layers. The origins of CDI and electrosorption can be traced back to the work of Helmholtz, who in 1853 developed the first EDL theory to describe a monolayer of counterions at the surface of an electrode in terms of a mechanism of charge storage similar to a capacitor.[501] In the early 1900s, Gouy revised this theory by claiming the electrolyte in the EDL to be mostly diffuse and by allowing both co-ions and counterions to spread over a large distance.[502] Chapman further improved the model by deriving the EDL differential capacitance for a symmetric binary electrolyte,[503] and Stern introduced a series capacitance to account for surface solvation.[504] The Gouy−Chapman−Stern (GCS) theory emerging from these developments has become the most widely used model to understand EDLs, and it is relevant for many electrosorption systems, especially in the dilute limit. The theory of electrocapillarity and EDLs was extensively discussed by Grahame in 1947,[657] and there have since been several publications addressing the application of this theory to electrosorption and molecular separations.[150,658,659]

CDI models were first proposed by Johnson and Newman in 1971 based on an equivalent circuit for charging of EDLs in porous electrodes, and the models included an empirical factor for salt removal efficiency.[660] The first self-consistent microscopic theory for EDL charging and salt removal, however, was not developed until the work of Bazant, Thornton, and Ajdari in 2004.[661] This theory was motivated by the modeling of induced-charge electrokinetic phenomena,[120,535] where large applied voltages at blocking porous electrodes, including voltage steps[661] and alternating voltages,[662] lead to nonlinear double-layer responses such as transient salt depletion and space charge formation. From this work, the first mathematical model for CDI with porous carbon electrodes, which bridged EDL theory with applications in water purification and desalination, was developed in 2010 by Biesheuvel and Bazant[663] and validated by direct numerical simulations with corrections for surface conduction.[664] Further extensions of the theory by Biesheuvel et al. include the addition of multicomponent asymmetric electrolytes, a generalized Frumkin−Butler−Volmer (FBV) model for parasitic Faradaic side reactions, a modified Donnan model for strongly overlapped EDLs, and a model for attractive ion image forces in metallic micropores.[665−668]

Storage of ions in EDLs for the purpose of water purification was first proposed and demonstrated in 1960. In the decades that followed, this area of research advanced slowly, although interest has grown quickly since 2010 with breakthroughs in theoretical modeling, experimental methods, material performance, and surface modifications.[115,154,635,669] The most widely used materials for ion electrosorption are microporous carbons due to their broad commercial availability, electrochemical stability, and high electrical conductivity.[115] Prominent examples of microporous carbons include activated carbon, carbon aerogels, graphene, and CNTs.[632] Early theoretical frameworks of electrosorption in these materials are rooted in EDL models for planar surfaces (e.g., Helmholtz, GCS).[661,663,670] One of the main theoretical advances in the past decade was to treat the EDLs in carbon micropores as EDLs in an IEM because geometric confinement in both cases leads to EDL overlapping. Current theories also assume a uniform potential in the liquid phase of a micropore as well as a Donnan potential drop between a micropore and its adjacent macropore. With these innovations, numerous modified Donnan-type models have been proposed and validated.[667,671−673] One benefit of such EDL models is their simplicity, which facilitates their integration into an electrode or cell-level transport theory.[674]

4.1.2. Ion Selectivity. Ions constitute a major subset of contaminants found in water. When present even at low concentration, ions like F^-, CrO_4^{2-}, AsO_4^{3-}, Hg^{2+}, and Pb^{2+} can pose a threat to the health of humans and animals.[675−677] For this reason, researchers have studied and developed platforms for targeted removal of ionic contaminants using CDI.[678−690] Selective adsorption by CDI can also be employed to recover valuable elements, such as lithium,[691−699] phosphorus,[700−705] and nitrogen.[704,706−713] In this section, we briefly review several experimental works that focus on selective separation of ions from multicomponent solutions using porous carbon electrodes. In particular, we focus on studies that involve either two monovalent ions or one monovalent and one divalent ion, and we exclude studies that involve mixtures of more than two competing ions because of the complexity of these systems.[714−723] We then discuss the quantification of ion selectivity via a separation factor. Next, we consider the use of composite and functionalized electrodes for enhancement of ion selectivity. Lastly, we present the foundations of selectivity modeling at equilibrium. Several studies focus on theories that capture selectivity based on charge, size, or affinity, which are not reviewed in detail here.[652,654,667]

Early work by Avraham et al. reported the possibility of selective removal of ions by tuning the pore size of microporous carbons.[724] In this work, the electrodes were modified by chemical vapor deposition (CVD) using toluene as a precursor. This treatment influenced the outer surface of the micropores and reduced their size, so only small enough ions could access the pores. Results of this study demonstrated facile storage of the smaller, monovalent cation (Na^+) with reduced storage of larger, divalent cations (Ca^{2+} and Mg^{2+}). A follow-up study by Noked et al. also used this CVD approach for selective removal of NO_3^- from a mixture of NO_3^- and Cl^-.[725] NO_3^- and Cl^- are hydrated anions of similar size, but the openings of the pores were controlled for NO_3^- to preferentially enter by virtue of stereoselectivity. That is, the size and structure of unhydrated NO_3^- was what determined the capacity for electrosorption. Cerón et al. tuned the pore size of hierarchical carbon aerogel monolith electrodes by adjusting the activation time to toggle selectivity toward either Na^+ or Ca^{2+}.[726] In this study, Ca^{2+} was nearly completely excluded from the small pores of the electrode. In the large pores, however, MD simulations suggested that Ca^{2+} selectivity is limited at high applied potential due to the competition between volume exclusion and electrostatic forces as well as the more favorable desolvation of Na^+. Zhang et al. studied cation selectivity via pore sieving, charge, and desolvation effects, and they also examined time-dependent ion swapping.[653] Han et al. further explored the impact of ion size and pore characteristics on selectivity.[727] Eliad et al. showed that the capacity of an EDL can be independent of ion size when the pores are much larger than the ions, which effectively disables ion sieving.[728]

https://doi.org/10.1021/acs.chemrev.1c00396
Chem. Rev. 2022, 122, 13547−13635

In addition to ion sieving, other widely employed strategies to selectively separate contaminants leverage the influence of ion charge and size on the EDL structure in micropores. Gabelich et al., for example, studied two different electrodes of aerogel carbon with relatively large nominal pore sizes (approximately 4 and 9 nm) and showed that charge had the greatest effect on electrosorption capacity.[729] They also found that smaller, monovalent ions showed improved storage relative to larger, divalent ions. These results prompted additional research, for example by Hou et al., who combined grand canonical Monte Carlo (GCMC) simulations with experiments using electrodes made of carbon aerogel.[730] When two ions of the same charge but different sizes were present in solution (e.g., K^+ and Li^+), the smaller ions favorably screened the surface charge while occupying a smaller volume in the liquid phase. This result was also predicted by using the closed-form Boublik−Mansoori−Carnahan−Starling−Leland (BMCSL) equation of state to model hydrated ions in the micropore EDLs as hard spheres,[652] building on earlier work using either local-density approximations for ion crowding in thin EDLs[535] or the Carnahan−Starling equation for overlapping EDLs[667] and consistent with later experimental observations.[686,693,731]

Ion separations in CDI are complicated, however, and cannot be fully explained by molecular or continuum models of equilibrium EDLs, especially in the presence of multivalent ions. For example, when a monovalent ion competes with a divalent ion (e.g., K^+ and Ca^{2+}), the GCMC simulations of Hou et al. predicted preferential electrosorption of the divalent ion (Ca^{2+}), but this result was not observed experimentally. This observation was later attributed to ion-specific electrosorption dynamics by Zhao et al.,[651] who developed a general theory of time-dependent ion-selectivity in CDI, based on the interplay of voltage-dependent adsorption capacities in the EDL and ion-specific transport resistances in the electrolyte. The theory was validated by experiments involving mixtures of Na^+ and Ca^{2+}, which also confirmed the prediction that selectivity toward Ca^{2+} would become high only after several hours of charging in their system.[651] To design more selective CDI electrodes for concentrated mixtures of multivalent ions, it may be important to extend these models to account for electrostatic correlations and hydration forces.[732] These effects can be incorporated using either local approximations based on the Bazant−Storey−Kornyshev (BSK) equation[537,538,541,542] or nonlocal weighted density approximations[733] based on fundamental measure theory[734] and charged-shell electrolyte models.[735]

Separations of anions using CDI have also been studied. Tang et al. observed moderate selectivity of Cl^- relative to F^- under constant voltage charging,[686] a result later observed and validated theoretically under constant current charging.[736] Selective removal of NO_3^- is a particularly common topic. Chen et al. studied a mixture of Cl^- and NO_3^- and showed that Cl^- is preferentially electrosorbed at early times, whereas Cl^- is displaced by NO_3^- in the EDLs at later times.[737] The time dependence of selectivity observed by Chen et al. was not observed for a mixture of SO_4^{2-} and Cl^-, from which neither anion was preferentially removed despite the difference in charge.[737] In contrast, Li et al. later observed dynamic replacement of Cl^- by both NO_3^- and SO_4^{2-} in separate experiments, and they suggested that selectivity and capacity are in fact determined by the hydration ratio, namely the ratio of the hydrated radius to the ionic radius.[738] This work reported that monovalent ions with lower hydration ratios exhibit greater electrosorption relative to other monovalent ions and that divalent ions are preferentially stored over monovalent ions at equilibrium, which supports the results of Zhao et al.[651] Nonetheless, there appear to be multiple mechanisms at play for the selective separation of NO_3^- from Cl^-. In addition to the work by Chen et al. and Li et al.,[737,738] Oyarzun et al. modeled the intrinsic selectivity of electrodes treated with cetyltrimethylammonium bromide (CTAB) toward NO_3^- using surface group−ion equilibrium constants, and they obtained an observable NO_3^- selectivity factor of 6.5 relative to Cl^-.[654] Using MD simulations, Hawks et al. examined NO_3^- selectivity in slit-shaped, subnanometer pores with approximately the same size as the hydrated diameters of NO_3^- and Cl^-. This study attributed the high selectivity to the slit-like shape and low hydration energy of NO_3^-, which allows its hydration shell to be removed more readily than those of Cl^- and SO_4^{2-}.[719] Mubita et al. found that the high selectivity of NO_3^- relative to Cl^- was maintained even when the pore size exceeded that of the hydrated ion.[739]

Selectivity between competing ions can be quantified by a separation factor, defined as the ratio of the molar electrosorption of ion i (Γ_i) to that of ion j (Γ_j) scaled by the respective feed concentrations, c_{i_0} and c_{j_0}:[652]

$$\beta_{i:j} = \frac{\Gamma_i / c_{i_0}}{\Gamma_j / c_{j_0}} \tag{7}$$

If $\beta_{i:j} > 1$, ion i is preferentially removed relative to ion j. We note that eq 7, as it is written, does not hold for batch mode operation because the feed concentrations vary during charging and discharging. Considering the hydrated radii of the ions studied by Nightingale,[740] Figure 21 shows that $\beta_{i:j}$ for competing monovalent ions, with ion i being the smaller of the two, is typically between one and five. One exception is for NO_3^-, which is larger than both Cl^- and Br^- but is selectively electrosorbed relative to these monatomic anions. For competing divalent (i) and monovalent (j) ions, $\beta_{i:j}$ is time dependent and can range from below 1 to more than 10.[651] Occasionally, selectivity is reported using a relation similar to the scaled retention selectivity introduced in section 3.5.2 for shock ED (see eq 5). The two definitions are related by rewriting the separation factor as $\beta_{i:j} = \frac{(1 - c_i / c_{i_0})}{(1 - c_j / c_{j_0})}$ provided the system is operated in a single pass; here, c_i and c_j are the concentrations in the desalinated product (see ref 741 for details on sample collection). Unlike in shock ED, selectivity in (membraneless) CDI arises due to the storage of ions in electrode pores. It is therefore preferable in CDI to use eq 7 because it explicitly accounts for ion electrosorption and also because effluent concentrations can vary in time even if pore concentrations reach steady state.

In addition to examining the mechanisms of selective electrosorption, researchers have sought to increase electrode capacity toward a specific ion by using composite carbon electrodes embedded with materials like polymers and metal oxides.[681,683,750] Kim et al. demonstrated this concept by coating the surface of a carbon anode with anion exchange resin that is selective toward NO_3^-, which more than doubled the separation of NO_3^- to Cl^- compared to the commercial AEM Neosepta.[683] By applying constant current to the device, the same group demonstrated even greater separation using the IEMs and composite electrodes reported by Kim and Choi.[681]

https://doi.org/10.1021/acs.chemrev.1c00396
Chem. Rev. 2022, 122, 13547−13635

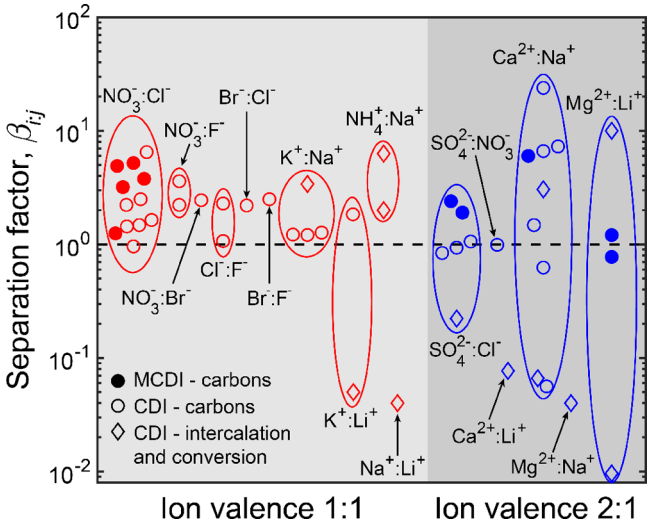

Figure 21. Separation factor $\beta_{i:j}$ calculated using eq 7 in MCDI, CDI with porous carbons, and CDI with intercalation or conversion electrodes for pairs of competing anions and cations. $\beta_{i:j} > 1$ implies selectivity toward ion i, $\beta_{i:j} < 1$ implies selectivity toward ion j, and $\beta_{i:j} = 1$ (dashed line) corresponds to no selectivity. Competing monovalent ions (ion valence 1:1) typically display $\beta_{i:j}$ between 1 and 10. Competing divalent and monovalent ions (ion valence 2:1) display a wider range of $\beta_{i:j}$, typically between 0.01 and 24. References for valence 1:1 ion pairs in alphabetical order: $Br^-:Cl^-$,[738] $Br^-:F^-$,[738] $Cl^-:F^-$,[686,738] $K^+:Li^+$,[691,693] $K^+:Na^+$,[715,731,738,742] $Na^+:Li^+$,[691] $NH_4^+:Na^+$,[743] $NO_3^-:Br^-$,[738] $NO_3^-:Cl^-$ (MCDI,[681,683] CDI[654,712,737,738]), and $NO_3^-:F^-$.[712,738] References for valence 2:1 ion pairs: $Ca^{2+}:Li^+$,[691] $Ca^{2+}:Na^+$ (MCDI,[744] CDI,[650,651,715,726] intercalation or conversion[745,746]) $Mg^{2+}:Li^+$,[691,692,747] $Mg^{2+}:Na^+$,[745] $SO_4^{2-}:Cl^-$,[737,748,749] and $SO_4^{2-}:NO_3^-$.[712]

Similarly, Tang et al. showed slight preferential removal of SO_4^{2-} by using an MCDI system operated at constant current.[751] It is important to distinguish composite electrodes, where materials are affixed directly to carbon, from MCDI, where free-standing membranes are layered onto the electrodes. MCDI can be used for selective removal of ions, as shown in Figure 21, but because ion selectivity in MCDI is primarily determined by the membranes rather than by the electrodes, we do not discuss this method further in this section. Besides using composites to tune selectivity, researchers have explored chemical treatments to functionalize electrode micropores for enhanced selectivity. Guyes et al. oxidized the negative electrode to add carboxylic groups to enhance ion selectivity based on size, which increased the selectivity factor of K^+ relative to Li^+ from approximately 1 to 1.84.[693] In a later study, Guyes et al. used a cell with a sulfonated cathode to increase the selective removal of Na^+ relative to Ca^{2+} at early charging times and high charging voltages.[650] Uwayid et al. then published the first demonstration of perfect Ca^{2+} selectivity relative to Na^+ in a CDI cell using a sulfonated cathode with long charging times and nonzero discharging voltages (i.e., only Ca^{2+} was removed during charging).[752]

The effects of ion size, chemical charge, and affinity can be mathematically modeled using continuum theories. Here, we briefly review the principles of modified Donnan (mD) EDL theory to describe some aspects of selectivity in porous carbon electrodes with micropores larger than the hydrated ions present in solution. In this framework, we spatially average over micropore volume to neglect the local pore structure and simplify the governing equations. We do not cover CDI models based on transport equations, which are needed to describe time-dependent electrosorption and selectivity.[650,753] An alternative yet related framework to the mD model, termed the amphoteric Donnan (amph-D) model, considers the electrodes to comprise separate regions of positive and negative surface charge.[754]

The mD model employs the Donnan approximation of spatially constant micropore potential and assumes equilibrium between the macropores and micropores, which results in a Boltzmann distribution for concentration:

$$c_{i,k}^{\mathrm{mi}} = c_{i,k}^{\mathrm{mA}} \exp(-z_i \Delta\phi_{\mathrm{D},k} - \Delta\mu_{i,k}^{\mathrm{ex}}) \tag{8}$$

The terms $c_{i,k}^{\mathrm{mi}}$ and $c_{i,k}^{\mathrm{mA}}$ are the micropore and macropore concentrations, respectively, of ion i in electrode k = A (anode) or C (cathode), $\Delta\phi_{\mathrm{D},k}$ is the dimensionless difference in potential between the micropores and macropores, $\Delta\mu_{i,k}^{\mathrm{ex}}$ is the dimensionless difference in excess chemical potential between the micropores and macropores, and z_i is valence; all potentials are scaled by the thermal voltage (see section 3.1.1). For single-pass operation and at cell equilibrium, it is usually assumed that the macropore concentration equals the feed concentration: $c_{i,k}^{\mathrm{mA}} = c_{i_0}$. The term $\Delta\mu_{i,k}^{\mathrm{ex}} = \mu_{i,k}^{\mathrm{ex,mi}} - \mu_{i,k}^{\mathrm{ex,mA}}$ accounts for nonideal effects, such as an affinity between the electrode surface and specific ions,[755] image forces acting on ions,[667] and hard-sphere interactions between ions.[652,693]

According to eq 8, higher background (macropore) concentration of a particular ion increases its micropore concentration. In the case of two competing ions with equal valence and excess potential, the ion with higher background concentration will be stored in larger quantities. In a charged cell, $\Delta\phi_{\mathrm{D,C}}$ is negative and so cations are stored in the cathode, while $\Delta\phi_{\mathrm{D,A}}$ is positive and so anions are stored in the anode. Because the Donnan potential is multiplied by valence, multivalent ($|z_i| > 1$) counterions are preferentially stored relative to monovalent ($|z_i| = 1$) counterions. As captured by the term $\Delta\mu_{i,k}^{\mathrm{ex}}$, a larger excess potential reduces ion concentration in micropores. Considering effects of volume exclusion due to finite ion size, a small ion has a lower excess potential and is thus preferentially stored relative to a larger ion with equal valence.[652] The value of $\Delta\mu_{i,k}^{\mathrm{ex}}$ is also affected by electrode properties such as the chemical charge of surface groups, which can be tuned to improve selectivity toward target ions.[693] Moreover, it was recently demonstrated that volume exclusion may enhance selective removal of larger ions with higher valence due to the complex interplay between electrostatic forces and volume-exclusion effects.[752]

4.1.3. Energy Consumption. Energy consumption by CDI has been extensively studied over the past five years.[90,639,756−764] Recently, Hawks et al. proposed metrics and methodologies to compare energy consumption between different CDI systems and other desalination technologies.[741] They suggested that a target separation should be implemented across all systems being compared by specifying feed concentration, c_0, concentration reduction, Δc, and water recovery, γ. The systems can then be compared in terms of volumetric energy consumption (in units of W h m^{-3} of treated water) versus productivity, $\mathcal{P}$, defined as the throughput of fresh water scaled by the projected cross-sectional area of the electrode and multiplied by the number of cells (see eq 24).[741] A related metric to quantify energy demand was used by Lin,[765] namely the specific energy consumption, SEC, scaled by either the amount of adsorbed salt[762,764]

https://doi.org/10.1021/acs.chemrev.1c00396
Chem. Rev. 2022, 122, 13547−13635

$$SEC_{ion} = \frac{E_{ch}}{M_{salt} Q t_{ch} \Delta c} \quad (9)$$

or the volume of produced water[741,765]

$$SEC_{w} = \frac{E_{ch}}{Q t_{ch}} \quad (10)$$

where E_{ch} is energy consumption during charging, M_{salt} is the molecular weight of the salt, Q is volumetric flow rate, and t_{ch} is charging time. Another common metric in the literature is energy normalized adsorbed salt (ENAS),[90,709,741] which equals SEC_{ion}^{-1}. To ensure repeatable results, energy consumption should be determined from the CDI cycle after the cell has reached a dynamic steady state.[90] Dynamic steady state is usually reached after 3−5 cycles, after which the system exhibits steady behavior and the amount of salt adsorbed during charging equals the amount released during discharging.

In CDI, energy can be recovered from the discharging step to reduce the total energy consumption.[759] Energy recovery is often quantified as the ratio of energy recovered during discharging to energy consumed during charging.[766−770] Early studies of energy recovery used either only the consumer unit, a CDI cell,[769] or only the storage unit, a buck-boost converter,[766−768] and reported recovery ratios of up to 83%. Kang et al. later examined a system comprising both a CDI cell and a buck-boost converter, which achieved recovery ratios of up to 50% and that decreased with lower feed concentrations and faster desalination rates.[770] Oyarzun et al. emphasized the importance of utilization efficiency, defined as the recovery efficiency over a full cycle, including charging and discharging of the DC−DC converter used for energy storage.[771] The nature of the power source used to drive the CDI cell is also an important consideration. As demonstrated by Tan et al.,[772−774] photovoltaics are an adequate power source due to the low applied voltage required for CDI cell charging (<1.2 V), which makes CDI a candidate for off-grid desalination.

The energy efficiency of CDI systems is normally reported as a thermodynamic efficiency, η_{thermo} (see eq 21),[90,150,760,764,765] defined as the ratio of the theoretical minimum energy needed to achieve a target separation (see eq 19) to the energy consumed in practice. For comparisons of η_{thermo} to be meaningful, the systems being compared should have the same productivity and realized ion separation.[764,775] Porada et al. presented an MCDI cell with an efficiency of 16.04% at a productivity of 11.8 L h^{-1} m^{-2} and current density of 18.5 mA m^{-2}.[639] Hemmatifar et al. analyzed a membraneless cell designed to achieve high efficiency with total recovery of the energy released during discharging.[90] This system achieved an efficiency of 8.89% at a productivity of 3 L h^{-1} m^{-2} and current density of 4 mA m^{-2}; increasing productivity to 6 L h^{-1} m^{-2} and current density to 8 mA m^{-2} lowered the efficiency to 6.81%. Ramachandran et al. reported a cell with an efficiency of 8% when operated at constant current and 5% when operated at constant voltage, assuming total energy recovery.[763] A comprehensive review of CDI efficiencies was presented recently,[764,765] and it reported values of up to approximately 6%.[753,776]

Three efficiency indicators have been proposed to study mechanisms of charge and energy loss: Coulombic efficiency, charge efficiency,[90,741,777−779] and flow efficiency.[639,660,761,763] Coulombic efficiency quantifies the ratio of charge released during discharging to charge delivered to the cell during charging. Values below one are due to parasitic Faradaic reactions that can occur during charging,[780] such as oxygen reduction at the cathode and carbon oxidation at the anode (see eq 11). Parasitic reactions, which can degrade salt storage capacity in the electrodes, are more likely to occur when operating at higher charging voltages and for longer times.[758,759,781−784] Charge efficiency is defined as the ratio of moles of salt removed from the feed to moles of electrons transferred between the electrodes during discharging,[778,785,786] and typical charge efficiencies in CDI systems are in the range of 60−90%.[115,787] Many strategies have been explored to improve charge efficiency, such as using high discharge voltages (with 0.3 V as a minimum value),[759,788] chemically functionalizing electrodes,[787] or layering IEMs over the electrodes, as in MCDI.[70,789] Flow efficiency is defined as moles of salt removed from the feed divided by moles of salt adsorbed by the electrodes,[763] and it captures unwanted effects like direct mixing of diluate and concentrate when switching between charging and discharging. Hawks et al. demonstrated that flow efficiency can be improved by adding a high throughput flush step between charging and discharging.[761]

In addition to energy losses caused by electrons participating in side reactions, there are also resistive losses caused by electronic and ionic resistances.[756,757,764,790] Electronic losses arise mainly from resistances of the external circuit components, contact resistance between current collectors and electrodes, and resistances in the solid phase of the electrodes.[760,764] Electronic losses can be reduced by improving contact between the current collectors and electrodes,[764] which can be achieved by surface treatments of the current collectors and electrodes[760] or by using conductive epoxies.[756] Electronic losses are expected to be greater when the cell is operated at constant voltage, as current can be high at early times.[90,758,759] Ionic losses occur mainly due to the resistance of the electrolyte in the separator and electrode. Common methods to lower these losses are to reduce spacer thickness or increase spacer porosity.[760] Although operating at constant current is often considered more energy efficient than operating at constant voltage,[758,791] Dykstra et al. showed that the reverse can be true when operating at certain conditions.[759]

Qin et al. recently analyzed brackish water desalination by RO and by CDI, and they concluded that RO is much more energy efficient, with no expected change in the future.[792,793] However, several serious issues with this analysis were later identified, including unrealistic values of electrical resistance, unphysical trends in energy consumption, and inaccurate predictions of performance.[794] Porada et al. also highlighted that the comparison by Qin et al. was done using inconsistent definitions of salt rejection.[639] While the common definition given by $R_j = 1 - c_D/c_0$ (where c_D is diluate concentration) was used for CDI, salt rejection in RO was defined as $R_j = 1 - c_D/c_B$ (where c_B is brine concentration).[792] Porada et al. thus repeated the analysis with consistent definitions of salt rejection and demonstrated that CDI can indeed be competitive with RO for brackish water desalination, especially when water recovery is high.[639]

Many applications in desalination and water purification demand high water recovery to reduce the volume of waste generated.[639,639,760,763,764,792] It was recently shown that water recovery in CDI could be significantly improved, with only a small increase in energy consumption, by decreasing the discharging flow rate.[763,795] For example, Ramachandran et al. found that setting the discharging flow rate to 10% of the charging flow rate was most suitable in their study,[763] and Tan

https://doi.org/10.1021/acs.chemrev.1c00396
Chem. Rev. 2022, 122, 13547−13635

et al. used a stopped flow discharge process.[795] Water recovery can also be improved by adjusting the operating parameters, which include charging and discharging times as well as charging and discharging voltages (or currents).[759] Another method to increase water recovery is by flowing the brine product through the cell as a washing solution during discharging.[796]

4.1.4. Flow Electrode Capacitive Deionization. Research and commercialization efforts in CDI have grown significantly over the past 10 years, and much of this growth has been catalyzed by the invention of new architectures and designs for CDI systems.[115,797,798] In 2011, Duduta et al.[799] introduced semisolid lithium-ion flow batteries with flowable intercalation electrodes, a concept that has since been applied to other rechargeable batteries[800−,802] as well as CDI. In 2013, Jeon et al. introduced flow electrodes for CDI, which were a suspension of carbon particles that are transported along with the flowing electrolyte, as shown in Figure 20a.[641] FCDI offers two major improvements to CDI with static electrodes, namely the ability to operate the system continuously rather than cyclically and an increased capacity for salt storage.[115] Transforming CDI into a continuous process requires discharge of the carbon particles (and formation of the brine) downstream, either in a mixing tank or in a second device.[644,803−810] FCDI has also demonstrated the possibility of desalinating feeds that are more concentrated than what is processed by static electrode CDI.[641,811]

FCDI is sometimes used to concentrate inorganic nutrients and organic molecules for later recovery.[702,703,812−815] Bian et al. introduced FCDI as an alternative to a complex and costly nutrient removal system for the extraction and up-concentration of inorganic nutrients, such as NH_4^+, NO_3^-, and PO_4^{3-}, from wastewater.[812] Although the system achieved a high recovery of NH_4^+ (89−99%), NO_3^- (83−99%), and PO_4^{3-} (49−91%), it required post-treatment to further separate inorganic nutrients from desalinated salts (e.g., NaCl). Several modifications of FCDI then enabled the recovery of inorganic nutrients, especially phosphorus. For instance, PO_4^{3-} was selectively recovered as H_3PO_4 by leveraging inevitable side reactions like the generation of H^+ by water splitting.[813] In this study, operating the system between 1.5 and 2.1 V resulted in the dissociation of water, while both PO_4^{3-} and Cl^- were adsorbed by the positively charged carbon particles. As a result, both H_3PO_4 and H^+ were produced at the same electrode. During regeneration, the electrode released most of the adsorbed Cl^- back into the original chamber, whereas neutral H_3PO_4 remained in the electrolyte (with a selectivity factor of >2 relative to Cl^-) to produce a solution rich in phosphorus.[813] Moreover, Zhang et al. recovered PO_4^{3-} with magnetic carbon particles (impregnated with Fe_3O_4) that showed strong affinity toward phosphorus.[703] This study proposed a two-step process for the recovery of highly purified PO_4^{3-} by concentrating the ion using FCDI and crystallizing it into vivianite (a hydrated iron phosphate mineral) using a fluidized bed crystallization column. The applications of FCDI have expanded to include recovery of carboxylates, such as acetate and oxalate, downstream of advanced oxidation processes.[814]

In contrast to solid carbon electrodes which have electrical conductivities in excess of 1000 mS cm^{-1}, flow electrodes have electrical conductivities mostly below 10 mS cm^{-1} because a suspension of carbon particles can form a largely discontinuous network for electron transport.[669,816] The electrical conductivity of flow electrodes is a function of the amount of suspended carbon, typically quantified by the weight fraction of carbon in the electrode (i.e., the dry weight of carbon particles divided by the total weight of the electrode). Increasing the fraction of carbon boosts electrical conductivity, although slurries used as flow electrodes become viscous and difficult to pump when the fraction of carbon exceeds about 20 wt %.[669] On the other hand, low electrical conductivity adversely impacts performance, particularly in the extreme case that the slurry does not percolate electric charge. In this limit, carbon particles through much of the network cannot be charged and do not store salt, and the mechanism of desalination reverts to that of an ED system driven by a steady Faradaic current.[642,817] This functionality is sometimes mistaken for capacitive storage of salt in carbon particles, which has led to spurious reports of unusually high salt adsorption capacities of flow electrodes.[817,818]

To overcome the limitations of weakly conductive flow electrodes, researchers have proposed new platforms that increase the loading of suspended carbon. These platforms include fluidized bed electrodes, a combination of these electrodes and slurry particles, conductive chemical additives, and redox electron mediators.[644,816,819−823] Fluidized bed electrodes are distinct from slurries used as flow electrodes because the former uses large ($\sim$100 μm), porous beads made of carbon that are pumped with the electrolyte vertically upward. The weight of the beads causes them to travel more slowly than the surrounding fluid, which leads to a densely packed electrode where the fraction of carbon can reach over 30 wt %.[644] Although these fluidized beds can be dense, the electrical conductivity often remains less than 1 mS cm^{-1}.[816] One way to further increase the loading of carbon beads is to enrich the bed with a slurry of smaller particles, which feel a negligible force due to gravity. Cohen et al. showed that although this slurry itself could have a conductivity greater than 1 mS cm^{-1}, the conductivity of the combined system would only just reach 1 mS cm^{-1}.[816] This result suggests that a more detailed understanding is needed of the relationship between the properties of carbon particles and the conductivity of the electrolyte. Ma et al. found that by adding redox-active quinone to a flow electrode with carbon particles of 100 μm loaded at 1 wt %, the rate of salt removal can be increased in potentiostatic mode.[819] Similarly, other researchers have attempted to increase the conductivity of flow electrodes by introducing conductive additives such as multiwalled CNTs and carbon black.[820,821] Recently, Halfon and Suss demonstrated a system that comprised metal particles under two operating modes: the first was a static mode in which conductivity exceeded 10 000 mS cm^{-1}, and the second was a flow mode in which the particles were discharged.[824] In the future, this concept may be adapted to FCDI by replacing the metal particles with carbon.

The latest advances in the field of FCDI have focused on scaling up, discovering innovative alternate applications, and better understanding the overall process. Today, FCDI is scaled up by either fabricating a stack with multiple unit cells or using three-dimensional honeycomb cells with multiple channels that are interconnected by porous carbon supports.[825−828] At the same time, researchers have adapted FCDI for capacitive neutralization desalination, double displacement reactions,[829] ion separations,[707,710,830−835] and resource recovery.[702,703] To better understand the process, theoretical models have been proposed,[807,836,837] and the governing

https://doi.org/10.1021/acs.chemrev.1c00396
Chem. Rev. 2022, 122, 13547−13635

transport mechanisms have been studied.[838] Overall, FCDI has the potential to be used for water purification, but for this field to reach its potential, the community must develop ways to either improve or compensate for the low electrical conductivity of flow electrodes.

4.1.5. Parasitic Faradaic Reactions. Faradaic side reactions in an electrochemical system are often (but not always) undesirable and can limit the performance and stability of the process.[655,839] The two reactions that are believed to have the greatest impact on the performance of CDI are carbon oxidation at the positive electrode and oxygen reduction at the negative electrode:[782,783]

$$\text{carbon oxidation: } C(H) + 2H_2O \rightarrow COO^-(H^+) + 4H^+ + 4e^-$$

$$\text{oxygen reduction: } O_2 + 2H^+ + 2e^- \rightarrow H_2O_2 \quad (11)$$

Managing the oxidative step in the corrosion of carbon plays a key role in the long term stability of a CDI device, as the electrodes are repeatedly charged and discharged. While this reaction can lower Coulombic efficiency, reduce the conductivity of the electrode, and distort its microporous structure, the most severe effect is likely the production of carboxyl surface groups (COO^-).[655,781,785] As the concentration of these surface groups increases in the micropores of the positive electrode, so does the concentration of co-ions to compensate for the increased negative charge.[787] The result is that a larger fraction of the applied current is consumed during charging to expel co-ions from the positive electrode, which lowers charge efficiency. This phenomenon was observed in the form of "inversion peaks" in the effluent concentration profile during charging after several cycles.[781,787] In addition, X-ray photoelectron spectroscopy revealed that, after cycling, the positive electrode was oxidized to the point that its surface was highly oxygenated,[781] and measurements of pH indicated asymmetric electrosorption as well as irreversible consumption of charge.[782] Although salt removal significantly decreases due to corrosion of the positive electrode,[840] charge storage capacitance often remains largely unaffected.[841] For a cell with an oxidized cathode, it was found that the anode was relatively stable during cycling, but the cathode degraded due to loss of its negative chemical charge.[693,784] Uwayid et al. recently compared the lifetimes of oxidized cathodes and sulfonated cathodes, and they found that the sulfonic acid groups led to a more stable cell.[842]

When no measures are taken to mitigate this corrosion, a CDI cell is often limited to 50 cycles before the capacity for salt adsorption exhibits a significant loss,[782,784,843] where FTE CDI cells are reported to degrade faster than FB cells.[643,844] Known strategies to mitigate corrosion include periodically reversing cell polarity to slow the oxidation of carbon,[781,845] optimizing the voltage window to reduce electrode degradation,[846,847] reducing the concentration of dissolved oxygen (DO) by sparging with gaseous nitrogen,[781] decorating the electrodes with titania to enhance electrochemical reduction and prevent DO from participating in corrosion reactions,[843] treating the surfaces of the positive electrode to make it negatively charged (inverted CDI),[845,848,849] and reducing the charging time to inhibit Faradaic reactions.[650,784] Other proposed methods include recovering the electrodes by thermal treatment[841] and adding an AEM between the main channel and the positive electrode to both reduce corrosion and extend cycle life.[115,638,850] While the positive electrode may still corrode, its capacitance can be preserved, as the AEM is the active element in this desalination.

By measuring the concentration of DO in the product, researchers discovered that oxygen is reduced at the negative electrode during charging, while the concentration of DO recovers during discharging.[782,783] It was proposed that DO reduction at the cathode contributes to corrosion of the anode carbon because it causes asymmetry in the electric potential[781] and produces hydrogen peroxide (see eq 11),[643,783,851] which accelerates oxidation of the positive electrode.[843] The reduction of oxygen, which dominates when the applied voltage is less than approximately 1 V, can severely diminish Coulombic efficiency under certain conditions.[782] The main approach to suppress this parasitic reaction is to dilute the DO by displacing it with gaseous nitrogen.[781] As with corrosion of carbon, the rate at which oxygen is reduced is lowered in MCDI systems[638] because the membranes impede transport of DO inside the device.

Besides the two reactions in eq 11, several other parasitic reactions may occur, although they usually have a minor impact on the performance of the cell.[655,689] One such reaction is electrolysis of water, which produces gaseous oxygen at the positive electrode and gaseous hydrogen at the negative electrode. The fact that this reaction is sluggish on carbon electrodes, however, reduces its impact on desalination by CDI. Moreover, electrolysis of water can be prevented by operating the system at or below the standard potential of water electrolysis (1.23 V). Recent studies of Faradaic side reactions in CDI with carbon electrodes have enabled researchers to limit the destructive effects of these reactions.[784,844,846] While the use of IEMs can reduce the impact of side reactions and increase cycle life, future work in this area should focus on delivering stable electrodes without the need for potentially costly membranes.

4.1.6. Fouling in Capacitive Deionization with Porous Carbon Electrodes. CDI devices with porous carbon electrodes are susceptible to fouling, which may either occur on electrode surfaces or block electrode pores. In MCDI devices, fouling can also occur on membrane surfaces or inside the membrane structure. Here, we discuss common types of fouling and their mechanisms in CDI; we limit the discussion to fouling of electrodes, as membrane fouling was explained in section 3.6. Fouling of electrodes by organic matter has received the most attention to date, and researchers generally report that salt capacity is reduced in the presence of organic matter.[561,729,852−858] Zhang et al. showed that the level of dissolved organic matter can determine the extent of fouling. In particular, treatment of lake water with low levels of organic matter led to little fouling and only a 13% loss in capacity over 2 weeks, whereas treatment of lake water with high levels of organic matter led to a 75% loss in capacity in the same amount of time.[853] Organic fouling also increases energy consumption due to adsorption of organic species that block active sites on the electrodes and inhibit fluid flow.[853,858] For example, Chen et al. found deposits of alginate gel and humic acid in the bulk electrode structure, and these deposits were more noticeable in the presence of Na^+ and Ca^{2+}.[858] The same authors observed similar deposits on the surfaces of IEMs in MCDI, although the alginate gels formed in the presence of Ca^{2+} were denser than those formed in the presence of Na^+. Organic foulants can also be adsorbed within carbon pores, although this adsorption may not significantly impact performance. Liu et al. found that while humic acid was adsorbed in

https://doi.org/10.1021/acs.chemrev.1c00396
Chem. Rev. 2022, 122, 13547−13635

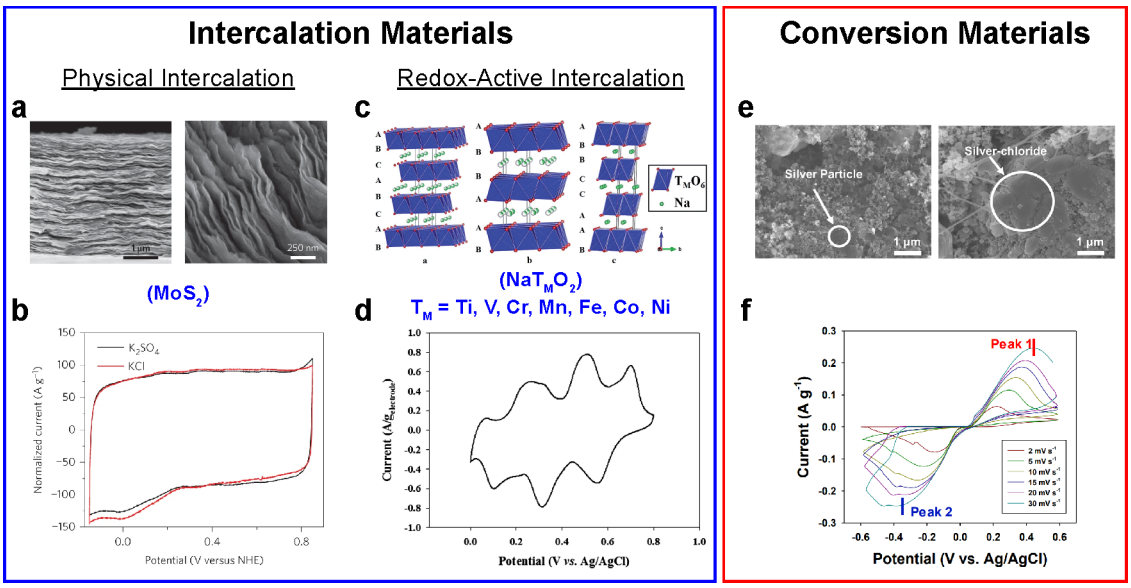

Figure 22. Representative intercalation and conversion electrodes used for electrochemical separations. Structural image and cyclic voltammetry of (a,b) MoS_2, (c,d) NMO, and (e,f) Ag/AgCl. (a,b) Reproduced with permission from ref 872. Copyright 2015 Springer Nature. (c) Reproduced with permission from ref 879. Copyright 2015 Royal Society of Chemistry. (d) Reproduced with permission from ref 850. Copyright 2014 Royal Society of Chemistry. (e,f) Reproduced with permission from ref 880. Copyright 2020 Elsevier.

both microporous and mesoporous activated carbons, salt capacity decreased by only 5% over 30 cycles.[855]

Mineral scale can form on the electrodes in CDI when ions such as Ca^{2+}, Mg^{2+}, HCO_3^-, and SO_4^{2-} are present in solution. Several studies found that scaling by Ca^{2+} and Mg^{2+} is minor,[852,853] although Mossad et al. observed that Fe^{3+}, even at concentrations as low as 2 mg L^{-1}, formed deposits which reduced salt removal by 7.4% and flow rate by 13% over 30 hours.[852] Moreover, Pb^{2+} and Cu^{2+} poorly desorb during cell discharging, which indicates that these species can remain bound to the electrode.[859]

A number of techniques have been studied to control fouling and prolong device lifetime, several of which are similar to the methods discussed in section 3.6. Pretreatment involves removing foulants and scalants upstream of CDI using chemical additives and antiscaling compounds. Often, these compounds are added directly to the feed, although in some cases they may interfere with the electrosorption process. Special electrodes (e.g., TiO_2−RGO nanocomposites[860]) can also be designed to have intrinsic antifouling properties. Finally, cleaning solutions such as citric acid, NaOH, and HCl are used to regularly remove deposits and restore performance. A more detailed review of methods to control fouling in CDI can be found in ref 861.

4.2. Capacitive Deionization With Intercalation and Conversion Electrodes

4.2.1. Faradaic Electrosorption Involving Electron Transfer Reactions. CDI cells have historically relied on porous carbon electrodes[110] because carbons are inexpensive, widely available, and capable of reversible positive and negative polarization across a wide range of potentials.[862−865] Despite these advantages, however, carbon electrodes have several limitations. First, the extent to which a porous carbon can store salt (expressed as the mass of stored material per unit mass of material available for storage, often in mg g^{-1}) is limited and rarely exceeds 20 mg g^{-1} for a typical salt like NaCl. Second, carbon electrodes must be charged to a relatively high voltage of 0.8−1.2 V for the amount of salt stored per unit charge to be meaningful. Third, the anode is unstable when exposed to water with a high concentration of DO, as discussed in section 4.1.5.[844,866] Researchers have thus sought to develop novel materials that can address the shortcomings of porous carbons.[867,868]

One class of intercalation materials traps ions between the closely spaced layers of the electrode mainly by electrostatic forces, although these materials often exhibit redox reactions as well. Examples of such materials include the inorganic compounds MXene[128,869−871] and MoS_2 (shown in Figure 22a,b),[872−875] both of which can be used as a cathode and, to a lesser extent, as an anode in CDI cells. Intercalation in these materials is largely driven by the electrostatic attraction between the ions and electrode, with only limited influence of redox reactions, as signified by wide "box-like" cyclic voltammograms such as the one shown in Figure 22b. MXenes have so far demonstrated electrosorption capacities of NaCl of up to 45 mg g^{-1} and charge efficiencies greater than 90%,[869,870] but degradation caused by oxidation and hydrolysis is a limiting factor.[876] Furthermore, these materials are susceptible to deformation (e.g., swelling) during operation because intercalation and ion exchange can alter the interlayer spacing,[877] as also observed in porous carbons adsorbing larger ions from room-temperature ionic liquids.[878] In MoS_2, salt capacity and charge efficiency have been shown to increase with increasing salt concentration in the feed, a trend opposite to what is observed in porous carbons.[873]

A second class of cells that do not use porous carbons involve asymmetric combinations of an electrostatic insertion cathode with a Faradaic conversion anode, such as Ag/AgCl,[881,882] Bi/BiOCl,[883] or MnO_2.[884,885] In this design, an important feature is that the metallic phase donates or accepts electrons in a redox reaction where ions are adsorbed from the liquid phase. The most familiar example of this process is the oxidation of Ag with Cl^-, which produces the solid salt AgCl on the surface of the electrode until the Ag is fully converted. As shown in Figure 22e,f, the reversible electron transfer

https://doi.org/10.1021/acs.chemrev.1c00396
Chem. Rev. 2022, 122, 13547−13635

reaction is associated with rate-dependent, symmetrically shifted peaks in the cyclic voltammograms, which are the most familiar waveforms observed in voltammetry.[886] Another such reaction is that of Bi with Cl^- to form BiOCl according to the chemical equation,[883]

$$Bi + Cl^- + H_2O \rightleftharpoons BiOCl + 2H^+ + 3e^- \quad (12)$$

and Bi-based electrodes enable high storage of Cl^- (~80 mg g^{-1}).[883] MnO_2 is also used as an anode because of its stability, high capacity for storage, and inhibition of parasitic side reactions,[884] and the redox reaction in which MnO_2 participates is analogous to that observed for Prussian Blue analogues (PBAs, discussed in more detail below).[887] Similarly, RuO_2 and TiO_2 increase electrosorption capacity when deposited onto a porous carbon electrode.[888,889] Overall, these inorganic materials are functional and selective, although they are limited in that only the primary atom in the host structure is reactive and that reactions of this kind can influence chemical structure.

Another class of intercalation materials is based on redox-active solid insertion electrodes, which enable ion storage throughout the (typically crystalline) solid bulk of the material.[867,890,891] In this section, redox-active crystalline solids are distinguished from redox-active polymers, which are discussed as a separate class of materials for Faradaic electrosorption in section 4.3. The reactions that enable ion storage in solid insertion electrodes typically require less than 1 V.[718,850,887,892] Moreover, a high diffusivity of ions within the crystal structure is desirable to facilitate ion insertion into the electrode, which increases the capacity of adsorption and reduces energy consumption.[88] High rates can also be achieved using nanoparticles with small diffusion lengths, as in most intercalation batteries.[358,893,894] The enhanced salt capacity in redox electrodes was described theoretically by He et al., who generalized the EDL theory used for capacitive CDI electrodes to include redox-active groups.[895]

So far, three major classes of redox-active materials have been explored for use in CDI, namely $Na_2Mn_5O_{10}$ (NMO, shown in Figure 22c,d),[850,879,896] metal phosphates,[892,897] and PBAs.[99,887,898] PBAs are analogues of Prussian Blue in which a fraction of the iron is replaced by another metal like nickel or copper, and they are widely investigated because of their potential longevity, high specific capacity, and facile intercalation of cations, particularly K^+.[718,742,899−903] Other materials have also been introduced in recent years, including V_2O_5,[904] TiS_2,[905] and sodium superionic conductors (NASICON), the last of which includes NMO. When subjected to an applied voltage, cations are selectively and reversibly inserted into the negatively charged crystal structure of these materials, whereas anions are electrostatically rejected. As the electrodes are charged more negatively (at increasingly positive cathodic potentials), the redox-active atoms are reduced further and more cations are drawn into the pores, which leads to desalination of the water surrounding the electrodes.[88] In practice, these materials are often combined with anodes such as Ag/AgCl and carbon to selectively adsorb the anions.[881,882,906,907]

Hybrid CDI (HCDI), first introduced by Lee et al.,[850] demonstrates this idea by pairing a redox-active electrode with a porous carbon anode.[697,884,888,903,908] Smith and Dmello discovered that redox-active materials can even be used as anodes as long as the two electrodes are separated by an IEM.[127] In the case of electrodes that selectively capture cations (e.g., NMO, metal phosphates, PBAs), the membrane must be an AEM, which functions as the anion selective surface in the device.[116,127,742] The AEM in this symmetric design partitions the feed into two channels in a way that resembles ED, except the electric field is still cyclic. This mode of operation was mathematically modeled by Singh et al.[88]

Recent advances in electrosorption with intercalation materials have provided opportunities for combined theoretical and experimental studies,[86,96,127,634,895] which build on earlier models of ion intercalation in porous electrodes of lithium-ion batteries.[358,780,893,894] Redox-active systems have an electric charge that depends on the applied potential, and this variable charge yields storage capacity and ionic selectivity.[105,909] In 2017, Smith used nickel hexacyanoferrate (NiHCF) and NMO electrodes in an ED cell and developed the first model to account for two-dimensional ion transport in ED with intercalation electrodes.[116] In 2018, He et al. proposed the first model to account for the thermodynamics of electrosorption based on variable chemical charge at electrodes whose surfaces were decorated with redox-active species.[895] This same framework was adapted to generate an equivalent circuit model to predict and validate the electroanalytical performance of intercalation materials.[910] He et al. further expanded the theory of electrosorption by redox-active materials by developing equivalent circuit models and a model based on coupled diffusion, convection, and electromigration with surface reaction kinetics.[910,911] Singh et al. also presented a theory for CDI with porous electrodes comprising nanoparticles made of a redox-active intercalation material, and the authors described the dynamics of this system in terms of concentration of the product, distribution of intercalated ions, cell potential, and energy consumption.[88] These models, however, neglect variations in ion concentration inside the particles and assume fast reactions with quasi-equilibrium adsorption isotherms. Inspired by recent progress in modeling intercalation batteries with multiphase layered materials,[780,893,894,912,913] it would be interesting to further consider the effects of coupled ion−electron transfer reactions, mechanical deformations, and phase transformations resulting from Faradaic electrosorption in porous electrodes.

Considering the many recent advances in intercalation materials, models, and cell designs summarized here, it is naturally useful to compare their desalination performances to those of traditional porous carbons. In a comparison of nine electrode materials, Pothanamkandathil et al. found that energy demands for NiHCF were lower than those of carbon materials when desalinating a 20 mM feed of NaCl without energy recovery; they were comparable, however, when assuming complete energy recovery.[914] Metzger et al. analyzed CDI with only intercalation electrodes and found that this CDI module costs approximately 27% of a typical MCDI module and is nearly four times smaller in volume due to the larger capacity of intercalation electrodes.[915] Liu et al. showed, however, that intercalation electrodes are more susceptible to declines in performance from organic fouling.[855]

4.2.2. The Role of Electron Transfer in Ion Intercalation. It is a common misconception that ion intercalation in solid host materials is a physical electroadsorption process, whenever the ion does not itself participate in redox reactions. Indeed, lithium-ion batteries derive their name from the fact that Li^+ is inserted reversibly in each electrode without being reduced to metallic lithium, effectively shuttling back and forth during battery cycling like a "rocking chair." This picture,

https://doi.org/10.1021/acs.chemrev.1c00396
Chem. Rev. 2022, 122, 13547−13635

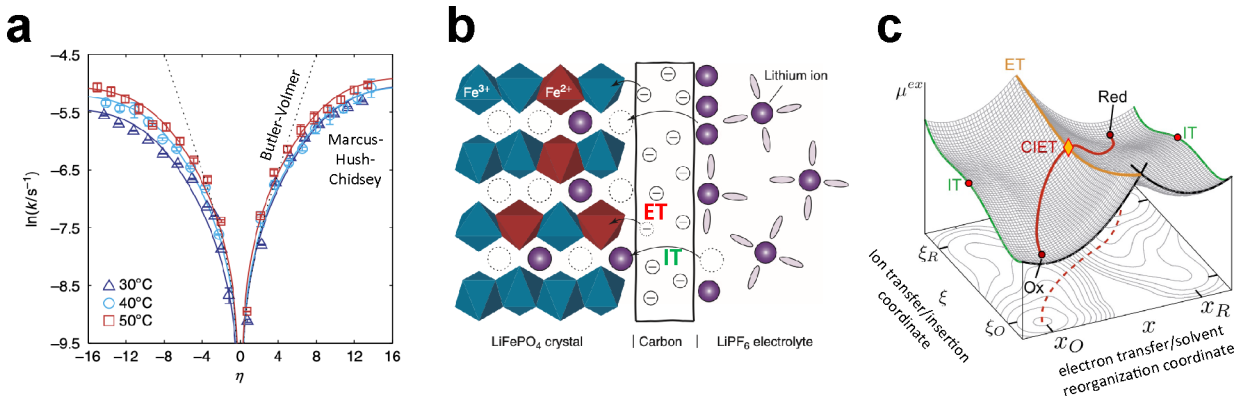

Figure 23. CIET mechanism for ion intercalation in redox-active solid electrodes. (a) Curved Tafel plots consistent with Marcus–Hush–Chidsey theory, indicating electron transfer limitation in $LiFePO_4$. (b) Sketch of lithium ion transfer (IT) coupled to electron transfer (ET) from the carbon coating to the nearest iron redox site. (c) Excess chemical potential landscape for CIET, combining the classical ion transfer coordinate with the solvent reorganization coordinate for quantum mechanical electron transfer. (a,b) Adapted with permission from ref 916. Copyright 2014 Nature Research. (c) Adapted with permission from ref 921. Copyright 2021 Elsevier.

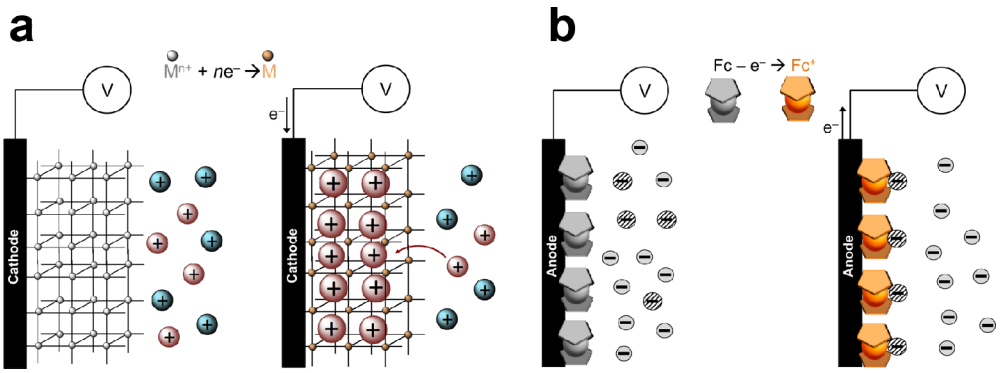

Figure 24. Overview of methods for water purification involving intercalation and conversion processes by (a) crystalline redox materials and (b) polymeric, single-site redox materials. Adapted with permission from ref 634. Copyright 2016 Wiley-VCH.

reminiscent of physical adsorption, might appear to be inconsistent with peaked voltammograms for lithium-ion battery materials, which clearly signify redox reactions, similar to those shown in Figure 22d for intercalation electrodes used in electrochemical separations.

In the context of lithium-ion batteries, the resolution of this paradox began with the discovery of Bai and Bazant in 2014 that ion intercalation can be limited by solid–solid electron transfer reactions that reduce and oxidize nearby transition metal ions in the host crystal.[916] The authors constructed Tafel plots (logarithm of current versus overpotential) for the high-rate cathode material Li_xFePO_4 in quantitative agreement with those predicted by the quantum mechanical Marcus theory of electron transfer,[780,917,918] specifically the Marcus–Hush–Chidsey formula for electron transfer from a metallic electrode (Figure 23a),[919,920] and they postulated a rate-limiting step of electron transfer from the carbon coating to the iron redox site, $Fe^{2+} \rightleftharpoons Fe^{3+} + e^-$ (Figure 23b). They also showed that the temperature-independent curvature of the Tafel plot (Figure 23a) is controlled by the reorganization energy, λ, of the local "solvent" (dielectric solid environment), which is well approximated by the Marcus estimate for outer-sphere electron transfer:

$$\lambda_o = \frac{e^2}{8\pi\varepsilon_0 k_B T}\left(\frac{1}{a_0} - \frac{1}{2d}\right)\left(\frac{1}{\varepsilon_{op}} - \frac{1}{\varepsilon_s}\right) \quad (13)$$

based on the optical and static dielectric constants of the solid, ε_{op} and ε_s, respectively, as well as the effective radius of the reactant a_0 and the distance for electron transfer d, each set to the Fe–O bond distance assuming direct contact of $FePO_4$ octahedra with a metallic (and sufficiently thick) carbon coating.

The emerging understanding is that both mechanisms occur simultaneously, as ion intercalation in redox-active solids occurs by coupled ion–electron transfer (CIET).[921] In this new picture, classical transfer of an ion over the intercalation energy barrier (dominated by the ion–electron Coulomb energy and the local dielectric response of the interface) facilitates the instantaneous quantum mechanical transfer of an electron tunneling between a localized state in the host crystal and a delocalized state in the electrode (Figure 23c). CIET theory is becoming widely used in modeling lithium-ion batteries,[894] and it could also be used to guide the design of Faradaic electrosorption systems from microscopic first principles. In contrast to the empirical Butler–Volmer equation, CIET theory predicts a reaction limited current, which can be modified by tuning the electrostatic and dielectric properties of the electrode–electrolyte interface and the electronic structure of the electrode.[921,922] For example, the theory attributes the enhanced intercalation rate in Li_xFePO_4 achieved experimentally by anionic surface charge modification[923] to lowering of the ion-transfer barrier of lithium. CIET theory also reveals the roles of dielectric

https://doi.org/10.1021/acs.chemrev.1c00396
Chem. Rev. 2022, 122, 13547–13635

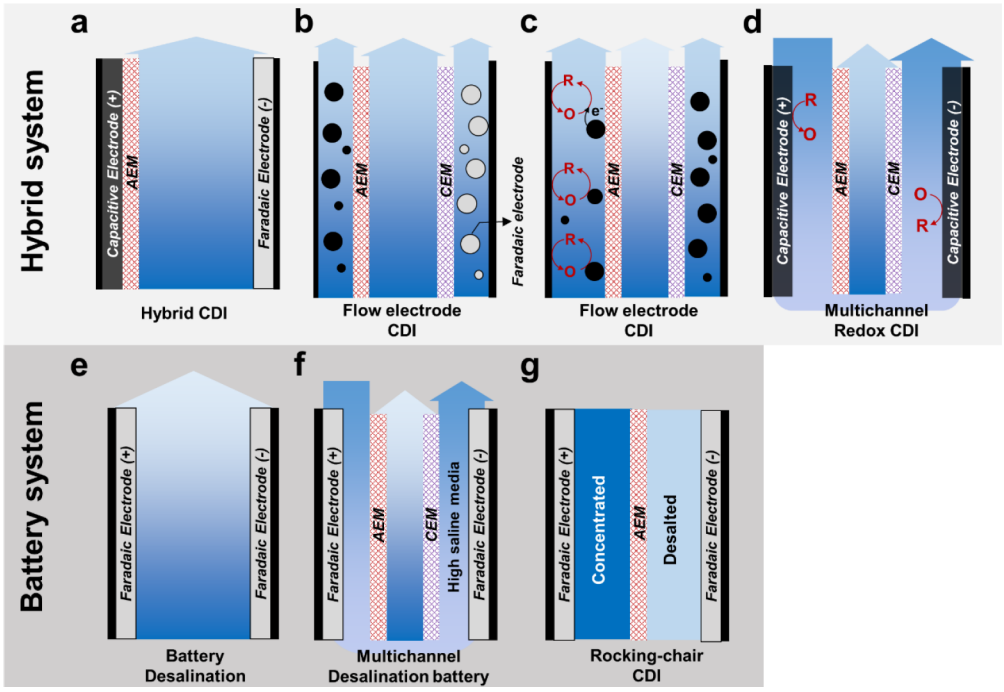

Figure 25. Schematic illustrations of CDI systems that use intercalation and conversion materials as electrodes. Adapted with permission from ref 936. Copyright 2020 Multidisciplinary Digital Publishing Institute.

properties and crystal structure of the intercalation host, including generalizations of eq 13 for the CIET barrier.[921]

4.2.3. Ion Selectivity in Intercalation Materials. Unlike the selectivity in capacitive materials described in section 4.1.2, selectivity in redox-active intercalation materials is achieved by insertion of specific ions into the crystalline structure, as shown in Figure 24a. Cyclic voltammetry of $NaTi_2(PO_4)_3$ and $Na_4Mn_9O_{18}$ indeed showed nearly one order of magnitude greater capacity for Na^+ compared to K^+, Ca^{2+}, and Al^{3+}. It was also concluded that the rate at which ions were removed from a dilute feed was limited by their transport from the bulk to the surfaces of the electrodes as well as by the concentration of noninserting (or electrochemically inert) ions.

In addition to the innovations already described in this section, several research groups developed novel device architectures and designs with the intent of selectively removing specific ions. For example, Pasta et al. created an asymmetric system in which one electrode was made of (redox-active) $Na_2Mn_5O_{10}$ and the other of (metallic) AgCl to desalinate seawater.[714] In contrast to carbon-based electrodes which are slightly selective toward K^+, this system could selectively remove Na^+ with a separation factor of approximately 2.8 relative to K^+. Separation factors of more than ten were also reported for electrodes made of (redox-active) $LiMn_2O_4$ in electrolytes comprising Li^+ as well as the competing cations Na^+, K^+, Ca^{2+}, and Mg^{2+}.[691] Kim et al. reported an even higher separation factor of 16 for Na^+ relative to K^+ in the presence of competing ions such as Ca^{2+} and Mg^{2+} by using (redox-active) $Na_{0.44}MnO_2$ and AgCl electrodes.[934] Among the most extreme separations of Li^+, however, were those achieved by Trócoli et al.,[924] who reported separation factors of 240 relative to Na^+ and 320 relative to K^+ by using (redox-active) $LiFePO_4$ and AgCl electrodes.[925,926] Recent studies that used PBAs for water desalination showed selectivity factors between 2.2 and 3.4 for K^+ relative to Na^+.[718,742,902] Although PBAs are usually selective toward monovalent cations, Singh et al. used the PBA vanadium hexacyanoferrate (VHCF) to preferentially remove Ca^{2+} in the presence of Na^+ with a selectivity factor of 3.5.[903]

Intercalation materials that are selective toward anions have also been examined in conventional CDI systems for the selective removal of PO_4^{3-} and F^-. For instance, Hong et al.[927] recently introduced ZnAl-layered double hydroxide (LDH, commonly used as an adsorbent for PO_4^{3-}) to an electrode material that is itself selective toward PO_4^{3-}.[928,929] LDH was composited with RGO to increase conductivity, and the LDH/RGO composite electrode (with activated carbon as the counter electrode) was used for selective separation of PO_4^{3-}. This composite electrode is selective toward PO_4^{3-} because as RGO boosts the conductivity of the composite electrode, the electron density of the transition metal sites in LDH is effectively reduced. The reduced metal sites then allow PO_4^{3-} to form inner-sphere complexations via an exchange reaction of ligands between the OH^- groups of the transition metal sites and PO_4^{3-}. As a result, the LDH/RGO composite electrode is selective toward PO_4^{3-} (with a selectivity factor of 6.1), even in the presence of Cl^- at 10 times the concentration of PO_4^{3-}.[927] Similarly, hydroxyapatite (HA) was composited with RGO and used to selectively remove F^-:[930] as RGO boosts the conductivity, the RGO/HA composite electrode forms a region concentrated with anions near the electrode, where ion exchange occurs efficiently between OH^- in the HA metal sites and F^-.[930,931] With this composite electrode, the CDI system exhibited five times greater removal of F^- compared to an equivalent system with activated carbon electrodes when both were applied to an equimolar solution of F^-, Cl^-, and NO_3^-.[930]

4.2.4. Electrochemical Systems Design With Redox Reactions. Various cell architectures have been developed to use intercalation and conversion materials more efficiently. For instance, HCDI (shown in Figure 25a) is designed to increase the extent of desalination by using the Faradaic electrode as a working electrode. Because this design slows desalination, a

https://doi.org/10.1021/acs.chemrev.1c00396
Chem. Rev. 2022, 122, 13547−13635

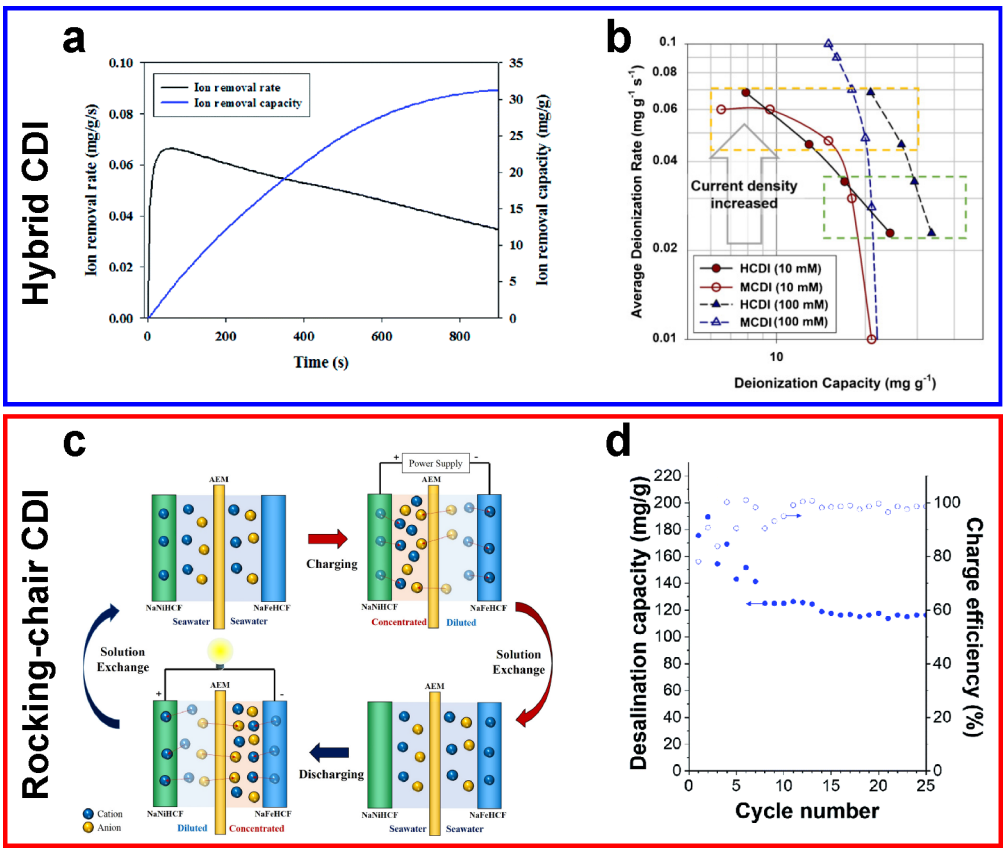

Figure 26. Representative results and mechanisms of CDI with intercalation and conversion electrodes. (a) Ion removal capacity and maximum removal rate in HCDI applied to a 10 mM solution of NaCl; the system is operated at 1.2 V for 15 min during the capture step and at −1.2 V for 15 min during the release step. Reproduced with permission from ref 850. Copyright 2014 Royal Society of Chemistry. (b) Ragone plot of HCDI (with $Na_2FeP_2O_7$) and MCDI for feed concentrations of 10 mM and 100 mM. Reproduced with permission from ref 892. Copyright 2016 Elsevier. (c) Mechanism and (d) performance metrics of RCDI applied to a 600 mM solution of NaCl; the system is operated at a cell voltage of 200 mV. (c) Reproduced with permission from ref 718. Copyright 2017 American Chemical Society. (d) Reproduced with permission from ref 937. Copyright 2019 Royal Society of Chemistry.

capacitive carbon electrode is included to mitigate the reduction in the rate of ion removal.[850,892,932] HCDI systems usually comprise intercalation or conversion materials, such as $Na_4Mn_9O_{18}$[850] and $Na_2FeP_2O_7$,[892] as the negative electrode to selectively capture Na^+, along with porous carbon and an AEM as the positive electrode to capture the anions. $Na_4Mn_9O_{18}$ and $Na_2FeP_2O_7$ could be categorized as one-dimensional insertion materials that store and diffuse cations, especially Na^+, in their tunnel structures.[933,934] Compared to a system with ordinary capacitive electrodes (which had a capacity of 13.5 mg g^{-1} and a maximum removal rate of 0.048 mg g^{-1} s^{-1}), Lee et al. demonstrated major improvements in the capacity (31.2 mg g^{-1}) and maximum removal rate (0.066 mg g^{-1} s^{-1}) by using HCDI with an NMO electrode, as shown in Figure 26a.[850] The HCDI system comprising $Na_2FeP_2O_7$ was also compared to an MCDI system based on capacity and rate capability using a CDI Ragone plot (see Figure 26b).[892] The Ragone plot of the HCDI system showed improvement in the capacity of ion removal by up to 150% relative to the MCDI system, which was attributed to the high capacity of $Na_2FeP_2O_7$. Moreover, the HCDI system achieved a rate capability comparable to that of its MCDI counterpart.[892] The hybrid use of electrodes has also been shown to enhance desalination performance in FCDI systems. As illustrated in Figure 25b, Chang et al. used copper hexacyanoferrate (CuHCF, a PBA) as the flow-negative electrode and activated carbon as the flow-positive electrode.[935] This system exhibited a higher rate of salt removal (up to 0.12 mg cm^{-2} min^{-1}) and a greater efficiency (up to 96%) compared to a system with only activated carbon electrodes.

Recently, several studies introduced dispersed redox species in various multichannel architectures to further improve performance.[819,938−941] By using two IEMs to provide different environmental conditions between the feed and electrolyte, the redox reaction can occur without contaminating the feed.[819,936,938−941] For instance, the use of redox-active species significantly improves charge transfer in FCDI by overcoming some of the limitations of charge transfer between current collectors and particles in the flow electrodes (see Figure 25c; details are provided in section 4.1.4).[819,938] Although many studies have suggested increasing either carbon content or salt concentration to reduce the internal resistance of the electrode channels, the conductivity of these channels could be compromised if the carbon particles were to aggregate.[819,942] Ma et al. thus proposed the use of hydroquinone (H_2Q) as an electron mediator that shuttles electrons from the current collector to the particles in the flow electrodes.[819] As a result, the deionization system exhibited an increase of 131% in the average rate of salt removal compared to the same system in the absence of H_2Q.[819] Kim et al. used redox species as an additional means for salt removal in the multichannel redox system (see Figure 25d).[939] In this system, the redox reaction

https://doi.org/10.1021/acs.chemrev.1c00396
Chem. Rev. 2022, 122, 13547−13635

between $Fe(CN_6)^{3-}$ and $Fe(CN_6)^{4-}$ further remove ions from the feed to maintain bulk electroneutrality in the electrolyte,[936] and the redox species are continuously regenerated as the redox couple circulates the electrodes. Overall, the desalination performance of this system (with a capacity of 67.8 mg g^{-1}) was improved by more than a factor of three compared to the same system in the absence of the redox species (with a capacity of 20.0 mg g^{-1}).[939]

Another active area of research is on the development of various configurations of battery desalination,[714,718,880,883,937,943−946] where both capacitive electrodes are replaced by intercalation or conversion materials. This concept, shown in Figure 25e, was first introduced by Pasta et al., who used NMO to capture Na^+ and Ag to capture Cl^-.[714] Following this study, several intercalation and conversion materials have been used in desalination battery systems to overcome the limited capacity of capacitive electrodes. Electrodes used to capture Na^+ include NMO,[714] $NaTi_2(PO_4)_3$,[883,945] and PBAs,[947] and electrodes used to capture Cl^- include Ag and Bi. Because conversion electrodes have high theoretical specific capacities, they are typically used as counter electrodes.[714,883,945,947−949] Conversion reactions, however, can lead to poor electrode stability due to repeated volume expansion and contraction over many cycles.[950] Despite this drawback, battery desalination systems have been used to recover Li^+ using selective electrodes such as LMO[948] and $LiFePO_4$[949] because of the structural advantages these materials exhibit toward Li^+. For instance, the tetrahedral sites of LMO and $LiNi_{0.5}Mn_{1.5}O_4$ are narrowly spaced and enable selective removal of Li^+ relative to larger cations.[951−953] Although the use of Faradaic materials can significantly increase the capacity of salt removal, they tend to limit the rate at which salt is removed.[117,954] Initial studies showed that CDI with activated carbon permits an applied current greater than 1 mA cm^{-2},[115] whereas intercalation electrodes limit the applied current to ∼100 μA cm^{-2}.[115,718,742]

Lee et al. recently proposed a multichannel desalination battery, as shown in Figure 25f, to overcome the mass transfer limitations of traditional desalination batteries.[946] The multichannel system was designed to have two independent channels (one for both electrodes and one for the feed) by placing an IEM at each interface.[946,955] The two electrodes (NaNiHCF and Ag) were exposed to a concentrated solution (1 M of NaCl) to reduce the resistance of the system, where the high salinity of the electrolyte significantly improved the capacity (52.9 mg g^{-1}) and removal rate (0.0576 mg g^{-1} s^{-1}).[946] Lee et al. also demonstrated the continuous battery desalination system known as "rocking-chair" CDI (RCDI; Figure 25g).[718] This configuration is usually made of two different PBAs, such as NaNiHCF and NaFeHCF, separated by an AEM. During the charging step, the working electrode (NaFeHCF) captures cations, while anions move to the counter electrode (NaNiHCF) to maintain bulk electroneutrality. During the discharging step, the working electrode is regenerated while the counter electrode captures cations, which enables continuous desalination with a removal capacity of 59.9 mg g^{-1} (Figure 26c).[718,943,944] In the same manner, the cation selective electrodes can be replaced with anion selective conversion electrodes such as Ag/AgCl for even greater continuous desalination (85[880] to 115[937] mg g^{-1}) at a low operating voltage (≈ 200 mV; Figure 26d).[880,937] During oxidation of the Ag electrode, Ag reacts with Cl^- in solution to form AgCl by breaking Ag−Ag bonds. Because both the oxidation and reduction peaks of Ag/AgCl occur at a low cell potential (220 mV versus SHE), this Faradaic process requires only a small input of energy (ranging between 2.5 k_BT ion^{-1}[937] and 10 kJ mol^{-1} of salt[880]). By adapting these cell architectures to existing designs, the desalination performance of conventional systems can be greatly improved using intercalation and conversion electrodes.

4.3. Electrosorption by Redox-Active Polymers

As illustrated in Figure 24, Faradaic redox reactions occur when there is transfer of n electrons at the surface of an electrode that changes the oxidation state of a reactant.[956,957] The equilibrium thermodynamics of these reversible Faradaic reactions are governed by the Nernst equation.[780,958−960] In this review, the notion of a Faradaic process encompasses reactions at electrodes regardless of the phase in or across which the reactants are moving or are present. For instance, a Faradaic process could be either a redox event at an electrode surface[86] or a variety of side reactions in which the electrons are transported across the electrolyte (e.g., water splitting, oxygen reduction).[89,961] Faradaic processes, combined with rich redox chemistry, have been extensively studied for a variety of applications, including energy storage,[962,963] bioelectrochemistry,[964] sensing,[965−967] and electrocatalysis.[968,969] As explained in section 2, nonelectrosorptive electrochemical methods rely on Faradaic reactions, be it through dissolution of a metal electrode or changes in the oxidation state of a dissolved species for plating. In the context of water purification by capacitive electrosorption, electron transfer and redox reactions are common, even without the use of external electroactive species. If left unregulated, these reactions could be parasitic and in turn degrade the electrodes, produce undesired byproducts, and reduce the efficiency of the primary electrochemical process.[150,961]

In this section, we focus on electrosorption promoted by redox reactions at active polymer electrodes, which boost energy efficiency and, more importantly, enable molecular selectivity. Materials with intrinsic Faradaic properties have long been studied and used for applications in energy storage.[970,971] Batteries, for example, store electric charge by Faradaic intercalation reactions and by changes in the oxidation state of a crystalline solid subjected to an electric field. These synthetic materials confine the redox reactions to within the solid electrode itself, without loss of electrons or transfer of ions across the electrolyte. Moreover, the surface reactions that occur usually promote specific binding of ions by creating sites of fixed charge that enable noncovalent interactions, such as hydrogen bonding, charge transfer processes, and hydrophobic transitions. From the perspective of electrochemical engineering, Faradaic materials also enable greater control of the window of operating voltages and suppress leakage currents and parasitic side reactions that would otherwise be detrimental to the longevity of the system.[909] The properties and applications of redox-active polymers are described in the sections below.

4.3.1. Overview of Redox-Active Polymers. Electrochemically tunable redox polymers, defined by the IUPAC as polymers with groups that can be either oxidized or reduced, play a key role as stimuli-responsive materials in many chemical and biochemical applications.[972] These materials have several properties that can be modulated electrochemically, such as reactivity,[973] mechanical actuation,[974] sensing,[975] and energy storage.[976] As shown in Figure 27, the redox group

https://doi.org/10.1021/acs.chemrev.1c00396
Chem. Rev. 2022, 122, 13547−13635

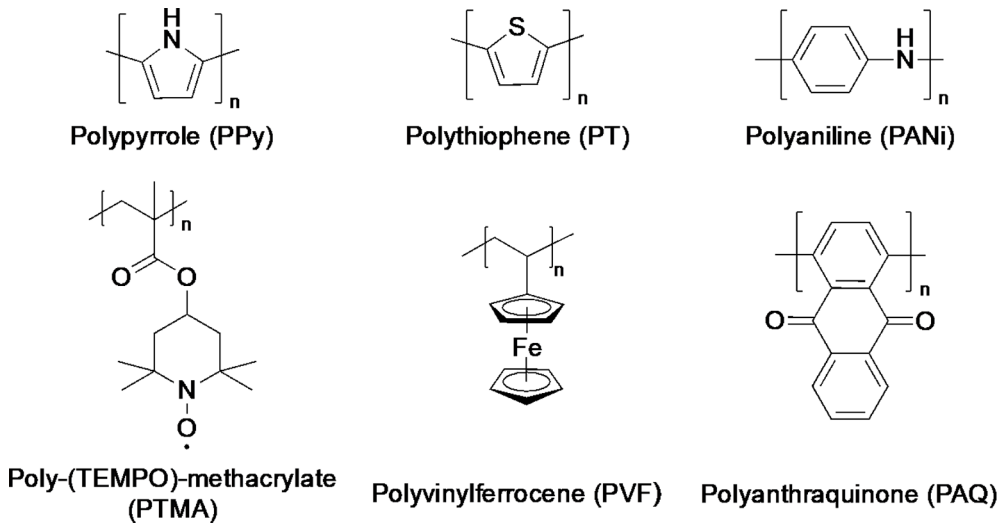

Figure 27. Chemical structures of representative redox-active and conducting polymers used to study selective electrochemical separations.

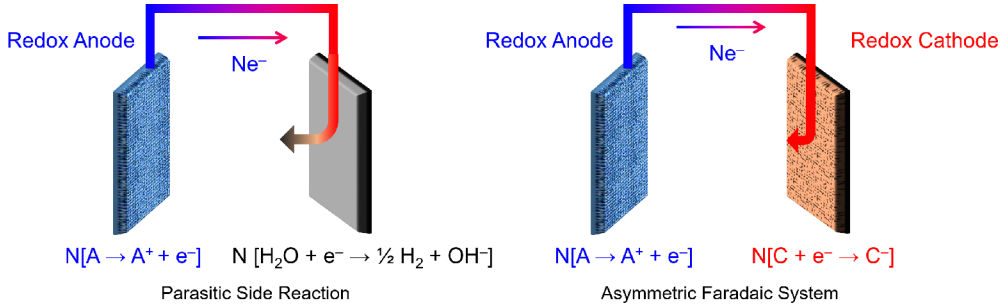

Figure 28. Suppression of side reactions using an asymmetric redox electrode configuration. Adapted with permission from ref 909. Copyright 2017 Royal Society of Chemistry.

can exist either directly on the backbone of the polymer chain, as is the case of polyanilines, polypyrroles, and polyquinones, or in pendant groups like ferrocene.[977] Redox-active polymers with electroactive units in the main chain are often conjugated[978] and comprise π-bonds that enable semiconductivity. While some of these semiconducting polymers have linear backbones, such as polyacetylene, many have conjugated backbones made of aromatic groups, such as polyaniline (PANI) and polypyrrole (PPy). Both PANI and PPy have been used extensively in electrosorption, particularly for enhanced CDI.[96,979−983] Redox polymers with active units in pendant groups, like pendant-group metallopolymers, are charged by a combination of bounded diffusion and electron hopping (or free diffusion).[984] Although these materials are less electrically conductive, they exhibit unique electronic properties and charge transfer interactions that make them highly selective toward target ions.[96,102,985]

Faradaic electrosorption relies on a change in the oxidation state of the electrode by electron transfer, which in turn influences the environment of the material. In a complementary manner, the solvent and immediate environment affect the behavior of redox polymers.[986,987] The oxidation or reduction of a redox polymer, for example, creates a fixed charge that selectively binds counterions by either ion exchange or insertion and release of the ions.[86,96,986−989] For redox systems that favor oxidation, the following chemical reactions are observed:

$$A^{n-} + n[P^+X^-] \leftrightarrow [P_n^+A^{n-}] + nX^- \quad (14a)$$

$$A^{n-} + P_n \leftrightarrow [P_n^+A^{n-}] + ne^- \quad (14b)$$

The first reaction describes a redox polymer P^+ (e.g., PPy) in which the weakly bound ion X^- is exchanged with the substituent ion A^{n-}. The second reaction describes a redox polymer P_n that is initially uncharged but, after undergoing oxidation (e.g., the transition from ferrocene to ferrocenium), can bind the counterion A^{n-} to a cationic group. In this process of binding, the affinity of the ions to the electrodes influences the electrochemical kinetics of adsorption. Ions that are strongly bound often facilitate electron transfer and shift the formal potentials, which makes the use of tunable redox polymers well suited for selective electrosorption and sensing.[985,990,991] Redox polymers, especially pendant-group metallopolymers, can also modulate electrode potentials, which prevents excursions in potential that would otherwise lead to side reactions. The suppression of parasitic side reactions (e.g., water splitting) improves performance and enables better control of water chemistry, as explained in Figure 28.[102,909,992] In the following sections, we describe recent advances in redox-active polymers for the separation of common pollutants like ions and uncharged contaminants.

4.3.2. Molecular Selectivity of Redox-Active Polymers. The main advantage of molecularly selective technologies is the ability to target a minority species in the presence of excess competing molecules. Redox-active polymers have facilitated the realization of this capability by enabling selective electrosorption and reversible release at fixed electric potentials. Because of their favorable electrochemical

https://doi.org/10.1021/acs.chemrev.1c00396
Chem. Rev. 2022, 122, 13547−13635

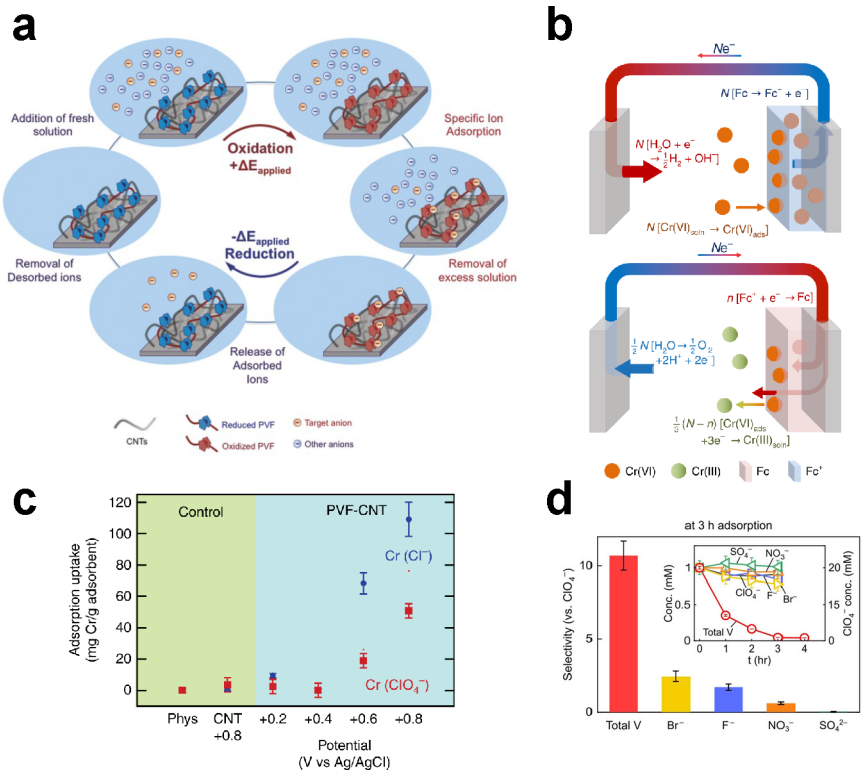

Figure 29. Electrochemical control of redox-active polymers for selective electrosorption. (a) Illustration of the concept of redox-based capture and release of a target anion. Reproduced with permission from ref 985. Copyright 2016 Wiley-VCH. (b) Selective separation of chromium at a PVF electrode; the schematic shows both charging and discharging steps as well as the reactions that occur at each counter electrode. (c) Results of adsorption uptake of chromium on PVF working electrodes as a function of potential. Reproduced with permission from ref 1021. Copyright 2018 Nature Research. (d) Calculated selectivity of individual anions (0.5 mM each) relative to a competing anion (20 mM of ClO_4^-) after 3 h of adsorption on PVF-CNT at 0.8 V versus Ag/AgCl. Reproduced with permission from ref 1022. Copyright 2020 Wiley-VCH.

kinetics, electroactive polymers have been considered for various applications in analytical sensing.[993−996] The mechanisms of selective ion sorption onto conducting polymers have been studied since the advent of ion exchange voltammetry.[997−999] For example, electroactive polymer films can be used as selective sensors by preconcentrating them with a certain counterion from the contacting solution phase.[1000,1001] Conducting polymers (e.g., PANI, PPy),[1002,1003] redox polymers,[989,1004−1006] and polymers entrapping redox units[1007−1009] have also been used for ion doping. These materials represent the archetypal systems of modified electrodes used during the development of electroanalytical chemistry.[958] The mechanisms of selectivity vary depending on the chemical structure of the redox monomer, the hydrophobicity of the polymer, and the electrostatic properties of the ions themselves. In general, the combination of controlled electric potentials and tailored molecular selectivity makes electroactive polymers a promising platform for energy efficient purification of water, recovery of valuable resources, and separation of fine chemicals.

Metallopolymers are one class of polymers that display electrochemically switchable properties, possess favorable electron transfer kinetics, and enable a diverse array of synthetic pathways for structural modification and tuning.[1010−1012] Recently, these materials were used as heterogeneous coatings on porous carbon to improve the capacity for energy storage. In particular, the noncovalent conjugation of polyvinylferrocene (denoted as PVF) with CNTs was demonstrated by both organic solution deposition and electrodeposition.[1013,1014] The resulting systems displayed high capacitances (1450 F g^{-1}) and energy densities (79.5 W h kg^{-1}).[1014] Through similar electrochemical methods, the charged moieties of metallopolymers can be used to capture and release anions efficiently. Films of PVF are oxidized in water over a range of positive potentials near 0.3 V versus Ag/AgCl,[1015] which is characteristic of stable electron transfer kinetics. Depending on the heterogeneity of the film, however, the applied voltage needed to fully charge all immobilized ferrocene units can be higher (in the range of 0.6−0.8 V versus Ag/AgCl), as was indicated by the large peak separation of different redox films in various electrolytes.

Redox-based electrosorption is cyclical and operates by electrochemical swings to capture target ions. During adsorption, electrodes become positively charged due to the formation of oxidized sites. Captured ions are then released by reversing the polarity due to the reduction of the redox adsorbent, as demonstrated in Figure 29a. The redox of PVF, for example, has been used to selectively extract organic anions such as carboxylates, phosphonates, and sulfonates from water in the presence of excess ions and without the use of chemical additives.[96,909,985,1016] Because many organic micropollutants like pesticides (e.g., metolachlor-based pesticide), microplastics, and pharmaceuticals (e.g., ethinyloestradiol contraceptive, propranolol hydrochloride beta blocker) are negatively charged,[1017−1019] electrosorption of negatively charged species is carried out by charging a redox polymer at the anode. In such a process, the functionalized redox electrode is immersed in an electrolyte comprising the minority organic anion (in

https://doi.org/10.1021/acs.chemrev.1c00396
Chem. Rev. 2022, 122, 13547−13635

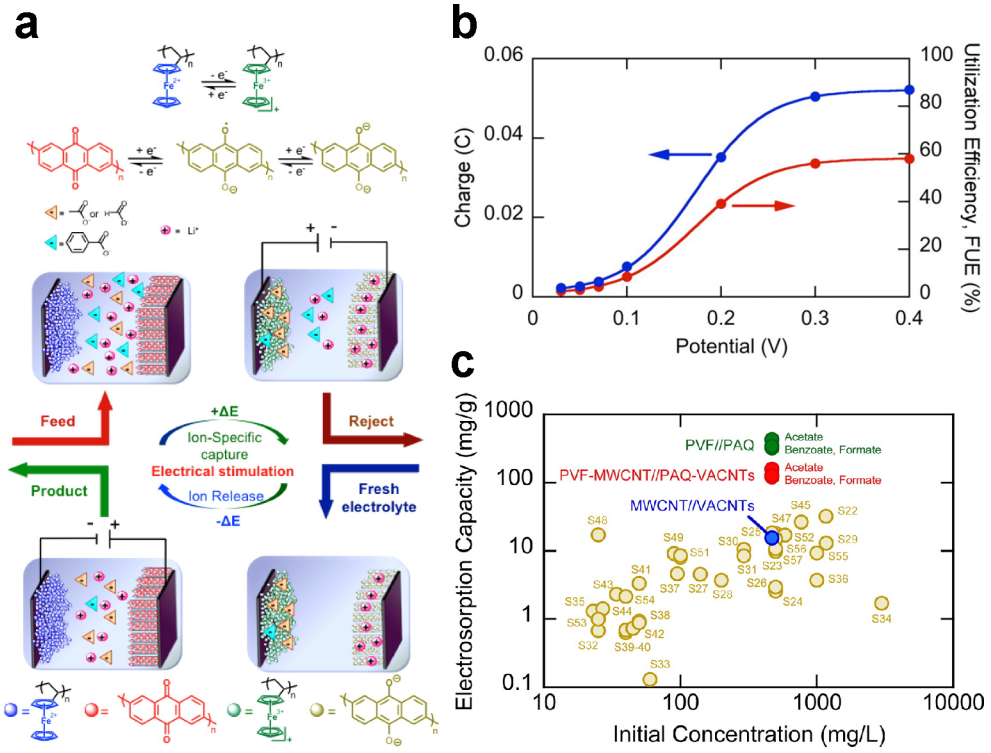

Figure 30. Operating principles of pseudocapacitive separation of ions. (a) Asymmetric PVF/PAQ system for electroregulated, selective recovery of lithiated carboxylates. (b) Variations in charge and ferrocene utilization efficiency (FUE) as functions of the applied potential. (c) Electrosorption capacity of this system compared to other supercapacitors reported in the literature (denoted by the light-colored symbols). Reproduced with permission from ref 1016. Copyright 2016 American Chemical Society.

concentrations ranging from 0.1 to 3 mM) as well as excess competing ions like ClO_4^- and Cl^- (in concentrations exceeding 100 mM). The transformation of ferrocene to ferrocenium results in a positively charged surface, which then electrostatically draws anions in solution to that surface. Systems based on PVF were also found to be stable over numerous cycles, and they generally display molecular selectivity, efficient use of energy, and a high capacity for uptake and storage of charge.[909] One example, shown in Figure 30a, is a system that paired a PVF anode with a polyanthraquinone (PAQ) cathode, which was effective compared to other systems at separating carboxylate, as quantified by an electrosorption capacity as high as 157 mg of anion per gram of adsorbent.[1016] Figure 30b reveals a relationship between the amount of oxidized species and the applied potential, and it shows that the utilization efficiency of ferrocene was lower than 100% during charging, which may be attributed to either active sites being inaccessible or redox units being kinetically trapped. In municipal wastewater, trace amounts of micropollutants usually exist in the range from micrograms to below a nanogram per liter.[1020] Future work demonstrating the effectiveness of redox-based electrochemical separations toward trace micropollutants will thus provide insight into industrial feasibility.

As illustrated in Figure 29, redox-active electrodes made of PVF were recently used to selectively extract toxic heavy metal oxyanions from water, namely chromate (CrO_4^{2-}), arsenate (AsO_4^{3-}), and vanadate (VO_4^{3-}).[102,1021,1022] The concentrations of chromium and arsenic were as low as 100 $\mu g\,L^{-1}$, and the experiments were performed in the presence of secondary wastewater components and excess competing ions at 200 times the concentration of the target ions. This process displayed high ion uptake (>100 mg of metal per gram of adsorbent; see Figure 29c), fast kinetics (<5 min of equilibrium uptake) at moderate potentials (≈ 0.8 V versus Ag/AgCl), and nearly complete electrochemical reversibility. The redox-based mechanisms of electrosorption for PVF were inferred from its electrochemical behavior, where an increase in the uptake of anions was correlated with an increase in redox charging.[1021] In situ measurements using transmission electron microscopy (TEM) supported the hypothesis that the insertion of ions into redox films was the main mechanism for selectivity, and there was no evidence of plating or phase change of the transition metal during electrosorption.[1021] Further analysis revealed that Cr(VI) (hexavalent) was reduced to the less toxic Cr(III) (trivalent) during the release step due to thermodynamic speciation at the electrified surface, favored by regulation of solvent pH at the counter electrode.[1021] This Faradaic reaction worked to the benefit of water purification because Cr(VI) (often produced in industrial processes) is carcinogenic, unlike Cr(III) which is an essential element in the human diet.[1023−1025]

When using metallopolymers for electrosorption, one of the main mechanisms of selectivity is charge transfer. Quantum calculations of electronic structure have pointed to a strong correlation between charge transfer at the redox moieties and the binding energy of the participating anion.[985,1021] For example, the binding energies of Cl^-, ClO_4^-, CrO_4^{2-}, and $HAsO_4^{2-}$ with ferrocenium were calculated to be 2.90, 3.47, 5.53, and 4.73 kcal/mol, respectively. These computations were performed using density functional theory (DFT) with corrections for entropic and solvation effects. Analysis of the binding of ferrocenium to anions, with supporting evidence from nuclear magnetic resonance (NMR) spectroscopy, has

https://doi.org/10.1021/acs.chemrev.1c00396
Chem. Rev. 2022, 122, 13547−13635

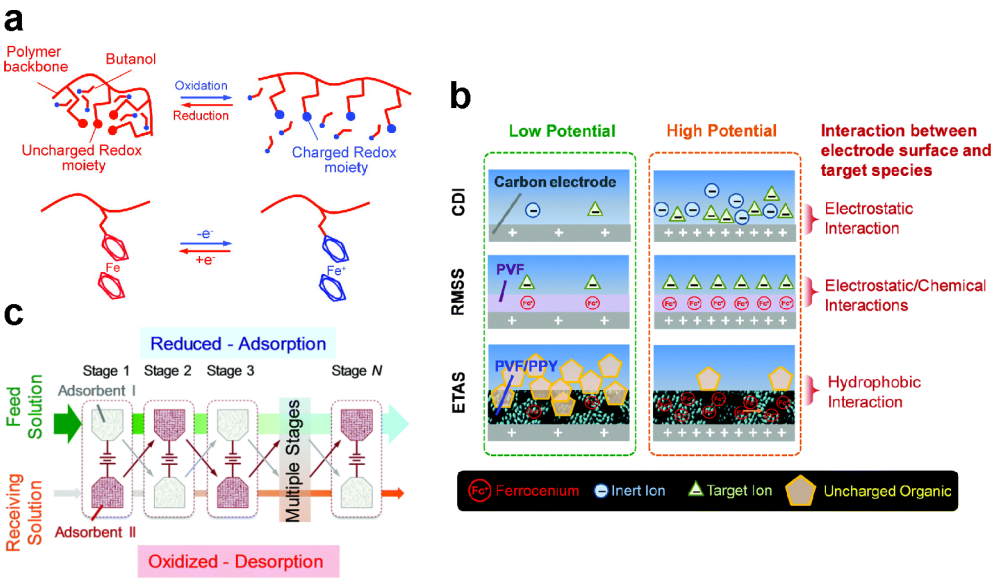

Figure 31. Faradaic systems with electrochemically tunable affinity for controlled capture of uncharged contaminants. (a) Redox of a ferrocene copolymer for separation of butanol from water. Reproduced with permission from ref 1036. Copyright 2011 American Chemical Society. (b) Comparison of the mechanisms of selectivity in CDI, RMSS, and ETAS. (c) Multistage electrochemical concentration of uncharged species using the ETAS process. Reproduced with permission from ref 103. Copyright 2018 Royal Society of Chemistry.

also underscored the role of cyclopentadienyl ligands on intermolecular binding. Once oxidized, ferrocenium (both the metal and the ligand) becomes a strong acceptor of charge that is selective toward anions. This selectivity was observed in both aqueous and organic solvents (e.g., acetonitrile), particularly during the removal of carboxylates in the presence of competing anions like hexafluorophosphate.[985,1016,1026,1027] The introduction of selective chemical interactions superimposing electrostatics enables selective separations by functionalized redox-metallopolymer electrodes.

More recently, radical-based redox polymers were also found to be highly effective at molecular separations for water purification. Kim et al. showed that TEMPO-based copolymers are effective at selective adsorption of per- and polyfluoroalkyl substances (PFAS) based on their affinity toward these polymers.[1028] PFAS contaminants are highly persistent and difficult to both capture and degrade due to their unique physicochemical properties. In the work by Kim et al., redox copolymers with amine functional groups and redox-active nitroxyl radical groups were used to achieve high selectivity and uptake of various PFAS compounds, with separation factors exceeding 500 relative to Cl^-. Furthermore, the use of BDD as the counter electrode reduced energy consumption and enabled degradation of PFAS, which was selectively adsorbed on the redox polymer electrode, in the electrode regeneration step. By tuning the ratio of amines to radical groups, the electrochemical regeneration and selectivity toward PFAS could be further improved.[1028]

4.3.3. Redox Separation of Uncharged Pollutants. Redox systems have recently been used to capture and release uncharged contaminants from water via hydrophilic-to-hydrophobic transitions. Many environmental micropollutants are uncharged pharmaceutical and personal care products (PPCPs) that are hazardous to humans and animals.[1029−1032] PPCPs have unique physicochemical properties and are often present in water in trace quantities, which complicates the removal of these contaminants by conventional methods such as adsorption, precipitation, biological treatment, and membrane filtration.[1031,1033−1035] As shown in Figure 31, Faradaic electrodes have been used to selectively capture uncharged micropollutants based on the electrochemically tunable affinity of these redox-active electrodes to the contaminants.

Prior work on chemical switching in redox polymers, shown in Figure 31a, revealed the possibility of extracting an uncharged compound such as butanol from water based on its affinity to a copolymer of hydroxybutyl methacrylate (HBMA) and vinylferrocene (VF).[1036] The selectivity of the redox gel to butanol in the reduced state was reported in terms of a separation factor equal to the ratio of the equilibrium distribution coefficients (see eq 15) of butanol and water, which was shown to exceed 5. This selectivity was attributed to the hydrophilic-to-hydrophobic transition and preferential swelling of the solvent within the gel.[1036] The concepts presented in this system served as the basis for electrochemically tunable affinity separations (ETAS), which leverage the redox switchable hydrophobicity of polymers to achieve targeted separations. Figure 31b compares the principles of electrostatic CDI, redox-mediated selective separations (RMSS), and ETAS.[103] In ETAS, a nanostructured blend of PVF and PPy was used to remove and concentrate a collection of uncharged organic pollutants, including dyes like methyl orange, endocrine disruptors like ethinylestradiol, and toxic chemicals like dichlorophenol and bisphenol. The PVF/PPy electrodes were synthesized by simultaneous electropolymerization of pyrrole and electrodeposition of PVF, which yielded a homogeneous coating of the PVF/PPy system onto a carbon cloth, as shown in Figure 32.[103,1037] These nanostructured hybrid materials also possess supercapacitive properties (>500 $F\,g^{-1}$) superior to those of their individual components (PVF with 79 $F\,g^{-1}$ and PPy with 27.3 $F\,g^{-1}$), without the use of carbon nanomaterials.[1037] Differential selectivity in ETAS was quantified using the distribution coefficient K_D:

$$K_D = \frac{Q_e}{c_e} \tag{15}$$

https://doi.org/10.1021/acs.chemrev.1c00396
Chem. Rev. 2022, 122, 13547−13635

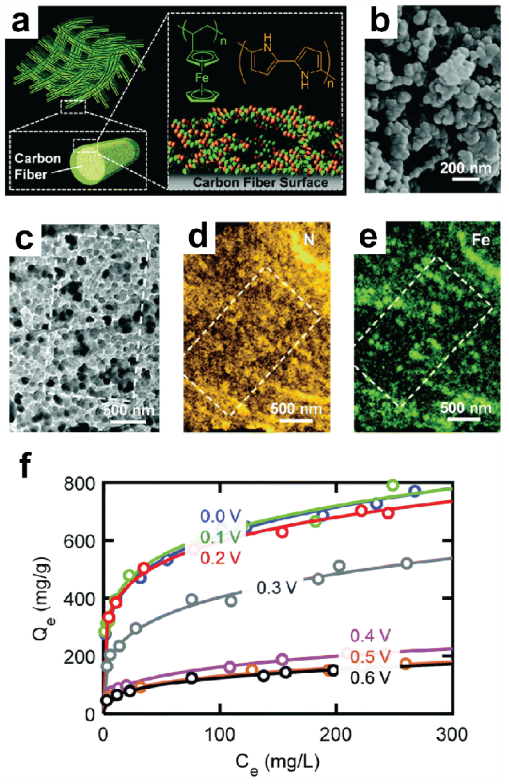

Figure 32. Imaging and analytical characterization of PVF/PPy coatings on a carbon cloth. (a) Schematic illustration of the ETAS adsorbent made of PVF/PPy coated on a flexible carbon substrate. Images of the PVF/PPy system using (b) SEM, (c) TEM, (d) energy dispersive X-ray spectroscopy (EDS) N mapping, and (e) EDS Fe mapping. (f) Adsorption isotherms of PVF/PPy at different potentials. Open circles represent experimental data and solid lines are fits based on the Freundlich adsorption model. Reproduced with permission from ref 103. Copyright 2018 Royal Society of Chemistry.

where Q_e is the adsorption capacity (in mg g^{-1}) and c_e is the concentration of the target contaminant at equilibrium. The distribution coefficient is a function of the applied electric potential (see Figure 32f) and the physicochemical properties of the contaminants.[103] As shown in Figure 31c, ETAS was implemented in a multistage cyclic batch process to concentrate target uncharged species by several orders of magnitude. The principle of hydrophobic transitions was taken a step further by using complementary asymmetric electrodes.[104]

4.3.4. Electrode Design for Faradaic Electrosorption.

As explained in section 4.1.5, parasitic reactions compromise the performance of electrochemical systems.[781,1038] These unwanted side reactions lower current efficiency and negatively impact the chemistry of the solution, for example, by producing hydroxides which lower selectivity toward anions. Asymmetric configurations of the electrodes have thus been proposed to mitigate parasitic reactions and improve efficiency. Innovations in this area encompass both Faradaic and non-Faradaic systems and involve the use of asymmetric membranes in CDI configurations,[1039] differential functionalization of the electrodes,[1040,1041] or implementation of asymmetric redox chemistries.[96,909,992] In one such example, the performance of CDI was improved by placing IEMs at the electrodes to improve selective adsorption of counterions and to prevent co-ions from escaping into the bulk, as shown in Figure 33.[671,1039]

Within the context of Faradaic systems, symmetric and asymmetric configurations have been proposed to improve charge storage in pseudocapacitors[1042−1044] and batteries.[1045−1047] Similar principles hold with regard to electroseparations: that is, the better the capacity for energy storage, the more ions will be separated and retained. Moreover, systems in which electron transfer occurs at a fixed, well-defined redox potential can help control the voltage window to limit side reactions and inhibit competing Faradaic reactions that result in current leakage.[909] These desirable properties can be achieved using asymmetric electrodes made of redox-active metallopolymers, as illustrated in Figure 34. Faradaic intercalation in crystalline systems can also be used to improve the efficiency of electrosorption. For example, symmetric electrodes of CuHCF have been used to reduce the amount of energy needed for desalination (down to 0.02 kW h m^{-3} for a

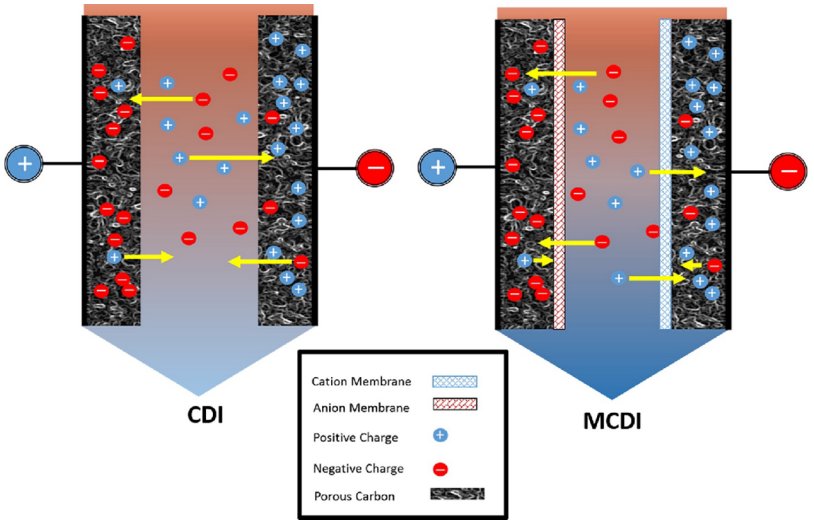

Figure 33. Comparison between the designs of conventional CDI and MCDI. Membranes in the latter repel co-ions and prevent them from escaping to the bulk, which in turn attracts more counterions to preserve electroneutrality. Reproduced with permission from ref 1039. Copyright 2014 American Chemical Society.

https://doi.org/10.1021/acs.chemrev.1c00396
Chem. Rev. 2022, 122, 13547−13635

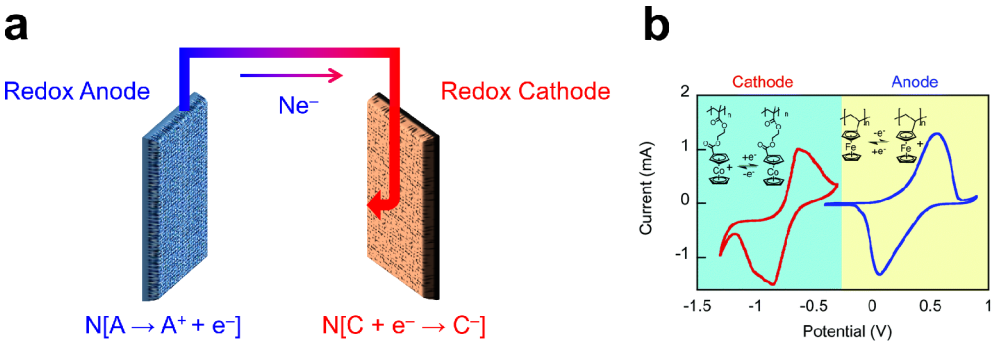

Figure 34. Asymmetric Faradaic systems for selective electrochemical separations. (a) Schematic of a Faradaic system with redox-active polymer electrodes, namely a ferrocene metallopolymer (PVF) for the anode and a cobaltocenium metallopolymer for the cathode. (b) Characterization of the electrochemical system and corresponding redox reactions by cyclic voltammetry. Reproduced with permission from ref 909. Copyright 2017 Royal Society of Chemistry.

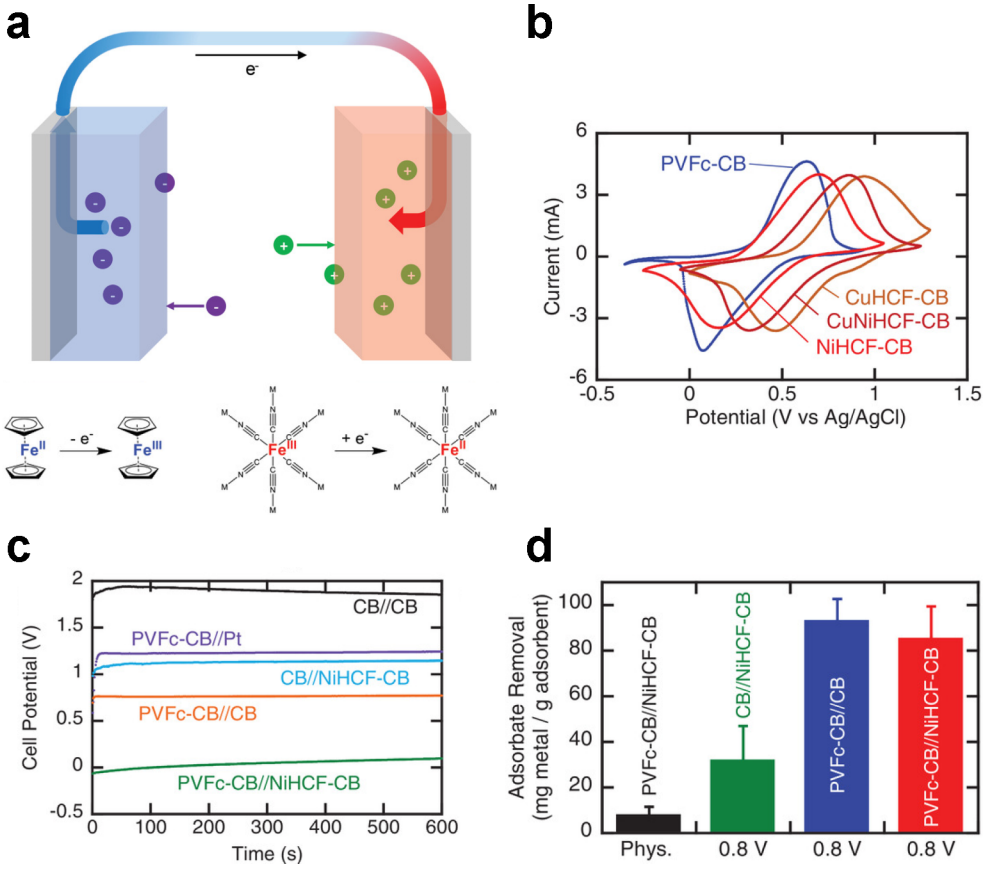

Figure 35. Asymmetric redox system using iron active centers for selective separations. (a) Schematic of the asymmetric Faradaic cell, in which a ferrocene metallopolymer is oxidized at the anode (blue) and an HCF crystal is reduced at the cathode (red). (b) Cyclic voltammetry shows that the HCF electrode can be structurally tuned to control the redox potential. (c) Cell potential during electrosorption and (d) recovery of molybdenum anions for different electrode chemistries. Reproduced with permission from ref 992. Copyright 2020 Wiley-VCH.

feed with an initial concentration of 25 mM and a final concentration of 17 mM).[944] This system was operated at a much lower cell voltage (i.e., 0.6 V) compared to a standard CDI cell, which reduced parasitic side reactions.[944]

Asymmetric configurations have the advantage of increasing energy storage at each of the electrodes by promoting the appropriate electron transfer reactions, namely oxidation at the anode during charging and reduction at the cathode. In the case of electrosorption, asymmetric Faradaic designs have been used to capture anions at the anode and cations at the cathode.[86,96,154,714] One example of redox-active systems that enabled selective electrochemical separations was made of ferrocene (PVF) and cobaltocenium metallopolymers on opposite electrodes, respectively.[909] The two electrodes operated within the window of water stability and, more importantly, their redox reactions allowed for selective capture of anions from solution and subsequent control of the voltage window with 96% current efficiency. By carrying out these redox reactions at low voltages (i.e., 0.4 and −0.6 V versus Ag/AgCl for the anode and cathode, respectively), the pH of the system was stable and there was significant improvement in the efficiency with which anions were removed from dilute

https://doi.org/10.1021/acs.chemrev.1c00396
Chem. Rev. 2022, 122, 13547−13635

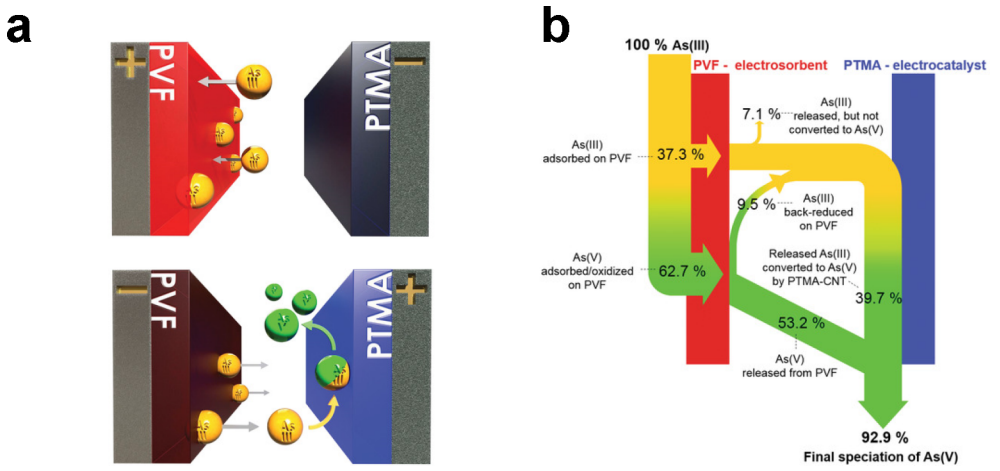

Figure 36. Simultaneous capture and conversion of As(III) into As(V) using redox-active electrodes. (a) Schematic of the asymmetric electrochemical system with electrodes made of PVF (electroadsorbent) and PTMA (electrocatalyst). (b) Flow diagram explaining the speciation of arsenic in this system. Reproduced with permission from ref 102. Copyright 2020 Wiley-VCH.

solutions. Furthermore, the selective properties of the PVF system were preserved upon capture of anions by preventing the formation of hydroxides.[909] In subsequent studies, it was shown that the organometallic cobalt center could be tuned using a tetraphenyl ligand,[1048] which enabled simultaneous recovery of cations and anions.[909]

More recently, hexacyanoferrate (HCF) electrodes were combined with redox-active polymers to achieve selective electrochemical separations that can be carried out with extremely small swings in voltage (<0.1 V) by redox matching at the electrodes.[992] As shown in Figure 35a, both anions and cations were selectively captured by combining an electrode made of PVF with another made of HCF. The redox potential of the cathode was shown to be tunable based on the content of mixed metal (see Figure 35b), which enabled structural control of the window of operating voltages down to ∼0.1 V at a current density of 1 A m^{-2} for a two-cell system. This feature also improved anion selectivity and separation efficiency, as demonstrated in Figure 35c,d, which highlights the potential of hybrid redox polymers with crystal electrodes for efficient separations.[992]

In addition to their high efficiency, asymmetric redox systems combine separations and reactions to chemically transform harmful contaminants into benign species. By combining an electrosorption working electrode with an electrocatalytic counter electrode, Kim et al. found that As(III) (trivalent) can be captured and transformed into As(V) (pentavalent), as shown in Figure 36a.[102] The former is a naturally and artificially occurring contaminant in groundwater that is highly toxic, even though it is often present at low concentrations.[1049−1051] Capturing this contaminant in the presence of competing species and transforming it into As(V) is a major challenge in water purification. Because of the affinity of PVF for charge transfer anions, PVF-CNT composite electrodes were used to capture AsO_4^{3-} and AsO_3^{3-} during oxidation of the working electrode.[985,1021] The counter electrode was coated with poly-TEMPO methacrylate (PTMA), which comprises stable nitroxide radicals that undergo oxidation by one-electron transfer. This system efficiently reduced the concentration of a contaminated solution from 100 ppb to below 10 ppb, the recommended maximum total exposure.[1052] Moreover, separation factors of over 49 relative to competing Cl^- were achieved during the capture of these oxyanions. Upon release, the PVF electrode liberated As(III), and the counter electrode transformed the anions into As(V) in both batch and flow configurations. By taking advantage of these redox processes, contaminants were simultaneously separated and converted, as described in Figure 36. This dual process reduced energy consumption to 0.45 kW h mol^{-1} of converted As and increased energy efficiency by an order of magnitude compared to systems that decouple separations from reactions.[102] This framework is similar to the use of PVF with a platinum counter electrode to capture and transform Cr(VI) into the less harmful Cr(III). In the latter process, however, the redox transformation occurs at a single PVF electrode which adsorbs Cr(VI) during oxidative charging and catalyzes its reduction during discharging, while water splitting occurs at the counter electrode to regulate pH.[1021] A study recently revealed the role of oxygen in ferrocene-mediated conversion of arsenic, where production of peroxide aided the regeneration of active ferrocenium units.[1053] The study also showed how PVF systems can be used for efficient remediation of groundwater contaminated with arsenic.

Asymmetric systems have been designed with complementary hydrophilic-to-hydrophobic transitions to increase the capacity of adsorption of uncharged organic contaminants.[104] As an example, one electrode was coated with the PVF/PPy hybrid introduced in section 4.3 and the other with PPy containing the amphiphilic surfactant dioctyl sulfosuccinate (DOSS, known commercially as AOT). When paired, these two electrodes exhibit hydrophilic-to-hydrophobic transitions that are complementary and occur at opposite electrodes. That is, the PVF/PPy electrode becomes hydrophilic when oxidized and hydrophobic when reduced, whereas the PPy/AOT electrode becomes hydrophobic when oxidized and hydrophilic when reduced. As shown in Figure 37, this design enables capture of hydrophobic molecules like Sudan Orange G (SOG), which is released from both loaded electrodes during charging (oxidation at PVF/PPy and reduction at PPy/AOT).[104] The PPy/AOT electrode was developed to achieve superhydrophobic properties and strong $\pi-\pi$ interactions with uncharged aromatic species.[1054] During electrostatic charging, the surfactant dopants are reoriented to modulate hydro-

https://doi.org/10.1021/acs.chemrev.1c00396
Chem. Rev. 2022, 122, 13547−13635

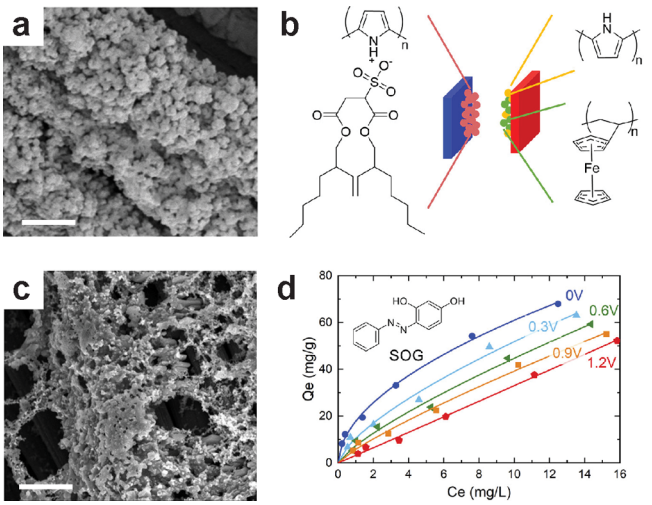

Figure 37. Asymmetric electrochemical system with tunable hydrophobicity. Complementary redox-active electrodes made of (a) PVF/PPy and (c) PPy/AOT nanostructures; scale bars are 10 μm. (b) Schematic of the asymmetric system with electrochemically modulated affinity toward uncharged organic molecules. (d) Adsorption isotherms of SOG for various applied potentials. Filled markers represent experimental data, and solid lines are fits based on the Freundlich adsorption model. Reproduced with permission from ref 104. Copyright 2019 American Chemical Society.

phobicity, an interaction that was explored in detail using DFT and MD simulations.[1054] While discharging, the asymmetric system of PVF/PPy and PPy/AOT was found to be nearly 20 times more energy efficient than systems based on activated carbon (12 J g^{-1} of adsorbent for the asymmetric redox system and 235 J g^{-1} of adsorbent for activated carbon).

Finally, these asymmetric systems have been redesigned into flow configurations, in which CNTs coated with PVF and PPy (doped with the anionic surfactant dodecylbenzenesulfonate, DBS) were used as the electrodes to selectively remove organic contaminants.[1055] This system integrated in situ ultraviolet, conductivity, and pH sensors for online monitoring, as shown in Figure 38, and it displayed a high capacity and rate of salt adsorption compared to CDI systems in the literature.[1056] On the basis of dynamic measurements of adsorption and release, the flow platform was also selective toward benzoate, a compound representative of toxic carboxylates, in the presence of competing electrolytes, which were 50 times more concentrated than the target anion. This work demonstrated the feasibility of using asymmetric redox designs as on-site systems for water purification.

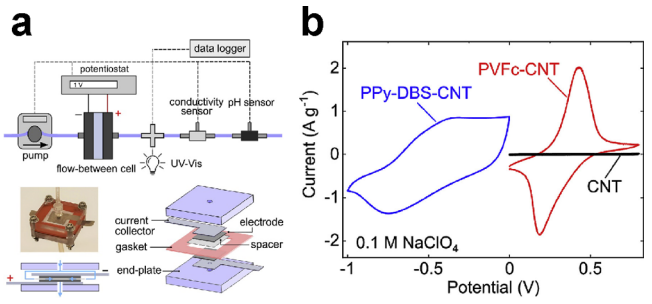

Figure 38. Selective adsorption of organic anions in a flow cell with asymmetric redox-active electrodes. (a) Schematic of the continuous electrosorption system with integrated sensing. (b) Cyclic voltammetry of carbon substrates functionalized with PVF-CNT, PPy-DBS-CNT, and CNT. Reproduced with permission from ref 1055. Copyright 2020 Elsevier.

5. INVERSE METHODS OF ENERGY CONVERSION

Generating clean, renewable energy is just as important as producing purified water for environmental sustainability. In this section, we introduce what are known as "inverse methods" of energy conversion and draw parallels between these systems and the methods of water purification discussed above. The electrochemical inverse methods that we describe here include reverse ED, capacitive mixing (CapMix), and battery mixing (BattMix). These technologies are similar in that they retrieve energy from the mixing of two streams between which there is a gradient in concentration (or more precisely in chemical potential), such as river water and seawater. They differ, however, in how they are designed and operated, but as we will show in this section, reverse ED, CapMix, and BattMix are in fact just ED, CDI, and Faradaic electrosorption, respectively, operated in reverse. For completeness, we also review electrokinetic conversion of mechanical energy to electrical energy based on harvesting the streaming current produced by pressure-driven flow in charged microchannels or porous media.

Although the scope of this review is limited to electrochemical methods, we note that there exists a physical, membrane-based inverse method known as pressure-retarded osmosis (PRO), which converts the free energy of mixing into useful electrical power.[1057−1062] In this process, two streams of different concentrations are separated by a semipermeable membrane that allows only water to pass by osmosis. The imbalance in chemical potential across the membrane promotes transport of water from diluate to concentrate. This osmotic flow can be stopped if enough hydraulic pressure is applied to the concentrate. The applied pressure needed to maintain osmotic equilibrium is called osmotic pressure and is determined entirely by the composition of the solution. PRO thus occurs as long as the applied pressure is less than the osmotic pressure, and because water flows against this gradient in hydraulic pressure, the free energy of mixing can be converted into mechanical work.

5.1. Inverse Electrokinetic Methods

5.1.1. Reverse Electrodialysis. In reverse ED, the system is fed dilute and concentrated streams that are partitioned by alternating AEMs and CEMs. This stack is sandwiched between metal electrodes that are connected through an external load to which power is delivered, as shown in Figure 39.[1063,1064] Transport of cations across the CEMs and anions across the AEMs produces a flux of electric charge between the electrodes. The magnitude of the resulting electric potential is related to the difference in chemical potentials of the salt in adjacent streams, and the voltages across each membrane are additive.[1063−1065] Natural runoffs and rivers in coastal areas are abundant sources of both dilute feed that is usually left to mix with seawater and energy that is produced without capture.[1066] It was estimated that 2.3 MJ of work could theoretically be extracted from each cubic meter of river water that flows into the sea.[1063,1066,1067] With the typical discharges of all rivers combined, the net power produced by this unconventional source of energy was estimated to be between 2.4 and 2.6 TW.[1063,1068] Of course, not all of this energy could be harvested by reverse ED, but the question is exactly how much

https://doi.org/10.1021/acs.chemrev.1c00396
Chem. Rev. 2022, 122, 13547−13635

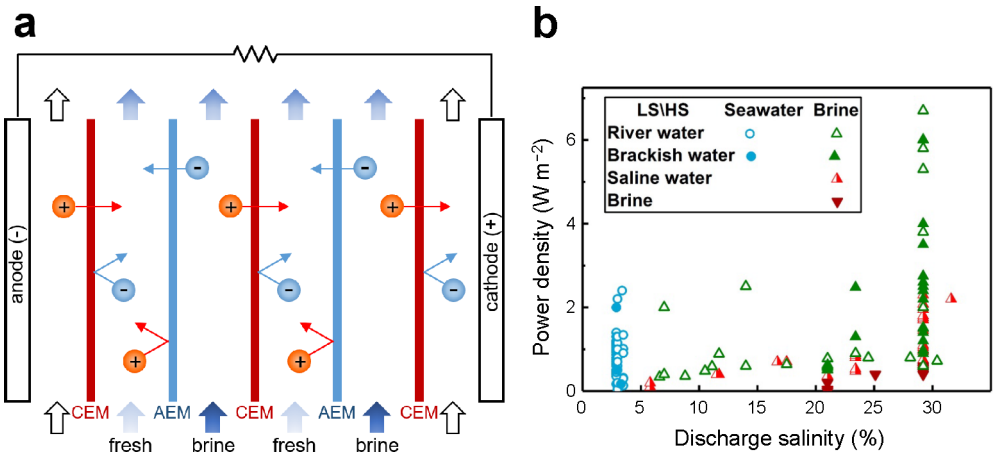

Figure 39. Operating principles and empirical results of reverse ED. (a) Dilute and concentrated streams are passed through a stack of alternating AEMs and CEMs. Differences in the chemical potentials of adjacent streams generate an electric potential across each membrane, and the total voltage is the sum of the potential differences across each membrane. In most reverse ED systems, reversible redox couples (e.g., Fe^{2+}/Fe^{3+}, $[Fe(CN)_6]^{4-}/[Fe(CN)_6]^{3-}$) in a supporting electrolyte (e.g., NaCl−HCl) are used as electrode streams to convert ion flux into electrical current.[1073−1075] (b) Power density versus discharge salinity for various pairs of low salinity (LS) and high salinity (HS) feeds. Reproduced with permission from ref 1076. Copyright 2018 Elsevier.

can be extracted? Forgacs conservatively predicted a yield of 0.35 MJ per cubic meter of river water,[1069] Audinos arrived at a similar yield and calculated an energy recovery of 21% (excluding losses due to pumping and power inversion),[1070] and Jagur-Grodzinski and Kramer experimentally determined a yield between 0.25 and 0.6 MJ per cubic meter of river water.[1071] Długołęcki et al. then derived an equation to calculate the maximum power output $\mathcal{P}_{max}$ based on the properties of the system and its components:[1072]

$$\mathcal{P}_{max} = NA\frac{[\alpha_{avg}RT/F\ \ln(a_c/a_d)]^2}{\mathcal{R}_{AEM} + \mathcal{R}_{CEM} + w_c/\kappa_c + w_d/\kappa_d} \quad (16)$$

where N is the number of membrane pairs, A is effective membrane area, α_{avg} is average membrane permselectivity, a is thermodynamic activity, $\mathcal{R}$ is membrane resistance (in $\Omega\ m^2$), w is compartment width, κ is electrolyte conductivity, and subscripts "c" and "d" represent the concentrate and diluate, respectively.

Early studies of reverse ED showed that little energy is recovered relative to what is theoretically available. Post et al. later investigated how much energy can be recovered in reverse ED by distinguishing between internal and external losses of energy and by focusing exclusively on the former[1066] (external losses arise due to pumping and power inversion and can only be quantified in a full-scale, optimized system). In the literature, it is explained that internal losses arise due to ionic shortcut currents,[1077] internal resistances (e.g., friction losses, pumping requirements, electrochemical overpotentials),[1071,1078,1079] concentration polarization,[1063,1080] and osmotic transport.[1081] Internal losses must therefore be reduced to improve energy efficiency, which can be achieved by developing improved electrode systems (to lower electrochemical overpotentials),[1082] introducing air bubbles to the feed (to decrease ionic shortcut currents),[1066,1077] improving stack hydrodynamics and spacer design (to reduce concentration polarization),[1080] and designing spiral wound modules (to decrease membrane area).[1083,1084] Using some of these principles, Post and Veerman et al. designed systems that, in the best case, recovered more than 80% of the work made available by mixing artificial river water and seawater.[1066,1077] Several other studies[1076] in the past decade also focused on optimizing the performance of reverse ED systems by modeling and developing new IEMs,[1085−1088] spacers,[1089] and electrodes.[1090] At the same time, researchers focused on improving the overall operation of the stack,[1091,1092] understanding the impact of fouling and mitigating it (see section 3.6),[1093−1096] and combining reverse ED with desalination technologies.[1097−1102]

The fastest growing areas of research over the past five years, however, are related to applications for energy storage,[1103,1104] developing micro- and nanofluidic reverse ED systems,[1105,1106] and pilot studies for commercial use.[1107−1110] Pilot studies are essential to bridge the gap between experimentation at the laboratory scale and implementation at the industrial scale. So far, pilot plants for reverse ED exist in only a few countries, including The Netherlands and Italy. The first of these plants was commissioned in 2014 in Afsluitdijk, a major dam in The Netherlands, and it features a dyke that is 32 km long which separates the IJssel Lake and the Wadden Sea.[1076] This plant produces electrical energy (the amount of which has not been made available to the public) from controlled mixing of fresh water with seawater. The pilot plant in Italy was commissioned near the Ettore e Infersa Saltworks in Trapani, and it mixes saturated brine from the saltworks with brackish water from a nearby shoreline well to produce an average of 0.8 W m^{-2} of membrane in total.[1076,1107,1108] Future work in this area will largely focus on improving power density, performing complete cost analyses, and building plants with greater capacity.[1064,1081]

5.1.2. Electrokinetic Energy Conversion. Although this review focuses on the interplay of electrical and chemical energy, we discuss here how linear electrokinetic phenomena (see section 3.3) can also be exploited to directly convert mechanical energy to electrical energy via the forced motion of liquid electrolytes in charged microchannels and pores. In 1964, Osterle introduced the basic idea of mechanical electrokinetic energy conversion by harvesting the streaming current produced by pressure-driven flow in a charged capillary.[1111] Morrison and Osterle then estimated a maximum

https://doi.org/10.1021/acs.chemrev.1c00396
Chem. Rev. 2022, 122, 13547−13635

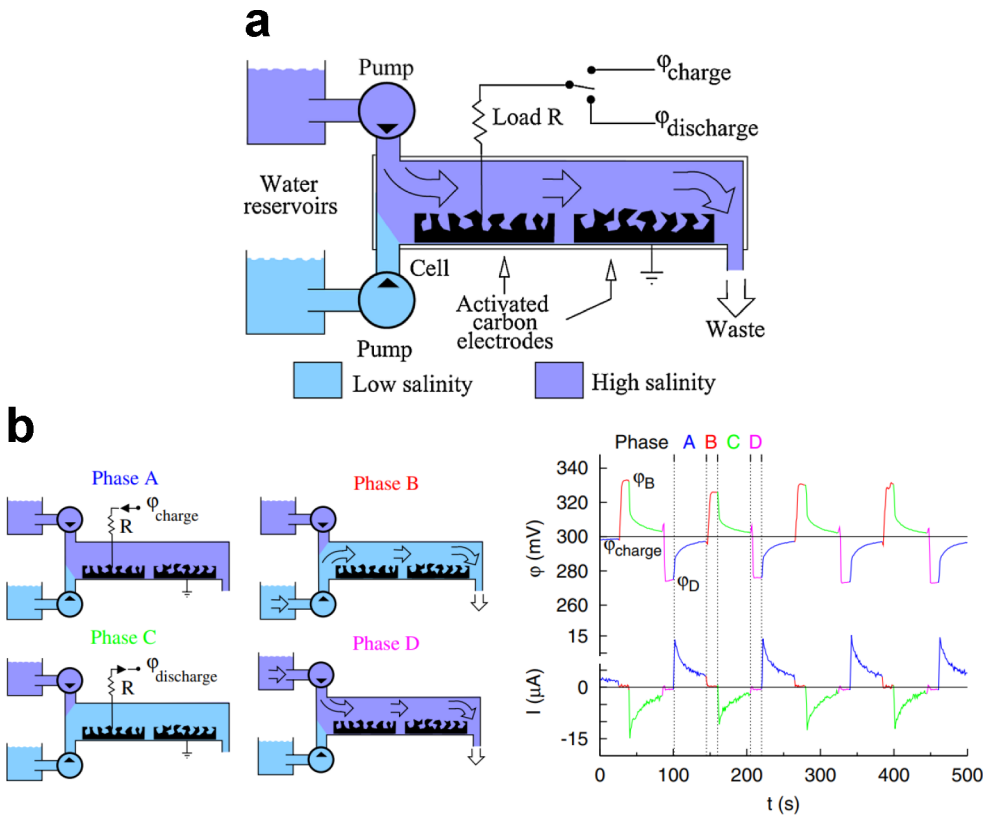

Figure 40. Schematic and operating procedure of CDLE, the original CapMix system. (a) The device comprises two electrodes made of porous activated carbon, and this pair of electrodes behaves as a capacitor that can be charged and discharged. Two reservoirs contain solutions with different concentrations that are pumped to the cell where they are mixed. (b) Graphical explanation of the four-step operating procedure of CDLE. In phase A, the electrical circuit is closed and the cell is charged; in phase B, the circuit is opened and the cell is flushed with fresh water to increase the electric potential; in phase C, the circuit is closed and the cell is discharged; and in phase D, the circuit is opened and the cell is flushed with salt water to decrease the electric potential. Reproduced with permission from ref 1134. Copyright 2009 American Physical Society.

efficiency of 0.9% for ultrafine water−glass capillaries.[1112] Gross and Osterle comprehensively analyzed energy conversion by linear electrokinetic phenomena (recently extended by Peters et al.[505]) and estimated a maximum electroosmotic conversion efficiency of 4%.[506] This approach had attracted relatively little attention until its rediscovery in the context of microfluidics.[1113] The possibility of measuring and controlling the streaming potential in single nanochannels renewed interest in advancing this classical method through nanoscale engineering.[1114−1117] Indeed, van der Heyden et al. predicted theoretical conversion efficiencies of up to 12%[1115] and experimentally demonstrated 3% efficiency in 75 nm-thick silica glass nanochannels using dilute KCl electrolytes.[1116] Considering conduction through the Stern layer can further reduce the theoretically predicted efficiency.[1118] Recent advances with soft, flexible microchannels have allowed for practical applications of electrokinetic energy conversion in wearable and portable self-powered devices.[1119,1120]

Significant developments have also followed from theoretical predictions of massive enhancement of electrokinetic phenomena for charged surfaces with hydrodynamic slip.[1121−1123] Ren and Stein predicted that hydrodynamic slip could increase nanofluidic energy conversion up to 40% for hydrophobic surfaces with slip lengths on the order of tens of nanometers and up to 70% in CNTs or graphitic systems based on reported apparent slip lengths.[1124] These theoretical values have proven difficult to achieve in electrokinetic energy conversion with homogeneous solid−liquid interfaces, and there are lingering signs of knowledge gaps in our understanding of electrokinetic phenomena under nanoconfinement.[491] For example, the apparent slip observed for CNTs is absent in crystallographically similar boron nitride nanotubes with different electronic structures.[497] As a possible alternative to homogeneous surfaces, Bagha et al.[1125] predicted that micropatterned, superhydrophobic surfaces with high slip and charged liquid−gas interfaces could increase efficiency at larger length scales, and this concept remains a subject of research.[1126−1128]

5.1.3. Reverse Electrowetting. Electrocapillary phenomena involve interactions between liquid electrolyte interfaces and charged solid surfaces or electrodes. The classical example is electrowetting, where an applied voltage changes the surface tension of a droplet via energy stored in EDL capacitors and thus manipulates the shape of an electrolyte droplet.[1129,1130] Krupenkin and Taylor first proposed the inverse effect of reverse electrowetting to convert mechanical energy to electrical energy, where immiscible electrolyte droplets were compressed by the motion of parallel-plate electrodes.[1131] Kolomeisky and Kornyshev suggested an alternative approach based on the reversible penetration of a liquid electrolyte into a solvophobic porous electrode, which could be used in a "double layer shoe" to harvest electricity from walking motion.[1132] Analogous to the use of moving wire electrodes in CDI for desalination,[862] capacitive rotors have been proposed to generate alternating current from mechanical motion by exploiting a time-varying EDL capacitance.[1133]

https://doi.org/10.1021/acs.chemrev.1c00396
Chem. Rev. 2022, 122, 13547−13635

5.2. Inverse Electrosorption Methods

5.2.1. CapMix. In 2009, Brogioli proposed a method (later called "capacitive double layer expansion," or CDLE) to extract energy from the concentration gradient between two feeds, as shown in Figure 40.[1134] Unlike reverse ED and PRO, CDLE was founded on the concept of an electrochemical capacitor (obtained by immersing two electrodes in an electrolyte),[151,1135,1136] which is the basis of water purification in CDI technologies.[110] CDLE can therefore be described as CDI operated in reverse: current is applied to the capacitor when filled with salt water, co-ions are repelled and counterions are attracted at each electrode, and EDLs are formed to store electric charge. After the EDLs are charged (an input of energy) the cell is flushed with fresh water to increase the electric potential, and in turn the electrostatic energy, of the system. The capacitor is then discharged (an output of energy) after which the cell is flushed with salt water to decrease the electric potential for a new cycle. This four-step cycle is demonstrated in Figure 40, and it reveals the possibility of extracting surplus energy due to a concentration gradient in the capacitor.

Brogioli explained the dynamics of EDLs in CDLE using the GCS theory[502−504,1137] and deduced that this process can achieve an energy output of 0.44 kW h per cubic meter of fresh water. By cycling the system at a rate of 1 Hz, the power output of CDLE would be comparable to that of membrane technologies for energy production. In 2011, Brogioli et al. assessed the performance of CDLE in a larger prototype and observed an efficiency of up to 20 times what was reported originally in ref 1134.[1138] To analyze the dynamics of CDLE and improve subsequent designs of these prototypes, Rica et al. mathematically modeled the electrodiffusion of ions as well as their adsorption and desorption in porous electrodes.[1139,1140] These models, which accounted for adsorption of both charge and salt, were based on a macroscopic formulation of ion diffusion and Ohm's law in porous media.

The original design by Brogioli had intrinsic technical deficiencies in that it was sensitive to impurities like DO and exhibited self-discharge.[1141] Several research groups improved the efficiency of energy conversion by introducing IEMs to the supercapacitor flow cell.[1142−1146] This system, which came to be known as capacitive Donnan potential (CDP), combined elements of reverse ED and Brogioli's capacitive method to both produce an electric potential across an IEM and store charge in the EDLs of porous electrodes.[1147] The method of Sales et al. was based on a fixed external resistance, and their work was followed by a study in which Liu et al. supplemented the charging cycle using an external power supply to ultimately draw more power.[1148] Shortly afterward, Brogioli et al. discovered that activated carbon behaves as a polarizable electrode on short time scales but reverts to its spontaneous (self) potential on long time scales, which limits the maximum power output of CapMix systems that use activated carbon as electrodes.[1149,1150] The authors attributed this effect to leakage of stored charge caused by unwanted electrochemical reactions.

To overcome the limitations of traditional carbon electrodes, researchers examined new geometries and arrangements for both the electrodes and IEMs, which enabled continuous operation[669,1151] and increased power output.[1152,1153] These advancements were accompanied by the use of novel materials for the electrodes, such as porous activated carbon coated with polyelectrolytes, to reduce the leakage current.[1154−1158] These so-called "soft electrodes" generate electrical energy in response to changes in both the capacitance of the EDL and the Donnan potential of the polyelectrolyte coat during exchange of electrolytes.

5.2.2. BattMix. In 2011, La Mantia et al. introduced a novel electrochemical system called the "mixing entropy battery" that extracted energy from a concentration gradient but then stored the energy in the bulk crystal structure of the electrodes.[896] The novelty of this BattMix system was in the use of a redox-active material, namely NMO, for the cathode (with Ag/AgCl for the anode), which improved the performance and efficiency of energy harvesting compared to supercapacitor electrodes made of activated carbon.[1159] The BattMix cell is first charged by applying an electric field that electrochemically transports Na^+ and Cl^- from the corresponding electrode into a dilute electrolyte. The cell is then discharged by exchanging this electrolyte for a concentrated one, which drives Na^+ to intercalate into the MnO_2 cathode and Ag to be oxidized to Ag^+ at the anode. Because the energy produced during discharging is greater than that expended during charging, net-positive energy can be harvested from this controlled mixing of two electrolytes. Following La Mantia et al., the scientific community developed and tested other redox-active materials (see section 4.2), such as PBAs,[1160−1164] inorganic compounds of metals,[1165−1167] and copper ammonia redox couples,[1168,1169] as well as conventional battery electrodes, such as zinc and silver.[1170,1171]

Like capacitive electrodes in CapMix, redox-active electrodes in BattMix are electrical accumulators that can store and release charge, and these two methods are broadly classified as accumulator mixing technologies.[1172] Marino et al. examined the electrochemical kinetics of these technologies and determined that supercapacitors (CapMix) can deliver a larger specific power than batteries (BattMix).[1173] The authors also observed that the kinetics of capacitive electrodes are controlled by the diffusion of ions in the electrolyte,[1140] whereas the kinetics of redox-active electrodes are controlled by the diffusion of intercalated sodium.[1174] To limit the shortcomings of each class of materials, Lee et al. designed a hybrid accumulator mixing system that comprised a battery electrode (NMO), a capacitive electrode (activated carbon), and an AEM.[1175] This system extracted an amount of energy per unit membrane area three times greater than that achieved by previous CapMix designs, including those with IEMs. Tan and Zhu also built a hybrid accumulator mixing system using CuHCF for the cathode and Bi/BiOCl for the anode.[1156] Instead of including an IEM, however, Tan and Zhu coated the electrodes with a polyelectrolyte material to boost power output. Future work in the area of electrochemical energy harvesting includes creating better and more cost-effective materials, improving device configuration and assembly, and carrying out pilot studies.[1176]

6. PERFORMANCE COMPARISONS AND PROCESS INTENSIFICATION

Now that we have presented and discussed the basic principles of emerging electrochemical methods for water purification, we compare the performance of these technologies by quantifying energy demand, energy efficiency, and performance trade-offs. A fair and comprehensive comparison of these metrics is generally difficult, and only a few studies have been published which mainly compare one electrochemical method (typically ED or CDI) with RO. In this section, we expand the existing

https://doi.org/10.1021/acs.chemrev.1c00396
Chem. Rev. 2022, 122, 13547−13635

work on performance comparisons by quantifying similarities and differences between the electrochemical methods discussed in this review. From these comparisons, we highlight the kinds of applications where each technology could provide the greatest benefit. Finally, we conclude this section by discussing pathways and challenges associated with scale up as well as opportunities for process intensification by combining electrochemical methods to achieve unique capabilities.

6.1. Energy Demand

Electrochemical methods have the potential to lower the cost of processing brackish water (<15 g of total dissolved solids per liter) as well as feeds that are dilute (<1 g of total dissolved solids per liter) but contaminated with hazardous substances.[123,1177] Unlike conventional desalination methods (e.g., distillation, RO), electrochemical processes are well suited for these tasks because their demand for electrical energy is often proportional to the amount of salt removed (for instance by electrokinetics or electrosorption) and not the volume of water treated. To demonstrate how this distinction influences energy demand, Hemmatifar[1178] compared RO with a generic electrochemical process (EC) based on the analyses in refs 1177 and 1179. RO consumes energy, $\hat{E}_{RO}$ (per unit volume of permeate), primarily in the form of mechanical work needed to overcome of the osmotic pressure of the feed:

$$\hat{E}_{RO} \approx \frac{1}{\gamma}(\Delta P + \Delta\pi) \tag{17}$$

where ΔP and $\Delta\pi$ are the differences in hydrodynamic and osmotic pressures, respectively, and γ is water recovery. The hydrodynamic pressure difference is related to productivity, $\mathcal{P}$ (volumetric throughput normalized by active surface area, in units of $L\,h^{-1}\,m^{-2}$), and membrane permeability, L_p (in units of $m\,s^{-1}\,Pa^{-1}$), by Fick's law: $\Delta P = \mathcal{P}/L_p$. The osmotic pressure difference is related to the difference in salt concentration, Δc, across the membrane by the van't Hoff equation: $\Delta\pi = iRT\Delta c$, where i (≈ 2) is the van't Hoff factor.

In contrast to RO, electrochemical processes consume electrical energy to transport ions and activate electrochemical reactions. These processes are subject to losses in the form of overpotentials, which represent energy lost as heat to the surroundings. Overpotentials in electrochemical systems are grouped into three categories, namely activation (the potential difference above the equilibrium value needed to produce a current in a redox event), concentration (the potential difference across a diffusion layer near the electrode), and resistance (the potential difference caused by resistances in conducting ions and electrons).[1180] Hemmatifar showed that the energy demand, $\hat{E}_{EC}$ (per unit volume of diluate), can be approximated based on ionic and Ohmic (resistive) losses:[90]

$$\hat{E}_{EC} \approx \frac{I^2\mathcal{R}_s}{\gamma Q} \tag{18}$$

where I is current (assumed to be constant under galvanostatic operation) and $\mathcal{R}_s$ is the equivalent resistance of ionic and Ohmic losses in series. This approximation holds unless the separation is slow and parasitic reactions dominate. Electrical current is related to the change in concentration as $I \approx FQ\Delta c/\Lambda$, where Λ is cycle efficiency. The quantity Λ equals the ratio of salt removed to electric charge fed (both in moles), and it is used to empirically account for coupled inefficiencies due to charge transfer, EDLs, and fluid flow.[1178,1181] Figure 2 presents estimates of the volumetric energy consumed by RO and EC using the equations above and the parameters in ref 1178.

These results confirm that although the energy required by RO is a linear function of concentration when the feed is salty (and $\Delta\pi$ is large compared to ΔP), it becomes nearly independent of concentration in the dilute limit. Thus, for feeds that would be classified as either brackish water or fresh water, $\hat{E}_{RO}$ is bounded by the mechanical work needed to sustain the hydrodynamic pressure, which is independent of concentration. The energy demand of EC, on the other hand, scales approximately as $(\Delta c)^2$ over the entire range of concentrations, which implies that electrochemical processes should in theory be significantly less energy intensive than RO for desalination of dilute feeds. Although the estimates in this analysis are based on a specific set of parameters (e.g., water recovery, productivity, cycle efficiency), the general trend in energy consumption can be generalized to any electrochemical method that removes solute from solvent. Electrochemical processes thus offer a unique opportunity to efficiently purify brackish water and other dilute but contaminated feeds.

6.2. Energy Efficiency

Although we have shown that electrochemical methods should theoretically be efficient in the dilute limit, the energy demand in practice has so far been tens or hundreds of times the thermodynamic minimum (see Figures 2 and 42). These values correspond to thermodynamic efficiencies, η_{thermo} (ratio of the free energy of separation to the input of electrical work), of only a few percent, which reveals the extent of dissipation (or energy loss) in state-of-the-art electrochemical systems. This gap between the thermodynamic limit and real efficiencies, however, is expected for emerging methods and presents an opportunity for the improvement of electrochemical technologies. In the early days of RO, for example, thermal distillation used to be the state-of-the-art method to desalinate seawater. But from the 1970s to 2008, the consumption of electrical power by RO systems was reduced by almost 90%, from approximately 16 to 1.8 $kW\,h\,m^{-3}$, which is near the theoretical minimum energy of 1.1 $kW\,h\,m^{-3}$ needed to desalinate seawater with a water recovery of 50%.[68] These improvements resulted in the widespread implementation of RO, which today is considered the leading process for seawater desalination based on installed capacity and annual growth.[12]

Dissipation in electrochemical systems leads to inefficiency and may be caused by the dynamics of electrokinetics and electrosorption, ionic and Ohmic losses, parasitic losses due to charge transfer, hydrodynamic dispersion and fluid mixing, or mechanical work required to pump the electrolyte. We emphasize that all electrochemical processes exhibit a complex trade-off between kinetics (measured in terms of productivity) and energetics.[90,741,760,762] As predicted by the simple model in eq 18, a fast process (one that is operated at high current) consumes more energy but achieves the same level of separation as a slow process,[762] although this fact holds for all desalination processes because more entropy is generated when operating farther from equilibrium.[72,1182] Similarly, a slow process may be inefficient because of the dominance of parasitic side reactions,[90,760] and so it is critical to understand these trade-offs and quantify the kinetics and energetics of the separation method under consideration.[741]

With these general guidelines established, researchers have sought to develop efficient electrochemical processes by

https://doi.org/10.1021/acs.chemrev.1c00396
Chem. Rev. 2022, 122, 13547−13635

engineering improved systems, materials, and operating conditions. Systems to improve energy efficiency were designed, such as cyclic recovery of stored energy, reduction of series resistances,[756,760] and use of membranes in electrosorption methods.[753,1183] Materials to suppress parasitic reactions were developed, including redox-active electrodes[96] and intercalation materials,[116,127,944] and operating parameters were tuned, like flow rate, current, and voltage.[753,758−760,763,1184,1185] The use of IEMs directly adjacent to the electrodes in electrosorption was first reported by Andelman and Walker,[1186] and this approach was since pursued by many researchers.[637,753,1183,1187,1188] The selectivity introduced by these membranes increases charge efficiency by allowing for voltage reversal and increasing the capacity of adsorption.[1188] One disadvantage of using IEMs, however, is that they can incur additional capital costs that exceed those of all other components in an electrochemical device.[741]

To suppress parasitic side reactions, which often severely compromise efficiency,[90] researchers have developed and used redox-active electrodes that guide the transfer of electrons toward redox groups.[96] For example, organometallic and metallopolymeric electrodes were used in an asymmetric Faradaic CDI system and led to no appreciable changes in the pH of the treated solution, which indicated that water reactions were indeed suppressed.[909] The authors also demonstrated stability of pH when the system was operated in batch mode before complete oxidation of the electrodes. A second class of materials that has been developed to control parasitic side reactions are intercalation electrodes.[944] For instance, Kim et al. developed a battery desalination system using identical sodium intercalation electrodes, namely CuHCF, with one or more IEMs to partition successive channels of diluate and concentrate. A triple-stack device with five IEMs showed a 10-fold reduction in energy consumption compared to an MCDI device operated under the same conditions. Again, these improvements in performance must be weighed against the capital cost incurred by using additional membranes.

The third standard approach to improve energy efficiency is to optimize the operating conditions of the process. One example is reported by Hemmatifar et al., who showed that careful selection of the operating conditions in CDI can increase the thermodynamic efficiency up to 9%.[760] These high efficiencies were achieved by operating the system at constant current, recovering energy during discharging, balancing the rates of charge transfer and fluid transport (which represent the rates of adsorption and ion advection, respectively), limiting the window of voltages to between 0.4 and 1 V (higher voltages trigger side reactions and smaller ones diminish charge efficiency), and lowering series resistances by using current collectors made of titanium mesh separated by thin (30 μm) spacers. In another study, Ramachandran et al. proposed the use of alternating electrical current and successfully removed much of the salt fed without compromising energy efficiency.[1185] The alternating current was sustained at the intrinsic resonant frequency of the system (equivalent to the time constant of an RC circuit), which was shown to be inversely proportional to the geometric mean of residence time and charging time. In a similar way to electrical current, the flow profile can be better controlled to improve performance, particularly in systems that are cyclic like CDI and Faradaic electrosorption. The main issue that arises in systems with uncontrolled flow profiles is hydrodynamic dispersion, which inadvertently mixes diluate (produced during adsorption) and concentrate (produced during desorption). A recent study showed that hydrodynamic dispersion (a phenomenon that increases mass diffusivity by an amount proportional to the square of the average fluid velocity) can be inhibited by reducing the flow rate during the discharging step.[763] Using this approach, water recovery was increased to about 90% (compared to 50% with the flow rate fixed) without compromising desalination, productivity, or energy efficiency. In fact, the increase in water recovery enhanced the thermodynamic efficiency by up to a factor of three. Management of electrical input and fluid flow can thus improve existing electrochemical systems at minimal cost.

6.3. Performance Trade-offs

Our discussion in the previous section would be incomplete without quantifying the performance of electrochemical methods because there are underlying trade-offs between kinetics and energetics in any separation process. For this reason, the desalination community uses productivity and energy consumption (per unit volume of diluate) as the two core measures to both quantify performance[126,1189,1190] and estimate the capital and operating costs of a plant.[741,762] In this section, we examine the relationship between these two parameters and how they collectively influence thermodynamic efficiency.

Constraining the extent of desalination, productivity and (volumetric) energy consumption reveal complex coupling, as shown in Figure 41. This plot condenses data obtained from 30 CDI experiments reported in ref 1178 into a single graph of energy versus productivity. As noted by Hawks et al.[741] and Wang et al.,[762] these quantities depend on conditions like water recovery, feed concentration, and average reduction in concentration. The data in Figure 41 are interpolated to obtain a curve that corresponds to the following conditions: water

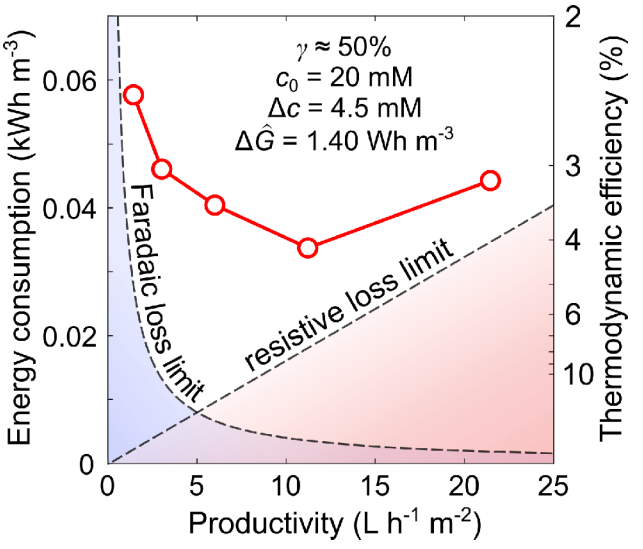

Figure 41. Graphical explanation of the relationship between productivity, energy consumption, and thermodynamic efficiency. Values were obtained by interpolation of data from 30 CDI experiments reported in ref 1178. In this plot, water recovery (γ), feed concentration (c_0), and average reduction in concentration (Δc) are prescribed. The dashed straight line and dashed curved line show qualitative lower limits imposed by resistive and Faradaic losses, respectively.

https://doi.org/10.1021/acs.chemrev.1c00396
Chem. Rev. 2022, 122, 13547−13635

recovery is 50%, feed concentration is 20 mM, and product concentration is 15.5 mM. The free energy of separation, $\Delta\hat{G}$ (per unit volume of diluate), is known and given by

$$\Delta\hat{G} = RT\sum_i \left[\frac{c_{i_0}}{\gamma}\ln\left(\frac{c_{i_B}}{c_{i_0}}\right) - c_{i_D}\ln\left(\frac{c_{i_B}}{c_{i_D}}\right)\right] \tag{19}$$

where the summation is taken over all ions in solution, c_{i_0} is the feed concentration of ion i, and $c_{i_D} = c_{i_0} - \Delta c_i$ and $c_{i_B} = c_{i_0} + \gamma\Delta c_i/(1-\gamma)$ are the concentrations of ion i in the diluate and concentrate (brine), respectively. For a univalent binary electrolyte of a single salt, eq 19 can be rewritten as[760]

$$\Delta\hat{G} = 2RT\left[\frac{c_0}{\gamma}\ln\left(\frac{c_B}{c_0}\right) - c_D\ln\left(\frac{c_B}{c_D}\right)\right] \tag{20}$$

The free energy of separation can then be used to determine the thermodynamic efficiency of a given desalination process:

$$\eta_{thermo} = \Delta\hat{G}/\hat{E} \tag{21}$$

where $\hat{E}$ is the energy consumed per unit volume of treated water.

Figure 41 shows the relationship between productivity and energy consumption in a general electrosorption process. This nonmonotonic behavior can be explained by the fact that energy consumption is governed primarily by resistive losses at high current and can be approximated as

$$\hat{E}_{EC} \approx A\mathcal{R}_s\left(\frac{F\Delta c}{\gamma\Lambda}\right)^2\mathcal{P} \tag{22}$$

where A is total active surface area and $\mathcal{P} = \gamma Q/A$. If cycle efficiency and total resistance are constant, energy consumption and productivity would be directly proportional (see refs 741 and 762 for similar conclusions). The dashed straight line in Figure 41 shows a qualitative lower limit imposed by resistive losses that dominates when productivity is high. At low current, on the hand, energy consumption is determined mainly by Faradaic losses[90] and can be approximated as

$$\hat{E}_{EC} \approx \frac{\mathcal{R}_s I_F^2}{A}\mathcal{P}^{-1} \tag{23}$$

where the charging current was replaced by the Faradaic leakage current, I_F. This simple model, represented by the dashed curved line in Figure 41, shows that energy consumption is inversely proportional to productivity. With the extent of desalination fixed, thermodynamic efficiency can be improved by carefully balancing the counteracting resistive and Faradaic losses.[90]

6.4. Desalination

In this section, we quantify the energy consumed by various electrochemical methods for desalination based on data reported in the literature. Figure 42 shows that the energy needed to desalinate brackish water by these methods ranges mostly between 10 and 100 times the theoretical minimum requirement. In contrast, optimized SWRO systems come within a factor of two (excluding pre- and post-treatment steps) of the thermodynamic limit.[68] As a result, much research is focused on improving electrochemical systems to reliably desalinate brackish water and remove trace contaminants from dilute feeds with energy inputs closer to the thermodynamic limit. Accomplishment of this task requires innovation and optimization of advanced technologies for ion separations. Electrochemical methods are well positioned to be at the forefront of this effort because, as shown in Figures 2 and 42, they can efficiently desalinate brackish water and dilute feeds under a broad range of operating conditions.

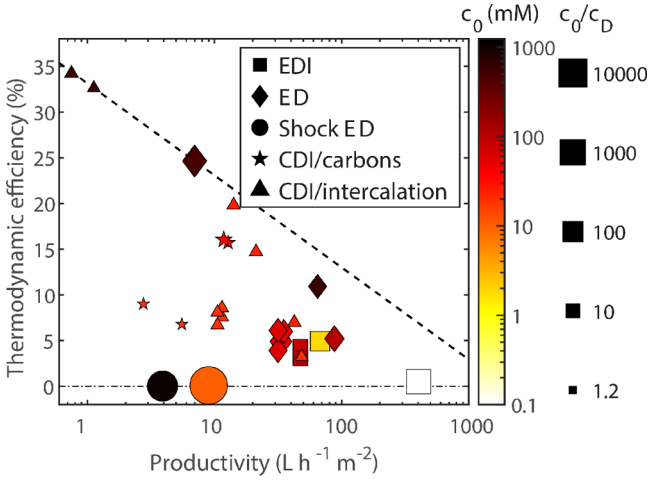

Figure 42. Thermodynamic energy efficiency as a function of productivity for various electrochemical methods performing laboratory-scale desalination of brackish and dilute water. Representative data are presented for EDI (squares),[626,1191,1192] ED (diamonds),[343,1193−1196] shock ED (circles),[87,587] and CDI with either carbon electrodes (stars)[639,760] or intercalation electrodes (triangles).[718,914,944] The color and size of each data marker represent feed concentration and the ratio c_0/c_D (see eq 19), respectively. The dashed line represents an (approximate) empirical efficiency limit and is given by $\eta_{thermo} = 0.331 - 0.101\log_{10}(\mathcal{P})$, where $\mathcal{P}$ is in units of L h^{-1} m^{-2}.

Figure 42 plots the thermodynamic efficiency (eq 21) versus productivity for several electrochemical systems used for desalination. Here, we use the definition of productivity given by Hawks et al.:[741]

$$\mathcal{P} = \frac{V_D}{nA} \tag{24}$$

where V_D is the volume of diluate, A is the projected membrane or electrode area of a single cell or a cell pair, and n is the number of cells or cell pairs (an alternative definition, which is not used here, is based on total membrane area and sets $n = 1$; this definition differs from eq 24 by a factor of two). The methods considered in Figure 42 include EDI (squares), ED (diamonds), shock ED (circles), and CDI with either carbon (stars) or intercalation (triangles) electrodes. The color of each marker represents feed concentration, and marker size corresponds to the ratio c_0/c_D, which quantifies salt rejection. The data in Figure 42 reveal a trade-off between energy consumption and productivity, where systems with higher productivity generally exhibit lower efficiency. We also observe a quantitative trend where all data points fall below a straight line, which we argue is an empirical efficiency limit at this time for desalination by the electrochemical methods considered in this review. Devices near this line are among the most efficient electrochemical systems currently used for desalination. In the

https://doi.org/10.1021/acs.chemrev.1c00396
Chem. Rev. 2022, 122, 13547−13635

future, further development and optimization will lead to devices that can surpass this empirical limit.

On the basis of Figure 42, CDI with membranes and intercalation electrodes as well as ED are the most efficient electrochemical systems for desalination, with maximum values of 34.2% for CDI ($\mathcal{P} < 1\,\mathrm{L\,h^{-1}\,m^{-2}}$) and 24.6% for ED ($\mathcal{P} = 7\mathrm{Lh^{-1}m^{-2}}$). At the same time, these systems have primarily been used to remove small quantities of salt (c_0/c_D equals up to 5.6 for carbon CDI, 1.5 for intercalation CDI, and 44 for ED). In contrast, methods like EDI and shock ED display lower energy efficiency but have mainly been used to deionize water (c_0/c_D equals up to 500 for EDI and 10^4 for shock ED). For nearly all the systems presented in Figure 42, water recovery ranges between 31% and 86% (in this context, water recovery is defined as the ratio of diluate volume to total feed volume, including electrode streams). One ED system, however, achieved only 4% water recovery ($\eta_{thermo} = 4.91\%$ and $\mathcal{P} = 33.3\,\mathrm{L\,h^{-1}\,m^{-2}}$) due to the high flow rates of the electrode streams, which were not recirculated.[1194]

6.5. Scale Up and Optimization

6.5.1. Electrodialysis. As explained in section 3.1, the cost of desalination by ED depends on the concentration of ions in the feed. In electromembrane processes, ion concentration determines current density and membrane area, both of which contribute to capital and operating costs and influence process efficiency. For example, a more conductive membrane results in faster ion transport, lower stack resistance, and less energy consumption. Faster ion transport also reduces the membrane area required by the device. Meanwhile, to separate the various components of a feed, the system needs a selective membrane. Numerous studies have focused on preparing IEMs with improved electrochemical properties, for example by employing functional nanomaterials and advanced surface modifications.[344,1197−1199] These efforts have shown noticeable improvements in the electrochemical properties of IEMs and ultimately in the performance of ED systems.[124] Today, ED stacks can operate at industrial throughputs and are commercially available from many companies, including PCCell, Suez Water Technologies and Solutions, Pure Water Group, and Hydro Volta. These ED systems have been deployed for a variety of applications, including brine desalination, wastewater treatment, nutrient recovery (e.g., nitrogen, phosphorus), whey and sugar demineralization, juice deacidification, and wine stabilization.[125,417,435,1200−1205]

In most of these applications, ED systems are subject to organic fouling, as discussed in section 3.6.[1206] Strong hydrophobic interactions between the membrane and organic species can lead to irreversible adsorption and an increase in membrane resistance.[1205,1206] Surface modifications with polyelectrolytes have thus attracted much interest in the design of fouling-resistant IEMs.[345,629,1207,1208] These modifications significantly increase the hydrophilicity of membrane surfaces and are simple to perform. Today, IEMs are manufactured by several companies, including DuPont (Nafion), Chemours (Nafion), ASTOM (Neosepta), AGC Chemicals (Selemion), and FUMATECH BWT (Fumasep), and much research has been devoted to improving the durability and lowering the cost of these membranes.[418,423,1209,1210]

In practice, an ED stack may comprise hundreds of membrane pairs to achieve a sufficient membrane area when operating at high throughput.[417] A large number of membrane pairs and compartments, however, increases the resistance of the stack, and so ED is usually built with thin spacers and gaskets (thicknesses are commonly in the range of 0.5−2.0 mm) to lower this resistance.[1211] The narrow channels and compartments created by these thin spacers also induce a high cross-flow velocity, which elevates the pressure difference between the diluate and concentrate compartments. This pressure difference must be controlled to prevent excessive stress on the membranes.[1212] Another effective way to decrease stack resistance and improve performance is to use thinner membranes.[1072,1213] Reducing the thickness of the membranes, however, must be accompanied by improving their mechanical properties, as thinner membranes can become mechanically delicate. Profiled (or patterned) membranes are some of the latest developed IEMs that are used to boost the performance of electromembrane processes. With their nonflat, patterned surfaces, profiled membranes enhance fluid mixing at interfaces and in turn improve ion transport.[1214] In the future, ED may even require no spacer, which would further reduce the stack resistance and fabrication cost of ED.

6.5.2. Electrodeionization. One aspect of EDI that remains an important research topic is resin configuration.[483] Devices with mixed-bed configurations are commonly used to boost the removal of ions present at low concentrations by exploiting water dissociation. Random contact between cation and anion exchange resins in this configuration, however, may negatively impact ion transport due to reverse junction leakage.[1215] Separated and layered beds are alternative configurations that improve current efficiency by providing more pathways for ion transport,[1215] although the stack may need additional compartments or special spacer designs to maintain the resin in layers.

The loose resin beads in EDI can accumulate at the end of compartments or near the electrolyte outlets, which increases the pressure drop across the device.[1216] Accumulation of resin beads can also lead to an uneven distribution of current and suboptimal ion transport. One solution to this problem is to introduce ion exchange resin wafers, which are made of resin beads bound and immobilized into a porous matrix.[83,457,466,1217−1219] These wafers ensure a mechanically stable distribution of the resin and prevent accumulation of resin beads. The binder material used in resin wafers could be either insulating[83] or conducting,[467] and water splitting could be promoted by incorporating a catalyst in Janus bipolar resin wafers.[466]

Additional design features have been introduced to EDI systems to further improve their performance. One example, known as fractional EDI, involves the division of an EDI cell into a sequence of stages to optimize the distribution of electrical current.[482,1220] A fractional EDI cell comprises two or more separated pairs of electrodes to divide the power supply into amounts appropriate for each pair. In this way, the energy consumption can be lowered, and selective separations based on the charge of the impurities can be achieved.[1220] Moreover, this design is better at limiting the formation of mineral scale because concentrates from different fractions are separated, which prevents interaction between multivalent ions from one fraction and the OH^- generated in another.

6.5.3. Shock Electrodialysis. The principles discussed in sections 6.5.1 and 6.5.2 are also relevant to the engineering of shock ED, although scaled-up commercial systems have yet to be demonstrated. As in ED or EDI, stacks of repeated layers may serve to lower the energy cost of driving electrical current

https://doi.org/10.1021/acs.chemrev.1c00396
Chem. Rev. 2022, 122, 13547−13635

at the electrodes relative to that of driving separations in all the layers,[1221] although it may be possible to achieve similar efficiency at lower cost and complexity by using fewer but thicker porous layers at the centimeter scale.[87,95] Performance of shock ED may also be improved by varying the charge and microstructure of the porous material.[529,585,1222] Similar hierarchical porous media as in EDI, such as immobilized beds of ion exchange resin,[83,466,467] could be used to boost electromigration (compared to surface conduction in a glass frit) and promote shock formation and ion separations in the depletion zone. It may also be possible to lower capital costs and improve performance by replacing the IEMs used to initiate shock waves with thin, nanoporous ceramic or polymer layers analogous to the nanochannel junctions used in microfluidic ICP.[93,553,557]

6.5.4. Capacitive Deionization. Today, CDI systems are available from several water technology companies. The first to develop a commercial CDI system was Voltea (founded in 2006), and it was followed by other companies including Ur-Water, Atlantis Technologies, Idropan dell'Orto Depuratori, EST Water Technologies, Siontech, and InnoDI Water Technologies.[1223,1224] As discussed in section 4.1.3, energy consumption by CDI has been extensively studied, and recent research demonstrated the possibility of combining photovoltaics and batteries to power a pilot CDI plant for remote applications.[795] Because pumping also contributes to the total energy demand, there has been growing interest in process design to reduce pumping costs.[795] For example, Nordstrand et al. recently designed a parallel arrangement of cells with symmetrically distributed flows to maintain a low pressure drop across the system.[648] Another challenge during scale up of CDI is to make the process continuous, which has been the focus of FCDI[809,825,826,1225] and multichannel MCDI[936,955,1226,1227] systems. The latter enables continuous production of both fresh and brine streams by periodically switching the products of the middle and side channels.[1226] Technoeconomic analyses of CDI also show the importance of achieving long system lifetimes, as capital costs (e.g., electrodes, membranes, frames, current collectors) are expected to outweigh operating costs (e.g., electricity, materials, labor).[775,1228,1229] In particular, it is necessary to understand and mitigate electrode degradation[655,785] (see section 4.1.5) and cell fouling (see section 4.1.6). Several other publications on CDI optimization and pilot systems provide additional design rules and principles for scale up.[648,774,795,825,1224,1225,1227,1230−1233]

6.5.5. Faradaic Electrosorption. Redox-based separation technologies remain an emerging area of research, and there are only a few preliminary studies on scale up and technoeconomic analysis. In one example, Joo et al. demonstrated a pilot electrochemical system using $LiMn_2O_4$ to selectively recover lithium from the desalination concentrate produced by RO and membrane distillation.[1234] This continuous system comprised 14 pairs of λ-MnO_2 and Ag electrodes arranged in parallel, and it was sequentially submerged in solutions for capturing, washing, and cleaning to recover the lithium. The system processed the desalination concentrate at a flow rate of 250 L h^{-1} and produced an up-concentrated lithium solution with 88% purity and an enrichment factor of 1800. Metzger et al. conducted a comprehensive technoeconomic analysis on MCDI, HCDI, and intercalation CDI.[915] This analysis showed that, compared to MCDI, intercalation CDI can achieve higher removal capacity and is more cost-effective and energy efficient.[915,1235] To treat equal volumes of water with similar performance, for example, an intercalation CDI module would cost only 27% of an MCDI module and would be four times smaller in size.

It has been shown, for certain applications, that electrochemical systems with redox reactions can be more cost-effective than conventional desalination methods. Kim et al. designed a system with redox-active electrodes to valorize proteins from whey waste and performed a preliminary technoeconomic analysis.[1236] To produce equal volumes of whey protein, the redox desalination system consumed up to 72% less energy than ED by driving redox reactions rather than water splitting. Moreover, the use of fewer IEMs in the redox system relative to ED lowered capital costs by 62%.[1236] Further progress in redox separation technologies requires a focus on device scale up, uncomplicated and economical synthesis of electrodes, long-term stability, and innovative stacking methods.[1237]

6.6. Process Intensification

Many of the methods discussed in this review are still under development, and it is anticipated that innovations in materials science, device engineering, and process design will continue to advance these technologies. In addition to these advancements, process intensification can be undertaken to achieve more holistic (or global) improvements in electrochemical methods for water purification. Process intensification is any integration of unit operations, functions, and phenomena that leads to a smaller, cleaner, safer, and more efficient technology.[1238,1239] Emerging electrochemical methods provide new opportunities for process intensification by combining these systems with either other emerging methods or established technologies that are complementary in function.[577,1240,1241] In an electrochemical method, the electric field enables selectivity and interfacial control, promotes fast reaction rates, and reduces energy consumption.[1240,1242] Advances in electrocatalysis have revealed that existing thermal and chemical methods can in fact be replaced by novel electrochemical processes.[1243,1244] Because of the importance of product purification, waste processing, and materials recycling, separations based on electrokinetics and electrosorption can play a key role in process intensification. Examples of process intensification for electroseparations include integration of reaction and separation using redox interfaces (as shown in Figure 29)[102,1021] as well as selective recovery of target species from waste streams using shock ED.[577]

The dual nature of electrochemical systems, highlighted by cells with asymmetrically configured electrodes, provides a new conceptual platform for process intensification.[102,909,1021] Although some Faradaic reactions are unwanted and can compromise efficiency, others can drive separations and promote catalysis.[96,655] In section 4.3, we explained that molecular design of Faradaic processes enables electrosorptive removal of heavy metal oxyanions and simultaneous redox transformation at the counter electrode. In one such example, As(III) was captured and transformed into As(V) using PVF and PTMA as electrodes,[102] and in another, Cr(VI) was captured and transformed into the less harmful Cr(III) using PVF and platinum as electrodes.[1021] Both of these systems involved electron transfer, which activated the redox units, and Faradaic reactions, which transformed the target metals into more benign products. Asymmetric combinations of intercalation systems and BDD electrodes have also been proposed

https://doi.org/10.1021/acs.chemrev.1c00396
Chem. Rev. 2022, 122, 13547−13635

for removal of both lithium and organic pollutants from industrial wastewater, as shown in Figure 43.[1245] Li^+ was

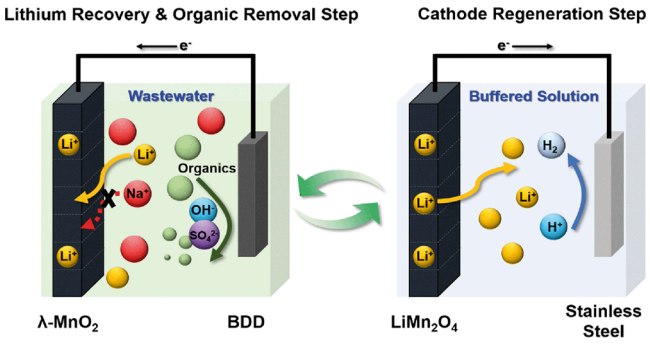

Figure 43. Schematic of an electrochemical system with $LiMn_2O_4$ and BDD as electrodes for removal of both lithium and organic pollutants from industrial wastewater. Reproduced with permission from ref 1245. Copyright 2018 Royal Society of Chemistry.

recovered (in excess of 98%) using an MnO_2 electrode with high selectivity toward Li^+ relative to Na^+, and more than 65% of the organic pollutant was decomposed at the stainless steel counter electrode. Kim et al. observed a trade-off, however, between the utilization efficiency of $LiMn_2O_4$ and the rate at which Li^+ could be recovered.[1245] Moving forward, we expect a growing set of concepts that combine separations and reactions for water purification.

Electrokinetic methods can also be used for molecular separations to effectively remove harmful contaminants or recover valuable targets.[479,577] For example, Li^+ can be selectively captured from a multicomponent mixture and recycled (or reused elsewhere) by integrating CDI with intercalation materials[88,655] as a second step following shock ED.[577] As shown in Figure 44, process intensification of this kind can in principle be achieved in two steps. In the first step, shock ED is used to concentrate waste in the brine, from which Li^+ is selectively captured in the CDI unit by intercalation into an appropriate electrode such as $LiFePO_4$ or $LiMn_2O_4$.[691,925,1246−1248] During this process, all cations are driven toward the intercalation electrode, but Li^+ will be predominantly inserted into its crystal lattice because the vacancies in $FePO_4$ are well fitted for this small monovalent cation. Moreover, the anions are inserted into a porous carbon electrode, so fluid leaving the device will be depleted of Li^+ and its counterion(s). In the second step, Li^+ and its counterion(s) are released from the electrodes by reversing the direction of the applied electric field, and the fresh stream produced by shock ED is passed through the CDI unit to collect these ions.

Process intensification of electrochemical methods not only enables targeted separations but also dramatically reduces energy consumption. By comparing the energetics of sequential and coupled Faradaic processes, Kim et al. lowered the energy needed to remove arsenic from 2.2 to 0.45 kW h mol^{-1}, as shown in Figure 45.[102] The basis of this energy integration was to reduce parasitic side reactions and improve current efficiency by using asymmetric redox systems. Relative to systems with nonselective electrodes (e.g., CDI with porous carbon electrodes), energy efficiency was improved by nearly an order of magnitude. Similarly, in recent work on PFAS capture by electrochemical mediation with TEMPO-based polymers, an asymmetric system of TEMPO copolymers with a BDD counter electrode achieved reactive separation of PFAS.[1028] During release of the PFAS by the redox polymer, the BDD electrode simultaneously broke down PFAS with little energy consumption and a defluorination efficiency over 50%. Electroseparations can therefore enable processes that would otherwise be prohibitively expensive or complex, such as purification of dilute feeds, recovery of metals, valorization of wastes, and isomeric separations of biochemicals and pharmaceutical compounds.[105,154,1241,1249] As shown in this review, electrokinetics and electrochemistry can improve energy efficiency and reduce secondary waste, which enables cleaner and more sustainable processes for water purification.

7. CONCLUSIONS AND OUTLOOK

Electrochemical methods for water purification use applied electric fields to remove contaminants by either degrading or converting them through redox reactions, driving their separations in a bulk electrolyte, electrostatically trapping them in an EDL (where they may undergo electrochemical reactions), or intercalating them in solid electrodes. The ability to remove contaminants directly from water, as opposed to removing the water from the contaminants, is the property that

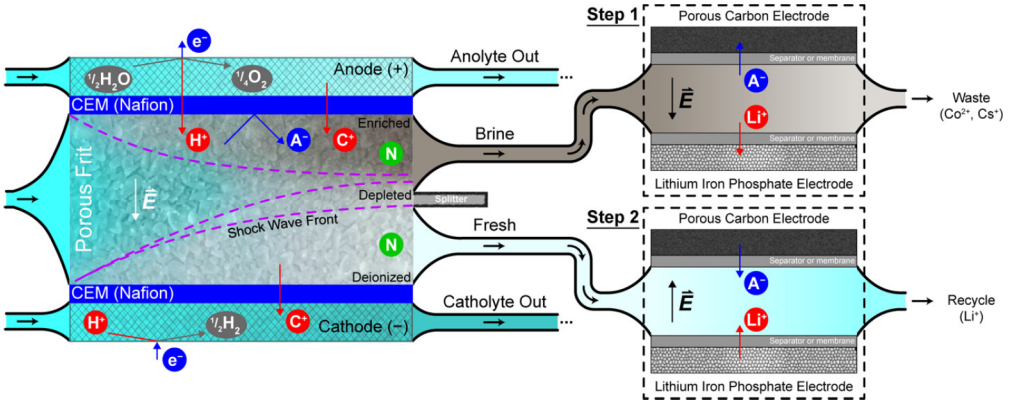

Figure 44. Process intensification of shock ED (left) by integrating CDI (right) to recycle Li^+ in two steps. The first step is selective capture of Li^+ in the intercalation electrode of a CDI unit from the brine discharged by shock ED. The second step is release of Li^+ into the fresh stream produced by shock ED by reversing the direction of the applied field. Cations other than Li^+ and H^+ are labeled C^+, anions are labeled A^-, and neutral species (unaffected by the electric fields) are labeled N; streams are colored based on the relative concentration of ions. Reproduced with permission from ref 577. Copyright 2019 American Chemical Society.

https://doi.org/10.1021/acs.chemrev.1c00396
Chem. Rev. 2022, 122, 13547−13635

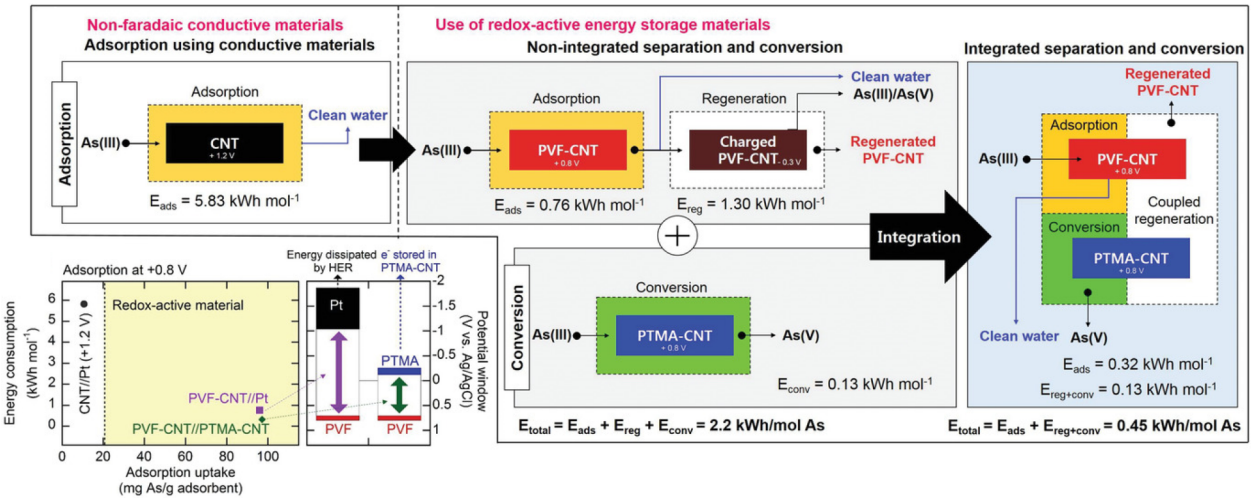

Figure 45. Analysis of energy integration and process intensification using redox electrochemistry with coated electrodes for reactive separations. Reproduced with permission from ref 102. Copyright 2020 Wiley-VCH.

enables most advantages of these methods. Nondestructive electrochemical methods, which are based on electrokinetic (ED, EDI, ICP, shock ED) and electrosorption (CDI, Faradaic electrosorption) processes, tend to be more energy efficient compared to physical methods when used for molecular separations or purification of dilute feeds. These systems have other attractive features including compactness, molecular selectivity, versatility, decreased generation of secondary waste, and the ability to combine reactions and separations. The selectivity and versatility of electrochemical systems enables unique combinations of technologies for exotic separations and recovery of high-value elements. In particular, the dual nature of these systems provides a new conceptual platform for process intensification of existing methods. Significant advances, however, are still needed both at the fundamental level (e.g., to impart higher molecular selectivity to electrodes for emerging applications) and in process engineering through the development of new hybrid systems for higher energy efficiency. Comprehensive work on technoeconomic analysis is also needed for these emerging methods to provide a comparative evaluation against other treatment technologies and identify limitations, areas of opportunity, and protocols for optimal operation. Here, we highlight emerging research directions, challenges, and opportunities in electrochemical methods for water purification, ion separations, and energy conversion.

7.1. Materials Design for Multicomponent Separations

Despite advances in redox-active materials, which have enabled new selectivity and higher uptake, there remain significant challenges in both fundamental studies and new areas of application.

7.1.1. Multifunctional Redox Materials. To enhance selectivity and overcome existing limitations, one promising approach has been to combine several distinct chemical groups. While redox homopolymers are efficient for applications that demand ion selectivity,[96] redox copolymers extend these capabilities by combining orthogonal properties. For example, redox copolymers have enhanced electrochemical regeneration, chemical binding of rare-earth elements,[1250] and control of hydrophobicity, affinity, and electrostatics within redox adsorbents for PFAS molecules and other micropollutants.[1028,1251,1252] Nanostructured combination of two distinct redox polymers has also enabled the reversible electrochemical binding and control of neutral molecules through redox-tunable hydrophobicity.[103] Similar concepts of hybrid materials may be generalized to redox crystals and various multicomponent separations, in which reversibility or selectivity could be enhanced through hybridization to achieve properties beyond the base chemical structure. Moving forward, we envision these multifunctional materials will provide a versatile platform for extraction of multiple desired elements simultaneously.

7.1.2. Computational Design and Operando Electrochemical Tools for Understanding Interactions. To guide the bottom-up design of materials, computational studies play a key role in the selection of chemistry and tuning of morphology. Tools such as MD[719] and electronic structure calculations[1253] have been critical in understanding selectivity in ultramicroporous carbon and redox-active materials, respectively. We envision molecular simulation tools will increase in utility due to the need for a greater understanding of selective interactions and their underlying mechanisms. In addition to computational tools, we expect that the integration of operando electrochemical tools such as vibrational spectroscopy will elucidate interfacial structure and binding mechanisms. These molecular tools, along with macroscopic transport modeling, can help advance the performance of electrochemical separation methods at multiple scales.

7.1.3. Advances in Membrane Materials. Advances in membrane materials can improve the efficiency of electrokinetic processes. Membrane fouling and poor stability under certain operating conditions remain longstanding challenges in electrokinetic systems. Besides, redox materials in electrokinetic systems could pass the membranes and contaminate the treated water. The introduction of more durable, cost-effective, and selective membranes is thus needed for more efficient and reliable electrokinetic systems. Structured nanomaterials are expected to play an important role in improving membrane performance.[1254,1255] Moreover, ion selectivity can be modulated through fine control of the structure, pore size, water permeability, and functional groups of the membranes.[1255,1256]

7.1.4. Multicomponent Mixtures for Separations. Many of the recent studies on selective removal and resource recovery have been performed using idealized simulated

https://doi.org/10.1021/acs.chemrev.1c00396
Chem. Rev. 2022, 122, 13547−13635

solutions. Real industrial and municipal effluents, however, involve complex speciation of ions and organic compounds, which affects both the selectivity and the lifetime of electrodes and membranes. Municipal effluents are often complex multicomponent mixtures that comprise organic substances, inorganic ions, and sometimes biological species,[145,1257] many of which could form unwanted deposits. Groundwater often contains significant organic matter, and the solution can exhibit a range of ionic strengths and pHs. As a result, there is a need to evaluate the performance of functional materials when exposed to real samples[1258] to quantify reliability and stability (e.g., electrochemical, chemical, mechanical). At a fundamental level, these studies may reveal the need for materials modification such as the use of antifouling coatings, which can provide a tunable balance between uptake, selectivity, and stability.

Nutrient recovery and metal recovery are two areas of emerging interest in the development of molecularly selective materials. There have been significant advances in the design of selective materials for nutrient recovery, especially using nanostructured porous carbons.[719] Improving selectivity further requires a deeper understanding of solvation, sterics, and electronic structure interactions due to the similarity in electric charge between nutrient species (particularly NO_3^-) and competing ions. At the same time, many electrosorption systems are still highly dependent on pH during separations,[1259,1260] and because many oxyanions have complex speciations that depend on pH, there have been approaches that leverage electrochemical swings in pH for the recovery of nutrients such as PO_4^{3-}.[813,1260]

The recovery of critical elements from mining, recycling, and industrial wastewater streams is another area of emerging importance for selective separations. Many of these transition metals are present in small amounts and are surrounded by excess competing species of similar valence and structure, which makes ion-selective electrosorption a "needle-in-a-haystack" challenge.[1253,1261] Functionalized carbons and redox-active electrodes have made significant strides toward efficient metal recovery and heavy metal removal.[649,1262,1263] However, there are key challenges still to be overcome, such as achieving higher selectivity between different transition metals within multicomponent mixtures. Rare-earth elements, for example, are often found in the presence of each other as well as other transition metals,[1264] which makes their separation a difficult and costly task. Many competing metals are electroactive at moderate potentials (e.g., copper, lead), and they can often interfere with selective electrosorption processes. Therefore, pretreatment and tuning of electrochemical potentials will be needed to selectively purify multicomponent mixtures.

7.2. Intensifying Water Treatment Processes Through Hybrid Approaches

Electrochemical methods can assist in process intensification by decreasing waste, lowering solvent use, and reducing the number of unit operations. In particular, areas for integration include the direct combination of electrochemical methods with renewable energy sources as well as the development of single-cell reactive separations.

7.2.1. Integrating Renewable Energy Sources and Electrochemical Methods. Coupled with global environmental crises, the development of sustainable manufacturing processes has become a major goal for industries. In this regard, combining electrochemical processes with renewable energy sources (e.g., solar panels) can reduce energy consumption and carbon intensity.[1265] Recently, electrochemical methods for water purification have been hybridized with dye-sensitized solar cells for direct conversion of light to electricity.[1266,1267] The photoanode uses desalinated chloride to generate reactive chlorine species, which can treat wastewater, while the cathode produces molecular hydrogen.[1268] The combination of photoelectrochemistry and redox-flow desalination enables continuous treatment, even in the absence of an external energy source. These systems demonstrate opportunities for the development of processes that integrate energy conversion and electrochemical separations.

7.2.2. Coupling Reaction and Separation. For persistent contaminants, degradation of these species is as important as their removal from water. The coupling of reaction and separation can be a powerful approach for providing modular water treatment, as in the case of capture and breakdown of PFAS.[992,1269] The integration of membrane technologies and electrochemical advanced oxidation processes has gained much attention for treatment of organic pollutants in wastewater. In these hybrid processes, a conductive membrane serves as a flow-through anode, which filters the wastewater and drives oxidation of the organic contaminants and pharmaceutical residues.[1270] Moreover, integration of redox processes and magnetic nanoparticles enables selective separation of various organic and inorganic micropollutants.[1252] We envision that emerging electrosorption and electrokinetic systems coupled with advanced oxidation processes can provide efficient process intensification for wastewater treatment.

7.3. Translation to Practical Applications

While there have been extensive studies of carbon electrode stability,[1271,1272] many of the emerging Faradaic materials have only been examined using idealized solutions. Demonstration of stability and reliability using real samples with relevant electrolyte concentrations is essential. For desalination, electrode stability can be improved by doping the carbon and creating hybrid materials.[1272,1273] It is also important to design materials that suppress parasitic reactions and function at lower potentials, especially when the side reactions involve chloride or oxygen, which often produce unwanted by-products.[655] Proof of economic feasibility is also critical for commercialization of electrochemical systems. Recently, there has been an increase in the number of publications on life cycle assessment and technoeconomic analysis.[1228,1274,1275] These technoeconomic analyses show that the costs of electrodes and membranes are key contributors to the overall capital and operating costs.[915,1228] In practice, technoeconomic analysis will provide a comprehensive framework for assessing feasible electrochemical approaches for water treatment.

In summary, electrochemical systems for water purification and resource recovery are already commercialized in many industries to treat water contaminated with various kinds of waste. Whether or not the emerging purification methods meet their expectations in the areas of water desalination, remediation, and separations, it seems likely that several of these methods will eventually be employed. In the near term, we expect that a deeper knowledge of the transport phenomena and electrochemical kinetics that govern these methods will facilitate their engineering and optimization. In the long term, work directed toward understanding and

https://doi.org/10.1021/acs.chemrev.1c00396
Chem. Rev. 2022, 122, 13547−13635

improving the design of these processes at scale may guide how commercial prototypes should be built for a given application.

AUTHOR INFORMATION

Corresponding Author

Martin Z. Bazant − *Department of Chemical Engineering, Massachusetts Institute of Technology, Cambridge, Massachusetts 02139, United States; Department of Mathematics, Massachusetts Institute of Technology, Cambridge, Massachusetts 02139, United States;* orcid.org/0000-0002-8200-4501; Email: bazant@mit.edu

Authors

Mohammad A. Alkhadra − *Department of Chemical Engineering, Massachusetts Institute of Technology, Cambridge, Massachusetts 02139, United States;* orcid.org/0000-0003-3866-709X

Xiao Su − *Department of Chemical and Biomolecular Engineering, University of Illinois at Urbana−Champaign, Urbana, Illinois 61801, United States;* orcid.org/0000-0001-7794-290X

Matthew E. Suss − *Faculty of Mechanical Engineering, Technion—Israel Institute of Technology, Haifa 3200003, Israel; Wolfson Department of Chemical Engineering and Nancy and Stephen Grand Technion Energy Program, Technion—Israel Institute of Technology, Haifa 3200003, Israel;* orcid.org/0000-0002-3813-2274

Huanhuan Tian − *Department of Chemical Engineering, Massachusetts Institute of Technology, Cambridge, Massachusetts 02139, United States;* orcid.org/0000-0001-5515-9105

Eric N. Guyes − *Faculty of Mechanical Engineering, Technion—Israel Institute of Technology, Haifa 3200003, Israel*

Amit N. Shocron − *Faculty of Mechanical Engineering, Technion—Israel Institute of Technology, Haifa 3200003, Israel;* orcid.org/0000-0002-9247-905X

Kameron M. Conforti − *Department of Chemical Engineering, Massachusetts Institute of Technology, Cambridge, Massachusetts 02139, United States*

J. Pedro de Souza − *Department of Chemical Engineering, Massachusetts Institute of Technology, Cambridge, Massachusetts 02139, United States;* orcid.org/0000-0003-3634-4991

Nayeong Kim − *Department of Chemical and Biomolecular Engineering, University of Illinois at Urbana−Champaign, Urbana, Illinois 61801, United States*

Michele Tedesco − *European Centre of Excellence for Sustainable Water Technology, Wetsus, 8911 MA Leeuwarden, The Netherlands;* orcid.org/0000-0002-3389-5168

Khoiruddin Khoiruddin − *Department of Chemical Engineering, Institut Teknologi Bandung, Bandung 40132, Indonesia; Research Center for Nanosciences and Nanotechnology, Institut Teknologi Bandung, Bandung 40132, Indonesia*

I Gede Wenten − *Department of Chemical Engineering, Institut Teknologi Bandung, Bandung 40132, Indonesia; Research Center for Nanosciences and Nanotechnology, Institut Teknologi Bandung, Bandung 40132, Indonesia*

Juan G. Santiago − *Department of Mechanical Engineering, Stanford University, Stanford, California 94305, United States;* orcid.org/0000-0001-8652-5411

T. Alan Hatton − *Department of Chemical Engineering, Massachusetts Institute of Technology, Cambridge, Massachusetts 02139, United States;* orcid.org/0000-0002-4558-245X

Complete contact information is available at: https://pubs.acs.org/10.1021/acs.chemrev.1c00396

Notes

The authors declare no competing financial interest.

Biographies

Mohammad A. Alkhadra graduated from UC San Diego in 2018 with both a B.S. and an M.S. in Chemical Engineering, after which he moved to Cambridge, MA, to begin his Ph.D. at MIT in the same major. At MIT, Mo focuses on ion separations using shock ED under the supervision of Prof. Martin Z. Bazant.

Xiao Su received his B.S. in Chemical Engineering from the University of Waterloo in 2011 and his Ph.D. in Chemical Engineering from MIT in 2017. He joined the faculty in the Department of Chemical and Biomolecular Engineering at the University of Illinois at Urbana−Champaign (UIUC) in 2019, where he focuses on electrochemical separations and process intensification. His research has been recognized by an NSF CAREER award in 2019 and the ACS Victor K. LaMer Award in 2020.

Matthew E. Suss heads the Cleantech Innovations Laboratory in the Faculty of Mechanical Engineering and Wolfson Department of Chemical Engineering at Technion—Israel Institute of Technology and is affiliated with the Grand Technion Energy Program and Grand Water Research Institute. Prof. Suss serves as a member of the Israel National Research Center for Electrochemical Propulsion (INREP) and as an Israeli delegate to the European Federation of Chemical Engineering (EFCE) working group on electrochemical engineering. Prof. Suss has won numerous national and international research awards, including the prestigious Alon Fellowship and an ARCHES award.

Huanhuan Tian joined the Department of Chemical Engineering at MIT in 2018 and is pursuing her Ph.D. under the supervision of Prof. Martin Z. Bazant. She received her B.S. and M.S. with honors in 2018 from the Department of Engineering Mechanics at Tsinghua University in China. Huanhuan is interested in issues related to energy and the environment, and her current research focuses on mathematical modeling of shock ED for selective ion separations.

Eric N. Guyes is a Ph.D. candidate at Technion under the supervision of Prof. Matthew E. Suss. He arrived at Technion in 2013 as a Fulbright Scholar and later joined Prof. Suss's group in 2014. His doctoral research focuses on the mechanisms and applications of selective ion removal in CDI for water desalination and treatment applications.

Amit N. Shocron is a Ph.D. candidate at Technion under the supervision of Prof. Matthew E. Suss. He received his B.S. and M.S. in Mechanical Engineering also at Technion. His research focuses on CDI for ion selective water treatment and water desalination.

Kameron M. Conforti received his Ph.D. in Chemical Engineering at MIT in 2019, after which he worked as a Postdoctoral Associate in the Department of Mechanical Engineering at MIT. He is currently a Senior Research Engineer in the Competency Research Lab at Saint-

https://doi.org/10.1021/acs.chemrev.1c00396
Chem. Rev. 2022, 122, 13547−13635

Gobain Research North America, where he specializes in modeling heat and mass transfer.

J. Pedro de Souza is a Ph.D. candidate in the Department of Chemical Engineering at MIT. He received his B.S. in chemical engineering at the University of Texas at Austin in 2016. He works with Prof. Martin Z. Bazant on theoretical modeling of the equilibrium structure and transport of ions at charged interfaces.

Nayeong Kim received her B.S. in Chemical and Biological Engineering from the University of Wisconsin−Madison in 2017 and her M.S. in the same major from Seoul National University in 2020 under the supervision of Prof. Jeyong Yoon. She is pursuing her Ph.D. at UIUC under the supervision of Prof. Xiao Su, where she focuses on environmental electrochemistry and integrated electrochemical separations.

Michele Tedesco has a Ph.D. in Chemical Engineering and is currently a scientific project manager at Wetsus. His research focuses on IEMs and related processes, including ED and reverse/bipolar ED, from fundamental modeling to experimental investigation.

Khoiruddin Khoiruddin is an assistant professor in the Department of Chemical Engineering at Institut Teknologi Bandung (ITB), Indonesia. He received his Ph.D. in Chemical Engineering from ITB in 2018. Formerly, he was a process engineer at the membrane company GDP Filter Indonesia from 2009 to 2018. His research interests include design of IEMs and applications of electromembrane processes.

I Gede Wenten is a professor in chemical engineering at ITB, Indonesia. He received his Ph.D. in Chemical Engineering from the Technical University of Denmark (DTU) in 1995. He has extensive experience in membrane technology, both in the industrial and academic settings, with a career spanning over three decades. His research interests include design, preparation, and fouling control of membranes.

Juan G. Santiago received his Ph.D. in Mechanical Engineering from UIUC in 1995. His research includes the development of microsystems for on-chip chemical and biochemical analysis, methods for DNA quantification and hybridization, and CDI. He is a Fellow of the American Physical Society, a Fellow of the American Society of Mechanical Engineering, and a Fellow of the American Institute for Medical and Biological Engineering. He serves and has served as an editor of several journals and cofounded several companies in microfluidics.

T. Alan Hatton is the Ralph Landau Professor and Director of the David H. Koch School of Chemical Engineering Practice at MIT. He earned his B.S. and M.S. from the University of Natal, Durban, and his Ph.D. from the University of Wisconsin−Madison in 1981. As part of the MIT Energy Initiative, Prof. Hatton codirects the Center for Carbon Capture, Utilization, and Storage. His research focuses on the development of electrochemical processes to facilitate chemical separations and to mediate the transformation of capture waste into useful commodity chemicals.

Martin Z. Bazant is the Edwin G. Roos (1944) Chair Professor of Chemical Engineering and Mathematics at MIT. He has made seminal theoretical contributions in electrokinetics and electrochemistry with applications in energy storage, water purification, and microfluidics. Prof. Bazant's awards include the 2015 Alexander Kuznetsov Prize in Theoretical Electrochemistry, the 2018 Andreas Acrivos Award for Professional Progress in Chemical Engineering (AIChE), and the 2019 MITx Prize for Teaching and Learning in Massive Open Online Courses. He consults extensively for industry and serves as the Chief Scientific Advisor for Saint-Gobain Research North America in Massachusetts.

ACKNOWLEDGMENTS

Part of this work was performed in the cooperation framework of Wetsus, European Centre of Excellence for Sustainable Water Technology. Wetsus is cofunded by the Dutch Ministry of Economic Affairs and Ministry of Infrastructure and Environment, the Province of Fryslân, and the Northern Netherlands Provinces (www.wetsus.eu). I Gede Wenten acknowledges financial support from the Indonesian Ministry of Research and Technology/National Agency for Research and Innovation and the Indonesian Ministry of Education and Culture under the World Class University program managed by ITB. J. Pedro de Souza acknowledges support from the NSF Graduate Research Fellowship (award no. 1,122,374). We thank Dr. Ali Hemmatifar for his significant contribution to the writing of this manuscript.

ABBREVIATIONS

AEM = anion exchange membrane
H_2Q = hydroquinone
AOT = brand name of DOSS
HA = hydroxyapatite
BattMix = battery mixing
HBMA = hydroxybutyl methacrylate
BDD = boron doped diamond
HCDI = hybrid capacitive deionization
BDI = battery deionization
HCF = hexacyanoferrate
BMCSL = Boublik−Mansoori−Carnahan−Starling−Leland
HS = high salinity
BSK = Bazant−Storey−Kornyshev
ICP = ion concentration polarization
BWRO = brackish water reverse osmosis
IEM = ion exchange membrane
CapMix = capacitive mixing
LDH = layered double hydroxide
CDI = capacitive deionization
LS = low salinity
CDLE = capacitive double layer expansion
MCDI = membrane capacitive deionization
CDP = capacitive Donnan potential
MD = molecular dynamics
CEM = cation exchange membrane
NASICON = sodium superionic conductors
CIET = coupled ion−electron transfer
NMO = sodium manganese oxide
CNT = carbon nanotube
NMR = nuclear magnetic resonance
CTAB = cetyltrimethylammonium bromide
PANI = polyaniline
CVD = chemical vapor deposition
PAQ = polyanthraquinone
DBS = dodecylbenzenesulfonate
PBA = Prussian blue analogue
DC = direct current
PFAS = polyfluoroalkyl substances
DFT = density functional theory
PNPS = Poisson−Nernst−Planck−Stokes
DO = dissolved oxygen
PPCP = pharmaceutical and personal care product

https://doi.org/10.1021/acs.chemrev.1c00396
Chem. Rev. 2022, 122, 13547−13635

DOSS = dioctyl sulfosuccinate
PPy = polypyrrole
DSA = dimensionally stable anode
PRO = pressure-retarded osmosis
EC = electrochemical process
PTMA = poly-TEMPO methacrylate
ED = electrodialysis
PVF = polyvinylferrocene
EDI = electrodeionization
RC = resistor−capacitor
EDL = electric double layer
RCDI = rocking-chair capacitive deionization
EDS = energy dispersive X-ray spectroscopy
RGO = reduced graphene oxide
EDTA = ethylenediaminetetraacetic acid
RMSS = redox-mediated selective separations
ENAS = energy normalized adsorbed salt
RO = reverse osmosis
ETAS = electrochemically tunable affinity separations
SEC = specific energy consumption
FB = flow-between
SEM = scanning electron microscopy
FBV = Frumkin−Butler−Volmer
SHE = standard hydrogen electrode
FCDI = flow electrode capacitive deionization
SOG = Sudan Orange G
FO = forward osmosis
SWRO = seawater reverse osmosis
FTE = flow-through electrode
TEM = transmission electron microscopy
FUE = ferrocene utilization efficiency
TEMPO = $(CH_2)_3(CMe_2)_2NO$
GCMC = grand canonical Monte Carlo
VF = vinylferrocene
GCS = Gouy−Chapman−Stern

REFERENCES

(1) Mekonnen, M. M.; Hoekstra, A. Y. Four billion people facing severe water scarcity. *Science Advances* **2016**, *2*, No. e1500323.
(2) Hoekstra, A. Y. *The Water Footprint of Modern Consumer Society*; Routledge, 2019.
(3) Kucera, J. *Desalination: Water from Water*; John Wiley & Sons, 2019.
(4) Al-Shammiri, M.; Safar, M. Multi-effect distillation plants: state of the art. *Desalination* **1999**, *126*, 45−59.
(5) Khawaji, A. D.; Kutubkhanah, I. K.; Wie, J.-M. Advances in seawater desalination technologies. *Desalination* **2008**, *221*, 47−69.
(6) Brogioli, D.; La Mantia, F.; Yip, N. Y. Thermodynamic analysis and energy efficiency of thermal desalination processes. *Desalination* **2018**, *428*, 29−39.
(7) Boysen, J. E.; Stevens, B. G. *Demonstration of the Natural Freeze−Thaw Process for the Desalination of Water from the Devils Lake Chain to Provide Water for the City of Devils Lake*; US Department of the Interior, Bureau of Reclamation, Technical Service Center, 2004.
(8) Xie, C.; Zhang, L.; Liu, Y.; Lv, Q.; Ruan, G.; Hosseini, S. S. A direct contact type ice generator for seawater freezing desalination using LNG cold energy. *Desalination* **2018**, *435*, 293−300.
(9) Kiezyk, P.; Mackay, D. Waste water treatment by solvent extraction. *Canadian Journal of Chemical Engineering* **1971**, *49*, 747−752.
(10) Van der Bruggen, B.; Vandecasteele, C. Distillation vs. membrane filtration: overview of process evolutions in seawater desalination. *Desalination* **2002**, *143*, 207−218.
(11) Cath, T. Y.; Childress, A. E.; Elimelech, M. Forward osmosis: principles, applications, and recent developments. *Journal of membrane science* **2006**, *281*, 70−87.
(12) Fritzmann, C.; Löwenberg, J.; Wintgens, T.; Melin, T. State-of-the-art of reverse osmosis desalination. *Desalination* **2007**, *216*, 1−76.
(13) Garcia-Rodriguez, L.; Palmero-Marrero, A. I.; Gómez-Camacho, C. Comparison of solar thermal technologies for applications in seawater desalination. *Desalination* **2002**, *142*, 135−142.
(14) Lienhard, J. H.; Thiel, G. P.; Warsinger, D. M.; Banchik, L. D. *Low Carbon Desalination: Status and Research, Development, and Demonstration Needs, Report of a Workshop Conducted at the Massachusetts Institute of Technology in Association with the Global Clean Water Desalination Alliance*; Massachusetts Institute of Technology, 2016.
(15) Godart, P. Design and simulation of a heat-driven direct reverse osmosis device for seawater desalination powered by solar thermal energy. *Applied Energy* **2021**, *284*, 116039.
(16) Davies, P. Wave-powered desalination: resource assessment and review of technology. *Desalination* **2005**, *186*, 97−109.
(17) Liebmann, A. J. History of distillation. *J. Chem. Educ.* **1956**, *33*, 166.
(18) Aly, S. Energy savings in distillation plants by using vapor thermo-compression. *Desalination* **1984**, *49*, 37−56.
(19) Al-Radif, A. Review of various combinations of a multiple effect desalination plant (MED) and a thermal vapour compression unit. *Desalination* **1993**, *93*, 119−125.
(20) Al-Najem, N. M.; Darwish, M.; Youssef, F. Thermovapor compression desalters: energy and availability—analysis of single-and multi-effect systems. *Desalination* **1997**, *110*, 223−238.
(21) Parekh, S.; Farid, M.; Selman, J.; Al-Hallaj, S. Solar desalination with a humidification-dehumidification technique—a comprehensive technical review. *Desalination* **2004**, *160*, 167−186.
(22) Narayan, G. P.; Sharqawy, M. H.; Summers, E. K.; Lienhard, J. H.; Zubair, S. M.; Antar, M. A. The potential of solar-driven humidification−dehumidification desalination for small-scale decentralized water production. *Renewable and Sustainable Energy Reviews* **2010**, *14*, 1187−1201.
(23) Narayan, G. P.; Sharqawy, M. H.; Lienhard, J. H., V; Zubair, S. M. Thermodynamic analysis of humidification dehumidification desalination cycles. *Desalination and Water Treatment* **2010**, *16*, 339−353.
(24) Dahmani, K.; Kherroub, D. E.; Belloul, M. *Materials Research and Applications*; Springer, 2021; pp 251−261.
(25) Rich, A.; Mandri, Y.; Bendaoud, N.; Mangin, D.; Abderafi, S.; Bebon, C.; Semlali, N.; Klein, J.-P.; Bounahmidi, T.; Bouhaouss, A.; Veesler, S. Freezing desalination of sea water in a static layer crystallizer. *Desalination and Water Treatment* **2010**, *13*, 120−127.
(26) Lu, Z.; Xu, L. Freezing desalination process. In *Thermal Desalination Processes* 2010, *2*.
(27) Gupta, V. K.; Ali, I.; Saleh, T. A.; Nayak, A.; Agarwal, S. Chemical treatment technologies for waste-water recycling—an overview. *Rsc Advances* **2012**, *2*, 6380−6388.
(28) Belfort, G.; Davis, R. H.; Zydney, A. L. The behavior of suspensions and macromolecular solutions in crossflow microfiltration. *Journal of membrane science* **1994**, *96*, 1−58.
(29) Rautenbach, R.; Vossenkaul, K.; Linn, T.; Katz, T. Waste water treatment by membrane processes—new development in ultrafiltration, nanofiltration and reverse osmosis. *Desalination* **1997**, *108*, 247−253.
(30) Schaefer, A.; Fane, A. G.; Waite, T. D. *Nanofiltration: Principles and Applications*; Elsevier, 2005.
(31) Peñate, B.; García-Rodríguez, L. Current trends and future prospects in the design of seawater reverse osmosis desalination technology. *Desalination* **2012**, *284*, 1−8.
(32) Kucera, J. *Reverse Osmosis: Industrial Processes and Applications*; John Wiley & Sons, 2015.
(33) Wenten, I.; Khoiruddin, K. Reverse osmosis applications: prospect and challenges. *Desalination* **2016**, *391*, 112−125.

https://doi.org/10.1021/acs.chemrev.1c00396
Chem. Rev. 2022, 122, 13547−13635

(34) Imbrogno, J.; Belfort, G. Membrane desalination: where are we, and what can we learn from fundamentals? *Annu. Rev. Chem. Biomol. Eng.* **2016**, *7*, 29−64.
(35) Zeman, L. J.; Zydney, A. *Microfiltration and Ultrafiltration: Principles and Applications*; CRC Press, 2017.
(36) Aryanti, P.; Hakim, A.; Widodo, S.; Widiasa, I.; Wenten, I. Prospect and Challenges of Tight Ultrafiltration Membrane in Drinking Water Treatment. *IOP Conference Series: Materials Science and Engineering* **2018**, *395*, 012012.
(37) Van der Bruggen, B. *Fundamental Modelling of Membrane Systems*; Elsevier, 2018; pp 25−70.
(38) Biesheuvel, P.; Porada, S.; Elimelech, M.; Dykstra, J. Tutorial review of reverse osmosis and electrodialysis. *J. Membr. Sci.* **2022**, *647*, 120221.
(39) Qiblawey, H. M.; Banat, F. Solar thermal desalination technologies. *Desalination* **2008**, *220*, 633−644.
(40) Kalogirou, S. A. *Solar Energy Engineering: Processes and Systems*; Academic Press, 2013.
(41) Wang, L. K.; Vaccari, D. A.; Li, Y.; Shammas, N. K. *Physicochemical Treatment Processes*; Springer, 2005; pp 141−197.
(42) Jiang, J.-Q. The role of coagulation in water treatment. *Current Opinion in Chemical Engineering* **2015**, *8*, 36−44.
(43) Bose, P.; Bose, M. A.; Kumar, S. Critical evaluation of treatment strategies involving adsorption and chelation for wastewater containing copper, zinc and cyanide. *Adv. Environ. Res.* **2002**, *7*, 179−195.
(44) Faust, S. D.; Aly, O. M. *Adsorption Processes for Water Treatment*; Elsevier, 2013.
(45) Collivignarelli, M. C.; Abbà, A.; Benigna, I.; Sorlini, S.; Torretta, V. Overview of the main disinfection processes for wastewater and drinking water treatment plants. *Sustainability* **2018**, *10*, 86.
(46) Rosso, D.; Larson, L. E.; Stenstrom, M. K. Aeration of large-scale municipal wastewater treatment plants: state of the art. *Water Sci. Technol.* **2008**, *57*, 973−978.
(47) Dabrowski, A.; Hubicki, Z.; Podkościelny, P.; Robens, E. Selective removal of the heavy metal ions from waters and industrial wastewaters by ion-exchange method. *Chemosphere* **2004**, *56*, 91−106.
(48) Li, J.; Wang, J. Advances in cement solidification technology for waste radioactive ion exchange resins: A review. *Journal of hazardous materials* **2006**, *135*, 443−448.
(49) Choppin, G.; Morgenstern, A. Radionuclide separations in radioactive waste disposal. *Journal of Radioanalytical and Nuclear Chemistry* **2000**, *243*, 45−51.
(50) Ashley, N. V.; Roach, D. J. Review of biotechnology applications to nuclear waste treatment. *J. Chem. Technol. Biotechnol.* **1990**, *49*, 381−394.
(51) Ghernaout, B.; Ghernaout, D.; Saiba, A. Algae and cyanotoxins removal by coagulation/flocculation: A review. *Desalination and Water Treatment* **2010**, *20*, 133−143.
(52) Verma, A. K.; Dash, R. R.; Bhunia, P. A review on chemical coagulation/flocculation technologies for removal of colour from textile wastewaters. *Journal of environmental management* **2012**, *93*, 154−168.
(53) Gupta, V. K.; Carrott, P.; Ribeiro Carrott, M.; Suhas. Low-cost adsorbents: growing approach to wastewater treatment—a review. *Critical reviews in environmental science and technology* **2009**, *39*, 783−842.
(54) Kim, H. D.; Kim, K. H. Water purification using aeration techniques in the lagoon. *Applied Mechanics and Materials* **2014**, *675-677*, 602−607.
(55) Dardor, D.; Minier-Matar, J.; Janson, A.; AlShamari, E.; Adham, S. The effect of Hydrogen sulfide oxidation with ultraviolet light and aeration on sour water treatment via membrane contactors. *Sep. Purif. Technol.* **2020**, *236*, 116262.
(56) Elwakeel, K. Z. Environmental application of chitosan resins for the treatment of water and wastewater: a review. *J. Dispersion Sci. Technol.* **2010**, *31*, 273−288.
(57) Hubicki, Z.; Kołodyńska, D. Selective removal of heavy metal ions from waters and waste waters using ion exchange methods. *Ion Exchange Technologies* **2012**, *7*, 193−240.
(58) Iizuka, A.; Yamashita, Y.; Nagasawa, H.; Yamasaki, A.; Yanagisawa, Y. Separation of lithium and cobalt from waste lithium-ion batteries via bipolar membrane electrodialysis coupled with chelation. *Sep. Purif. Technol.* **2013**, *113*, 33−41.
(59) Kaur, M.; Zhang, H.; Martin, L.; Todd, T.; Qiang, Y. Conjugates of Magnetic Nanoparticle−Actinide Specific Chelator for Radioactive Waste Separation. *Environ. Sci. Technol.* **2013**, *47*, 11942−11959.
(60) Shkolnikov, V.; Bahga, S. S.; Santiago, J. G. Desalination and hydrogen, chlorine, and sodium hydroxide production via electrophoretic ion exchange and precipitation. *Phys. Chem. Chem. Phys.* **2012**, *14*, 11534−11545.
(61) Arar, Ö.; Yüksel, Ü.; Kabay, N.; Yüksel, M. Various applications of electrodeionization (EDI) method for water treatment—A short review. *Desalination* **2014**, *342*, 16−22.
(62) Pham, T. C. T.; Docao, S.; Hwang, I. C.; Song, M. K.; Choi, D. Y.; Moon, D.; Oleynikov, P.; Yoon, K. B. Capture of iodine and organic iodides using silica zeolites and the semiconductor behaviour of iodine in a silica zeolite. *Energy Environ. Sci.* **2016**, *9*, 1050−1062.
(63) Manahan, S. E. *Fundamentals of Environmental Chemistry*; CRC Press, 2001; pp 1−42.
(64) Qasim, M.; Badrelzaman, M.; Darwish, N. N.; Darwish, N. A.; Hilal, N. Reverse osmosis desalination: A state-of-the-art review. *Desalination* **2019**, *459*, 59−104.
(65) Shannon, M. A.; Bohn, P. W.; Elimelech, M.; Georgiadis, J. G.; Marinas, B. J.; Mayes, A. M. *Nanoscience and Technology: A Collection of Reviews from Nature Journals*; World Scientific, 2010; pp 337−346.
(66) Sauvet-Goichon, B. Ashkelon desalination plant - A successful challenge. *Desalination* **2007**, *203*, 75−81.
(67) Semiat, R. Energy Issues in Desalination Processes. *Environ. Sci. Technol.* **2008**, *42*, 8193−8201.
(68) Elimelech, M.; Phillip, W. A. The Future of Seawater Desalination: Energy, Technology, and the Environment. *Science* **2011**, *333*, 712−717.
(69) Kim, J.; Park, K.; Yang, D. R.; Hong, S. A comprehensive review of energy consumption of seawater reverse osmosis desalination plants. *Applied Energy* **2019**, *254*, 113652.
(70) Zhao, R.; Porada, S.; Biesheuvel, P. M.; Van der Wal, A. Energy consumption in membrane capacitive deionization for different water recoveries and flow rates, and comparison with reverse osmosis. *Desalination* **2013**, *330*, 35−41.
(71) Zhou, J.; Chang, V. W. C.; Fane, A. G. Environmental life cycle assessment of brackish water reverse osmosis desalination for different electricity production models. *Energy Environ. Sci.* **2011**, *4*, 2267−2278.
(72) Spiegler, K. S.; El-Sayed, Y. M. The energetics of desalination processes. *Desalination* **2001**, *134*, 109−128.
(73) Ayoub, J.; Alward, R. Water requirements and remote arid areas: the need for small-scale desalination. *Desalination* **1996**, *107*, 131−147.
(74) Song, J.; Li, T.; Wright-Contreras, L.; Law, A. W.-K. A review of the current status of small-scale seawater reverse osmosis desalination. *Water international* **2017**, *42*, 618−631.
(75) Azwanida, N. N. A review on the extraction methods use in medicinal plants, principle, strength and limitation. *Med. Aromat. Plants* **2015**, *4*, 2167−0412.
(76) Crini, G.; Lichtfouse, E. Advantages and disadvantages of techniques used for wastewater treatment. *Environmental Chemistry Letters* **2019**, *17*, 145−155.
(77) Zhang, Y.; Bian, T.; Zhang, Y.; Zheng, X.; Li, Z. Chelation resin efficient removal of Cu (II), Cr (III), Ni (II) in electroplating wastewater. *Fullerenes, Nanotubes and Carbon Nanostructures* **2018**, *26*, 765−776.
(78) Drikas, M.; Chow, C. W.; House, J.; Burch, M. D. Using coagulation, flocculation, and settling to remove toxic cyanobacteria. *Journal-American Water Works Association* **2001**, *93*, 100−111.

https://doi.org/10.1021/acs.chemrev.1c00396
Chem. Rev. 2022, 122, 13547−13635

(79) Zhang, S.; Zheng, H.; Tang, X.; Zhao, C.; Zheng, C.; Gao, B. Sterilization by flocculants in drinking water treatment. *Chemical Engineering Journal* **2020**, *382*, 122961.
(80) Teh, C. Y.; Budiman, P. M.; Shak, K. P. Y.; Wu, T. Y. Recent advancement of coagulation−flocculation and its application in wastewater treatment. *Ind. Eng. Chem. Res.* **2016**, *55*, 4363−4389.
(81) de Wolf, C. A.; Bang, E.; Bouwman, A.; Braun, W.; De Oliveira, E.; Nasr El-Dinothers, H. *Evaluation of Environmentally Friendly Chelating Agents for Applications in the Oil and Gas Industry*; SPE International Symposium and Exhibition on Formation Damage Control, 2014.
(82) Chen, J. P. *Decontamination of Heavy Metals: Processes, Mechanisms, And Applications*; CRC Press, 2012.
(83) Pan, S.-Y.; Snyder, S. W.; Ma, H.-W.; Lin, Y. J.; Chiang, P.-C. Development of a resin wafer electrodeionization process for impaired water desalination with high energy efficiency and productivity. *Acs Sustainable Chemistry & Engineering* **2017**, *5*, 2942−2948.
(84) Tarpeh, W. A.; Barazesh, J. M.; Cath, T. Y.; Nelson, K. L. Electrochemical stripping to recover nitrogen from source-separated urine. *Environ. Sci. Technol.* **2018**, *52*, 1453−1460.
(85) Mu, L.; Wang, Y.; Tarpeh, W. A. Validation and Mechanism of a Low-Cost Graphite Carbon Electrode for Electrochemical Brine Valorization. *ACS Sustainable Chem. Eng.* **2020**, *8*, 8648−8654.
(86) Su, X.; Hatton, T. A. Electrosorption at functional interfaces: from molecular-level interactions to electrochemical cell design. *Phys. Chem. Chem. Phys.* **2017**, *19*, 23570−23584.
(87) Schlumpberger, S.; Lu, N. B.; Suss, M. E.; Bazant, M. Z. Scalable and Continuous Water Deionization by Shock Electrodialysis. *Environmental Science & Technology Letters* **2015**, *2*, 367−372.
(88) Singh, K.; Bouwmeester, H.; De Smet, L.; Bazant, M.; Biesheuvel, P. Theory of water desalination with intercalation materials. *Physical review applied* **2018**, *9*, 064036.
(89) He, D.; Wong, C. E.; Tang, W. W.; Kovalsky, P.; Waite, T. D. Faradaic Reactions in Water Desalination by Batch-Mode Capacitive Deionization. *Environmental Science & Technology Letters* **2016**, *3*, 222−226.
(90) Hemmatifar, A.; Palko, J. W.; Stadermann, M.; Santiago, J. G. Energy breakdown in capacitive deionization. *Water Res.* **2016**, *104*, 303−311.
(91) Squires, T. M. Particles in electric fields. *Fluids, Colloids and Soft Materials: An Introduction to Soft Matter Physics* **2016**, 59−79.
(92) Mani, A.; Zangle, T. A.; Santiago, J. G. On the propagation of concentration polarization from microchannel-nanochannel interfaces Part I: analytical model and characteristic analysis. *Langmuir* **2009**, *25*, 3898−3908.
(93) Zangle, T. A.; Mani, A.; Santiago, J. G. On the propagation of concentration polarization from microchannel-nanochannel interfaces Part II: numerical and experimental study. *Langmuir* **2009**, *25*, 3909−3916.
(94) Mani, A.; Bazant, M. Z. Deionization shocks in microstructures. *Phys. Rev. E* **2011**, *84*, 061504.
(95) Deng, D.; Dydek, E. V.; Han, J.-H.; Schlumpberger, S.; Mani, A.; Zaltzman, B.; Bazant, M. Z. Overlimiting current and shock electrodialysis in porous media. *Langmuir* **2013**, *29*, 16167−16177.
(96) Su, X.; Hatton, T. A. Redox-electrodes for selective electrochemical separations. *Adv. Colloid Interface Sci.* **2017**, *244*, 6−20.
(97) Comninellis, C.; Chen, G. *Electrochemistry for the Environment*; Springer, 2010; Vol. *2015*; Chapter 12.
(98) Mousset, E.; Doudrick, K. A review of electrochemical reduction processes to treat oxidized contaminants in water. *Current Opinion in Electrochemistry* **2020**, *22*, 221−227.
(99) Lilga, M. A.; Orth, R. J.; Sukamto, J.; Haight, S.; Schwartz, D. Metal ion separations using electrically switched ion exchange. *Sep. Purif. Technol.* **1997**, *11*, 147−158.
(100) Jeerage, K. M.; Schwartz, D. T. Characterization of cathodically deposited nickel hexacyanoferrate for electrochemically switched ion exchange. *Sep. Sci. Technol.* **2000**, *35*, 2375−2392.
(101) Dong, H.; Wei, L.; Tarpeh, W. A. Electro-assisted regeneration of pH-sensitive ion exchangers for sustainable phosphate removal and recovery. *Water Res.* **2020**, *184*, 116167.
(102) Kim, K.; Cotty, S.; Elbert, J.; Chen, R.; Hou, C.-H.; Su, X. Asymmetric Redox-Polymer Interfaces for Electrochemical Reactive Separations: Synergistic Capture and Conversion of Arsenic. *Adv. Mater.* **2020**, *32*, 1906877.
(103) Mao, X.; Tian, W.; Ren, Y.; Chen, D.; Curtis, S. E.; Buss, M. T.; Rutledge, G. C.; Hatton, T. A. Energetically efficient electrochemically tunable affinity separation using multicomponent polymeric nanostructures for water treatment. *Energy Environ. Sci.* **2018**, *11*, 2954−2963.
(104) Ren, Y.; Mao, X.; Hatton, T. A. An Asymmetric Electrochemical System with Complementary Tunability in Hydrophobicity for Selective Separations of Organics. *ACS Central Science* **2019**, *5*, 1396−1406.
(105) Su, X.; Hübner, J.; Kauke, M. J.; Dalbosco, L.; Thomas, J.; Gonzalez, C. C.; Zhu, E.; Franzreb, M.; Jamison, T. F.; Hatton, T. A. Redox Interfaces for Electrochemically Controlled Protein−Surface Interactions: Bioseparations and Heterogeneous Enzyme Catalysis. *Chem. Mater.* **2017**, *29*, 5702−5712.
(106) Wood, J.; Gifford, J.; Arba, J.; Shaw, M. Production of ultrapure water by continuous electrodeionization. *Desalination* **2010**, *250*, 973−976.
(107) Hakim, A. N; Khoiruddin; Wenten, I. G Mechanism of Ion Transfer in Electrodeionization (EDI) System. *Adv. Sci. Lett.* **2017**, *23*, 5640−5642.
(108) Rathi, B. S.; Kumar, P. S.; Parthiban, R. A review on recent advances in electrodeionization for various environmental applications. *Chemosphere* **2022**, *289*, 133223.
(109) Conforti, K. M.; Bazant, M. Z. Continuous ion-selective separations by shock electrodialysis. *AIChE J.* **2020**, *66*, No. e16751.
(110) Oren, Y. Capacitive deionization (CDI) for desalination and water treatment—past, present and future (a review). *Desalination* **2008**, *228*, 10−29.
(111) Huyskens, C.; Helsen, J.; de Haan, A. Capacitive deionization for water treatment: Screening of key performance parameters and comparison of performance for different ions. *Desalination* **2013**, *328*, 8−16.
(112) Guo, L.; Huang, Y. X.; Ding, M.; Leong, Z. Y.; Vafakhah, S.; Yang, H. Y. A high performance electrochemical deionization method to desalinate brackish water with an FePO4/RGO nanocomposite. *Journal of Materials Chemistry A* **2018**, *6*, 8901−8908.
(113) Guo, L.; Mo, R. W.; Shi, W. H.; Huang, Y. X.; Leong, Z. Y.; Ding, M.; Chen, F. M.; Yang, H. Y. A Prussian blue anode for high performance electrochemical deionization promoted by the Faradaic mechanism. *Nanoscale* **2017**, *9*, 13305−13312.
(114) Strathmann, H. Electrodialysis, a mature technology with a multitude of new applications. *Desalination* **2010**, *264*, 268−288.
(115) Suss, M.; Porada, S.; Sun, X.; Biesheuvel, P.; Yoon, J.; Presser, V. Water desalination via capacitive deionization: what is it and what can we expect from it? *Energy Environ. Sci.* **2015**, *8*, 2296−2319.
(116) Smith, K. C. Theoretical evaluation of electrochemical cell architectures using cation intercalation electrodes for desalination. *Electrochim. Acta* **2017**, *230*, 333−341.
(117) Suss, M. E.; Presser, V. Water desalination with energy storage electrode materials. *Joule* **2018**, *2*, 10−15.
(118) Suresh, A.; Hill, G. T.; Hoenig, E.; Liu, C. Electrochemically mediated deionization: a review. *Molecular Systems Design & Engineering* **2021**, *6*, 25−51.
(119) Bazant, M. Z.; Squires, T. M. Induced-charge electrokinetic phenomena: theory and microfluidic applications. *Phys. Rev. Lett.* **2004**, *92*, 066101.
(120) Bazant, M. Z.; Squires, T. M. Induced-charge electrokinetic phenomena. *Curr. Opin. Colloid Interface Sci.* **2010**, *15*, 203−213.
(121) Goldstein, A. L. Electrodialysis on the American continent. *Desalination* **1979**, *30*, 49−58.
(122) Bernardes, A.; Rodrigues, M.; Ferreira, J. *Electrodialysis and Water Reuse*; Springer, 2016.

https://doi.org/10.1021/acs.chemrev.1c00396
Chem. Rev. 2022, 122, 13547−13635

(123) Sillanpää, M.; Shestakova, M. *Electrochemical Water Treatment Methods: Fundamentals, Methods and Full Scale Applications*; Butterworth-Heinemann, 2017.
(124) Campione, A.; Gurreri, L.; Ciofalo, M.; Micale, G.; Tamburini, A.; Cipollina, A. Electrodialysis for water desalination: A critical assessment of recent developments on process fundamentals, models and applications. *Desalination* **2018**, *434*, 121−160.
(125) Gurreri, L.; Tamburini, A.; Cipollina, A.; Micale, G. Electrodialysis Applications in Wastewater Treatment for Environmental Protection and Resources Recovery: A Systematic Review on Progress and Perspectives. *Membranes* **2020**, *10*, 146.
(126) Alvarado, L.; Chen, A. Electrodeionization: Principles, Strategies and Applications. *Electrochim. Acta* **2014**, *132*, 583−597.
(127) Smith, K. C.; Dmello, R. Na-Ion Desalination (NID) Enabled by Na-Blocking Membranes and Symmetric Na-Intercalation: Porous-Electrode Modeling. *J. Electrochem. Soc.* **2016**, *163*, A530−A539.
(128) Srimuk, P.; Kaasik, F.; Kruner, B.; Tolosa, A.; Fleischmann, S.; Jackel, N.; Tekeli, M. C.; Aslan, M.; Suss, M. E.; Presser, V. MXene as a novel intercalation-type pseudocapacitive cathode and anode for capacitive deionization. *Journal of Materials Chemistry A* **2016**, *4*, 18265−18271.
(129) Balcajin, O.; Noy, A.; Fornasiero, F.; Grigoropoulos, C. P.; Holt, J. K.; In, J. B.; Kim, S.; Park, H. G. *Nanotechnology Applications for Clean Water*; Elsevier, 2009; pp 77−93.
(130) Roelofs, S. H.; van den Berg, A.; Odijk, M. Microfluidic desalination techniques and their potential applications. *Lab Chip* **2015**, *15*, 3428−3438.
(131) Särkkä, H.; Vepsäläinen, M.; Sillanpää, M. Natural organic matter (NOM) removal by electrochemical methods—A review. *J. Electroanal. Chem.* **2015**, *755*, 100−108.
(132) Martínez-Huitle, C. A.; Rodrigo, M. A.; Sirés, I.; Scialdone, O. Single and coupled electrochemical processes and reactors for the abatement of organic water pollutants: a critical review. *Chem. Rev.* **2015**, *115*, 13362−13407.
(133) Chaplin, B. P. Critical review of electrochemical advanced oxidation processes for water treatment applications. *Environ. Sci.: Proc. Impacts* **2014**, *16*, 1182−1203.
(134) Panizza, M.; Bocca, C.; Cerisola, G. Electrochemical treatment of wastewater containing polyaromatic organic pollutants. *Water Res.* **2000**, *34*, 2601−2605.
(135) Martínez-Huitle, C. A.; Brillas, E. Decontamination of wastewaters containing synthetic organic dyes by electrochemical methods: a general review. *Applied Catalysis B: Environmental* **2009**, *87*, 105−145.
(136) Sirés, I.; Brillas, E. Remediation of water pollution caused by pharmaceutical residues based on electrochemical separation and degradation technologies: a review. *Environ. Int.* **2012**, *40*, 212−229.
(137) Brillas, E.; Martínez-Huitle, C. A. Decontamination of wastewaters containing synthetic organic dyes by electrochemical methods. An updated review. *Applied Catalysis B: Environmental* **2015**, *166*, 603−643.
(138) Grimm, J.; Bessarabov, D.; Sanderson, R. Review of electro-assisted methods for water purification. *Desalination* **1998**, *115*, 285−294.
(139) Chen, G. Electrochemical technologies in wastewater treatment. *Sep. Purif. Technol.* **2004**, *38*, 11−41.
(140) Pulkka, S.; Martikainen, M.; Bhatnagar, A.; Sillanpää, M. Electrochemical methods for the removal of anionic contaminants from water−a review. *Sep. Purif. Technol.* **2014**, *132*, 252−271.
(141) Alsheyab, M.; Jiang, J.-Q.; Stanford, C. On-line production of ferrate with an electrochemical method and its potential application for wastewater treatment−A review. *Journal of Environmental Management* **2009**, *90*, 1350−1356.
(142) Särkkä, H.; Bhatnagar, A.; Sillanpää, M. Recent developments of electro-oxidation in water treatment—a review. *J. Electroanal. Chem.* **2015**, *754*, 46−56.
(143) Martínez-Huitle, C. A.; Brillas, E. Electrochemical alternatives for drinking water disinfection. *Angew. Chem., Int. Ed.* **2008**, *47*, 1998−2005.
(144) Kraft, A. Electrochemical water disinfection: a short review. *Platinum metals review* **2008**, *52*, 177−185.
(145) Garcia-Segura, S.; Ocon, J. D.; Chong, M. N. Electrochemical oxidation remediation of real wastewater effluents—a review. *Process Safety and Environmental Protection* **2018**, *113*, 48−67.
(146) Sirés, I.; Brillas, E.; Oturan, M. A.; Rodrigo, M. A.; Panizza, M. Electrochemical advanced oxidation processes: today and tomorrow. A review. *Environmental Science and Pollution Research* **2014**, *21*, 8336−8367.
(147) Miklos, D. B.; Remy, C.; Jekel, M.; Linden, K. G.; Drewes, J. E.; Hübner, U. Evaluation of advanced oxidation processes for water and wastewater treatment−A critical review. *Water research* **2018**, *139*, 118−131.
(148) Trojanowicz, M.; Bojanowska-Czajka, A.; Bartosiewicz, I.; Kulisa, K. Advanced oxidation/reduction processes treatment for aqueous perfluorooctanoate (PFOA) and perfluorooctanesulfonate (PFOS)−a review of recent advances. *Chemical Engineering Journal* **2018**, *336*, 170−199.
(149) Khan, S.; Sayed, M.; Sohail, M.; Shah, L. A.; Raja, M. A. Advanced oxidation and reduction processes. *Advances in Water Purification Techniques* **2019**, 135−164.
(150) Porada, S.; Zhao, R.; van der Wal, A.; Presser, V.; Biesheuvel, P. M. Review on the science and technology of water desalination by capacitive deionization. *Prog. Mater. Sci.* **2013**, *58*, 1388−1442.
(151) Yip, N. Y.; Brogioli, D.; Hamelers, H. V.; Nijmeijer, K. Salinity gradients for sustainable energy: primer, progress, and prospects. *Environ. Sci. Technol.* **2016**, *50*, 12072−12094.
(152) Bazinet, L.; Geoffroy, T. R. Electrodialytic processes: Market overview, membrane phenomena, recent developments and sustainable strategies. *Membranes* **2020**, *10*, 221.
(153) Wenten, I.; Khoiruddin, K.; Alkhadra, M. A.; Tian, H.; Bazant, M. Z. Novel ionic separation mechanisms in electrically driven membrane processes. *Adv. Colloid Interface Sci.* **2020**, *284*, 102269.
(154) Srimuk, P.; Su, X.; Yoon, J.; Aurbach, D.; Presser, V. Charge-transfer materials for electrochemical water desalination, ion separation and the recovery of elements. *Nature Reviews Materials* **2020**, *5*, 517−538.
(155) Marek, J. State-of-the-Art Water Treatment in Czech Power Sector: Industry-Proven Case Studies Showing Economic and Technical Benefits of Membrane and Other Novel Technologies for Each Particular Water Cycle. *Membranes* **2021**, *11*, 98.
(156) Koren, J.; Syversen, U. State-of-the-art electroflocculation. *Filtration and Separation* **1995**, *32*, 153−156.
(157) Alinsafi, A.; Khemis, M.; Pons, M.-N.; Leclerc, J.-P.; Yaacoubi, A.; Benhammou, A.; Nejmeddine, A. Electro-coagulation of reactive textile dyes and textile wastewater. *Chem. Eng. Proc.: Proc. Intensification* **2005**, *44*, 461−470.
(158) Mollah, M. Y. A.; Schennach, R.; Parga, J. R.; Cocke, D. L. Electrocoagulation (EC) - science and applications. *Journal of Hazardous Materials* **2001**, *84*, 29−41.
(159) Rodrigo, M.; Oturan, N.; Oturan, M. A. Electrochemically assisted remediation of pesticides in soils and water: a review. *Chem. Rev.* **2014**, *114*, 8720−8745.
(160) Azimi, A.; Azari, A.; Rezakazemi, M.; Ansarpour, M. Removal of heavy metals from industrial wastewaters: a review. *ChemBioEng. Reviews* **2017**, *4*, 37−59.
(161) Liu, C.; Wu, T.; Hsu, P.-C.; Xie, J.; Zhao, J.; Liu, K.; Sun, J.; Xu, J.; Tang, J.; Ye, Z.; Lin, D.; Cui, Y. Direct/alternating current electrochemical method for removing and recovering heavy metal from water using graphene oxide electrode. *ACS Nano* **2019**, *13*, 6431−6437.
(162) Wang, F.; Stahl, S. S. Electrochemical oxidation of organic molecules at lower overpotential: Accessing broader functional group compatibility with electron-proton transfer mediators. *Accounts of chemical research* **2020**, *53*, 561−574.
(163) Wang, J. L.; Xu, L. J. Advanced oxidation processes for wastewater treatment: formation of hydroxyl radical and application. *Critical reviews in environmental science and technology* **2012**, *42*, 251−325.

https://doi.org/10.1021/acs.chemrev.1c00396
Chem. Rev. 2022, 122, 13547−13635

(164) Hayyan, M.; Hashim, M. A.; AlNashef, I. M. Superoxide ion: generation and chemical implications. *Chem. Rev.* **2016**, *116*, 3029−3085.
(165) Martínez-Huitle, C. A.; Rodrigo, M. A.; Scialdone, O. *Electrochemical Water and Wastewater Treatment*; Butterworth-Heinemann, 2018.
(166) Xia, X.; Zhu, F.; Li, J.; Yang, H.; Wei, L.; Li, Q.; Jiang, J.; Zhang, G.; Zhao, Q. A review study on sulfate-radical-based advanced oxidation processes for domestic/industrial wastewater treatment: degradation, efficiency, and mechanism. *Front. Chem.* **2020**, *8*, 592056.
(167) Kim, S.; Sin, A.; Nam, H.; Park, Y.; Lee, H.; Han, C. Advanced oxidation processes for microplastics degradation: A recent trend. *Chemical Engineering Journal Advances* **2022**, *9*, 100213.
(168) Moreira, F. C.; Boaventura, R. A.; Brillas, E.; Vilar, V. J. Electrochemical advanced oxidation processes: a review on their application to synthetic and real wastewaters. *Applied Catalysis B: Environmental* **2017**, *202*, 217−261.
(169) Du, J.; Zhang, B.; Li, J.; Lai, B. Decontamination of heavy metal complexes by advanced oxidation processes: A review. *Chin. Chem. Lett.* **2020**, *31*, 2575−2582.
(170) da Silva, S. W.; Welter, J. B.; Albornoz, L. L.; Heberle, A. N. A.; Ferreira, J. Z.; Bernardes, A. M. Advanced Electrochemical Oxidation Processes in the Treatment of Pharmaceutical Containing Water and Wastewater: a Review. *Curr. Pollution Rep.* **2021**, *7*, 121−124.
(171) Sen, C.; Packer, L.; Hänninen, O. *Handbook of Oxidants and Antioxidants in Exercise*; Elsevier, 2000.
(172) Halliwell, B.; Gutteridge, J. M. *Free Radicals in Biology and Medicine*; Oxford University Press, 2015.
(173) Bielski, B. H.; Cabelli, D. E.; Arudi, R. L.; Ross, A. B. Reactivity of HO2/O- 2 radicals in aqueous solution. *Journal of physical and chemical reference data* **1985**, *14*, 1041−1100.
(174) Zhang, H.; Wu, J.; Wang, Z.; Zhang, D. Electrochemical oxidation of crystal violet in the presence of hydrogen peroxide. *J. Chem. Technol. Biotechnol.* **2010**, *85*, 1436−1444.
(175) R Buettner, G. Superoxide dismutase in redox biology: the roles of superoxide and hydrogen peroxide. *Anti-Cancer Agents Med. Chem.* **2011**, *11*, 341−346.
(176) Ai, Z.; Gao, Z.; Zhang, L.; He, W.; Yin, J. J. Core−shell structure dependent reactivity of Fe@ Fe2O3 nanowires on aerobic degradation of 4-chlorophenol. *Environ. Sci. Technol.* **2013**, *47*, 5344−5352.
(177) Dimić, D. S.; Milenković, D. A.; Avdović, E. H.; Nakarada, DJ. J.; Dimitrić Marković, J. M. D.; Marković, Z. S. Advanced oxidation processes of coumarins by hydroperoxyl radical: An experimental and theoretical study, and ecotoxicology assessment. *Chemical Engineering Journal* **2021**, *424*, 130331.
(178) Watts, R. J.; Bottenberg, B. C.; Hess, T. F.; Jensen, M. D.; Teel, A. L. Role of reductants in the enhanced desorption and transformation of chloroaliphatic compounds by modified Fenton's reactions. *Environ. Sci. Technol.* **1999**, *33*, 3432−3437.
(179) Teel, A. L.; Watts, R. J. Degradation of carbon tetrachloride by modified Fenton's reagent. *Journal of Hazardous Materials* **2002**, *94*, 179−189.
(180) Mitchell, S. M.; Ahmad, M.; Teel, A. L.; Watts, R. J. Degradation of perfluorooctanoic acid by reactive species generated through catalyzed H2O2 propagation reactions. *Environmental Science & Technology Letters* **2014**, *1*, 117−121.
(181) Bai, L.; Jiang, Y.; Xia, D.; Wei, Z.; Spinney, R.; Dionysiou, D. D.; Minakata, D.; Xiao, R.; Xie, H.-B.; Chai, L. *Mechanistic Understanding of Superoxide Radical-Mediated Degradation of Perfluorocarboxylic Acids*; Environmental Science & Technology, 2021.
(182) Watts, R. J.; Teel, A. L. Hydroxyl radical and non-hydroxyl radical pathways for trichloroethylene and perchloroethylene degradation in catalyzed H2O2 propagation systems. *Water research* **2019**, *159*, 46−54.
(183) Buxton, G. V.; Greenstock, C. L.; Helman, W. P.; Ross, A. B. Critical Review of rate constants for reactions of hydrated electrons, hydrogen atoms and hydroxyl radicals (·OH/ ·O⁻ in Aqueous Solution. *Journal of physical and chemical reference data* **1988**, *17*, 513−886.
(184) Naumczyk, J.; Szpyrkowicz, L.; Zilio-Grandi, F. Electrochemical treatment of textile wastewater. *Water Sci. Technol.* **1996**, *34*, 17−24.
(185) Comninellis, C.; Nerini, A. Anodic oxidation of phenol in the presence of NaCl for wastewater treatment. *J. Appl. Electrochem.* **1995**, *25*, 23−28.
(186) Martinez-Huitle, C. A.; Ferro, S. Electrochemical oxidation of organic pollutants for the wastewater treatment: direct and indirect processes. *Chem. Soc. Rev.* **2006**, *35*, 1324−1340.
(187) Li, H.; Ni, J. Electrogeneration of disinfection byproducts at a boron-doped diamond anode with resorcinol as a model substance. *Electrochimica acta* **2012**, *69*, 268−274.
(188) Li, H.; Long, Y.; Zhu, X.; Tian, Y.; Ye, J. Influencing factors and chlorinated byproducts in electrochemical oxidation of bisphenol A with boron-doped diamond anodes. *Electrochim. Acta* **2017**, *246*, 1121−1130.
(189) Carboneras, M. B.; Cañizares, P.; Rodrigo, M. A.; Villaseñor, J.; Fernandez-Morales, F. J. Improving biodegradability of soil washing effluents using anodic oxidation. *Bioresource technology* **2018**, *252*, 1−6.
(190) Urtiaga, A.; Rueda, A.; Anglada, Á.; Ortiz, I. Integrated treatment of landfill leachates including electrooxidation at pilot plant scale. *Journal of Hazardous Materials* **2009**, *166*, 1530−1534.
(191) Zöllig, H.; Remmele, A.; Morgenroth, E.; Udert, K. M. Removal rates and energy demand of the electrochemical oxidation of ammonia and organic substances in real stored urine. *Environ. Sci.: Water Res. Technol.* **2017**, *3*, 480−491.
(192) Dirany, A.; Sirés, I.; Oturan, N.; Özcan, A.; Oturan, M. A. Electrochemical treatment of the antibiotic sulfachloropyridazine: kinetics, reaction pathways, and toxicity evolution. *Environ. Sci. Technol.* **2012**, *46*, 4074−4082.
(193) Comninellis, C.; Pulgarin, C. Electrochemical oxidation of phenol for wastewater treatment using SnO_2 anodes. *J. Appl. Electrochem.* **1993**, *23*, 108−112.
(194) Comninellis, C. Electrocatalysis in the electrochemical conversion/combustion of organic pollutants for waste water treatment. *Electrochim. Acta* **1994**, *39*, 1857−1862.
(195) Gandini, D.; Mahé, E.; Michaud, P. A.; Haenni, W.; Perret, A.; Comninellis, C. Oxidation of carboxylic acids at boron-doped diamond electrodes for wastewater treatment. *J. Appl. Electrochem.* **2000**, *30*, 1345−1350.
(196) Wala, M.; Simka, W. Effect of Anode Material on Electrochemical Oxidation of Low Molecular Weight Alcohols—A Review. *Molecules* **2021**, *26*, 2144.
(197) Martínez-Huitle, C. A.; Panizza, M. Electrochemical oxidation of organic pollutants for wastewater treatment. *Current Opinion in Electrochemistry* **2018**, *11*, 62−71.
(198) Panizza, M.; Cerisola, G. Direct and mediated anodic oxidation of organic pollutants. *Chem. Rev.* **2009**, *109*, 6541−6569.
(199) Oturan, N.; Ganiyu, S. O.; Raffy, S.; Oturan, M. A. Sub-stoichiometric titanium oxide as a new anode material for electro-Fenton process: application to electrocatalytic destruction of antibiotic amoxicillin. *Applied Catalysis B: Environmental* **2017**, *217*, 214−223.
(200) Qiao, J.; Xiong, Y. Electrochemical oxidation technology: A review of its application in high-efficiency treatment of wastewater containing persistent organic pollutants. *Journal of Water Process Engineering* **2021**, *44*, 102308.
(201) Palma-Goyes, R.; Vazquez-Arenas, J.; Torres-Palma, R.; Ostos, C.; Ferraro, F.; González, I. The abatement of indigo carmine using active chlorine electrogenerated on ternary Sb2O5-doped Ti/RuO2-ZrO2 anodes in a filter-press FM01-LC reactor. *Electrochim. Acta* **2015**, *174*, 735−744.
(202) Duan, X.; Zhao, C.; Liu, W.; Zhao, X.; Chang, L. Fabrication of a novel PbO2 electrode with a graphene nanosheet interlayer for

https://doi.org/10.1021/acs.chemrev.1c00396
Chem. Rev. 2022, 122, 13547−13635

electrochemical oxidation of 2-chlorophenol. *Electrochim. Acta* **2017**, *240*, 424−436.
(203) Zuo, J.; Zhu, J.; Zhang, M.; Hong, Q.; Han, J.; Liu, J. Synergistic photoelectrochemical performance of La-doped RuO2-TiO2/Ti electrodes. *Appl. Surf. Sci.* **2020**, *502*, 144288.
(204) Wang, W.; Wang, K.; Hao, W.; Zhang, T.; Liu, Y.; Yu, L.; Li, W. Preparation of Ti-based Yb-doped SnO2−RuO2 electrode and electrochemical oxidation treatment of coking wastewater. *Journal of Rare Earths* **2022**, *40*, 763−771.
(205) Zhang, C.; Tang, J.; Peng, C.; Jin, M. Degradation of perfluorinated compounds in wastewater treatment plant effluents by electrochemical oxidation with Nano-ZnO coated electrodes. *J. Mol. Liq.* **2016**, *221*, 1145−1150.
(206) Man, S.; Bao, H.; Yang, H.; Xu, K.; Li, A.; Xie, Y.; Jian, Y.; Yang, W.; Mo, Z.; Li, X. Preparation and characterization of Nano-SiC doped PbO2 electrode for degradation of toluene diamine. *J. Alloys Compd.* **2021**, *859*, 157884.
(207) Kasian, O.; Luk'Yanenko, T.; Demchenko, P.; Gladyshevskii, R.; Amadelli, R.; Velichenko, A. Electrochemical properties of thermally treated platinized Ebonex® with low content of Pt. *Electrochim. Acta* **2013**, *109*, 630−637.
(208) Geng, P.; Su, J.; Miles, C.; Comninellis, C.; Chen, G. Highly-ordered Magnéli Ti4O7 nanotube arrays as effective anodic material for electro-oxidation. *Electrochim. Acta* **2015**, *153*, 316−324.
(209) Ioroi, T.; Yasuda, K. Highly reversal-tolerant anodes using Ti4O7-supported platinum with a very small amount of water-splitting catalyst. *J. Power Sources* **2020**, *450*, 227656.
(210) Lin, H.; Niu, J.; Liang, S.; Wang, C.; Wang, Y.; Jin, F.; Luo, Q.; Huang, Q. Development of macroporous Magnéli phase Ti4O7 ceramic materials: As an efficient anode for mineralization of poly-and perfluoroalkyl substances. *Chemical Engineering Journal* **2018**, *354*, 1058−1067.
(211) Ganiyu, S. O.; Oturan, N.; Raffy, S.; Esposito, G.; van Hullebusch, E. D.; Cretin, M.; Oturan, M. A. Use of sub-stoichiometric titanium oxide as a ceramic electrode in anodic oxidation and electro-Fenton degradation of the beta-blocker propranolol: degradation kinetics and mineralization pathway. *Electrochim. Acta* **2017**, *242*, 344−354.
(212) Ganiyu, S. O.; Oturan, N.; Raffy, S.; Cretin, M.; Causserand, C.; Oturan, M. A. Efficiency of plasma elaborated sub-stoichiometric titanium oxide (Ti4O7) ceramic electrode for advanced electrochemical degradation of paracetamol in different electrolyte media. *Sep. Purif. Technol.* **2019**, *208*, 142−152.
(213) Han, Z.; Xu, Y.; Zhou, S.; Zhu, P. Preparation and electrochemical properties of Al-based composite coating electrode with Ti4O7 ceramic interlayer for electrowinning of nonferrous metals. *Electrochim. Acta* **2019**, *325*, 134940.
(214) Iniesta, J.; Michaud, P.; Panizza, M.; Cerisola, G.; Aldaz, A.; Comninellis, C. Electrochemical oxidation of phenol at boron-doped diamond electrode. *Electrochim. Acta* **2001**, *46*, 3573−3578.
(215) Anglada, A.; Urtiaga, A.; Ortiz, I. Contributions of electrochemical oxidation to waste-water treatment: fundamentals and review of applications. *J. Chem. Technol. Biotechnol.* **2009**, *84*, 1747−1755.
(216) Reddy, C. V.; Reddy, K. R.; Harish, V. a.; Shim, J.; Shankar, M.; Shetti, N. P.; Aminabhavi, T. M. Metal-organic frameworks (MOFs)-based efficient heterogeneous photocatalysts: synthesis, properties and its applications in photocatalytic hydrogen generation, CO2 reduction and photodegradation of organic dyes. *Int. J. Hydrogen Energy* **2020**, *45*, 7656−7679.
(217) Elgarahy, A. M.; Elwakeel, K. Z.; Akhdhar, A.; Hamza, M. F. Recent advances in greenly synthesized nanoengineered materials for water/wastewater remediation: an overview. *Nanotechnol. Environ. Eng.* **2021**, *6*, 1−24.
(218) Du, X.; Oturan, M. A.; Zhou, M.; Belkessa, N.; Su, P.; Cai, J.; Trellu, C.; Mousset, E. Nanostructured electrodes for electrocatalytic advanced oxidation processes: From materials preparation to mechanisms understanding and wastewater treatment applications. *Applied Catalysis B: Environmental* **2021**, *296*, 120332.
(219) Michaud, P.-A.; Mahé, E.; Haenni, W.; Perret, A.; Comninellis, C. Preparation of peroxodisulfuric acid using boron-doped diamond thin film electrodes. *Electrochem. Solid-State Lett.* **1999**, *3*, 77.
(220) Serrano, K.; Michaud, P.; Comninellis, C.; Savall, A. Electrochemical preparation of peroxodisulfuric acid using boron doped diamond thin film electrodes. *Electrochim. Acta* **2002**, *48*, 431−436.
(221) Saha, M. S.; Furuta, T.; Nishiki, Y. Electrochemical synthesis of sodium peroxycarbonate at boron-doped diamond electrodes. *Electrochem. Solid-State Lett.* **2003**, *6*, D5.
(222) Wang, J.; Wang, S. Activation of persulfate (PS) and peroxymonosulfate (PMS) and application for the degradation of emerging contaminants. *Chemical Engineering Journal* **2018**, *334*, 1502−1517.
(223) Hasanzadeh, A.; Khataee, A.; Zarei, M.; Zhang, Y. Two-electron oxygen reduction on fullerene C60-carbon nanotubes covalent hybrid as a metal-free electrocatalyst. *Sci. Rep.* **2019**, *9*, 13780.
(224) Zhang, Z.; Meng, H.; Wang, Y.; Shi, L.; Wang, X.; Chai, S. Fabrication of graphene@ graphite-based gas diffusion electrode for improving H2O2 generation in Electro-Fenton process. *Electrochim. Acta* **2018**, *260*, 112−120.
(225) Su, P.; Zhou, M.; Lu, X.; Yang, W.; Ren, G.; Cai, J. Electrochemical catalytic mechanism of N-doped graphene for enhanced H2O2 yield and in-situ degradation of organic pollutant. *Applied Catalysis B: Environmental* **2019**, *245*, 583−595.
(226) Wang, W.; Lu, X.; Su, P.; Li, Y.; Cai, J.; Zhang, Q.; Zhou, M.; Arotiba, O. Enhancement of hydrogen peroxide production by electrochemical reduction of oxygen on carbon nanotubes modified with fluorine. *Chemosphere* **2020**, *259*, 127423.
(227) Carneiro, J. F.; Rocha, R. S.; Hammer, P.; Bertazzoli, R.; Lanza, M. Hydrogen peroxide electrogeneration in gas diffusion electrode nanostructured with Ta2O5. *Applied Catalysis A: General* **2016**, *517*, 161−167.
(228) Carneiro, J. F.; Silva, F. L.; Martins, A. S.; Dias, R. M.; Titato, G. M.; Santos-Neto, A. J.; Bertazzoli, R.; Lanza, M. R. Simultaneous degradation of hexazinone and diuron using ZrO2-nanostructured gas diffusion electrode. *Chemical Engineering Journal* **2018**, *351*, 650−659.
(229) Paz, E. C.; Aveiro, L. R.; Pinheiro, V. S.; Souza, F. M.; Lima, V. B.; Silva, F. L.; Hammer, P.; Lanza, M. R.; Santos, M. C. Evaluation of H2O2 electrogeneration and decolorization of Orange II azo dye using tungsten oxide nanoparticle-modified carbon. *Applied Catalysis B: Environmental* **2018**, *232*, 436−445.
(230) Yuan, S.; Gou, N.; Alshawabkeh, A. N.; Gu, A. Z. Efficient degradation of contaminants of emerging concerns by a new electro-Fenton process with Ti/MMO cathode. *Chemosphere* **2013**, *93*, 2796−2804.
(231) He, Y.; Ma, Y.; Meng, J.; Zhang, X.; Xia, Y. Dual electrochemical catalysis of Bi2Mo3O12/Ti cathode for hydrogen peroxide production in electro-Fenton system. *Journal of catalysis* **2019**, *373*, 297−305.
(232) Pitchai, R.; Thavasi, V.; Mhaisalkar, S. G.; Ramakrishna, S. Nanostructured cathode materials: a key for better performance in Li-ion batteries. *J. Mater. Chem.* **2011**, *21*, 11040−11051.
(233) Rajkumar, C.; Veerakumar, P.; Chen, S.-M.; Thirumalraj, B.; Lin, K.-C. Ultrathin sulfur-doped graphitic carbon nitride nanosheets as metal-free catalyst for electrochemical sensing and catalytic removal of 4-nitrophenol. *ACS Sustainable Chem. Eng.* **2018**, *6*, 16021−16031.
(234) Li, Z.; Shen, C.; Liu, Y.; Ma, C.; Li, F.; Yang, B.; Huang, M.; Wang, Z.; Dong, L.; Wolfgang, S. Carbon nanotube filter functionalized with iron oxychloride for flow-through electro-Fenton. *Applied Catalysis B: Environmental* **2020**, *260*, 118204.
(235) dos Santos Cunha, G.; de Souza-Chaves, B. M.; Bila, D. M.; Bassin, J. P.; Vecitis, C. D.; Dezotti, M. Insights into estrogenic activity removal using carbon nanotube electrochemical filter. *Sci. Total Environ.* **2019**, *678*, 448−456.
(236) Pleskov, Y. V.; Krotova, M.; Elkin, V.; Varnin, V.; Teremetskaya, I.; Saveliev, A.; Ralchenko, V. Benzene oxidation at

https://doi.org/10.1021/acs.chemrev.1c00396
Chem. Rev. 2022, 122, 13547−13635

diamond electrodes: Comparison of microcrystalline and nanocrystalline diamonds. *ChemPhysChem* **2012**, *13*, 3047−3052.
(237) Vecitis, C. D.; Gao, G.; Liu, H. Electrochemical carbon nanotube filter for adsorption, desorption, and oxidation of aqueous dyes and anions. *J. Phys. Chem. C* **2011**, *115*, 3621−3629.
(238) Cao, J.; Zhao, H.; Cao, F.; Zhang, J.; Cao, C. Electrocatalytic degradation of 4-chlorophenol on F-doped PbO2 anodes. *Electrochim. Acta* **2009**, *54*, 2595−2602.
(239) Bessegato, G. G.; Cardoso, J. C.; Zanoni, M. V. B. Enhanced photoelectrocatalytic degradation of an acid dye with boron-doped TiO2 nanotube anodes. *Catal. Today* **2015**, *240*, 100−106.
(240) Chen, Y.; Zhang, G.; Ma, J.; Zhou, Y.; Tang, Y.; Lu, T. Electro-oxidation of methanol at the different carbon materials supported Pt nano-particles. *international journal of hydrogen energy* **2010**, *35*, 10109−10117.
(241) Li, S.-H.; Zhao, Y.; Chu, J.; Li, W.-W.; Yu, H.-Q.; Liu, G. Electrochemical degradation of methyl orange on Pt−Bi/C nanostructured electrode by a square-wave potential method. *Electrochim. Acta* **2013**, *92*, 93−101.
(242) Li, D.; Guo, X.; Song, H.; Sun, T.; Wan, J. Preparation of RuO2-TiO2/Nano-graphite composite anode for electrochemical degradation of ceftriaxone sodium. *Journal of hazardous materials* **2018**, *351*, 250−259.
(243) Chang, X.; Thind, S. S.; Chen, A. Electrocatalytic enhancement of salicylic acid oxidation at electrochemically reduced TiO2 nanotubes. *ACS Catal.* **2014**, *4*, 2616−2622.
(244) Kim, C.; Kim, S.; Choi, J.; Lee, J.; Kang, J. S.; Sung, Y.-E.; Lee, J.; Choi, W.; Yoon, J. Blue TiO2 nanotube array as an oxidant generating novel anode material fabricated by simple cathodic polarization. *Electrochim. Acta* **2014**, *141*, 113−119.
(245) Yoon, J.-H.; Shim, Y.-B.; Lee, B.-s.; Choi, S.-Y.; Won, M.-S. Electrochemical degradation of phenol and 2-chlorophenol using Pt/Ti and boron-doped diamond electrodes. *Bulletin of the Korean Chemical Society* **2012**, *33*, 2274−2278.
(246) Huang, L.; Li, D.; Liu, J.; Yang, L.; Dai, C.; Ren, N.; Feng, Y. Construction of TiO2 nanotube clusters on Ti mesh for immobilizing Sb-SnO2 to boost electrocatalytic phenol degradation. *Journal of Hazardous Materials* **2020**, *393*, 122329.
(247) Dos Santos, E. V.; Sena, S. F. M.; da Silva, D. R.; Ferro, S.; De Battisti, A.; Martínez-Huitle, C. A. Scale-up of electrochemical oxidation system for treatment of produced water generated by Brazilian petrochemical industry. *Environmental Science and Pollution Research* **2014**, *21*, 8466−8475.
(248) Chaplin, B. P. The prospect of electrochemical technologies advancing worldwide water treatment. *Accounts of chemical research* **2019**, *52*, 596−604.
(249) Stirling, R.; Walker, W. S.; Westerhoff, P.; Garcia-Segura, S. Techno-economic analysis to identify key innovations required for electrochemical oxidation as point-of-use treatment systems. *Electrochim. Acta* **2020**, *338*, 135874.
(250) Coha, M.; Farinelli, G.; Tiraferri, A.; Minella, M.; Vione, D. Advanced oxidation processes in the removal of organic substances from produced water: Potential, configurations, and research needs. *Chemical Engineering Journal* **2021**, *414*, 128668.
(251) Ganiyu, S. O.; Sable, S.; El-Din, M. G. Advanced oxidation processes for the degradation of dissolved organics in produced water: A review of process performance, degradation kinetics and pathway. *Chemical Engineering Journal* **2022**, *429*, 132492.
(252) Brillas, E.; Sirés, I.; Oturan, M. A. Electro-Fenton process and related electrochemical technologies based on Fenton's reaction chemistry. *Chem. Rev.* **2009**, *109*, 6570−6631.
(253) Nidheesh, P.; Gandhimathi, R. Trends in electro-Fenton process for water and wastewater treatment: an overview. *Desalination* **2012**, *299*, 1−15.
(254) García-Espinoza, J. D.; Robles, I.; Durán-Moreno, A.; Godínez, L. A. Photo-assisted electrochemical advanced oxidation processes for the disinfection of aqueous solutions: A review. *Chemosphere* **2021**, *274*, 129957.
(255) Anwer, A. H.; Khan, M. D.; Khan, M. Z.; Joshi, R. *Modern Age Waste Water Problems*; Springer, 2020; pp 339−360.
(256) Pérez-García, J. A.; Bacame-Valenzuela, F. J.; Hernández, A. P.; Castañeda-Zaldivar, F.; Espejel-Ayala, F.; Reyes-Vidal, Y. *The Future of Effluent Treatment Plants*; Elsevier, 2021; pp 287−306.
(257) Cheng, S.; Mao, Z.; Sun, Y.; Yang, J.; Yu, Z.; Gu, R. A novel electrochemical oxidation-methanogenesis system for simultaneously degrading antibiotics and reducing CO2 to CH4 with low energy costs. *Science of The Total Environment* **2021**, *750*, 141732.
(258) Ramírez-Vargas, C. A.; Prado, A.; Arias, C. A.; Carvalho, P. N.; Esteve-Núñez, A.; Brix, H. Microbial electrochemical technologies for wastewater treatment: principles and evolution from microbial fuel cells to bioelectrochemical-based constructed wetlands. *Water* **2018**, *10*, 1128.
(259) Oturan, M. A.; Aaron, J.-J. Advanced oxidation processes in water/wastewater treatment: principles and applications. A review. *Critical Reviews in Environmental Science and Technology* **2014**, *44*, 2577−2641.
(260) Peng, H.; Guo, J. Removal of chromium from wastewater by membrane filtration, chemical precipitation, ion exchange, adsorption electrocoagulation, electrochemical reduction, electrodialysis, electrodeionization, photocatalysis and nanotechnology: a review. *Environ. Chem. Lett.* **2020**, *18*, 2055−2068.
(261) Yang, Q.; Yao, F.; Zhong, Y.; Wang, D.; Chen, F.; Sun, J.; Hua, S.; Li, S.; Li, X.; Zeng, G. Catalytic and electrocatalytic reduction of perchlorate in water−A review. *Chemical Engineering Journal* **2016**, *306*, 1081−1091.
(262) Garcia-Segura, S.; Lanzarini-Lopes, M.; Hristovski, K.; Westerhoff, P. Electrocatalytic reduction of nitrate: Fundamentals to full-scale water treatment applications. *Applied Catalysis B: Environmental* **2018**, *236*, 546−568.
(263) Sun, C.; Baig, S. A.; Lou, Z.; Zhu, J.; Wang, Z.; Li, X.; Wu, J.; Zhang, Y.; Xu, X. Electrocatalytic dechlorination of 2, 4-dichlorophenoxyacetic acid using nanosized titanium nitride doped palladium/nickel foam electrodes in aqueous solutions. *Applied Catalysis B: Environmental* **2014**, *158*, 38−47.
(264) Mao, R.; Zhao, X.; Lan, H.; Liu, H.; Qu, J. Graphene-modified Pd/C cathode and Pd/GAC particles for enhanced electrocatalytic removal of bromate in a continuous three-dimensional electrochemical reactor. *Water research* **2015**, *77*, 1−12.
(265) Mousset, E.; Puce, M.; Pons, M.-N. Advanced Electro-Oxidation with Boron-Doped Diamond for Acetaminophen Removal from Real Wastewater in a Microfluidic Reactor: Kinetics and Mass-Transfer Studies. *ChemElectroChem.* **2019**, *6*, 2908−2916.
(266) Mao, R.; Zhao, X.; Lan, H.; Liu, H.; Qu, J. Efficient electrochemical reduction of bromate by a Pd/rGO/CFP electrode with low applied potentials. *Applied Catalysis B: Environmental* **2014**, *160*, 179−187.
(267) Gennero De Chialvo, M. R.; Chialvo, A. Kinetics of hydrogen evolution reaction with Frumkin adsorption: re-examination of the Volmer−Heyrovsky and Volmer−Tafel routes. *Electrochimica Acta* **1998**, *44*, 841−851.
(268) Yao, F.; Yang, Q.; Sun, J.; Chen, F.; Zhong, Y.; Yin, H.; He, L.; Tao, Z.; Pi, Z.; Wang, D.; Li, X. Electrochemical reduction of bromate using noble metal-free nanoscale zero-valent iron immobilized activated carbon fiber electrode. *Chem. Eng. J.* **2020**, *389*, 123588.
(269) Sun, C.; Lou, Z.; Liu, Y.; Fu, R.; Zhou, X.; Zhang, Z.; Baig, S. A.; Xu, X. Influence of environmental factors on the electrocatalytic dechlorination of 2,4-dichlorophenoxyacetic acid on nTiN doped Pd/Ni foam electrode. *Chemical Engineering Journal* **2015**, *281*, 183−191.
(270) Wong, M. S.; Alvarez, P. J.; Fang, Y.-l.; Akçin, N.; Nutt, M. O.; Miller, J. T.; Heck, K. N. Cleaner water using bimetallic nanoparticle catalysts. *Journal of Chemical Technology & Biotechnology: International Research in Process, Environmental & Clean Technology* **2009**, *84*, 158−166.
(271) Nutt, M. O.; Hughes, J. B.; Wong, M. S. Designing Pd-on-Au bimetallic nanoparticle catalysts for trichloroethene hydrodechlorination. *Environ. Sci. Technol.* **2005**, *39*, 1346−1353.

https://doi.org/10.1021/acs.chemrev.1c00396
Chem. Rev. 2022, 122, 13547−13635

(272) Lan, H.; Mao, R.; Tong, Y.; Liu, Y.; Liu, H.; An, X.; Liu, R. Enhanced electroreductive removal of bromate by a supported Pd−In Bimetallic catalyst: kinetics and mechanism investigation. *Environ. Sci. Technol.* **2016**, *50*, 11872−11878.
(273) Lou, Z.; Zhou, J.; Sun, M.; Xu, J.; Yang, K.; Lv, D.; Zhao, Y.; Xu, X. MnO_2 enhances electrocatalytic hydrodechlorination by Pd/Ni foam electrodes and reduces Pd needs. *Chemical Engineering Journal* **2018**, *352*, 549−557.
(274) Song, S.; Liu, Q.; Fang, J.; Yu, W. Enhanced electrocatalytic dechlorination of 2,4-dichlorophenoxyacetic acid on in situ prepared Pd-anchored $Ni(OH)_2$ bifunctional electrodes: synergistic effect between H· formation on $Ni(OH)_2$ and dechlorination steps on Pd. *Catalysis Science & Technology* **2019**, *9*, 5130−5141.
(275) Gennaro, A.; Isse, A. A.; Bianchi, C. L.; Mussini, P. R.; Rossi, M. Is glassy carbon a really inert electrode material for the reduction of carbon−halogen bonds? *Electrochemistry communications* **2009**, *11*, 1932−1935.
(276) Zhang, Y.; Mu, S.; Deng, B.; Zheng, J. Electrochemical removal and release of perchlorate using poly (aniline-co-o-aminophenol). *J. Electroanal. Chem.* **2010**, *641*, 1−6.
(277) Ding, L.; Li, Q.; Cui, H.; Tang, R.; Xu, H.; Xie, X.; Zhai, J. Electrocatalytic reduction of bromate ion using a polyaniline-modified electrode: An efficient and green technology for the removal of BrO_3^- in aqueous solutions. *Electrochimica acta* **2010**, *55*, 8471−8475.
(278) Bellomunno, C.; Bonanomi, D.; Falciola, L.; Longhi, M.; Mussini, P.; Doubova, L.; Di Silvestro, G. Building up an electrocatalytic activity scale of cathode materials for organic halide reductions. *Electrochimica acta* **2005**, *50*, 2331−2341.
(279) Gütz, C.; Bänziger, M.; Bucher, C.; Galvão, T. R.; Waldvogel, S. R. Development and scale-up of the electrochemical dehalogenation for the synthesis of a key intermediate for NS5A inhibitors. *Org. Process Res. Dev.* **2015**, *19*, 1428−1433.
(280) Möhle, S.; Zirbes, M.; Rodrigo, E.; Gieshoff, T.; Wiebe, A.; Waldvogel, S. R. Modern electrochemical aspects for the synthesis of value-added organic products. *Angew. Chem., Int. Ed.* **2018**, *57*, 6018−6041.
(281) Vik, E. A.; Carlson, D. A.; Eikum, A. S.; Gjessing, E. T. Electrocoagulation of potable water. *Water research* **1984**, *18*, 1355−1360.
(282) Holt, P. K.; Barton, G. W.; Mitchell, C. A. The future for electrocoagulation as a localised water treatment technology. *Chemosphere* **2005**, *59*, 355−367.
(283) Mickova, I. L. Advanced electrochemical technologies in wastewater treatment. Part I: electrocoagulation. *Am. Sci. Res. J. Eng., Technol. Sci.* **2015**, *14*, 233−257.
(284) Mickova, I. L. Advanced electrochemical technologies in wastewater treatment. Part II: electro-flocculation and electro-flotation. *Am. Sci. Res. J. Eng., Technol. Sci.* **2015**, *14*, 273−294.
(285) Nidheesh, P.; Kumar, A.; Babu, D. S.; Scaria, J.; Kumar, M. S. Treatment of mixed industrial wastewater by electrocoagulation and indirect electrochemical oxidation. *Chemosphere* **2020**, *251*, 126437.
(286) Dieterich, A. E. Electric water-purifier. U.S. US823671A, 1906.
(287) Moreno C, H. A.; Cocke, D. L.; Gomes, J. A.; Morkovsky, P.; Parga, J.; Peterson, E.; Garcia, C. Electrochemical reactions for electrocoagulation using iron electrodes. *Ind. Eng. Chem. Res.* **2009**, *48*, 2275−2282.
(288) Canizares, P.; Carmona, M.; Lobato, J.; Martinez, F.; Rodrigo, M. A. Electrodissolution of aluminum electrodes in electrocoagulation processes. *Ind. Eng. Chem. Res.* **2005**, *44*, 4178−4185.
(289) Ofir, E.; Oren, Y.; Adin, A. Electroflocculation: the effect of zeta-potential on particle size. *Desalination* **2007**, *204*, 33−38.
(290) Darban, A.; Shahedi, A.; Taghipour, F.; Jamshidi-Zanjani, A. A review on industrial wastewater treatment via electrocoagulation processes. *Curr. Opin. Electrochem.* **2020**, *22*, 154−169.
(291) Al-Hanif, E. T.; Bagastyo, A. Y. Electrocoagulation for drinking water treatment: a review. *IOP Conf. Ser.: Earth Environ. Scii.* **2021**, *623*, 012016.
(292) Bandaru, S. R. S.; van Genuchten, C. M.; Kumar, A.; Glade, S.; Hernandez, D.; Nahata, M.; Gadgil, A. Rapid and Efficient Arsenic Removal by Iron Electrocoagulation Enabled with in Situ Generation of Hydrogen Peroxide. *Environ. Sci. Technol.* **2020**, *54* (10), 6094−6103, DOI: 10.1021/acs.est.0c00012.
(293) Tahreen, A.; Jami, M. S.; Ali, F. Role of electrocoagulation in wastewater treatment: A developmental review. *Journal of Water Process Engineering* **2020**, *37*, 101440.
(294) Mahesh, S.; Prasad, B.; Mall, I. D.; Mishra, I. M. Electrochemical degradation of pulp and paper mill wastewater. Part 1. COD and color removal. *Ind. Eng. Chem. Res.* **2006**, *45*, 2830−2839.
(295) Heidmann, I.; Calmano, W. Removal of Zn(II), Cu(II), Ni(II), Ag(I) and Cr(VI) present in aqueous solutions by aluminium electrocoagulation. *Journal of Hazardous Materials* **2008**, *152*, 934−941.
(296) Merzouk, B.; Gourich, B.; Sekki, A.; Madani, K.; Chibane, M. Removal turbidity and separation of heavy metals using electrocoagulation-electroflotation technique A case study. *Journal of Hazardous Materials* **2009**, *164*, 215−222.
(297) Zongo, I.; Leclerc, J. P.; Maiga, H. A.; Wethe, J.; Lapicque, F. Removal of hexavalent chromium from industrial wastewater by electrocoagulation: A comprehensive comparison of aluminium and iron electrodes. *Sep. Purif. Technol.* **2009**, *66*, 159−166.
(298) Shen, F.; Chen, X. M.; Gao, P.; Chen, G. H. Electrochemical removal of fluoride ions from industrial wastewater. *Chem. Eng. Sci.* **2003**, *58*, 987−993.
(299) Ölmez, T. The optimization of Cr (VI) reduction and removal by electrocoagulation using response surface methodology. *Journal of Hazardous Materials* **2009**, *162*, 1371−1378.
(300) Mamelkina, M. A.; Cotillas, S.; Lacasa, E.; Sáez, C.; Tuunila, R.; Sillanpää, M.; Häkkinen, A.; Rodrigo, M. A. Removal of sulfate from mining waters by electrocoagulation. *Sep. Purif. Technol.* **2017**, *182*, 87−93.
(301) Wang, C.-T.; Chou, W.-L.; Kuo, Y.-M. Removal of COD from laundry wastewater by electrocoagulation/electroflotation. *Journal of hazardous materials* **2009**, *164*, 81−86.
(302) Phalakornkule, C.; Sukkasem, P.; Mutchimsattha, C. Hydrogen recovery from the electrocoagulation treatment of dye-containing wastewater. *Int. J. Hydrogen Energy* **2010**, *35*, 10934−10943.
(303) Can, O. T.; Bayramoglu, M.; Kobya, M. Decolorization of reactive dye solutions by electrocoagulation using aluminum electrodes. *Ind. Eng. Chem. Res.* **2003**, *42*, 3391−3396.
(304) Ingelsson, M.; Yasri, N.; Roberts, E. P. Electrode Passivation, Faradaic Efficiency, and Performance Enhancement Strategies in Electrocoagulation—A Review. *Water Res.* **2020**, *187*, 116433.
(305) Garcia-Segura, S.; Eiband, M. M. S.; de Melo, J. V.; Martínez-Huitle, C. A. Electrocoagulation and advanced electrocoagulation processes: A general review about the fundamentals, emerging applications and its association with other technologies. *J. Electroanal. Chem.* **2017**, *801*, 267−299.
(306) Hakizimana, J. N.; Gourich, B.; Chafi, M.; Stiriba, Y.; Vial, C.; Drogui, P.; Naja, J. Electrocoagulation process in water treatment: A review of electrocoagulation modeling approaches. *Desalination* **2017**, *404*, 1−21.
(307) Chen, X. M.; Chen, G. H.; Yue, P. L. Novel electrode system for electroflotation of wastewater. *Environ. Sci. Technol.* **2002**, *36*, 778−783.
(308) Ge, J. T.; Qu, J. H.; Lei, P. J.; Liu, H. J. New bipolar electrocoagulation-electroflotation process for the treatment of laundry wastewater. *Sep. Purif. Technol.* **2004**, *36*, 33−39.
(309) Mollah, M. Y. A.; Morkovsky, P.; Gomes, J. A. G.; Kesmez, M.; Parga, J.; Cocke, D. L. Fundamentals, present and future perspectives of electrocoagulation. *Journal of Hazardous Materials* **2004**, *114*, 199−210.
(310) Kolesnikov, V.; Il'in, V.; Kolesnikov, A. Electroflotation in wastewater treatment from oil products, dyes, surfactants, ligands, and biological pollutants: a review. *Theoretical Foundations of Chemical Engineering* **2019**, *53*, 251−273.
(311) Elmore, A. S. Apparatus for concentrating ores. U.S. US865334A, 1907.

(312) Khosla, N.; Venkatachalam, S.; Somasundaran, P. Pulsed electrogeneration of bubbles for electroflotation. *J. Appl. Electrochem.* **1991**, *21*, 986−990.
(313) Emamjomeh, M. M.; Sivakumar, M. Review of pollutants removed by electrocoagulation and electrocoagulation/flotation processes. *Journal of environmental management* **2009**, *90*, 1663−1679.
(314) Matis, K.; Peleka, E. Alternative flotation techniques for wastewater treatment: focus on electroflotation. *Sep. Sci. Technol.* **2010**, *45*, 2465−2474.
(315) Mohtashami, R.; Shang, J. Q. Electroflotation for Treatment of Industrial Wastewaters: A Focused Review. *Environmental Processes* **2019**, *6*, 325−353.
(316) Peleka, E. N.; Gallios, G. P.; Matis, K. A. A perspective on flotation: a review. *J. Chem. Technol. Biotechnol.* **2018**, *93*, 615−623.
(317) Tadesse, B.; Albijanic, B.; Makuei, F.; Browner, R. Recovery of fine and ultrafine mineral particles by electroflotation−A review. *Mineral Processing and Extractive Metallurgy Review* **2019**, *40*, 108−122.
(318) Agrawal, A.; Kumari, S.; Sahu, K. K. Iron and Copper Recovery/Removal from Industrial Wastes: A Review. *Ind. Eng. Chem. Res.* **2009**, *48*, 6145−6161.
(319) Vasudevan, S.; Oturan, M. A. Electrochemistry: as cause and cure in water pollution-an overview. *Environmental Chemistry Letters* **2014**, *12*, 97−108.
(320) Rahimi, M.; Schoener, Z.; Zhu, X.; Zhang, F.; Gorski, C. A.; Logan, B. E. Removal of copper from water using a thermally regenerative electrodeposition battery. *Journal of hazardous materials* **2017**, *322*, 551−556.
(321) Peng, C.; Liu, Y.; Bi, J.; Xu, H.; Ahmed, A.-S. Recovery of copper and water from copper-electroplating wastewater by the combination process of electrolysis and electrodialysis. *Journal of hazardous materials* **2011**, *189*, 814−820.
(322) Guimarães, Y. F.; Santos, I. D.; Dutra, A. J. Direct recovery of copper from printed circuit boards (PCBs) powder concentrate by a simultaneous electroleaching−electrodeposition process. *Hydrometallurgy* **2014**, *149*, 63−70.
(323) Janin, A.; Zaviska, F.; Drogui, P.; Blais, J. F.; Mercier, G. Selective recovery of metals in leachate from chromated copper arsenate treated wastes using electrochemical technology and chemical precipitation. *Hydrometallurgy* **2009**, *96*, 318−326.
(324) Sulonen, M. L. K.; Kokko, M. E.; Lakaniemi, A. M.; Puhakka, J. A. Simultaneous removal of tetrathionate and copper from simulated acidic mining water in bioelectrochemical and electrochemical systems. *Hydrometallurgy* **2018**, *176*, 129−138.
(325) Anastassakis, G. N.; Bevilacqua, P.; De Lorenzi, L. Recovery of residual copper from low-content tailings derived from waste electrical cable treatment. *Int. J. Miner. Process.* **2015**, *143*, 105−111.
(326) Müller, S.; Holzer, F.; Haas, O. Optimized zinc electrode for the rechargeable zinc−air battery. *Journal of applied electrochemistry* **1998**, *28*, 895−898.
(327) Lai, Q.; Zhang, H.; Li, X.; Zhang, L.; Cheng, Y. A novel single flow zinc−bromine battery with improved energy density. *J. Power Sources* **2013**, *235*, 1−4.
(328) Gong, K.; Ma, X.; Conforti, K. M.; Kuttler, K. J.; Grunewald, J. B.; Yeager, K. L.; Bazant, M. Z.; Gu, S.; Yan, Y. A zinc−iron redox-flow battery under $100 per kW h of system capital cost. *Energy Environ. Sci.* **2015**, *8*, 2941−2945.
(329) Horstmann, B.; Danner, T.; Bessler, W. G. Precipitation in aqueous lithium−oxygen batteries: a model-based analysis. *Energy Environ. Sci.* **2013**, *6*, 1299−1314.
(330) Gilroy, D.; Conway, B. Kinetic theory of inhibition and passivation in electrochemical reactions. *J. Phys. Chem.* **1965**, *69*, 1259−1267.
(331) Lyklema, J.; Minor, M. On surface conduction and its role in electrokinetics. *Colloids Surf., A* **1998**, *140*, 33−41.
(332) Lyklema, J. *Fundamentals of Interface and Colloid Science: Soft Colloids*; Elsevier, 2005; Vol. *5*.
(333) Israelachvili, J. N. *Intermolecular and Surface Forces*; Academic Press, 2015.
(334) Ricart, M.; Pazos, M.; Gouveia, S.; Cameselle, C.; Sanroman, M. Removal of organic pollutants and heavy metals in soils by electrokinetic remediation. *Journal of Environmental Science and Health Part A* **2008**, *43*, 871−875.
(335) Ribeiro, A. B.; Mateus, E. P.; Rodríguez-Maroto, J.-M. Removal of organic contaminants from soils by an electrokinetic process: the case of molinate and bentazone. Experimental and modeling. *Sep. Purif. Technol.* **2011**, *79*, 193−203.
(336) Handojo, L.; Wardani, A.; Regina, D.; Bella, C.; Kresnowati, M.; Wenten, I. Electro-membrane processes for organic acid recovery. *RSC Adv.* **2019**, *9*, 7854−7869.
(337) Wen, D.; Fu, R.; Li, Q. Removal of inorganic contaminants in soil by electrokinetic remediation technologies: A review. *Journal of Hazardous Materials* **2021**, *401*, 123345.
(338) Strathmann, H. *Ion-Exchange Membrane Separation Processes*; Elsevier, 2004.
(339) Probstein, R. *Physicochemical Hydrodynamics: An Introduction*; John Wiley & Sons: New York, 1994.
(340) Hellferich, F. *Ion Exchange*; McGraw-Hill: New York, 1962.
(341) Hwang, S.-T.; Kammermeyer, K. *Membranes in Separation*; Wiley: New York, 1975.
(342) Nikonenko, V.; Yaroslavtsev, A.; Pourcelly, G. In *Ion Transfer in and through Charged Membranes*; Ciferri, A., Perico, A., Eds.; John Wiley & Sons, 2012; pp 267−336.
(343) Chen, Q.-B.; Wang, J.; Liu, Y.; Zhao, J.; Li, P. Novel energy-efficient electrodialysis system for continuous brackish water desalination: Innovative stack configurations and optimal inflow modes. *Water Res.* **2020**, *179*, 115847.
(344) Ladole, M. R.; Patil, S. S.; Paraskar, P. M.; Pokale, P. B.; Patil, P. D. *Sustainable Materials and Systems for Water Desalination*; Springer, 2021; pp 15−38.
(345) Xu, T. Ion exchange membranes: State of their development and perspective. *Journal of membrane science* **2005**, *263*, 1−29.
(346) Luo, T.; Abdu, S.; Wessling, M. Selectivity of ion exchange membranes: A review. *Journal of membrane science* **2018**, *555*, 429−454.
(347) Sonin, A.; Probstein, R. A hydrodynamic theory of desalination by electrodialysis. *Desalination* **1968**, *5*, 293−329.
(348) Kim, Y.; Walker, W. S.; Lawler, D. F. Competitive separation of di-vs. mono-valent cations in electrodialysis: Effects of the boundary layer properties. *water research* **2012**, *46*, 2042−2056.
(349) Deen, W. *Analysis of Transport Phenomena*, 2nd ed.; Oxford University Press: Oxford, 2012.
(350) Geissler, S.; Heits, H.; Werner, U. Description of fluid flow through spacers in flat-channel filtration systems. *Filtration & separation* **1995**, *32*, 538−544.
(351) Balster, J.; Stamatialis, D.; Wessling, M. Membrane with integrated spacer. *J.Membr. Sci.* **2010**, *360*, 185−189.
(352) Dukhin, S. S.; Deriagin, B. V. *Electrokinetic Phenomena*, 1974.
(353) Dukhin, S. S. Electrokinetic phenomena of the second kind and their applications. *Advances in colloid and interface science* **1991**, *35*, 173−196.
(354) Yaroshchuk, A. What makes a nano-channel? A limiting-current criterion. *Microfluid. Nanofluid.* **2012**, *12*, 615−624.
(355) Bouhidel, K.-E.; Benslimane, S. Ion exchange membrane modification by weak electrolytes and glycine: reduction and elimination of the concentration polarization plateau in electrodialysis. *Desalination* **2006**, *199*, 67−69.
(356) Peers, A. *Disc. Faraday Soc. 21*. **1956**.
(357) Rosenberg, N.; Tirrell, C. Limiting currents in membrane cells. *Industrial & Engineering Chemistry* **1957**, *49*, 780−784.
(358) Newman, J.; Thomas-Alyea, K. E. *Electrochemical Systems*; John Wiley & Sons, 2012.
(359) Bird, R. B.; Stewart, W. E.; Lightfoot, E. N.; Klingenberg, D. J. *Introductory Transport Phenomena*; Wiley: New York, 2015; Vol. *1*.
(360) Mareev, S.; Butylskii, D.; Kovalenko, A.; Petukhova, A.; Pismenskaya, N.; Dammak, L.; Larchet, C.; Nikonenko, V. Accounting for the concentration dependence of electrolyte diffusion

https://doi.org/10.1021/acs.chemrev.1c00396
Chem. Rev. 2022, 122, 13547−13635

coefficient in the Sand and the Peers equations. *Electrochim. Acta* **2016**, *195*, 85−93.
(361) Lévêque, M. Les Lois de la Transmission de Chaleur par Convection. Doctoral Dissertation, 1928.
(362) Kundu, P. K.; Cohen, I. M. *Fluid Mechanics*; Elsevier, 2001.
(363) Braff, W. A.; Buie, C. R.; Bazant, M. Z. Boundary layer analysis of membraneless electrochemical cells. *J. Electrochem. Soc.* **2013**, *160*, A2056−A2063.
(364) Cowan, D. A.; Brown, J. H. Effect of turbulence on limiting current in electrodialysis cells. *Industrial & Engineering Chemistry* **1959**, *51*, 1445−1448.
(365) Belfort, G.; Guter, G. A. An experimental study of electrodialysis hydrodynamics. *Desalination* **1972**, *10*, 221−262.
(366) Belfort, G.; Guter, G. An electrical analogue for electrodialysis. *Desalination* **1968**, *5*, 267−291.
(367) Atlas, I.; Wu, J.; Shocron, A. N.; Suss, M. E. Spatial variations of pH in electrodialysis stacks: Theory. *Electrochim. Acta* **2022**, *413*, 140151.
(368) Mubita, T.; Porada, S.; Biesheuvel, P.; van der Wal, A.; Dykstra, J. Strategies to increase ion selectivity in electrodialysis. *Sep. Purif. Technol.* **2022**, *292*, 120944.
(369) Nikonenko, V. V.; Kovalenko, A. V.; Urtenov, M. K.; Pismenskaya, N. D.; Han, J.; Sistat, P.; Pourcelly, G. Desalination at overlimiting currents: State-of-the-art and perspectives. *Desalination* **2014**, *342*, 85−106.
(370) Nikonenko, V. V.; Pismenskaya, N. D.; Belova, E. I.; Sistat, P.; Huguet, P.; Pourcelly, G.; Larchet, C. Intensive current transfer in membrane systems: Modelling, mechanisms and application in electrodialysis. *Adv. Colloid Interface Sci.* **2010**, *160*, 101−123.
(371) Westall, J.; Hohl, H. A comparison of electrostatic models for the oxide/solution interface. *Adv. Colloid Interface Sci.* **1980**, *12*, 265−294.
(372) Marinova, K.; Alargova, R.; Denkov, N.; Velev, O.; Petsev, D.; Ivanov, I.; Borwankar, R. Charging of oil- water interfaces due to spontaneous adsorption of hydroxyl ions. *Langmuir* **1996**, *12*, 2045−2051.
(373) Behrens, S. H.; Grier, D. G. The charge of glass and silica surfaces. *J. Chem. Phys.* **2001**, *115*, 6716−6721.
(374) Nap, R. J.; Božič, A. L.; Szleifer, I.; Podgornik, R. The role of solution conditions in the bacteriophage PP7 capsid charge regulation. *Biophysical journal* **2014**, *107*, 1970−1979.
(375) Safinya, C. R.; Radler, J. *Handbook of Lipid Membranes: Molecular, Functional, and Materials Aspects*; CRC Press, 2018; Chapter 9.
(376) Trefalt, G.; Behrens, S. H.; Borkovec, M. Charge regulation in the electrical double layer: ion adsorption and surface interactions. *Langmuir* **2016**, *32*, 380−400.
(377) Tian, H.; Wang, M. Electrokinetic mechanism of wettability alternation at oil-water-rock interface. *Surf. Sci. Rep.* **2017**, *72*, 369−391.
(378) Kharkats, Y. I.; Sokirko, A. Theory of the effect of migration current exaltation taking into account dissociation-recombination reactions. *Journal of electroanalytical chemistry and interfacial electrochemistry* **1991**, *303*, 27−44.
(379) Andersen, M.; van Soestbergen, M.; Mani, A.; Bruus, H.; Biesheuvel, P.; Bazant, M. Current-induced membrane discharge. *Phys. Rev. Lett.* **2012**, *109*, 108301.
(380) Rubinstein, I.; Zaltzman, B. Equilibrium Electroconvective Instability. *Phys. Rev. Lett.* **2015**, *114*, 114502.
(381) Rubinstein, I.; Zaltzman, B. Extended space charge in concentration polarization. *Advances in colloid and interface science* **2010**, *159*, 117−129.
(382) Zaltzman, B.; Rubinstein, I. Electro-osmotic slip and electroconvective instability. *J. Fluid Mech.* **2007**, *579*, 173−226.
(383) Rubinstein, S.; Manukyan, G.; Staicu, A.; Rubinstein, I.; Zaltzman, B.; Lammertink, R.; Mugele, F.; Wessling, M. Direct observation of a nonequilibrium electro-osmotic instability. *Phys. Rev. Lett.* **2008**, *101*, 236101.
(384) Yossifon, G.; Chang, H.-C. Selection of nonequilibrium overlimiting currents: universal depletion layer formation dynamics and vortex instability. *Phys. Rev. Lett.* **2008**, *101*, 254501.
(385) Pham, S.; Li, Z.; Lim, K.; White, J.; Han, J. Direct numerical simulation of electroconvective instability and hysteretic current-voltage response of permselective membrane. *Phys. Rev. E* **2012**, *86*, 046310.
(386) Kwak, R.; Pham, V.; Lim, K.; Han, J. Shear flow of an electrically charged fluid by ion concentration polarization: scaling laws for convection vortices. *Phys. Rev. Lett.* **2013**, *110*, 114501.
(387) Chang, H.-C.; Yossifon, G.; Demekhin, E. A. Nanoscale electrokinetics and microvortices: How microhydrodynamics affects nanofluidic ion flux. *Annu. Rev. Fluid Mech.* **2012**, *44*, 401−426.
(388) Davidson, S. M.; Wessling, M.; Mani, A. On the dynamical regimes of pattern-accelerated electroconvection. *Sci. Rep.* **2016**, *6*, 22505.
(389) Xu, B.; Gu, Z.; Liu, W.; Huo, P.; Zhou, Y.; Rubinstein, S.; Bazant, M.; Zaltzman, B.; Rubinstein, I.; Deng, D. Electro-osmotic instability of concentration enrichment in curved geometries for an aqueous electrolyte. *Physical Review Fluids* **2020**, *5*, 091701.
(390) Wessling, M.; Morcillo, L. G.; Abdu, S. Nanometer-thick lateral polyelectrolyte micropatterns induce macrosopic electro-osmotic chaotic fluid instabilities. *Sci. Rep.* **2015**, *4*, 4294.
(391) Roghmans, F.; Evdochenko, E.; Stockmeier, F.; Schneider, S.; Smailji, A.; Tiwari, R.; Mikosch, A.; Karatay, E.; Kuhne, A.; Walther, A.; Mani, A.; Wessling, M. 2D Patterned Ion-Exchange Membranes Induce Electroconvection. *Advanced Materials Interfaces* **2019**, *6*, 1801309.
(392) Zyryanova, S.; Mareev, S.; Gil, V.; Korzhova, E.; Pismenskaya, N.; Sarapulova, V.; Rybalkina, O.; Boyko, E.; Larchet, C.; Dammak, L.; Nikonenko, V. How Electrical Heterogeneity Parameters of Ion-Exchange Membrane Surface Affect the Mass Transfer and Water Splitting Rate in Electrodialysis. *Int. J. Mol. Sci.* **2020**, *21*, 973.
(393) Butylskii, D.; Moroz, I.; Tsygurina, K.; Mareev, S. Effect of Surface Inhomogeneity of Ion-Exchange Membranes on the Mass Transfer Efficiency in Pulsed Electric Field Modes. *Membranes* **2020**, *10*, 40.
(394) Mishchuk, N. Perspectives of the electrodialysis intensification. *Desalination* **1998**, *117*, 283−295.
(395) Mishchuk, N.; Koopal, L.; Gonzalez-Caballero, F. Intensification of electrodialysis by applying a non-stationary electric field. *Colloids Surf., A* **2001**, *176*, 195−212.
(396) Lemay, N.; Mikhaylin, S.; Bazinet, L. Voltage spike and electroconvective vortices generation during electrodialysis under pulsed electric field: Impact on demineralization process efficiency and energy consumption. *Innovative food science & emerging technologies* **2019**, *52*, 221−231.
(397) Lemay, N.; Mikhaylin, S.; Mareev, S.; Pismenskaya, N.; Nikonenko, V.; Bazinet, L. How demineralization duration by electrodialysis under high frequency pulsed electric field can be the same as in continuous current condition and that for better performances? *J. Membr. Sci.* **2020**, *603*, 117878.
(398) Gonzalez-Vogel, A.; Rojas, O. J. Exploiting electroconvective vortices in electrodialysis with high-frequency asymmetric bipolar pulses for desalination in overlimiting current regimes. *Desalination* **2020**, *474*, 114190.
(399) Huth, J.; Swinney, H.; Mccormick, W.; Kuhn, A.; Argoul, F. *Phys. Rev. E* **1995**, *51*, 3444−3458.
(400) Bai, P.; Li, J.; Brushett, F. R.; Bazant, M. Z. Transition of lithium growth mechanisms in liquid electrolytes. *Energy Environ. Sci.* **2016**, *9*, 3221−3229.
(401) He, Y.; Ge, L.; Ge, Z.; Zhao, Z.; Sheng, F.; Liu, X.; Ge, X.; Yang, Z.; Fu, R.; Liu, Z.; Wu, L.; Xu, T. Monovalent cations permselective membranes with zwitterionic side chains. *J. Membr. Sci.* **2018**, *563*, 320−325.
(402) Chandra, A.; Bhuvanesh, E.; Mandal, P.; Chattopadhyay, S. Surface modification of anion exchange membrane using layer-by-layer polyelectrolytes deposition facilitating monovalent organic acid transport. *Colloids Surf., A* **2018**, *558*, 579−590.

https://doi.org/10.1021/acs.chemrev.1c00396
Chem. Rev. 2022, 122, 13547−13635

(403) Merino-Garcia, I.; Kotoka, F.; Portugal, C. A.; Crespo, J. G.; Velizarov, S. Characterization of poly (Acrylic) acid-modified heterogenous anion exchange membranes with improved monovalent permselectivity for RED. *Membranes* **2020**, *10*, 134.
(404) Ahdab, Y. D.; Rehman, D.; Lienhard, J. H. Brackish water desalination for greenhouses: Improving groundwater quality for irrigation using monovalent selective electrodialysis reversal. *J. Membr. Sci.* **2020**, *610*, 118072.
(405) Ahdab, Y. D.; Rehman, D.; Schücking, G.; Barbosa, M.; Lienhard, J. H. Treating irrigation water using high-performance membranes for monovalent selective electrodialysis. *ACS ES&T Water* **2021**, *1*, 117−124.
(406) Tian, H.; Wang, Y.; Pei, Y.; Crittenden, J. C. Unique applications and improvements of reverse electrodialysis: A review and outlook. *Applied Energy* **2020**, *262*, 114482.
(407) Liu, L.; Cheng, Q. Mass transfer characteristic research on electrodialysis for desalination and regeneration of solution: A comprehensive review. *Renewable and Sustainable Energy Reviews* **2020**, *134*, 110115.
(408) Wenten, I.; Khoiruddin, K.; Wardani, A. K.; Widiasa, I. *Synthetic Polymeric Membranes for Advanced Water Treatment, Gas Separation, and Energy Sustainability*; Elsevier, 2020; pp 71−101.
(409) Ariono, D; Khoiruddin; Subagjo; Wenten, I G. Heterogeneous structure and its effect on properties and electrochemical behavior of ion-exchange membrane. *Mater. Res. Express* **2017**, *4*, 024006.
(410) Andreeva, M.; Gil, V.; Pismenskaya, N.; Nikonenko, V.; Dammak, L.; Larchet, C.; Grande, D.; Kononenko, N. Effect of homogenization and hydrophobization of a cation-exchange membrane surface on its scaling in the presence of calcium and magnesium chlorides during electrodialysis. *J. Membr. Sci.* **2017**, *540*, 183−191.
(411) Hosseini, S.; Rafiei, N.; Salabat, A.; Ahmadi, A. Fabrication of new type of barium ferrite/copper oxide composite nanoparticles blended polyvinylchloride based heterogeneous ion exchange membrane. *Arabian Journal of Chemistry* **2020**, *13*, 2470−2482.
(412) Mareev, S.; Butylskii, D. Y.; Pismenskaya, N.; Larchet, C.; Dammak, L.; Nikonenko, V. Geometric heterogeneity of homogeneous ion-exchange Neosepta membranes. *Journal of membrane science* **2018**, *563*, 768−776.
(413) Vasil'eva, V.; Goleva, E.; Pismenskaya, N.; Kozmai, A.; Nikonenko, V. Effect of surface profiling of a cation-exchange membrane on the phenylalanine and NaCl separation performances in diffusion dialysis. *Sep. Purif. Technol.* **2019**, *210*, 48−59.
(414) Belloň, T.; Slouka, Z. Overlimiting behavior of surface-modified heterogeneous anion-exchange membranes. *J. Membr. Sci.* **2020**, *610*, 118291.
(415) Gil, V.; Porozhnyy, M.; Rybalkina, O.; Butylskii, D.; Pismenskaya, N. The Development of Electroconvection at the Surface of a Heterogeneous Cation-Exchange Membrane Modified with Perfluorosulfonic Acid Polymer Film Containing Titanium Oxide. *Membranes* **2020**, *10*, 125.
(416) Akberova, E.; Vasil'eva, V. Effect of the resin content in cation-exchange membranes on development of electroconvection. *Electrochem. Commun.* **2020**, *111*, 106659.
(417) Al-Amshawee, S.; Yunus, M. Y. B. M.; Azoddein, A. A. M.; Hassell, D. G.; Dakhil, I. H.; Hasan, H. A. Electrodialysis desalination for water and wastewater: A review. *Chemical Engineering Journal* **2020**, *380*, 122231.
(418) Mikhaylin, S.; Bazinet, L. Fouling on ion-exchange membranes: Classification, characterization and strategies of prevention and control. *Advances in colloid and interface science* **2016**, *229*, 34−56.
(419) Hansima, M.; Makehelwala, M.; Jinadasa, K.; Wei, Y.; Nanayakkara, K.; Herath, A. C.; Weerasooriya, R. Fouling of ion exchange membranes used in the electrodialysis reversal advanced water treatment: A review. *Chemosphere* **2020**, *263*, 127951.
(420) Tong, X.; Zhang, B.; Chen, Y. Fouling resistant nanocomposite cation exchange membrane with enhanced power generation for reverse electrodialysis. *J. Membr. Sci.* **2016**, *516*, 162−171.
(421) Li, Y.; Shi, S.; Cao, H.; Zhao, Z.; Su, C.; Wen, H. Improvement of the antifouling performance and stability of an anion exchange membrane by surface modification with graphene oxide (GO) and polydopamine (PDA). *J. Membr. Sci.* **2018**, *566*, 44−53.
(422) Liu, Y.; Yang, S.; Chen, Y.; Liao, J.; Pan, J.; Sotto, A.; Shen, J. Preparation of water-based anion-exchange membrane from PVA for anti-fouling in the electrodialysis process. *J. Membr. Sci.* **2019**, *570*, 130−138.
(423) Bdiri, M.; Larchet, C.; Dammak, L. A Review on Ion-exchange Membranes Fouling and Antifouling During Electrodialysis Used in Food Industry: Cleanings and Strategies of Prevention. *Chemistry Africa* **2020**, *3*, 609−633.
(424) Huang, C.; Xu, T. Electrodialysis with bipolar membranes for sustainable development. *Environ. Sci. Technol.* **2006**, *40*, 5233−5243.
(425) Nikonenko, V.; Urtenov, M.; Mareev, S.; Pourcelly, G. Mathematical Modeling of the Effect of Water Splitting on Ion Transfer in the Depleted Diffusion Layer Near an Ion-Exchange Membrane. *Membranes* **2020**, *10*, 22.
(426) Pärnamäe, R.; Mareev, S.; Nikonenko, V.; Melnikov, S.; Sheldeshov, N.; Zabolotskii, V.; Hamelers, H.; Tedesco, M. Bipolar membranes: A review on principles, latest developments, and applications. *J. Membr. Sci.* **2020**, *617*, 118538.
(427) Nagasubramanian, K.; Chlanda, F.; Liu, K.-J. Use of bipolar membranes for generation of acid and base—an engineering and economic analysis. *J. Membr. Sci.* **1977**, *2*, 109−124.
(428) Bayramoğlu, G.; Tuzun, I.; Celik, G.; Yilmaz, M.; Arica, M. Y. Biosorption of mercury (II), cadmium (II) and lead (II) ions from aqueous system by microalgae Chlamydomonas reinhardtii immobilized in alginate beads. *Int. J. Miner. Process.* **2006**, *81*, 35−43.
(429) Wilhelm, F.; Pünt, I.; Van Der Vegt, N.; Wessling, M.; Strathmann, H. Optimisation strategies for the preparation of bipolar membranes with reduced salt ion leakage in acid−base electrodialysis. *J. Membr. Sci.* **2001**, *182*, 13−28.
(430) Mafé, S.; Ramırez, P.; Alcaraz, A. Electric field-assisted proton transfer and water dissociation at the junction of a fixed-charge bipolar membrane. *Chem. Phys. Lett.* **1998**, *294*, 406−412.
(431) Zabolotskii, V.; Sharafan, M.; Shel'deshov, N. Influence of the nature of membrane ionogenic groups on water dissociation and electrolyte ion transport: A rotating membrane disk study. *Russian Journal of Electrochemistry* **2008**, *44*, 1127−1134.
(432) Zabolotskii, V.; Sheldeshov, N.; Melnikov, S. Heterogeneous bipolar membranes and their application in electrodialysis. *Desalination* **2014**, *342*, 183−203.
(433) Mareev, S.; Evdochenko, E.; Wessling, M.; Kozaderova, O.; Niftaliev, S.; Pismenskaya, N.; Nikonenko, V. A comprehensive mathematical model of water splitting in bipolar membranes: Impact of the spatial distribution of fixed charges and catalyst at bipolar junction. *J. Membr. Sci.* **2020**, *603*, 118010.
(434) Zhang, X.; Li, C.; Wang, Y.; Luo, J.; Xu, T. Recovery of acetic acid from simulated acetaldehyde wastewaters: Bipolar membrane electrodialysis processes and membrane selection. *Journal of membrane science* **2011**, *379*, 184−190.
(435) Ghyselbrecht, K.; Huygebaert, M.; Van der Bruggen, B.; Ballet, R.; Meesschaert, B.; Pinoy, L. Desalination of an industrial saline water with conventional and bipolar membrane electrodialysis. *Desalination* **2013**, *318*, 9−18.
(436) Ilhan, F.; Kabuk, H. A.; Kurt, U.; Avsar, Y.; Gonullu, M. T. Recovery of mixed acid and base from wastewater with bipolar membrane electrodialysis—a case study. *Desalination and Water Treatment* **2016**, *57*, 5165−5173.
(437) Sun, X.; Lu, H.; Wang, J. Recovery of citric acid from fermented liquid by bipolar membrane electrodialysis. *Journal of Cleaner Production* **2017**, *143*, 250−256.
(438) Bunani, S.; Arda, M.; Kabay, N.; Yoshizuka, K.; Nishihama, S. Effect of process conditions on recovery of lithium and boron from water using bipolar membrane electrodialysis (BMED). *Desalination* **2017**, *416*, 10−15.

https://doi.org/10.1021/acs.chemrev.1c00396
Chem. Rev. 2022, 122, 13547−13635

(439) Noguchi, M.; Nakamura, Y.; Shoji, T.; Iizuka, A.; Yamasaki, A. Simultaneous removal and recovery of boron from waste water by multi-step bipolar membrane electrodialysis. *Journal of Water Process Engineering* **2018**, *23*, 299−305.
(440) Lin, J.; Lin, F.; Chen, X.; Ye, W.; Li, X.; Zeng, H.; Van der Bruggen, B. Sustainable management of textile wastewater: A hybrid tight ultrafiltration/bipolar-membrane electrodialysis process for resource recovery and zero liquid discharge. *Ind. Eng. Chem. Res.* **2019**, *58*, 11003−11012.
(441) Cherif, A. T.; Molenat, J.; Elmidaoui, A. Nitric acid and sodium hydroxide generation by electrodialysis using bipolar membranes. *Journal of Applied Electrochemistry* **1997**, *27*, 1069−1074.
(442) Abu Khalla, S.; Suss, M. Desalination via chemical energy: An electrodialysis cell driven by spontaneous electrode reactions. *Desalination* **2019**, *467*, 257−262.
(443) Atlas, I.; Suss, M. Theory of simultaneous desalination and electricity generation via an electrodialysis cell driven by spontaneous redox reactions. *Electrochim. Acta* **2019**, *319*, 813−821.
(444) Ghahari, M.; Rashid-Nadimi, S.; Bemana, H. Metal-air desalination battery: Concurrent energy generation and water desalination. *J. Power Sources* **2019**, *412*, 197−203.
(445) Wang, L.; Zhang, Y.; Moh, K.; Presser, V. From capacitive deionization to desalination batteries and desalination fuel cells. *Current Opinion in Electrochemistry* **2021**, *29*, 100758.
(446) Chen, X.; Xia, X.; Liang, P.; Cao, X.; Sun, H.; Huang, X. Stacked microbial desalination cells to enhance water desalination efficiency. *Environ. Sci. Technol.* **2011**, *45*, 2465−2470.
(447) Qu, Y.; Feng, Y.; Wang, X.; Liu, J.; Lv, J.; He, W.; Logan, B. E. Simultaneous water desalination and electricity generation in a microbial desalination cell with electrolyte recirculation for pH control. *Bioresource technology* **2012**, *106*, 89−94.
(448) Atlas, I.; Abu Khalla, S.; Suss, M. Thermodynamic Energy Efficiency of Electrochemical Systems Performing Simultaneous Water Desalination and Electricity Generation. *J. Electrochem. Soc.* **2020**, *167*, 134517.
(449) Zhang, Y.; Wang, L.; Presser, V. Electrocatalytic fuel cell desalination for continuous energy and freshwater generation. *Cell Reports Physical Science* **2021**, *2*, 100416.
(450) Abu Khalla, S.; Atlas, I.; Litster, S.; Suss, M. E. Desalination Fuel Cells with High Thermodynamic Energy Efficiency. *Environ. Sci. Technol.* **2022**, *56*, 1413−1422.
(451) Amikam, G.; Manor-Korin, N.; Nativ, P.; Gendel, Y. Separation of ions from water and wastewater using micro-scale capacitive-faradaic fuel cells (CFFCs), powered by H2 (g) and air. *Sep. Purif. Technol.* **2020**, *253*, 117494.
(452) Suss, M. E.; Zhang, Y.; Atlas, I.; Gendel, Y.; Ruck, E.; Presser, V. Emerging, hydrogen-driven electrochemical water purification. *Electrochem. Commun.* **2022**, *136*, 107211.
(453) Bhat, Z. M.; Pandit, D.; Ardo, S.; Thimmappa, R.; Kottaichamy, A. R.; Dargily, N. C.; Devendrachari, M. C.; Thotiyl, M. O. An electrochemical neutralization cell for spontaneous water desalination. *Joule* **2020**, *4*, 1730−1742.
(454) Abdalla, S.; Khalla, S. A.; Suss, M. E. Voltage loss breakdown in desalination fuel cells. *Electrochem. Commun.* **2021**, *132*, 107136.
(455) Asokan, A.; Abu-Khalla, S.; Abdalla, S.; Suss, M. E. Chloride-Tolerant, Inexpensive Fe/N/C Catalysts for Desalination Fuel Cell Cathodes. *ACS Applied Energy Materials* **2022**, *5*, 1743−1754.
(456) Bouhidel, K.-E.; Lakehal, A. Influence of voltage and flow rate on electrodeionization (EDI) process efficiency. *Desalination* **2006**, *193*, 411−421.
(457) Pan, S.-Y.; Snyder, S. W.; Ma, H.-W.; Lin, Y. J.; Chiang, P.-C. Energy-efficient resin wafer electrodeionization for impaired water reclamation. *Journal of Cleaner Production* **2018**, *174*, 1464−1474.
(458) Zhao, C.; Zhang, L.; Ge, R.; Zhang, A.; Zhang, C.; Chen, X. Treatment of low-level Cu (II) wastewater and regeneration through a novel capacitive deionization-electrodeionization (CDI-EDI) technology. *Chemosphere* **2019**, *217*, 763−772.
(459) Lee, H.-J.; Song, J.-H.; Moon, S.-H. Comparison of electrodialysis reversal (EDR) and electrodeionization reversal (EDIR) for water softening. *Desalination* **2013**, *314*, 43−49.
(460) Rathi, B. S.; Kumar, P. S. Electrodeionization theory, mechanism and environmental applications. A review. *Environmental Chemistry Letters* **2020**, *18*, 1209−1227.
(461) Arar, Ö.; Yüksel, Ü.; Kabay, N.; Yüksel, M. Demineralization of geothermal water reverse osmosis (RO) permeate by electrodeionization (EDI) with layered bed configuration. *Desalination* **2013**, *317*, 48−54.
(462) Song, J.-H.; Song, M.-C.; Yeon, K.-H.; Kim, J.-B.; Lee, K.-J.; Moon, S.-H. Purification of a primary coolant in a nuclear power plant using a magnetic filter—electrodeionization hybrid separation system. *J. Radioanal. Nuclear Chem.* **2005**, *262*, 725−732.
(463) Ganzi, G.; Egozy, Y.; Giuffrida, A.; Jha, A. High purity water by electrodeionization performance of the ionpure continuous deionization system. *Ultrapure Water* **1987**, *4*, 43−50.
(464) Shaposhnik, V.; Kuzminykh, V.; Grigorchuk, O.; Vasil'eva, V. Analytical model of laminar flow electrodialysis with ion-exchange membranes. *Journal of membrane science* **1997**, *133*, 27−37.
(465) Fu, L.; Wang, J.; Su, Y. Removal of low concentrations of hardness ions from aqueous solutions using electrodeionization process. *Sep. Purif. Technol.* **2009**, *68*, 390−396.
(466) Jordan, M. L.; Valentino, L.; Nazyrynbekova, N.; Palakkal, V. M.; Kole, S.; Bhattacharya, D.; Lin, Y. J.; Arges, C. G. Promoting water-splitting in Janus bipolar ion-exchange resin wafers for electrodeionization. *Molecular Systems Design & Engineering* **2020**, *5*, 922−935.
(467) Palakkal, V. M.; Valentino, L.; Lei, Q.; Kole, S.; Lin, Y. J.; Arges, C. G. Advancing electrodeionization with conductive ionomer binders that immobilize ion-exchange resin particles into porous wafer substrates. *NPJ Clean Water* **2020**, *3*, 5.
(468) Yeon, K.; Seong, J.; Rengaraj, S.; Moon, S. Electrochemical characterization of ion-exchange resin beds and removal of cobalt by electrodeionization for high purity water production. *Sep. Sci. Technol.* **2003**, *38*, 443−462.
(469) Mahmoud, A.; Muhr, L.; Grévillot, G.; Valentin, G.; Lapicque, F. Ohmic drops in the ion-exchange bed of cationic electrodeionisation cells. *Journal of applied electrochemistry* **2006**, *36*, 277−285.
(470) Alvarado, L.; Rodríguez-Torres, I.; Balderas, P. Investigation of Current Routes in Electrodeionization System Resin Beds During Chromium Removal. *Electrochim. Acta* **2015**, *182*, 763−768.
(471) Sauer, M.; Southwick, P.; Spiegler, K.; Wyllie, M. Electrical conductance of porous plugs-ion exchange resin-solution systems. *Industrial & Engineering Chemistry* **1955**, *47*, 2187−2193.
(472) Strathmann, H.; Krol, J.; Rapp, H.-J.; Eigenberger, G. Limiting current density and water dissociation in bipolar membranes. *J. Membr. Sci.* **1997**, *125*, 123−142.
(473) Nikonenko, V.; Mareev, S.; Pis'menskaya, N.; Uzdenova, A.; Kovalenko, A.; Urtenov, M. K.; Pourcelly, G. Effect of electroconvection and its use in intensifying the mass transfer in electrodialysis. *Russian Journal of Electrochemistry* **2017**, *53*, 1122−1144.
(474) Mani, A.; Wang, K. M. Electroconvection Near Electrochemical Interfaces: Experiments, Modeling, and Computation. *Annu. Rev. Fluid Mech.* **2020**, *52*, 509−529.
(475) Park, S.; Kwak, R. Microscale electrodeionization: In situ concentration profiling and flow visualization. *Water research* **2020**, *170*, 115310.
(476) Stockmeier, F.; Schatz, M.; Habermann, M.; Linkhorst, J.; Mani, A.; Wessling, M. Direct 3D observation and unraveling of electroconvection phenomena during concentration polarization at ion-exchange membranes. *J. Membr. Sci.* **2021**, *640*, 119846.
(477) Wen, R.; Deng, S.; Zhang, Y. The removal of silicon and boron from ultra-pure water by electrodeionization. *Desalination* **2005**, *181*, 153−159.

https://doi.org/10.1021/acs.chemrev.1c00396
Chem. Rev. 2022, 122, 13547−13635

(478) Lounis, A.; Setti, L.; Djennane, A.; Melikchi, R. Separation of Molybdenum-Uranium by a process combining ion exchange resin and membranes. *J. Appl. Sci.* **2007**, *7*, 1963−1967.
(479) Taghdirian, H. R.; Moheb, A.; Mehdipourghazi, M. Selective separation of Ni (II)/Co (II) ions from dilute aqueous solutions using continuous electrodeionization in the presence of EDTA. *J. Membr. Sci.* **2010**, *362*, 68−75.
(480) Ervan, Y.; Wenten, I. G. Study on the influence of applied voltage and feed concentration on the performance of electro-deionization. *Songklanakarin J. Sci. Technol.* **2002**, *24*, 955−963.
(481) Monzie, I.; Muhr, L.; Lapicque, F.; Grévillot, G. Mass transfer investigations in electrodeionization processes using the microcolumn technique. *Chemical engineering science* **2005**, *60*, 1389−1399.
(482) Hakim, A. N.; Khoiruddin, K.; Ariono, D.; Wenten, I. Ionic Separation in Electrodeionization System: Mass Transfer Mechanism and Factor Affecting Separation Performance. *Separ. Purif. Rev.* **2019**, *49*, 294−316.
(483) Otero, C.; Urbina, A.; Rivero, E. P.; Rodríguez, F. A. Desalination of brackish water by electrodeionization: Experimental study and mathematical modeling. *Desalination* **2021**, *504*, 114803.
(484) Verbeek, H.; Fürst, L.; Neumeister, H. Digital simulation of an electrodeionization process. *Computers & chemical engineering* **1998**, *22*, S913−S916.
(485) Lu, J.; Wang, Y.-X.; Zhu, J. Numerical simulation of the electrodeionization (EDI) process accounting for water dissociation. *Electrochimica acta* **2010**, *55*, 2673−2686.
(486) Lu, J.; Ma, X.-Y.; Wang, Y.-X. Numerical simulation of the electrodeionization (EDI) process with layered resin bed for deeply separating salt ions. *Desalination and Water Treatment* **2016**, *57*, 10546−10559.
(487) Zahakifar, F.; Keshtkar, A.; Souderjani, E. Z.; Moosavian, M. Use of response surface methodology for optimization of thorium (IV) removal from aqueous solutions by electrodeionization (EDI). *Progress in Nuclear Energy* **2020**, *124*, 103335.
(488) Glueckauf, E. Electro-deionization through a packed bed. *Br. Chem. Eng.* **1959**, *4*, 646−651.
(489) Dobrevsky, I.; Zvezdov, A. Investigation of pore structure of ion exchange membranes. *Desalination* **1979**, *28*, 283−289.
(490) Yaroslavtsev, A. B.; Nikonenko, V. V.; Zabolotsky, V. I. Ion transfer in ion-exchange and membrane materials. *Russian chemical reviews* **2003**, *72*, 393−421.
(491) Faucher, S.; Aluru, N.; Bazant, M. Z.; Blankschtein, D.; Brozena, A. H.; Cumings, J.; Pedro de Souza, J.; Elimelech, M.; Epsztein, R.; Fourkas, J. T.; Rajan, A. G.; Kulik, H. J.; Levy, A.; Majumdar, A.; Martin, C.; McEldrew, M.; Misra, R. P.; Noy, A.; Pham, T. A.; Reed, M.; Schwegler, E.; Siwy, Z.; Wang, Y.; Strano, M. Critical knowledge gaps in mass transport through single-digit nanopores: a review and perspective. *J. Phys. Chem. C* **2019**, *123*, 21309−21326.
(492) Berezina, N.; Kononenko, N.; Dyomina, O.; Gnusin, N. Characterization of ion-exchange membrane materials: properties vs structure. *Advances in colloid and interface science* **2008**, *139*, 3−28.
(493) Nagarale, R.; Gohil, G.; Shahi, V. K. Recent developments on ion-exchange membranes and electro-membrane processes. *Advances in colloid and interface science* **2006**, *119*, 97−130.
(494) Goh, P.; Ismail, A.; Ng, B. Carbon nanotubes for desalination: performance evaluation and current hurdles. *Desalination* **2013**, *308*, 2−14.
(495) Das, R.; Ali, M. E.; Hamid, S. B. A.; Ramakrishna, S.; Chowdhury, Z. Z. Carbon nanotube membranes for water purification: a bright future in water desalination. *Desalination* **2014**, *336*, 97−109.
(496) Holt, J. K.; Park, H. G.; Wang, Y.; Stadermann, M.; Artyukhin, A. B.; Grigoropoulos, C. P.; Noy, A.; Bakajin, O. Fast mass transport through sub-2-nanometer carbon nanotubes. *Science* **2006**, *312*, 1034−1037.
(497) Secchi, E.; Marbach, S.; Niguès, A.; Stein, D.; Siria, A.; Bocquet, L. Massive radius-dependent flow slippage in carbon nanotubes. *Nature* **2016**, *537*, 210−213.
(498) Wang, E. N.; Karnik, R. Graphene cleans up water. *Nature Nanotechnol.* **2012**, *7*, 552−554.
(499) Aghigh, A.; Alizadeh, V.; Wong, H. Y.; Islam, M. S.; Amin, N.; Zaman, M. Recent advances in utilization of graphene for filtration and desalination of water: a review. *Desalination* **2015**, *365*, 389−397.
(500) Wang, L.; Boutilier, M. S.; Kidambi, P. R.; Jang, D.; Hadjiconstantinou, N. G.; Karnik, R. Fundamental transport mechanisms, fabrication and potential applications of nanoporous atomically thin membranes. *Nature Nanotechnol.* **2017**, *12*, 509−522.
(501) Helmholtz, H. v. Ueber einige Gesetze der Vertheilung elektrischer Ströme in körperlichen Leitern, mit Anwendung auf die thierisch-elektrischen Versuche (Schluss.). *Annalen der Physik* **1853**, *165*, 353−377.
(502) Gouy, M. Sur la constitution de la charge électrique à la surface d'un électrolyte. *J. Phys. Theor. Appl.* **1910**, *9*, 457−468.
(503) Chapman, D. L. A contribution to the theory of electro-capillarity. *London, Edinburgh, and Dublin philosophical magazine and journal of science* **1913**, *25*, 475−481.
(504) Stern, O. Zur theorie der elektrolytischen doppelschicht. *Zeit. Elektrochem. Angew. Phys. Chem,* **1924**, *30*, 508−516.
(505) Peters, P.; Van Roij, R.; Bazant, M. Z.; Biesheuvel, P. Analysis of electrolyte transport through charged nanopores. *Phys. Rev. E* **2016**, *93*, 053108.
(506) Gross, R. J.; Osterle, J. Membrane transport characteristics of ultrafine capillaries. *J. Chem. Phys.* **1968**, *49*, 228−234.
(507) Nielsen, C. P.; Bruus, H. Concentration polarization, surface currents, and bulk advection in a microchannel. *Phys. Rev. E* **2014**, *90*, 043020.
(508) Alizadeh, S.; Mani, A. Multiscale model for electrokinetic transport in networks of pores, Part I: model derivation. *Langmuir* **2017**, *33*, 6205−6219.
(509) Alizadeh, S.; Mani, A. Multiscale model for electrokinetic transport in networks of pores, Part II: computational algorithms and applications. *Langmuir* **2017**, *33*, 6220−6231.
(510) Alizadeh, S.; Bazant, M. Z.; Mani, A. Impact of network heterogeneity on electrokinetic transport in porous media. *J. Colloid Interface Sci.* **2019**, *553*, 451−464.
(511) Mirzadeh, M.; Zhou, T.; Amooie, M. A.; Fraggedakis, D.; Ferguson, T. R.; Bazant, M. Z. Vortices of electro-osmotic flow in heterogeneous porous media. *Physical Review Fluids* **2020**, *5*, 103701.
(512) Sasidhar, V.; Ruckenstein, E. Electrolyte osmosis through capillaries. *J. Colloid Interface Sci.* **1981**, *82*, 439−457.
(513) Yaroshchuk, A.; Bruening, M. L.; Zholkovskiy, E. Modelling nanofiltration of electrolyte solutions. *Adv. Colloid Interface Sci.* **2019**, *268*, 39−63.
(514) Lanteri, Y.; Szymczyk, A.; Fievet, P. Membrane potential in multi-ionic mixtures. *J. Phys. Chem. B* **2009**, *113*, 9197−9204.
(515) Yang, Y.; Pintauro, P. N. Multicomponent space-charge transport model for ion-exchange membranes. *AIChE journal* **2000**, *46*, 1177−1190.
(516) Huisman, I. H.; Prádanos, P.; Calvo, J. I.; Hernández, A. Electroviscous effects, streaming potential, and zeta potential in polycarbonate track-etched membranes. *J. Membr. Sci.* **2000**, *178*, 79−92.
(517) Sasidhar, V.; Ruckenstein, E. Anomalous effects during electrolyte osmosis across charged porous membranes. *J. Colloid Interface Sci.* **1982**, *85*, 332−362.
(518) Shang, W.-J.; Wang, X.-L.; Yu, Y.-X. Theoretical calculation on the membrane potential of charged porous membranes in 1−1, 1−2, 2−1 and 2−2 electrolyte solutions. *Journal of membrane science* **2006**, *285*, 362−375.
(519) Ramirez, P.; Aguilella-Arzo, M.; Alcaraz, A.; Cervera, J.; Aguilella, V. Theoretical description of the ion transport across nanopores with titratable fixed charges. *Cell Biochem. Biophys.* **2006**, *44*, 287−312.
(520) Manghi, M.; Palmeri, J.; Yazda, K.; Henn, F.; Jourdain, V. Role of charge regulation and flow slip in the ionic conductance of nanopores: An analytical approach. *Phys. Rev. E* **2018**, *98*, 012605.

https://doi.org/10.1021/acs.chemrev.1c00396
Chem. Rev. 2022, 122, 13547−13635

(521) Zhang, W.; Wang, Q.; Zeng, M.; Zhao, C. Thermoelectric effect and temperature-gradient-driven electrokinetic flow of electrolyte solutions in charged nanocapillaries. *Int. J. Heat Mass Transfer* **2019**, *143*, 118569.
(522) Zhang, L.; Biesheuvel, P.; Ryzhkov, I. Theory of ion and water transport in electron-conducting membrane pores with pH-dependent chemical charge. *Physical Review Applied* **2019**, *12*, 014039.
(523) Ryzhkov, I. I.; Lebedev, D. V.; Solodovnichenko, V. S.; Minakov, A. V.; Simunin, M. M. On the origin of membrane potential in membranes with polarizable nanopores. *Journal of membrane science* **2018**, *549*, 616−630.
(524) Bontha, J.; Pintauro, P. N. Water orientation and ion solvation effects during multicomponent salt partitioning in a Nafion cation exchange membrane. *Chemical engineering science* **1994**, *49*, 3835−3851.
(525) Lanteri, Y.; Szymczyk, A.; Fievet, P. Influence of steric, electric, and dielectric effects on membrane potential. *Langmuir* **2008**, *24*, 7955−7962.
(526) Szymczyk, A.; Sbaï, M.; Fievet, P.; Vidonne, A. Transport properties and electrokinetic characterization of an amphoteric nanofilter. *Langmuir* **2006**, *22*, 3910−3919.
(527) Hawkins Cwirko, E.; Carbonell, R. Transport of electrolytes in charged pores: analysis using the method of spatial averaging. *J. Colloid Interface Sci.* **1989**, *129*, 513−531.
(528) Dydek, E. V.; Zaltzman, B.; Rubinstein, I.; Deng, D.; Mani, A.; Bazant, M. Z. Overlimiting current in a microchannel. *Physical review letters* **2011**, *107*, 118301.
(529) Dydek, E. V.; Bazant, M. Z. Nonlinear dynamics of ion concentration polarization in porous media: The leaky membrane model. *AIChE J.* **2013**, *59*, 3539−3555.
(530) Levy, A.; de Souza, J. P.; Bazant, M. Z. Breakdown of electroneutrality in nanopores. *J. Colloid Interface Sci.* **2020**, *579*, 162−176.
(531) Maffeo, C.; Bhattacharya, S.; Yoo, J.; Wells, D.; Aksimentiev, A. Modeling and simulation of ion channels. *Chem. Rev.* **2012**, *112* (12), 6250−6284.
(532) de Souza, J. P.; Levy, A.; Bazant, M. Z. Electroneutrality breakdown in nanopore arrays. *Phys. Rev. E* **2021**, *104*, No. 044803.
(533) Zhou, X.; Wang, Z.; Epsztein, R.; Zhan, C.; Li, W.; Fortner, J. D.; Pham, T. A.; Kim, J.-H.; Elimelech, M. Intrapore energy barriers govern ion transport and selectivity of desalination membranes. *Sci. Adv.* **2020**, *6*, No. abdd9045.
(534) Kornyshev, A. A. Double-Layer in Ionic Liquids: Paradigm Change? *J. Phys. Chem. B* **2007**, *111* (20), 5545−5557.
(535) Bazant, M. Z.; Kilic, M. S.; Storey, B. D.; Ajdari, A. Towards an understanding of induced-charge electrokinetics at large applied voltages in concentrated solutions. *Advances in colloid and interface science* **2009**, *152*, 48−88.
(536) Qiao, R.; Aluru, N. R. Ion concentrations and velocity profiles in nanochannel electroosmotic flows. *J. Chem. Phys.* **2003**, *118*, 4692−4701.
(537) Storey, B. D.; Bazant, M. Z. Effects of electrostatic correlations on electrokinetic phenomena. *Phys. Rev. E* **2012**, *86*, 056303.
(538) Stout, R. F.; Khair, A. S. A continuum approach to predicting electrophoretic mobility reversals. *J. Fluid Mech.* **2014**, *752*, R1.
(539) Kilic, M. S.; Bazant, M. Z.; Ajdari, A. Steric effects in the dynamics of electrolytes at large applied voltages. I. Double-layer charging. *Phys. Rev. E* **2007**, *75*, 021502.
(540) Kilic, M. S.; Bazant, M. Z.; Ajdari, A. Steric effects in the dynamics of electrolytes at large applied voltages. II. Modified Poisson-Nernst-Planck equations. *Phys. Rev. E* **2007**, *75*, 021503.
(541) Bazant, M. Z.; Storey, B. D.; Kornyshev, A. A. Double layer in ionic liquids: Overscreening versus crowding. *Phys. Rev. Lett.* **2011**, *106*, 046102.
(542) de Souza, J. P.; Bazant, M. Z. Continuum theory of electrostatic correlations at charged surfaces. *J. Phys. Chem. C* **2020**, *124*, 11414−11421.
(543) Wesselingh, J.; Vonk, P.; Kraaijeveld, G. Exploring the Maxwell-Stefan description of ion exchange. *Chemical Engineering Journal and The Biochemical Engineering Journal* **1995**, *57*, 75−89.
(544) de Lint, W. B. S.; Benes, N. E. Predictive charge-regulation transport model for nanofiltration from the theory of irreversible processes. *J. Membr. Sci.* **2004**, *243*, 365−377.
(545) Tedesco, M.; Hamelers, H.; Biesheuvel, P. Nernst-Planck transport theory for (reverse) electrodialysis: II. Effect of water transport through ion-exchange membranes. *J. Membr. Sci.* **2017**, *531*, 172−182.
(546) Oren, Y.; Biesheuvel, P. Theory of ion and water transport in reverse-osmosis membranes. *Physical Review Applied* **2018**, *9*, 024034.
(547) Biesheuvel, P.; Bazant, M. Analysis of ionic conductance of carbon nanotubes. *Phys. Rev. E* **2016**, *94*, 050601.
(548) Secchi, E.; Niguès, A.; Jubin, L.; Siria, A.; Bocquet, L. Scaling behavior for ionic transport and its fluctuations in individual carbon nanotubes. *Physical review letters* **2016**, *116*, 154501.
(549) Vangara, R.; Brown, D.; van Swol, F.; Petsev, D. Electrolyte solution structure and its effect on the properties of electric double layers with surface charge regulation. *J. Colloid Interface Sci.* **2017**, *488*, 180−189.
(550) Ramirez, P.; Manzanares, J. A.; Cervera, J.; Gomez, V.; Ali, M.; Nasir, S.; Ensinger, W.; Mafe, S. Surface charge regulation of functionalized conical nanopore conductance by divalent cations and anions. *Electrochim. Acta* **2019**, *325*, 134914.
(551) Werkhoven, B.; Everts, J. C.; Samin, S.; Van Roij, R. Flow-induced surface charge heterogeneity in electrokinetics due to Stern-layer conductance coupled to reaction kinetics. *Physical review letters* **2018**, *120*, 264502.
(552) Werkhoven, B.; Samin, S.; van Roij, R. Dynamic Stern layers in charge-regulating electrokinetic systems: three regimes from an analytical approach. *European Physical Journal Special Topics* **2019**, *227*, 2539−2557.
(553) Kim, S. J.; Wang, Y.-C.; Lee, J. H.; Jang, H.; Han, J. Concentration polarization and nonlinear electrokinetic flow near a nanofluidic channel. *Physical review letters* **2007**, *99*, 044501.
(554) Kim, S. J.; Li, L. D.; Han, J. Amplified electrokinetic response by concentration polarization near nanofluidic channel. *Langmuir* **2009**, *25*, 7759−7765.
(555) Kim, S. J.; Song, Y.-A.; Han, J. Nanofluidic concentration devices for biomolecules utilizing ion concentration polarization: theory, fabrication, and applications. *Chem. Soc. Rev.* **2010**, *39*, 912−922.
(556) Zangle, T. A.; Mani, A.; Santiago, J. G. Theory and experiments of concentration polarization and ion focusing at microchannel and nanochannel interfaces. *Chem. Soc. Rev.* **2010**, *39*, 1014−1035.
(557) Kim, S. J.; Ko, S. H.; Kang, K. H.; Han, J. Direct seawater desalination by ion concentration polarization. *Nature Nanotechnol.* **2010**, *5*, 297−301.
(558) Kim, S. J.; Ko, S. H.; Kang, K. H.; Han, J. Erratum: Direct seawater desalination by ion concentration polarization. *Nature Nanotechnol.* **2013**, *8*, 609.
(559) Nam, S.; Cho, I.; Heo, J.; Lim, G.; Bazant, M. Z.; Moon, D. J.; Sung, G. Y.; Kim, S. J. Experimental verification of overlimiting current by surface conduction and electro-osmotic flow in micro-channels. *Physical review letters* **2015**, *114*, 114501.
(560) Wang, Y.-C.; Stevens, A. L.; Han, J. Million-fold preconcentration of proteins and peptides by nanofluidic filter. *Analytical chemistry* **2005**, *77*, 4293−4299.
(561) Kim, Y.-J.; Hur, J.; Bae, W.; Choi, J.-H. Desalination of brackish water containing oil compound by capacitive deionization process. *Desalination* **2010**, *253*, 119−123.
(562) Rica, R. A.; Bazant, M. Z. Electrodiffusiophoresis: Particle motion in electrolytes under direct current. *Phys. Fluids* **2010**, *22*, 112109.
(563) Křivánková, L.; Pantůčková, P.; Boček, P. Isotachophoresis in zone electrophoresis. *Journal of Chromatography A* **1999**, *838*, 55−70.

https://doi.org/10.1021/acs.chemrev.1c00396
Chem. Rev. 2022, 122, 13547−13635

(564) Jung, B.; Bharadwaj, R.; Santiago, J. G. On-chip millionfold sample stacking using transient isotachophoresis. *Analytical chemistry* **2006**, *78*, 2319−2327.
(565) Ghosal, S.; Chen, Z. Nonlinear waves in capillary electrophoresis. *Bulletin of mathematical biology* **2010**, *72*, 2047−2066.
(566) Bahga, S. S.; Santiago, J. G. Coupling isotachophoresis and capillary electrophoresis: a review and comparison of methods. *Analyst* **2013**, *138*, 735−754.
(567) Gu, Z.; Xu, B.; Huo, P.; Rubinstein, S. M.; Bazant, M. Z.; Deng, D. Deionization shock driven by electroconvection in a circular channel. *Physical Review Fluids* **2019**, *4*, 113701.
(568) Yaroshchuk, A.; Zholkovskiy, E.; Pogodin, S.; Baulin, V. Coupled concentration polarization and electroosmotic circulation near micro/nanointerfaces: Taylor−Aris model of hydrodynamic dispersion and limits of its applicability. *Langmuir* **2011**, *27*, 11710−11721.
(569) Yaroshchuk, A. Over-limiting currents and deionization "shocks" in current-induced polarization: Local-equilibrium analysis. *Advances in colloid and interface science* **2012**, *183*, 68−81.
(570) Han, J.-H.; Khoo, E.; Bai, P.; Bazant, M. Z. Over-limiting current and control of dendritic growth by surface conduction in nanopores. *Sci. Rep.* **2015**, *4*, 7056.
(571) Schmuck, M.; Bazant, M. Z. Homogenization of the Poisson−Nernst−Planck equations for ion transport in charged porous media. *SIAM Journal on Applied Mathematics* **2015**, *75*, 1369−1401.
(572) Choi, J.; Baek, S.; Kim, H. C.; Chae, J.-H.; Koh, Y.; Seo, S. W.; Lee, H.; Kim, S. J. Nanoelectrokinetic Selective Preconcentration Based on Ion Concentration Polarization. *BioChip Journal* **2020**, *14*, 100−109.
(573) Han, J.-H.; Wang, M.; Bai, P.; Brushett, F. R.; Bazant, M. Z. Dendrite suppression by shock electrodeposition in charged porous media. *Sci. Rep.* **2016**, *6*, 28054.
(574) Han, J.-H.; Muralidhar, R.; Waser, R.; Bazant, M. Z. Resistive switching in aqueous nanopores by shock electrodeposition. *Electrochimica acta* **2016**, *222*, 370−375.
(575) Zhi, J.; Li, S.; Han, M.; Chen, P. Biomolecule-guided cation regulation for dendrite-free metal anodes. *Science Advances* **2020**, *6*, No. eabb1342.
(576) Deng, D.; Aouad, W.; Braff, W. A.; Schlumpberger, S.; Suss, M. E.; Bazant, M. Z. Water purification by shock electrodialysis: Deionization, filtration, separation, and disinfection. *Desalination* **2015**, *357*, 77−83.
(577) Alkhadra, M. A.; Conforti, K. M.; Gao, T.; Tian, H.; Bazant, M. Z. Continuous Separation of Radionuclides from Contaminated Water by Shock Electrodialysis. *Environ. Sci. Technol.* **2020**, *54*, 527−536.
(578) Matijevic, E.; Good, R. J. *Surface and Colloid Science*; Springer Science & Business Media, 2012; Vol. *12*.
(579) Culbertson, C. T.; Ramsey, R. S.; Ramsey, J. M. Electroosmotically induced hydraulic pumping on microchips: differential ion transport. *Anal. Chem.* **2000**, *72*, 2285−2291.
(580) McKnight, T. E.; Culbertson, C. T.; Jacobson, S. C.; Ramsey, J. M. Electroosmotically induced hydraulic pumping with integrated electrodes on microfluidic devices. *Anal. Chem.* **2001**, *73*, 4045−4049.
(581) Suss, M. E.; Mani, A.; Zangle, T. A.; Santiago, J. G. Electroosmotic pump performance is affected by concentration polarizations of both electrodes and pump. *Sensors and Actuators A: Physical* **2011**, *165*, 310−315.
(582) Schlumpberger, S.; Smith, R. B.; Tian, H.; Mani, A.; Bazant, M. Z. Deionization shocks in crossflow. *AIChE J.* **2021**, *67*, No. e17274.
(583) Tian, H.; Alkhadra, M. A.; Bazant, M. Z. Theory of shock electrodialysis I: Water dissociation and electrosmotic vortices. *J. Colloid Interface Sci.* **2021**, *589*, 605−615.
(584) Tian, H.; Alkhadra, M. A.; Conforti, K.; Bazant, M. Z. Continuous and Selective Removal of Lead from Drinking Water by Shock Electrodialysis. In *Environment Science & Technology: Water*, 2021.
(585) Čížek, J.; Cvejn, P.; Marek, J.; Tvrzník, D. Desalination Performance Assessment of Scalable, Multi-Stack Ready Shock Electrodialysis Unit Utilizing Anion-Exchange Membranes. *Membranes* **2020**, *10*, 347.
(586) Conforti, K. M. Continuous Ion-Selective Separation by Shock Electrodialysis. Ph.D. Thesis. Massachusetts Institute of Technology, 2019.
(587) Alkhadra, M. A.; Gao, T.; Conforti, K. M.; Tian, H.; Bazant, M. Z. Small-scale desalination of seawater by shock electrodialysis. *Desalination* **2020**, *476*, 114219.
(588) Menyah, K.; Wolde-Rufael, Y. CO2 emissions, nuclear energy, renewable energy and economic growth in the US. *Energy Policy* **2010**, *38*, 2911−2915.
(589) Saidi, K.; Ben Mbarek, M. Nuclear energy, renewable energy, CO2 emissions, and economic growth for nine developed countries: Evidence from panel Granger causality tests. *Progress in Nuclear Energy* **2016**, *88*, 364−374.
(590) Lister, D. The Transport of Radioactive Corrosion Products in High-Temperature Water II. The Activation of Isothermal Steel Surfaces. *Nuclear Science and Engineering* **1976**, *59*, 406−426.
(591) Honda, T.; Izumiya, M.; Minato, A.; Ohsumi, K.; Matsubayashi, H. Radiation buildup on stainless steel in a boiling water reactor environment. *Nuclear Technology* **1984**, *64*, 35−42.
(592) Choo, K.-H.; Kwon, D.-J.; Lee, K.-W.; Choi, S.-J. Selective removal of cobalt species using nanofiltration membranes. *Environ. Sci. Technol.* **2002**, *36*, 1330−1336.
(593) Kikuchi, M.; Ga, E.; Funabashi, K.; Yusa, H.; Uchida, S.; Fujita, K. Removal of radioactive cobalt ion in high temperature water using titanium oxide. *Nucl. Eng. Des.* **1979**, *53*, 387−392.
(594) Cox, B.; Wu, C. Transient effects of lithium hydroxide and boric acid on Zircaloy corrosion. *Journal of nuclear materials* **1995**, *224*, 169−178.
(595) Sengupta, S. K.; Hooper, E.; Dubost, E. *Processing of Nuclear Power Plant Waste Streams Containing Boric Acid (Technical Report)*; International Atomic Energy Agency, 2019; p 49.
(596) Liu, X.; Wu, J.; Wang, J. Removal of Cs (I) from simulated radioactive wastewater by three forward osmosis membranes. *Chemical Engineering Journal* **2018**, *344*, 353−362.
(597) Ryan, P. B.; Huet, N.; MacIntosh, D. L. Longitudinal investigation of exposure to arsenic, cadmium, and lead in drinking water. *Environ. Health Perspect.* **2000**, *108*, 731−735.
(598) *Lead in Drinking Water*; World Health Organization, 2012.
(599) Tian, H.; Alkhadra, M. A.; Bazant, M. Z. Theory of shock electrodialysis II: Mechanisms of selective ion removal. *J. Colloid Interface Sci.* **2021**, *589*, 616−621.
(600) Abrams, I. *Studies in Environmental Science*; Elsevier, 1982; Vol. *19*; pp 213−224.
(601) Anupkumar, B.; Rao, T.; Satpathy, K. Microbial fouling of an anion exchange resin. *Current Sci.* **2001**, *80*, 1104−1107.
(602) Asraf-Snir, M.; Gilron, J.; Oren, Y. Gypsum scaling of anion exchange membranes in electrodialysis. *J. Membr. Sci.* **2016**, *520*, 176−186.
(603) Zhao, D.; Lee, L. Y.; Ong, S. L.; Chowdhury, P.; Siah, K. B.; Ng, H. Y. Electrodialysis reversal for industrial reverse osmosis brine treatment. *Sep. Purif. Technol.* **2019**, *213*, 339−347.
(604) Andreeva, M.; Gil, V.; Pismenskaya, N.; Dammak, L.; Kononenko, N.; Larchet, C.; Grande, D.; Nikonenko, V. Mitigation of membrane scaling in electrodialysis by electroconvection enhancement, pH adjustment and pulsed electric field application. *J. Membr. Sci.* **2018**, *549*, 129−140.
(605) Turek, M.; Waś, J.; Mitko, K. Scaling prediction in electrodialytic desalination. *Desalination and Water Treatment* **2012**, *44*, 255−260.
(606) Casademont, C.; Farias, M. A.; Pourcelly, G.; Bazinet, L. Impact of electrodialytic parameters on cation migration kinetics and fouling nature of ion-exchange membranes during treatment of solutions with different magnesium/calcium ratios. *Journal of membrane Science* **2008**, *325*, 570−579.

https://doi.org/10.1021/acs.chemrev.1c00396
Chem. Rev. 2022, 122, 13547−13635

(607) Ben Salah Sayadi, I.; Sistat, P.; Ben Amor, M.; Tlili, M. Brackish water desalination by electrodialysis: CaCO3 scaling monitoring during batch recirculation operation. *Int. J. Chem. Reactor Eng.* **2013**, *11*, 517−525.
(608) Tanaka, Y. Water dissociation in ion-exchange membrane electrodialysis. *J. Membr. Sci.* **2002**, *203*, 227−244.
(609) Cifuentes-Araya, N.; Astudillo-Castro, C.; Bazinet, L. Mechanisms of mineral membrane fouling growth modulated by pulsed modes of current during electrodialysis: Evidences of water splitting implications in the appearance of the amorphous phases of magnesium hydroxide and calcium carbonate. *J. Colloid Interface Sci.* **2014**, *426*, 221−234.
(610) Mikhaylin, S.; Nikonenko, V.; Pourcelly, G.; Bazinet, L. Intensification of demineralization process and decrease in scaling by application of pulsed electric field with short pulse/pause conditions. *Journal of membrane science* **2014**, *468*, 389−399.
(611) Dufton, G.; Mikhaylin, S.; Gaaloul, S.; Bazinet, L. Positive impact of pulsed electric field on lactic acid removal, demineralization and membrane scaling during acid whey electrodialysis. *International journal of molecular sciences* **2019**, *20*, 797.
(612) Lee, H.-J.; Park, J.-S.; Kang, M.-S.; Moon, S.-H. Effects of silica sol on ion exchange membranes: Electrochemical characterization of anion exchange membranes in electrodialysis of silica sol containing-solutions. *Korean Journal of Chemical Engineering* **2003**, *20*, 889−895.
(613) Korngold, E. Prevention of colloidal-fouling in electrodialysis by chlorination. *Desalination* **1971**, *9*, 213−216.
(614) Mondor, M.; Ippersiel, D.; Lamarche, F.; Masse, L. Fouling characterization of electrodialysis membranes used for the recovery and concentration of ammonia from swine manure. *Bioresource technology* **2009**, *100*, 566−571.
(615) Yiantsios, S.; Karabelas, A. The effect of colloid stability on membrane fouling. *Desalination* **1998**, *118*, 143−152.
(616) Tanaka, N.; Nagase, M.; Higa, M. Organic fouling behavior of commercially available hydrocarbon-based anion-exchange membranes by various organic-fouling substances. *Desalination* **2012**, *296*, 81−86.
(617) De Jaegher, B.; Larumbe, E.; De Schepper, W.; Verliefde, A.; Nopens, I. Data on ion-exchange membrane fouling by humic acid during electrodialysis. *Data in Brief* **2020**, *31*, 105763.
(618) De Jaegher, B.; Larumbe, E.; De Schepper, W.; Verliefde, A.; Nopens, I. Colloidal fouling in electrodialysis: A neural differential equations model. *Sep. Purif. Technol.* **2020**, *249*, 116939.
(619) Talebi, S.; Chen, G. Q.; Freeman, B.; Suarez, F.; Freckleton, A.; Bathurst, K.; Kentish, S. E. Fouling and in-situ cleaning of ion-exchange membranes during the electrodialysis of fresh acid and sweet whey. *Journal of Food Engineering* **2019**, *246*, 192−199.
(620) Persico, M.; Mikhaylin, S.; Doyen, A.; Firdaous, L.; Nikonenko, V.; Pismenskaya, N.; Bazinet, L. Prevention of peptide fouling on ion-exchange membranes during electrodialysis in overlimiting conditions. *J. Membr. Sci.* **2017**, *543*, 212−221.
(621) Verliefde, A. R.; Cornelissen, E. R.; Heijman, S. G.; Hoek, E. M.; Amy, G. L.; Bruggen, B. V. d.; Van Dijk, J. C. Influence of solute-membrane affinity on rejection of uncharged organic solutes by nanofiltration membranes. *Environ. Sci. Technol.* **2009**, *43*, 2400−2406.
(622) Lee, H.-J.; Hong, M.-K.; Han, S.-D.; Cho, S.-H.; Moon, S.-H. Fouling of an anion exchange membrane in the electrodialysis desalination process in the presence of organic foulants. *Desalination* **2009**, *238*, 60−69.
(623) Guo, H.; Xiao, L.; Yu, S.; Yang, H.; Hu, J.; Liu, G.; Tang, Y. Analysis of anion exchange membrane fouling mechanism caused by anion polyacrylamide in electrodialysis. *Desalination* **2014**, *346*, 46−53.
(624) Katz, W. E. The electrodialysis reversal (EDR) process. *Desalination* **1979**, *28*, 31−40.
(625) Chao, Y.-M.; Liang, T. A feasibility study of industrial wastewater recovery using electrodialysis reversal. *Desalination* **2008**, *221*, 433−439.
(626) Sun, X.; Lu, H.; Wang, J. Brackish water desalination using electrodeionization reversal. *Chemical Engineering and Processing: Process Intensification* **2016**, *104*, 262−270.
(627) Tamersit, S.; Bouhidel, K.-E.; Zidani, Z. Investigation of electrodialysis anti-fouling configuration for desalting and treating tannery unhairing wastewater: Feasibility of by-products recovery and water recycling. *Journal of environmental management* **2018**, *207*, 334−340.
(628) Zhao, J.; Chen, Q.; Ren, L.; Wang, J. Fabrication of hydrophilic cation exchange membrane with improved stability for electrodialysis: An excellent anti-scaling performance. *J. Membr. Sci.* **2021**, *617*, 118618.
(629) Mulyati, S.; Takagi, R.; Fujii, A.; Ohmukai, Y.; Maruyama, T.; Matsuyama, H. Improvement of the antifouling potential of an anion exchange membrane by surface modification with a polyelectrolyte for an electrodialysis process. *J. Membr. Sci.* **2012**, *417*, 137−143.
(630) Khoiruddin, K.; Ariono, D.; Subagjo, S.; Wenten, I. Improved anti-organic fouling of polyvinyl chloride-based heterogeneous anion-exchange membrane modified by hydrophilic additives. *Journal of Water Process Engineering* **2021**, *41*, 102007.
(631) Gil, V.; Andreeva, M.; Jansezian, L.; Han, J.; Pismenskaya, N.; Nikonenko, V.; Larchet, C.; Dammak, L. Impact of heterogeneous cation-exchange membrane surface modification on chronopotentiometric and current−voltage characteristics in NaCl, CaCl2 and MgCl2 solutions. *Electrochim. Acta* **2018**, *281*, 472−485.
(632) Cheng, Y.; Hao, Z.; Hao, C.; Deng, Y.; Li, X.; Li, K.; Zhao, Y. A review of modification of carbon electrode material in capacitive deionization. *RSC Adv.* **2019**, *9*, 24401−24419.
(633) Ying, T.-Y.; Yang, K.-L.; Yiacoumi, S.; Tsouris, C. Electrosorption of ions from aqueous solutions by nanostructured carbon aerogel. *J. Colloid Interface Sci.* **2002**, *250*, 18−27.
(634) Su, X.; Hatton, T. A. Electrosorption. *Kirk-Othmer Encyclopedia of Chemical Technology* **2016**, 1−11.
(635) Gamaethiralalage, J.; Singh, K.; Sahin, S.; Yoon, J.; Elimelech, M.; Suss, M.; Liang, P.; Biesheuvel, P.; Zornitta, R. L.; de Smet, L. Recent advances in ion selectivity with capacitive deionization. *Energy Environ. Sci.* **2021**, *14*, 1095−1120.
(636) Lester, Y.; Shaulsky, E.; Epsztein, R.; Zucker, I. Capacitive deionization for simultaneous removal of salt and uncharged organic contaminants from water. *Sep. Purif. Technol.* **2020**, *237*, 116388.
(637) Lee, J. B.; Park, K. K.; Eum, H. M.; Lee, C. W. Desalination of a thermal power plant wastewater by membrane capacitive deionization. *Desalination* **2006**, *196*, 125−134.
(638) Tang, W.; He, D.; Zhang, C.; Kovalsky, P.; Waite, T. D. Comparison of Faradaic reactions in capacitive deionization (CDI) and membrane capacitive deionization (MCDI) water treatment processes. *Water research* **2017**, *120*, 229−237.
(639) Porada, S.; Zhang, L.; Dykstra, J. Energy consumption in membrane capacitive deionization and comparison with reverse osmosis. *Desalination* **2020**, *488*, 114383.
(640) Yang, J.; Bu, Y.; Liu, F.; Zhang, W.; Cai, D.; Sun, A.; Wu, Y.; Zhou, R.; Zhang, C. Potential Application of Membrane Capacitive Deionization for Heavy Metal Removal from Water: A Mini-Review. *Int. J. Electrochem. Sci.* **2020**, *15*, 7848−7859.
(641) Jeon, S.-i.; Park, H.-r.; Yeo, J.-g.; Yang, S.; Cho, C. H.; Han, M. H.; Kim, D. K. Desalination via a new membrane capacitive deionization process utilizing flow-electrodes. *Energy Environ. Sci.* **2013**, *6*, 1471−1475.
(642) Ma, J.; He, C.; He, D.; Zhang, C.; Waite, T. D. Analysis of capacitive and electrodialytic contributions to water desalination by flow-electrode CDI. *Water research* **2018**, *144*, 296−303.
(643) Zhang, C.; He, D.; Ma, J.; Tang, W.; Waite, T. D. Comparison of Faradaic reactions in flow-through and flow-by capacitive deionization (CDI) systems. *Electrochim. Acta* **2019**, *299*, 727−735.
(644) Doornbusch, G. J.; Dykstra, J. E.; Biesheuvel, P. M.; Suss, M. E. Fluidized bed electrodes with high carbon loading for water desalination by capacitive deionization. *Journal of Materials Chemistry A* **2016**, *4*, 3642−3647.

https://doi.org/10.1021/acs.chemrev.1c00396
Chem. Rev. 2022, 122, 13547−13635

(645) Zhang, X.; Zuo, K.; Zhang, X.; Zhang, C.; Liang, P. Selective ion separation by capacitive deionization (CDI) based technologies: a state-of-the-art review. *Environ. Sci. Water Res. Technol.* **2020**, *6*, 243−257.
(646) Suss, M. E.; Baumann, T. F.; Bourcier, W. L.; Spadaccini, C. M.; Rose, K. A.; Santiago, J. G.; Stadermann, M. Capacitive desalination with flow-through electrodes. *Energy Environ. Sci.* **2012**, *5*, 9511−9519.
(647) Remillard, E. M.; Shocron, A. N.; Rahill, J.; Suss, M. E.; Vecitis, C. D. A direct comparison of flow-by and flow-through capacitive deionization. *Desalination* **2018**, *444*, 169−177.
(648) Nordstrand, J.; Dutta, J. Design principles for enhanced up-scaling of flow-through capacitive deionization for water desalination. *Desalination* **2021**, *500*, 114842.
(649) Chen, R.; Sheehan, T.; Ng, J. L.; Brucks, M.; Su, X. Capacitive deionization and electrosorption for heavy metal removal. *Environ. Sci.: Water Res. Technol.* **2020**, *6*, 258−282.
(650) Guyes, E. N.; Shocron, A. N.; Chen, Y.; Diesendruck, C. E.; Suss, M. E. Long-lasting, monovalent-selective capacitive deionization electrodes. *NPJ Clean Water* **2021**, *4*, 22.
(651) Zhao, R.; Van Soestbergen, M.; Rijnaarts, H.; Van der Wal, A.; Bazant, M.; Biesheuvel, P. Time-dependent ion selectivity in capacitive charging of porous electrodes. *J. Colloid Interface Sci.* **2012**, *384*, 38−44.
(652) Suss, M. E. Size-based ion selectivity of micropore electric double layers in capacitive deionization electrodes. *J. Electrochem. Soc.* **2017**, *164*, No. E270.
(653) Zhang, Y.; Peng, J.; Feng, G.; Presser, V. Hydration shell energy barrier differences of sub-nanometer carbon pores enable ion sieving and selective ion removal. *Chemical Engineering Journal* **2021**, *419*, 129438.
(654) Oyarzun, D. I.; Hemmatifar, A.; Palko, J. W.; Stadermann, M.; Santiago, J. G. Ion selectivity in capacitive deionization with functionalized electrode: Theory and experimental validation. *Water Research X* **2018**, *1*, 100008.
(655) Zhang, C.; He, D.; Ma, J.; Tang, W.; Waite, T. D. Faradaic reactions in capacitive deionization (CDI)-problems and possibilities: A review. *Water research* **2018**, *128*, 314−330.
(656) Yoon, H.; Lee, J.; Kim, S.; Yoon, J. Review of concepts and applications of electrochemical ion separation (EIONS) process. *Sep. Purif. Technol.* **2019**, *215*, 190−207.
(657) Grahame, D. C. The electrical double layer and the theory of electrocapillarity. *Chem. Rev.* **1947**, *41*, 441−501.
(658) De Levie, R. On porous electrodes in electrolyte solutions: I. Capacitance effects. *Electrochimica acta* **1963**, *8*, 751−780.
(659) Burt, R.; Birkett, G.; Zhao, X. A review of molecular modelling of electric double layer capacitors. *Phys. Chem. Chem. Phys.* **2014**, *16*, 6519−6538.
(660) Johnson, A. M.; Newman, J. Desalting by Means of Porous Carbon Electrodes. *J. Electrochem. Soc.* **1971**, *118*, 510.
(661) Bazant, M. Z.; Thornton, K.; Ajdari, A. Diffuse-charge dynamics in electrochemical systems. *Phys. Rev. E* **2004**, *70*, 021506.
(662) Højgaard Olesen, L. H.; Bazant, M. Z.; Bruus, H. Strongly nonlinear dynamics of electrolytes in large ac voltages. *Phys. Rev. E* **2010**, *82*, 011501.
(663) Biesheuvel, P.; Bazant, M. Nonlinear dynamics of capacitive charging and desalination by porous electrodes. *Phys. Rev. E* **2010**, *81*, 031502.
(664) Mirzadeh, M.; Gibou, F.; Squires, T. M. Enhanced charging kinetics of porous electrodes: Surface conduction as a short-circuit mechanism. *Physical review letters* **2014**, *113*, 097701.
(665) Biesheuvel, P.; Fu, Y.; Bazant, M. Z. Diffuse charge and Faradaic reactions in porous electrodes. *Phys. Rev. E* **2011**, *83*, 061507.
(666) Biesheuvel, P.; Fu, Y.; Bazant, M. Electrochemistry and capacitive charging of porous electrodes in asymmetric multi-component electrolytes. *Russian Journal of Electrochemistry* **2012**, *48*, 580−592.
(667) Biesheuvel, P.; Porada, S.; Levi, M.; Bazant, M. Z. Attractive forces in microporous carbon electrodes for capacitive deionization. *J. Solid State Electrochem.* **2014**, *18*, 1365−1376.
(668) Shocron, A. N.; Suss, M. E. The effect of surface transport on water desalination by porous electrodes undergoing capacitive charging. *J. Phys.: Condens. Matter* **2017**, *29*, 084003.
(669) Porada, S.; Weingarth, D.; Hamelers, H. V. M.; Bryjak, M.; Presser, V.; Biesheuvel, P. M. Carbon flow electrodes for continuous operation of capacitive deionization and capacitive mixing energy generation. *Journal of Materials Chemistry A* **2014**, *2*, 9313−9321.
(670) Gabitto, J.; Tsouris, C. Volume averaging study of the capacitive deionization process in homogeneous porous media. *Transport in Porous Media* **2015**, *109*, 61−80.
(671) Biesheuvel, P.; Zhao, R.; Porada, S.; Van der Wal, A. Theory of membrane capacitive deionization including the effect of the electrode pore space. *J. Colloid Interface Sci.* **2011**, *360*, 239−248.
(672) Porada, S.; Bryjak, M.; Van Der Wal, A.; Biesheuvel, P. Effect of electrode thickness variation on operation of capacitive deionization. *Electrochim. Acta* **2012**, *75*, 148−156.
(673) Wang, L.; Biesheuvel, P.; Lin, S. Reversible thermodynamic cycle analysis for capacitive deionization with modified Donnan model. *J. Colloid Interface Sci.* **2018**, *512*, 522−528.
(674) Shocron, A. N.; Suss, M. E. Should we pose a closure problem for capacitive charging of porous electrodes? *EPL (Europhysics Letters)* **2020**, *130*, 34003.
(675) Akpor, O. B.; Muchie, M. Remediation of heavy metals in drinking water and wastewater treatment systems: Processes and applications. *Int. J. Phys. Sci.* **2010**, *5*, 1807−1817.
(676) Chaudhary, V.; Kumar, M.; Sharma, M.; Yadav, B. Fluoride, boron and nitrate toxicity in ground water of northwest Rajasthan, India. *Environmental monitoring and assessment* **2010**, *161*, 343−348.
(677) Mohod, C. V.; Dhote, J. Review of heavy metals in drinking water and their effect on human health. *Int. J. Innovative Res. Sci., Eng. Technol.* **2013**, *2*, 2992−2996.
(678) Xu, P.; Drewes, J. E.; Heil, D.; Wang, G. Treatment of brackish produced water using carbon aerogel-based capacitive deionization technology. *Water Res.* **2008**, *42*, 2605−2617.
(679) Broséus, R.; Cigana, J.; Barbeau, B.; Daines-Martinez, C.; Suty, H. Removal of total dissolved solids, nitrates and ammonium ions from drinking water using charge-barrier capacitive deionisation. *Desalination* **2009**, *249*, 217−223.
(680) Li, H.; Zou, L.; Pan, L.; Sun, Z. Using graphene nano-flakes as electrodes to remove ferric ions by capacitive deionization. *Sep. Purif. Technol.* **2010**, *75*, 8−14.
(681) Kim, Y.-J.; Choi, J.-H. Selective removal of nitrate ion using a novel composite carbon electrode in capacitive deionization. *Water Res.* **2012**, *46*, 6033−6039.
(682) Mossad, M.; Zou, L. A study of the capacitive deionisation performance under various operational conditions. *Journal of Hazardous Materials* **2012**, *213-214*, 491−497.
(683) Kim, Y.-J.; Kim, J.-H.; Choi, J.-H. Selective removal of nitrate ions by controlling the applied current in membrane capacitive deionization (MCDI). *J. Membr. Sci.* **2013**, *429*, 52−57.
(684) Macías, C.; Lavela, P.; Rasines, G.; Zafra, M. C.; Tirado, J. L.; Ania, C. O. Improved electro-assisted removal of phosphates and nitrates using mesoporous carbon aerogels with controlled porosity. *J. Appl. Electrochem.* **2014**, *44*, 963−976.
(685) Wang, H.; Na, C. Binder-Free Carbon Nanotube Electrode for Electrochemical Removal of Chromium. *ACS Appl. Mater. Interfaces* **2014**, *6*, 20309−20316.
(686) Tang, W.; Kovalsky, P.; Cao, B.; Waite, T. D. Investigation of fluoride removal from low-salinity groundwater by single-pass constant-voltage capacitive deionization. *Water Res.* **2016**, *99*, 112−121.
(687) Tang, W.; Kovalsky, P.; He, D.; Waite, T. D. Fluoride and nitrate removal from brackish groundwaters by batch-mode capacitive deionization. *Water Res.* **2015**, *84*, 342−349.

https://doi.org/10.1021/acs.chemrev.1c00396
Chem. Rev. 2022, 122, 13547−13635

(688) Huang, Z.; Lu, L.; Cai, Z.; Ren, Z. J. Individual and competitive removal of heavy metals using capacitive deionization. *Journal of Hazardous Materials* **2016**, *302*, 323−331.
(689) Lado, J. J.; Pérez-Roa, R. E.; Wouters, J. J.; Tejedor-Tejedor, M. I.; Federspill, C.; Ortiz, J. M.; Anderson, M. A. Removal of nitrate by asymmetric capacitive deionization. *Sep. Purif. Technol.* **2017**, *183*, 145−152.
(690) Hu, C.; Dong, J.; Wang, T.; Liu, R.; Liu, H.; Qu, J. Nitrate electro-sorption/reduction in capacitive deionization using a novel Pd/NiAl-layered metal oxide film electrode. *Chemical Engineering Journal* **2018**, *335*, 475−482.
(691) Lee, D.-H.; Ryu, T.; Shin, J.; Ryu, J. C.; Chung, K.-S.; Kim, Y. H. Selective lithium recovery from aqueous solution using a modified membrane capacitive deionization system. *Hydrometallurgy* **2017**, *173*, 283−288.
(692) Shi, W.; Liu, X.; Ye, C.; Cao, X.; Gao, C.; Shen, J. Efficient lithium extraction by membrane capacitive deionization incorporated with monovalent selective cation exchange membrane. *Sep. Purif. Technol.* **2019**, *210*, 885−890.
(693) Guyes, E. N.; Malka, T.; Suss, M. E. Enhancing the ion-size-based selectivity of capacitive deionization electrodes. *Environ. Sci. Technol.* **2019**, *53*, 8447−8454.
(694) Ha, Y.; Jung, H. B.; Lim, H.; Jo, P. S.; Yoon, H.; Yoo, C. Y.; Pham, T. K.; Ahn, W.; Cho, Y. Continuous lithium extraction from aqueous solution using flow-electrode capacitive deionization. *Energies* **2019**, *12*, 2913.
(695) Siekierka, A.; Tomaszewska, B.; Bryjak, M. Lithium capturing from geothermal water by hybrid capacitive deionization. *Desalination* **2018**, *436*, 8−14.
(696) Siekierka, A.; Bryjak, M. Novel anion exchange membrane for concentration of lithium salt in hybrid capacitive deionization. *Desalination* **2019**, *452*, 279−289.
(697) Siekierka, A.; Bryjak, M. Selective sorbents for recovery of lithium ions by hybrid capacitive deionization. *Desalination* **2021**, *520*, 115324.
(698) Kim, B.; Seo, J. Y.; Chung, C.-H. Electrochemical Desalination and Recovery of Lithium from Saline Water upon Operation of a Capacitive Deionization Cell Combined with a Redox Flow Battery. *ACS ES&T Water* **2021**, *1*, 1047−1054.
(699) Hu, B.; Shang, X.; Nie, P.; Zhang, B.; Yang, J.; Liu, J. Lithium ion sieve modified three-dimensional graphene electrode for selective extraction of lithium by capacitive deionization. *J. Colloid Interface Sci.* **2022**, *612*, 392−400.
(700) Huang, X.; He, D.; Tang, W.; Kovalsky, P.; Waite, T. D. Investigation of pH-dependent phosphate removal from wastewaters by membrane capacitive deionization (MCDI). *Environ. Sci.: Water Res. Technol.* **2017**, *3*, 875−882.
(701) Jiang, J.; Kim, D. I.; Dorji, P.; Phuntsho, S.; Hong, S.; Shon, H. K. Phosphorus removal mechanisms from domestic wastewater by membrane capacitive deionization and system optimization for enhanced phosphate removal. *Proc. Safe. Environ. Protect.* **2019**, *126*, 44−52.
(702) Zhang, C.; Cheng, X.; Wang, M.; Ma, J.; Collins, R.; Kinsela, A.; Zhang, Y.; Waite, T. D. Phosphate recovery as vivianite using a flow-electrode capacitive desalination (FCDI) and fluidized bed crystallization (FBC) coupled system. *Water Res.* **2021**, *126*, 194.
(703) Zhang, C.; Wang, M.; Xiao, W.; Ma, J.; Sun, J.; Mo, H.; Waite, T. D. Phosphate selective recovery by magnetic iron oxide impregnated carbon flow-electrode capacitive deionization (FCDI). *Water Res.* **2021**, *189*, 116653.
(704) Shocron, A.; Guyes, E.; Biesheuvel, P.; Rijnaarts, H.; Suss, M.; Dykstra, J. Electrochemical removal of amphoteric ions. *Proc. Natl. Acad. Sci. U. S. A.* **2021**, *118*, No. e2108240118.
(705) Zornitta, R. L.; Ruotolo, L. A.; de Smet, L. C. High-Performance Carbon Electrodes Modified with Polyaniline for Stable and Selective Anion Separation. *Sep. Purif. Technol.* **2022**, *290*, 120807.
(706) Kim, Y. J.; Kim, J. H.; Choi, J. H. Selective removal of nitrate ions by controlling the applied current in membrane capacitive deionization (MCDI). *J. Membr. Sci.* **2013**, *429*, 52−57.
(707) Zhang, C.; Ma, J.; Song, J.; He, C.; Waite, T. D. Continuous Ammonia Recovery from Wastewaters Using an Integrated Capacitive Flow Electrode Membrane Stripping System. *Environ. Sci. Technol.* **2018**, *52*, 14275−14285.
(708) Fang, K.; Gong, H.; He, W.; Peng, F.; He, C.; Wang, K. Recovering ammonia from municipal wastewater by flow-electrode capacitive deionization. *Chem. Eng. J.* **2018**, *348*, 301−309.
(709) Oyarzun, D. I.; Hemmatifar, A.; Palko, J. W.; Stadermann, M.; Santiago, J. G. Adsorption and capacitive regeneration of nitrate using inverted capacitive deionization with surfactant functionalized carbon electrodes. *Sep. Purif. Technol.* **2018**, *194*, 410−415.
(710) Zhang, C.; Ma, J.; Waite, T. D. Ammonia-Rich Solution Production from Wastewaters Using Chemical-Free Flow-Electrode Capacitive Deionization. *ACS Sustainable Chem. Eng.* **2019**, *7*, 6480−6485.
(711) Sakar, H.; Celik, I.; Balcik-Canbolat, C.; Keskinler, B.; Karagunduz, A. Ammonium removal and recovery from real digestate wastewater by a modified operational method of membrane capacitive deionization unit. *J. Cleaner Prod.* **2019**, *215*.14151423
(712) Gan, L.; Wu, Y.; Song, H.; Zhang, S.; Lu, C.; Yang, S.; Wang, Z.; Jiang, B.; Wang, C.; Li, A. Selective removal of nitrate ion using a novel activated carbon composite carbon electrode in capacitive deionization. *Sep. Purif. Technol.* **2019**, *212*, 728−736.
(713) Fang, K.; He, W.; Peng, F.; Wang, K. Ammonia recovery from concentrated solution by designing novel stacked FCDI cell. *Sep. Purif. Technol.* **2020**, *250*, 117066.
(714) Pasta, M.; Wessells, C.; Cui, Y.; La Mantia, F. A desalination battery. *Nano Lett.* **2012**, *12*, 839−843.
(715) Hou, C.-H.; Huang, C.-Y. A comparative study of electrosorption selectivity of ions by activated carbon electrodes in capacitive deionization. *Desalination* **2013**, *314*, 124−129.
(716) Yeo, J.-H.; Choi, J.-H. Enhancement of nitrate removal from a solution of mixed nitrate, chloride and sulfate ions using a nitrate-selective carbon electrode. *Desalination* **2013**, *320*, 10−16.
(717) Kim, S.; Yoon, H.; Shin, D.; Lee, J.; Yoon, J. Electrochemical selective ion separation in capacitive deionization with sodium manganese oxide. *J. Colloid Interface Sci.* **2017**, *506*, 644−648.
(718) Lee, J.; Kim, S.; Yoon, J. Rocking chair desalination battery based on Prussian Blue electrodes. *Acs Omega* **2017**, *2*, 1653−1659.
(719) Hawks, S. A.; Cerón, M. R.; Oyarzun, D. I.; Pham, T. A.; Zhan, C.; Loeb, C. K.; Mew, D.; Deinhart, A.; Wood, B. C.; Santiago, J. G.; Stadermann, M.; Campbell, P. G. Using ultramicroporous carbon for the selective removal of nitrate with capacitive deionization. *Environ. Sci. Technol.* **2019**, *53*, 10863−10870.
(720) Dong, Q.; Guo, X.; Huang, X.; Liu, L.; Tallon, R.; Taylor, B.; Chen, J. Selective removal of lead ions through capacitive deionization: Role of ion-exchange membrane. *Chemical Engineering Journal* **2019**, *361*, 1535−1542.
(721) Seo, S. J.; Jeon, H.; Lee, J. K.; Kim, G. Y.; Park, D.; Nojima, H.; Lee, J.; Moon, S. H. Investigation on removal of hardness ions by capacitive deionization (CDI) for water softening applications. *Water Res.* **2010**, *44*, 2267−2275.
(722) Hassanvand, A.; Chen, G. Q.; Webley, P. A.; Kentish, S. E. A comparison of multicomponent electrosorption in capacitive deionization and membrane capacitive deionization. *Water Res.* **2018**, *131*, 100−109.
(723) Sahin, S.; Zuilhof, H.; Zornitta, R. L.; de Smet, L. C. Enhanced monovalent over divalent cation selectivity with polyelectrolyte multilayers in membrane capacitive deionization via optimization of operational conditions. *Desalination* **2022**, *522*, 115391.
(724) Avraham, E.; Yaniv, B.; Soffer, A.; Aurbach, D. Developing Ion Electroadsorption Stereoselectivity, by Pore Size Adjustment with Chemical Vapor Deposition onto Active Carbon Fiber Electrodes. Case of Ca2+/Na+ Separation in Water Capacitive Desalination. *J. Phys. Chem. C* **2008**, *112*, 7385−7389.

https://doi.org/10.1021/acs.chemrev.1c00396
Chem. Rev. 2022, 122, 13547−13635

(725) Noked, M.; Avraham, E.; Bohadana, Y.; Soffer, A.; Aurbach, D. Development of Anion Stereoselective, Activated Carbon Molecular Sieve Electrodes Prepared by Chemical Vapor Deposition. *J. Phys. Chem. C* **2009**, *113*, 7316−7321.
(726) Cerón, M. R.; Aydin, F.; Hawks, S. A.; Oyarzun, D. I.; Loeb, C. K.; Deinhart, A.; Zhan, C.; Pham, T. A.; Stadermann, M.; Campbell, P. G. Cation Selectivity in Capacitive Deionization: Elucidating the Role of Pore Size, Electrode Potential, and Ion Dehydration. *ACS Appl. Mater. Interfaces* **2020**, *12*, 42644−42652.
(727) Han, L.; Karthikeyan, K. G.; Anderson, M. A.; Gregory, K. B. Exploring the impact of pore size distribution on the performance of carbon electrodes for capacitive deionization. *J. Colloid Interface Sci.* **2014**, *430*, 93−99.
(728) Eliad, L.; Salitra, G.; Soffer, A.; Aurbach, D. Ion Sieving Effects in the Electrical Double Layer of Porous Carbon Electrodes: Estimating Effective Ion Size in Electrolytic Solutions. *J. Phys. Chem. B* **2001**, *105*, 6880−6887.
(729) Gabelich, C. J.; Tran, T. D.; Suffet, I. H. Electrosorption of Inorganic Salts from Aqueous Solution Using Carbon Aerogels. *Environ. Sci. Technol.* **2002**, *36*, 3010−3019.
(730) Hou, C.-H.; Taboada-Serrano, P.; Yiacoumi, S.; Tsouris, C. Electrosorption selectivity of ions from mixtures of electrolytes inside nanopores. *J. Chem. Phys.* **2008**, *129*, 224703.
(731) Dykstra, J.; Dijkstra, J.; van der Wal, A.; Hamelers, H.; Porada, S. On-line method to study dynamics of ion adsorption from mixtures of salts in capacitive deionization. *Desalination* **2016**, *390*, 47−52.
(732) Misra, R. P.; de Souza, J. P.; Blankschtein, D.; Bazant, M. Z. Theory of surface forces in multivalent electrolytes. *Langmuir* **2019**, *35*, 11550−11565.
(733) Levin, Y. Electrostatic correlations: from plasma to biology. *Rep. Prog. Phys.* **2002**, *65*, 1577.
(734) Roth, R. Fundamental measure theory for hard-sphere mixtures: a review. *J. Phys.: Condens. Matter* **2010**, *22*, 063102.
(735) de Souza, J. P.; Goodwin, Z. A.; McEldrew, M.; Kornyshev, A. A.; Bazant, M. Z. Interfacial layering in the electric double layer of ionic liquids. *Phys. Rev. Lett.* **2020**, *125*, 116001.
(736) Tang, W.; Kovalsky, P.; Cao, B.; He, D.; Waite, T. D. Fluoride removal from brackish groundwaters by constant current capacitive deionization (CDI). *Environ. Sci. Technol.* **2016**, *50*, 10570−10579.
(737) Chen, Z.; Zhang, H.; Wu, C.; Wang, Y.; Li, W. A study of electrosorption selectivity of anions by activated carbon electrodes in capacitive deionization. *Desalination* **2015**, *369*, 46−50.
(738) Li, Y.; Zhang, C.; Jiang, Y.; Wang, T.-J.; Wang, H. Effects of the hydration ratio on the electrosorption selectivity of ions during capacitive deionization. *Desalination* **2016**, *399*, 171−177.
(739) Mubita, T. M.; Dykstra, J. E.; Biesheuvel, P. M.; van der Wal, A.; Porada, S. Selective adsorption of nitrate over chloride in microporous carbons. *Water Res.* **2019**, *164*, 114885.
(740) Nightingale, E. R. Phenomenological Theory of Ion Solvation. Effective Radii of Hydrated Ions. *J. Phys. Chem.* **1959**, *63*, 1381−1387.
(741) Hawks, S. A.; Ramachandran, A.; Porada, S.; Campbell, P. G.; Suss, M. E.; Biesheuvel, P. M.; Santiago, J. G.; Stadermann, M. Performance Metrics for the Objective Assessment of Capacitive Deionization Systems. *Water Res.* **2019**, *152*, 126−137.
(742) Porada, S.; Shrivastava, A.; Bukowska, P.; Biesheuvel, P. M.; Smith, K. C. Nickel Hexacyanoferrate Electrodes for Continuous Cation Intercalation Desalination of Brackish Water. *Electrochim. Acta* **2017**, *255*, 369−378.
(743) Kim, T.; Gorski, C. A.; Logan, B. E. Ammonium Removal from Domestic Wastewater Using Selective Battery Electrodes. *Environmental Science & Technology Letters* **2018**, *5*, 578−583.
(744) Choi, J.; Lee, H.; Hong, S. Capacitive deionization (CDI) integrated with monovalent cation selective membrane for producing divalent cation-rich solution. *Desalination* **2016**, *400*, 38−46.
(745) Singh, K.; Qian, Z.; Biesheuvel, P.; Zuilhof, H.; Porada, S.; de Smet, L. C. Nickel hexacyanoferrate electrodes for high mono/divalent ion-selectivity in capacitive deionization. *Desalination* **2020**, *481*, 114346.
(746) Xu, Y.; Zhou, H.; Wang, G.; Zhang, Y.; Zhang, H.; Zhao, H. Selective Pseudocapacitive Deionization of Calcium Ions in Copper Hexacyanoferrate. *ACS Appl. Mater. Interfaces* **2020**, *12*, 41437−41445.
(747) Shang, X.; Hu, B.; Nie, P.; Shi, W.; Hussain, T.; Liu, J. LiNi0.5Mn1.5O4-based hybrid capacitive deionization for highly selective adsorption of lithium from brine. *Sep. Purif. Technol.* **2021**, *258*, 118009.
(748) Zuo, K.; Kim, J.; Jain, A.; Wang, T.; Verduzco, R.; Long, M.; Li, Q. Novel Composite Electrodes for Selective Removal of Sulfate by the Capacitive Deionization Process. *Environ. Sci. Technol.* **2018**, *52*, 9486−9494.
(749) Chang, J.; Li, Y.; Duan, F.; Su, C.; Li, Y.; Cao, H. Selective removal of chloride ions by bismuth electrode in capacitive deionization. *Sep. Purif. Technol.* **2020**, *240*, 116600.
(750) Kim, J. S.; Jeon, Y. S.; Rhim, J. W. Application of poly(vinyl alcohol) and polysulfone based ionic exchange polymers to membrane capacitive deionization for the removal of mono- and divalent salts. *Sep. Purif. Technol.* **2016**, *157*, 45−52.
(751) Tang, W.; He, D.; Zhang, C.; Waite, T. D. Optimization of sulfate removal from brackish water by membrane capacitive deionization (MCDI). *Water Res.* **2017**, *121*, 302−310.
(752) Uwayid, R.; Guyes, E. N.; Shocron, A. N.; Gilron, J.; Elimelech, M.; Suss, M. E. Perfect divalent cation selectivity with capacitive deionization. *Water Res.* **2022**, *210*, 117959.
(753) Zhao, R.; Biesheuvel, P. M.; van der Wal, a. Energy consumption and constant current operation in membrane capacitive deionization. *Energy Environ. Sci.* **2012**, *5*, 9520−9527.
(754) Gaoa, X.; Porada, S.; Omosebi, A.; Liu, K.-L.; Biesheuvel, P. M.; Landon, J. Complementary surface charge for enhanced capacitive deionization. *Water Res.* **2016**, *92*, 275−282.
(755) Hemmatifar, A.; Stadermann, M.; Santiago, J. G. Two-Dimensional Porous Electrode Model for Capacitive Deionization. *J. Phys. Chem. C* **2015**, *119*, 24681−24694.
(756) Qu, Y.; Baumann, T. F.; Santiago, J. G.; Stadermann, M. Characterization of Resistances of a Capacitive Deionization System. *Environ. Sci. Technol.* **2015**, *49*, 9699−9706.
(757) Dykstra, J.; Zhao, R.; Biesheuvel, P.; van der Wal, A. Resistance identification and rational process design in Capacitive Deionization. *Water Res.* **2016**, *88*, 358−370.
(758) Qu, Y.; Campbell, P. G.; Gu, L.; Knipe, J. M.; Dzenitis, E.; Santiago, J. G.; Stadermann, M. Energy consumption analysis of constant voltage and constant current operations in capacitive deionization. *Desalination* **2016**, *400*, 18−24.
(759) Dykstra, J. E.; Porada, S.; van der Wal, A.; Biesheuvel, P. M. Energy consumption in capacitive deionization − Constant current versus constant voltage operation. *Water Res.* **2018**, *143*, 367−375.
(760) Hemmatifar, A.; Ramachandran, A.; Liu, K.; Oyarzun, D. I.; Bazant, M. Z.; Santiago, J. G. Thermodynamics of Ion Separation by Electrosorption. *Environ. Sci. Technol.* **2018**, *52*, 10196−10204.
(761) Hawks, S. A.; Knipe, J. M.; Campbell, P. G.; Loeb, C. K.; Hubert, M. A.; Santiago, J. G.; Stadermann, M. Quantifying the flow efficiency in constant-current capacitive deionization. *Water Res.* **2018**, *129*, 327−336.
(762) Wang, L.; Lin, S. Intrinsic tradeoff between kinetic and energetic efficiencies in membrane capacitive deionization. *Water Res.* **2018**, *129*, 394−401.
(763) Ramachandran, A.; Oyarzun, D. I.; Hawks, S. A.; Stadermann, M.; Santiago, J. G. High water recovery and improved thermodynamic efficiency for capacitive deionization using variable flowrate operation. *Water research* **2019**, *155*, 76−85.
(764) Wang, L.; Dykstra, J. E.; Lin, S. Energy Efficiency of Capacitive Deionization. *Environ. Sci. Technol.* **2019**, *53*, 3366−3378.
(765) Lin, S. Energy Efficiency of Desalination: Fundamental Insights from Intuitive Interpretation. *Environ. Sci. Technol.* **2020**, *54*, 76−84.
(766) Alkuran, M.; Orabi, M. Utilization of a buck boost converter and the method of segmented capacitors in a CDI water purification

https://doi.org/10.1021/acs.chemrev.1c00396
Chem. Rev. 2022, 122, 13547−13635

system. In *2008 12th International Middle-East Power System Conference*, 2008; pp 470−474.
(767) Pernía, A. M.; Norniella, J. G.; Martín-Ramos, J. A.; Díaz, J.; Martínez, J. A. Up−Down Converter for Energy Recovery in a CDI Desalination System. *IEEE Transactions on Power Electronics* **2012**, *27*, 3257−3265.
(768) Pernía, A. M.; Alvarez-Gonzalez, F. J.; Prieto, M. A. J.; Villegas, P. J.; Nuno, F. New Control Strategy of an Up−Down Converter for Energy Recovery in a CDI Desalination System. *IEEE Transactions on Power Electronics* **2014**, *29*, 3573−3581.
(769) Długołęcki, P.; Van Der Wal, A. Energy recovery in membrane capacitive deionization. *Environ. Sci. Technol.* **2013**, *47*, 4904−4910.
(770) Kang, J.; Kim, T.; Shin, H.; Lee, J.; Ha, J.-I.; Yoon, J. Direct energy recovery system for membrane capacitive deionization. *Desalination* **2016**, *398*, 144−150.
(771) Oyarzun, D. I.; Hawks, S. A.; Campbell, P. G.; Hemmatifar, A.; Krishna, A.; Santiago, J. G.; Stadermann, M. Energy transfer for storage or recovery in capacitive deionization using a DC-DC converter. *J. Power Sources* **2020**, *448*, 227409.
(772) Zhang, W.; Mossad, M.; Yazdi, J. S.; Zou, L. A statistical experimental investigation on arsenic removal using capacitive deionization. *Desalination and Water Treatment* **2016**, *57*, 3254−3260.
(773) Wu, T.; Wang, G.; Dong, Q.; Zhan, F.; Zhang, X.; Li, S.; Qiao, H.; Qiu, J. Starch Derived Porous Carbon Nanosheets for High-Performance Photovoltaic Capacitive Deionization. *Environ. Sci. Technol.* **2017**, *51*, 9244−9251.
(774) Tan, C.; He, C.; Tang, W.; Kovalsky, P.; Fletcher, J.; Waite, T. D. Integration of photovoltaic energy supply with membrane capacitive deionization (MCDI) for salt removal from brackish waters. *Water Res.* **2018**, *147*, 276−286.
(775) Hand, S.; Guest, J. S.; Cusick, R. D. Technoeconomic Analysis of Brackish Water Capacitive Deionization: Navigating Tradeoffs between Performance, Lifetime, and Material Costs. *Environ. Sci. Technol.* **2019**, *53*, 13353−13363.
(776) Kang, J.; Kim, T.; Jo, K.; Yoon, J. Comparison of salt adsorption capacity and energy consumption between constant current and constant voltage operation in capacitive deionization. *Desalination* **2014**, *352*, 52−57.
(777) Avraham, E.; Noked, M.; Bouhadana, Y.; Soffer, A.; Aurbach, D. Limitations of charge efficiency in capacitive deionization: II. On the behavior of CDI cells comprising two activated carbon electrodes. *J. Electrochem. Soc.* **2009**, *156*, P157.
(778) Avraham, E.; Noked, M.; Bouhadana, Y.; Soffer, A.; Aurbach, D. Limitations of charge efficiency in capacitive deionization processes III: The behavior of surface oxidized activated carbon electrodes. *Electrochim. Acta* **2010**, *56*, 441−447.
(779) Shanbhag, S.; Whitacre, J. F.; Mauter, M. S. The Origins of Low Efficiency in Electrochemical De-Ionization Systems. *J. Electrochem. Soc.* **2016**, *163*, E363−E371.
(780) Bazant, M. Z. Theory of chemical kinetics and charge transfer based on nonequilibrium thermodynamics. *Accounts of chemical research* **2013**, *46*, 1144−1160.
(781) Bouhadana, Y.; Avraham, E.; Noked, M.; Ben-Tzion, M.; Soffer, A.; Aurbach, D. Capacitive deionization of NaCl solutions at non-steady-state conditions: Inversion functionality of the carbon electrodes. *J. Phys. Chem. C* **2011**, *115*, 16567−16573.
(782) Holubowitch, N.; Omosebi, A.; Gao, X.; Landon, J.; Liu, K. Quasi-Steady-State Polarization Reveals the Interplay of Capacitive and Faradaic Processes in Capacitive Deionization. *ChemElectroChem.* **2017**, *4*, 2404−2413.
(783) He, D.; Wong, C. E.; Tang, W.; Kovalsky, P.; Waite, T. D. Faradaic Reactions in Water Desalination by Batch-Mode Capacitive Deionization. *Environmental Science & Technology Letters* **2016**, *3*, 222−226.
(784) Uwayid, R.; Seraphim, N. M.; Guyes, E. N.; Eisenberg, D.; Suss, M. E. Characterizing and mitigating the degradation of oxidized cathodes during capacitive deionization cycling. *Carbon* **2021**, *173*, 1105−1114.
(785) Cohen, I.; Avraham, E.; Noked, M.; Soffer, A.; Aurbach, D. Enhanced Charge Efficiency in Capacitive Deionization Achieved by Surface-Treated Electrodes and by Means of a Third Electrode. *J. Phys. Chem. C* **2011**, *115*, 19856−19863.
(786) Gao, X.; Omosebi, A.; Landon, J.; Liu, K. Enhancement of charge efficiency for a capacitive deionization cell using carbon xerogel with modified potential of zero charge. *Electrochem. Commun.* **2014**, *39*, 22−25.
(787) Biesheuvel, P. M.; Hamelers, H. V. M.; Suss, M. E. Theory of Water Desalination by Porous Electrodes with Immobile Chemical Charge. *Colloids and Interface Science Communications* **2015**, *9*, 1−5.
(788) Kim, T.; Dykstra, J.; Porada, S.; van der Wal, A.; Yoon, J.; Biesheuvel, P. Enhanced charge efficiency and reduced energy use in capacitive deionization by increasing the discharge voltage. *J. Colloid Interface Sci.* **2015**, *446*, 317−326.
(789) McNair, R.; Szekely, G.; Dryfe, R. A. Ion-exchange materials for membrane capacitive deionization. *ACS ES&T Water* **2021**, *1*, 217−239.
(790) Liu, X.; Shanbhag, S.; Natesakhawat, S.; Whitacre, J. F.; Mauter, M. S. Performance Loss of Activated Carbon Electrodes in Capacitive Deionization: Mechanisms and Material Property Predictors. *Environ. Sci. Technol.* **2020**, *54*, 15516−15526.
(791) Han, L.; Karthikeyan, K. G.; Gregory, K. B. Energy Consumption and Recovery in Capacitive Deionization Using Nanoporous Activated Carbon Electrodes. *J. Electrochem. Soc.* **2015**, *162*, E282−E288.
(792) Qin, M.; Deshmukh, A.; Epsztein, R.; Patel, S. K.; Owoseni, O. M.; Walker, W. S.; Elimelech, M. Comparison of energy consumption in desalination by capacitive deionization and reverse osmosis. *Desalination* **2019**, *455*, 100−114.
(793) Qin, M.; Deshmukh, A.; Epsztein, R.; Patel, S. K.; Owoseni, O. M.; Walker, W. S.; Elimelech, M. Response to comments on "comparison of energy consumption in desalination by capacitive deionization and reverse osmosis. *Desalination* **2019**, *462*, 48−55.
(794) Ramachandran, A.; Oyarzun, D. I.; Hawks, S. A.; Campbell, P. G.; Stadermann, M.; Santiago, J. G. Comments on "Comparison of Energy Consumption in Desalination by Capacitive Deionization and Reverse Osmosis". *Desalination*, **2019**, *461*, 30−36.
(795) Tan, C.; He, C.; Fletcher, J.; Waite, T. D. Energy recovery in pilot scale membrane CDI treatment of brackish waters. *Water Res.* **2020**, *168*, 115146.
(796) García-Quismondo, E.; Santos, C.; Soria, J.; Palma, J.; Anderson, M. A. New Operational Modes to Increase Energy Efficiency in Capacitive Deionization Systems. *Environ. Sci. Technol.* **2016**, *50*, 6053−6060.
(797) Subramani, A.; Jacangelo, J. G. Emerging desalination technologies for water treatment: a critical review. *Water research* **2015**, *75*, 164−187.
(798) Jia, B.; Zhang, W. Preparation and application of electrodes in capacitive deionization (CDI): a state-of-art review. *Nanoscale Res. Lett.* **2016**, *11*, 64.
(799) Duduta, M.; Ho, B.; Wood, V. C.; Limthongkul, P.; Brunini, V. E.; Carter, W. C.; Chiang, Y. M. Semi-solid lithium rechargeable flow battery. *Adv. Energy Mater.* **2011**, *1* (4), 511−516.
(800) Park, M.; Ryu, J.; Wang, W.; Cho, J. Material design and engineering of next-generation flow-battery technologies. *Nat. Rev. Mater.* **2017**, *2* (1), 1−18.
(801) Chen, H.; Lu, Y. C. A High-Energy-Density Multiple Redox Semi-Solid-Liquid Flow Battery. *Adv. Energy Mater.* **2016**, *6* (8), 150−183.
(802) Narayanan, T. M.; Zhu, Y. G.; Gencer, E.; McKinley, G.; Shao-Horn, Y. Low-cost manganese dioxide semi-solid electrode for flow batteries. *Joule* **2021**, *5* (11), 2934−2954.
(803) Jeon, S.-i.; Yeo, J.-g.; Yang, S.; Choi, J.; Kim, D. K. Ion storage and energy recovery of a flow-electrode capacitive deionization process. *Journal of Materials Chemistry A* **2014**, *2*, 6378−6383.
(804) Hatzell, K. B.; Iwama, E.; Ferris, A.; Daffos, B.; Urita, K.; Tzedakis, T.; Chauvet, F.; Taberna, P.-L.; Gogotsi, Y.; Simon, P. Capacitive deionization concept based on suspension electrodes

https://doi.org/10.1021/acs.chemrev.1c00396
Chem. Rev. 2022, 122, 13547−13635

without ion exchange membranes. *Electrochem. Commun.* **2014**, *43*, 18−21.
(805) Rommerskirchen, A.; Gendel, Y.; Wessling, M. Single module flow-electrode capacitive deionization for continuous water desalination. *Electrochem. Commun.* **2015**, *60*, 34−37.
(806) Zhang, C.; Wu, L.; Ma, J.; Pham, A. N.; Wang, M.; Waite, T. D. Integrated Flow-Electrode Capacitive Deionization and Microfiltration System for Continuous and Energy-Efficient Brackish Water Desalination. *Environ. Sci. Technol.* **2019**, *53*, 13364−13373.
(807) Rommerskirchen, A.; Linnartz, C. J.; Müller, D.; Willenberg, L. K.; Wessling, M. Energy Recovery and Process Design in Continuous Flow-Electrode Capacitive Deionization Processes. *ACS Sustainable Chem. Eng.* **2018**, *6*, 13007−13015.
(808) Ma, J.; Liang, P.; Sun, X.; Zhang, H.; Bian, Y.; Yang, F.; Bai, J.; Gong, Q.; Huang, X. Energy recovery from the flow-electrode capacitive deionization. *J. Power Sources* **2019**, *421*, 50−55.
(809) Zhang, C.; Ma, J.; Wu, L.; Sun, J.; Wang, L.; Li, T.; Waite, T. D. Flow Electrode Capacitive Deionization (FCDI): Recent Developments, Environmental Applications, and Future Perspectives. *Environ. Sci. Technol.* **2021**, *55*, 4243−4267.
(810) Yang, F.; He, Y.; Rosentsvit, L.; Suss, M. E.; Zhang, X.; Gao, T.; Liang, P. Flow-electrode capacitive deionization: A review and new perspectives. *Water Res.* **2021**, *200*, 117222.
(811) Rommerskirchen, A.; Linnartz, C. J.; Egidi, F.; Kendir, S.; Wessling, M. Flow-electrode capacitive deionization enables continuous and energy-efficient brine concentration. *Desalination* **2020**, *490*, 114453.
(812) Bian, Y.; Chen, X.; Lu, L.; Liang, P.; Ren, Z. J. Concurrent nitrogen and phosphorus recovery using flow-electrode capacitive deionization. *ACS Sustainable Chem. Eng.* **2019**, *7*, 7844−7850.
(813) Xu, L.; Yu, C.; Tian, S.; Mao, Y.; Zong, Y.; Zhang, X.; Zhang, B.; Zhang, C.; Wu, D. Selective recovery of phosphorus from synthetic urine using flow-electrode capacitive deionization (FCDI)-based technology. *ACS ES&T Water* **2021**, *1*, 175−184.
(814) Yu, C.; Xu, L.; Mao, Y.; Zong, Y.; Wu, D. Efficient recovery of carboxylates from the effluents treated by advanced oxidation processes using flow-electrode capacitive deionization in short-circuited closed-cycle operation. *Sep. Purif. Technol.* **2021**, *275*, 119151.
(815) Fang, K.; Peng, F.; San, E.; Wang, K. The impact of concentration in electrolyte on ammonia removal in flow-electrode capacitive deionization system. *Sep. Purif. Technol.* **2021**, *255*, 117337.
(816) Cohen, H.; Eli, S. E.; Jõgi, M.; Suss, M. E. Suspension Electrodes Combining Slurries and Upflow Fluidized Beds. *ChemSusChem* **2016**, *9*, 3045−3048.
(817) Nativ, P.; Badash, Y.; Gendel, Y. New insights into the mechanism of flow-electrode capacitive deionization. *Electrochem. Commun.* **2017**, *76*, 24−28.
(818) Gendel, Y.; Rommerskirchen, A. K. E.; David, O.; Wessling, M. Batch mode and continuous desalination of water using flowing carbon deionization (FCDI) technology. *Electrochem. Commun.* **2014**, *46*, 152−156.
(819) Ma, J.; He, D.; Tang, W.; Kovalsky, P.; He, C.; Zhang, C.; Waite, T. Development of redox-active flow electrodes for high-performance capacitive deionization. *Environ. Sci. Technol.* **2016**, *50*, 13495−13501.
(820) Yang, S.; Park, H.-r.; Yoo, J.; Kim, H.; Choi, J.; Han, M. H.; Kim, D. K. Plate-Shaped Graphite for Improved Performance of Flow-Electrode Capacitive Deionization. *J. Electrochem. Soc.* **2017**, *164*, E480−E488.
(821) Liang, P.; Sun, X.; Bian, Y.; Zhang, H.; Yang, X.; Jiang, Y.; Liu, P.; Huang, X. Optimized desalination performance of high voltage flow-electrode capacitive deionization by adding carbon black in flow-electrode. *Desalination* **2017**, *420*, 63−69.
(822) Akuzum, B.; Agartan, L.; Locco, J.; Kumbur, E. Effects of particle dispersion and slurry preparation protocol on electrochemical performance of capacitive flowable electrodes. *J. Appl. Electrochem.* **2017**, *47*, 369−380.
(823) Akuzum, B.; Singh, P.; Eichfeld, D. A.; Agartan, L.; Uzun, S.; Gogotsi, Y.; Kumbur, E. C. Percolation characteristics of conductive additives for capacitive flowable (semi-solid) electrodes. *ACS Appl. Mater. Interfaces* **2020**, *12*, 5866−5875.
(824) Halfon, E. B.; Suss, M. E. Measurements of the electric conductivity of an electrode as it transitions between static and flowable modes. *Electrochem. Commun.* **2019**, *99*, 61−64.
(825) Yang, S.; Jeon, S. I.; Kim, H.; Choi, J.; Yeo, J. G.; Park, H. R.; Kim, D. K. Stack Design and Operation for Scaling Up the Capacity of Flow-Electrode Capacitive Deionization Technology. *ACS Sustainable Chem. Eng.* **2016**, *4*, 4174−4180.
(826) Cho, Y.; Lee, K. S.; Yang, S.; Choi, J.; Park, H.-r.; Kim, D. K. A novel three-dimensional desalination system utilizing honeycomb-shaped lattice structures for flow-electrode capacitive deionization. *Energy Environ. Sci.* **2017**, *10*, 1746−1750.
(827) Ma, J.; Ma, J.; Zhang, C.; Song, J.; Dong, W.; Waite, T. D. Flow-electrode capacitive deionization (FCDI) scale-up using a membrane stack configuration. *Water research* **2020**, *168*, 115186.
(828) Linnartz, C. J.; Rommerskirchen, A.; Walker, J.; Plankermann-Hajduk, J.; Köller, N.; Wessling, M. Membrane-electrode assemblies for flow-electrode capacitive deionization. *J. Membr. Sci.* **2020**, *605*, 118095.
(829) Linnartz, C. J.; Rommerskirchen, A.; Wessling, M.; Gendel, Y. Flow-Electrode Capacitive Deionization for Double Displacement Reactions. *ACS Sustainable Chem. Eng.* **2017**, *5*, 3906−3912.
(830) Wang, M.; Hou, S.; Liu, Y.; Xu, X.; Lu, T.; Zhao, R.; Pan, L. Capacitive neutralization deionization with flow electrodes. *Electrochim. Acta* **2016**, *216*, 211−218.
(831) Nativ, P.; Lahav, O.; Gendel, Y. Separation of divalent and monovalent ions using flow-electrode capacitive deionization with nanofiltration membranes. *Desalination* **2018**, *425*, 123−129.
(832) He, C.; Ma, J.; Zhang, C.; Song, J.; Waite, T. D. Short-Circuited Closed-Cycle Operation of Flow-Electrode CDI for Brackish Water Softening. *Environ. Sci. Technol.* **2018**, *52*, 9350−9360.
(833) Song, J.; Ma, J.; Zhang, C.; He, C.; Waite, T. D. Implication of non-electrostatic contribution to deionization in flow-electrode CDI: Case study of nitrate removal from contaminated source waters. *Front. Chem.* **2019**, *7*, 146.
(834) Ma, J.; Zhang, Y.; Collins, R. N.; Tsarev, S.; Aoyagi, N.; Kinsela, A. S.; Jones, A. M.; Waite, T. D. Flow-Electrode CDI Removes the Uncharged Ca-UO2-CO3 Ternary Complex from Brackish Potable Groundwater: Complex Dissociation, Transport, and Sorption. *Environ. Sci. Technol.* **2019**, *53*, 2739−2747.
(835) Jiang, H.; Zhang, J.; Luo, K.; Xing, W.; Du, J.; Dong, Y.; Li, X.; Tang, W. Effective fluoride removal from brackish groundwaters by flow-electrode capacitive deionization (FCDI) under a continuous-flow mode. *Sci. Total Environ.* **2022**, *804*, 150166.
(836) Rommerskirchen, A.; Alders, M.; Wiesner, F.; Linnartz, C. J.; Kalde, A.; Wessling, M. Process model for high salinity flow-electrode capacitive deionization processes with ion-exchange membranes. *J. Membr. Sci.* **2020**, *616*, 118614.
(837) Wang, L.; Zhang, C.; He, C.; Waite, T. D.; Lin, S. Equivalent film-electrode model for flow-electrode capacitive deionization: Experimental validation and performance analysis. *Water Res.* **2020**, *181*, 115917.
(838) Rommerskirchen, A.; Kalde, A.; Linnartz, C. J.; Bongers, L.; Linz, G.; Wessling, M. Unraveling charge transport in carbon flow-electrodes: Performance prediction for desalination applications. *Carbon* **2019**, *145*, 507−520.
(839) Eifert, L.; Jusys, Z.; Behm, R.; Zeis, R. Side reactions and stability of pre-treated carbon felt electrodes for vanadium redox flow batteries: A DEMS study. *Carbon* **2020**, *158*, 580−587.
(840) Cohen, I.; Avraham, E.; Bouhadana, Y.; Soffer, A.; Aurbach, D. Long term stability of capacitive de-ionization processes for water desalination: The challenge of positive electrodes corrosion. *Electrochim. Acta* **2013**, *106*, 91−100.
(841) Li, B.; Zheng, T.; Ran, S.; Sun, M.; Shang, J.; Hu, H.; Lee, P. H.; Boles, S. T. Performance Recovery in Degraded Carbon-Based

Electrodes for Capacitive Deionization. *Environ. Sci. Technol.* **2020**, *54*, 1848−1856.
(842) Uwayid, R.; Diesendruck, C. E.; Suss, M. E. Emerging investigator series: a comparison of strong and weak-acid functionalized carbon electrodes in capacitive deionization. *Environ. Sci.: Water Res. Technol.* **2022**, *8*, 949−956.
(843) Srimuk, P.; Zeiger, M.; Jäckel, N.; Tolosa, A.; Krüner, B.; Fleischmann, S.; Grobelsek, I.; Aslan, M.; Shvartsev, B.; Suss, M. E.; Presser, V. Enhanced performance stability of carbon/titania hybrid electrodes during capacitive deionization of oxygen saturated saline water. *Electrochim. Acta* **2017**, *224*, 314−328.
(844) Cohen, I.; Avraham, E.; Bouhadana, Y.; Soffer, A.; Aurbach, D. The effect of the flow-regime, reversal of polarization, and oxygen on the long term stability in capacitive de-ionization processes. *Electrochim. Acta* **2015**, *153*, 106−114.
(845) Gao, X.; Omosebi, A.; Landon, J.; Liu, K. Voltage-Based Stabilization of Microporous Carbon Electrodes for Inverted Capacitive Deionization. *J. Phys. Chem. C* **2018**, *122*, 1158−1168.
(846) Lu, D.; Cai, W.; Wang, Y. Optimization of the voltage window for long-term capacitive deionization stability. *Desalination* **2017**, *424*, 53−61.
(847) Lee, J.-H.; Bae, W.-S.; Choi, J.-H. Electrode reactions and adsorption/desorption performance related to the applied potential in a capacitive deionization process. *Desalination* **2010**, *258*, 159−163.
(848) Gao, X.; Omosebi, A.; Landon, J.; Liu, K. Surface charge enhanced carbon electrodes for stable and efficient capacitive deionization using inverted adsorption−desorption behavior. *Energy Environ. Sci.* **2015**, *8*, 897−909.
(849) Gao, X.; Omosebi, A.; Holubowitch, N.; Landon, J.; Liu, K. Capacitive Deionization Using Alternating Polarization: Effect of Surface Charge on Salt Removal. *Electrochim. Acta* **2017**, *233*, 249−255.
(850) Lee, J.; Kim, S.; Kim, C.; Yoon, J. Hybrid capacitive deionization to enhance the desalination performance of capacitive techniques. *Energy Environ. Sci.* **2014**, *7*, 3683−3689.
(851) Kim, T.; Yu, J.; Kim, C.; Yoon, J. Hydrogen peroxide generation in fl ow-mode capacitive deionization. *J. Electroanal. Chem.* **2016**, *776*, 101−104.
(852) Mossad, M.; Zou, L. Study of fouling and scaling in capacitive deionisation by using dissolved organic and inorganic salts. *Journal of hazardous materials* **2013**, *244*, 387−393.
(853) Zhang, W.; Mossad, M.; Zou, L. A study of the long-term operation of capacitive deionisation in inland brackish water desalination. *Desalination* **2013**, *320*, 80−85.
(854) Wang, C.; Song, H.; Zhang, Q.; Wang, B.; Li, A. Parameter optimization based on capacitive deionization for highly efficient desalination of domestic wastewater biotreated effluent and the fouled electrode regeneration. *Desalination* **2015**, *365*, 407−415.
(855) Liu, X.; Whitacre, J. F.; Mauter, M. S. Mechanisms of humic acid fouling on capacitive and insertion electrodes for electrochemical desalination. *Environ. Sci. Technol.* **2018**, *52*, 12633−12641.
(856) Wang, T.; Zhang, C.; Bai, L.; Xie, B.; Gan, Z.; Xing, J.; Li, G.; Liang, H. Scaling behavior of iron in capacitive deionization (CDI) system. *Water research* **2020**, *171*, 115370.
(857) Wang, T.; Bai, L.; Zhang, C.; Zhu, X.; Xing, J.; Guo, Y.; Wang, J.; Lin, D.; Li, G.; Liang, H. Formation mechanism of iron scale in membrane capacitive deionization (MCDI) system. *Desalination* **2020**, *495*, 114636.
(858) Chen, L.; Wang, C.; Liu, S.; Hu, Q.; Zhu, L.; Cao, C. Investigation of the long-term desalination performance of membrane capacitive deionization at the presence of organic foulants. *Chemosphere* **2018**, *193*, 989−997.
(859) Li, Y.; Stewart, T. C.; Tang, H. L. A comparative study on electrosorptive rates of metal ions in capacitive deionization. *Journal of water process engineering* **2018**, *26*, 257−263.
(860) Zhang, W.; Jia, B. Toward anti-fouling capacitive deionization by using visible-light reduced TiO2/graphene nanocomposites. *MRS Commun.* **2015**, *5*, 613−617.
(861) Liu, E.; Lee, L. Y.; Ong, S. L.; Ng, H. Y. Treatment of industrial brine using capacitive deionization (CDI) towards zero liquid discharge−challenges and optimization. *Water Res.* **2020**, *183*, 116059.
(862) Porada, S.; Weinstein, L.; Dash, R.; Van Der Wal, A.; Bryjak, M.; Gogotsi, Y.; Biesheuvel, P. Water desalination using capacitive deionization with microporous carbon electrodes. *ACS Appl. Mater. Interfaces* **2012**, *4*, 1194−1199.
(863) Porada, S.; Borchardt, L.; Oschatz, M.; Bryjak, M.; Atchison, J.; Keesman, K.; Kaskel, S.; Biesheuvel, P.; Presser, V. Direct prediction of the desalination performance of porous carbon electrodes for capacitive deionization. *Energy Environ. Sci.* **2013**, *6*, 3700−3712.
(864) Huang, Z.-H.; Yang, Z.; Kang, F.; Inagaki, M. Carbon electrodes for capacitive deionization. *Journal of Materials Chemistry A* **2017**, *5*, 470−496.
(865) Ratajczak, P.; Suss, M. E.; Kaasik, F.; Béguin, F. Carbon electrodes for capacitive technologies. *Energy Storage Materials* **2019**, *16*, 126−145.
(866) Li, B.; Zheng, T.; Ran, S.; Lee, P.-H.; Liu, B.; Boles, S. T. Role of metastable-adsorbed charges in the stability degradation of carbon-based electrodes for capacitive deionization. *Environ. Sci.: Water Res.; Technol.* **2018**, *4*, 1172−1180.
(867) Singh, K.; Porada, S.; de Gier, H.; Biesheuvel, P.; de Smet, L. Timeline on the application of intercalation materials in Capacitive Deionization. *Desalination* **2019**, *455*, 115−134.
(868) Han, B.; Cheng, G.; Wang, Y.; Wang, X. Structure and functionality design of novel carbon and faradaic electrode materials for high-performance capacitive deionization. *Chemical Engineering Journal* **2019**, *360*, 364−384.
(869) Srimuk, P.; Halim, J.; Lee, J.; Tao, Q.; Rosen, J.; Presser, V. Two-dimensional molybdenum carbide (MXene) with divacancy ordering for brackish and seawater desalination via cation and anion intercalation. *ACS Sustainable Chem. Eng.* **2018**, *6*, 3739−3747.
(870) Bao, W.; Tang, X.; Guo, X.; Choi, S.; Wang, C.; Gogotsi, Y.; Wang, G. Porous cryo-dried MXene for efficient capacitive deionization. *Joule* **2018**, *2*, 778−787.
(871) Shen, X.; Xiong, Y.; Hai, R.; Yu, F.; Ma, J. An All-MXene-Based Integrated Membrane Electrode Constructed using $Ti_3C_2T_x$ as an Intercalating Agent for High Performance Desalination. *Environ. Sci. Technol.* **2020**, *54*, 4554−4563.
(872) Acerce, M.; Voiry, D.; Chhowalla, M. Metallic 1T phase MoS_2 nanosheets as supercapacitor electrode materials. *Nature Nanotechnol.* **2015**, *10*, 313−318.
(873) Srimuk, P.; Lee, J.; Fleischmann, S.; Choudhury, S.; Jackel, N.; Zeiger, M.; Kim, C.; Aslan, M.; Presser, V. Faradaic deionization of brackish and sea water via pseudocapacitive cation and anion intercalation into few-layered molybdenum disulfide. *Journal of Materials Chemistry A* **2017**, *5*, 15640−15649.
(874) Xing, F.; Li, T.; Li, J.; Zhu, H.; Wang, N.; Cao, X. Chemically exfoliated MoS2 for capacitive deionization of saline water. *Nano Energy* **2017**, *31*, 590−595.
(875) Cai, Y.; Zhang, W.; Fang, R.; Zhao, D.; Wang, Y.; Wang, J. Well-dispersed few-layered MoS2 connected with robust 3D conductive architecture for rapid capacitive deionization process and its specific ion selectivity. *Desalination* **2021**, *520*, 115325.
(876) Huang, S.; Mochalin, V. N. Hydrolysis of 2D Transition-Metal Carbides (MXenes) in Colloidal Solutions. *Inorg. Chem.* **2019**, *58*, 1958−1966.
(877) Verger, L.; Natu, V.; Ghidiu, M.; Barsoum, M. W. Effect of Cationic Exchange on the Hydration and Swelling Behavior of $Ti_3C_2T_z$ MXenes. *J. Phys. Chem. C* **2019**, *123*, 20044−20050.
(878) Kaasik, F.; Tamm, T.; Hantel, M. M.; Perre, E.; Aabloo, A.; Lust, E.; Bazant, M. Z.; Presser, V. Anisometric charge dependent swelling of porous carbon in an ionic liquid. *Electrochemistry communications* **2013**, *34*, 196−199.
(879) Han, M. H.; Gonzalo, E.; Singh, G.; Rojo, T. A comprehensive review of sodium layered oxides: powerful cathodes for Na-ion batteries. *Energy Environ. Sci.* **2015**, *8*, 81−102.

https://doi.org/10.1021/acs.chemrev.1c00396
Chem. Rev. 2022, 122, 13547−13635

(880) Ahn, J.; Lee, J.; Kim, S.; Kim, C.; Lee, J.; Biesheuvel, P.; Yoon, J. High performance electrochemical saline water desalination using silver and silver-chloride electrodes. *Desalination* **2020**, *476*, 114216.
(881) Chen, F.; Huang, Y.; Guo, L.; Ding, M.; Yang, H. Y. A dual-ion electrochemistry deionization system based on AgCl-$Na_{0.44}MnO_2$ electrodes. *Nanoscale* **2017**, *9*, 10101−10108.
(882) Zhao, W.; Guo, L.; Ding, M.; Huang, Y.; Yang, H. Y. Ultrahigh-Desalination-Capacity Dual-Ion Electrochemical Deionization Device Based on $Na_3V_2(PO_4)_3$@C−AgCl Electrodes. *ACS Appl. Mater. Interfaces* **2018**, *10*, 40540−40548.
(883) Nam, D.-H.; Choi, K.-S. Bismuth as a new chloride-storage electrode enabling the construction of a practical high capacity desalination battery. *J. Am. Chem. Soc.* **2017**, *139*, 11055−11063.
(884) Wu, T.; Wang, G.; Wang, S.; Zhan, F.; Fu, Y.; Qiao, H.; Qiu, J. Highly stable hybrid capacitive deionization with a MnO_2 anode and a positively charged cathode. *Environmental Science & Technology Letters* **2018**, *5*, 98−102.
(885) Yang, J.; Zou, L.; Song, H.; Hao, Z. Development of novel MnO2/nanoporous carbon composite electrodes in capacitive deionization technology. *Desalination* **2011**, *276*, 199−206.
(886) Compton, R. G.; Banks, C. E. *Understanding Voltammetry*; World Scientific, 2018.
(887) Karyakin, A. A. Prussian blue and its analogues: electrochemistry and analytical applications. *Electroanalysis: An International Journal Devoted to Fundamental and Practical Aspects of Electroanalysis* **2001**, *13*, 813−819.
(888) Ma, X.; Chen, Y.-A.; Zhou, K.; Wu, P.-C.; Hou, C.-H. Enhanced desalination performance via mixed capacitive-Faradaic ion storage using RuO2-activated carbon composite electrodes. *Electrochim. Acta* **2019**, *295*, 769−777.
(889) Ding, M.; Fan, S.; Huang, S.; Pam, M. E.; Guo, L.; Shi, Y.; Yang, H. Y. Tunable Pseudocapacitive Behavior in Metal−Organic Framework-Derived TiO 2 @Porous Carbon Enabling High-Performance Membrane Capacitive Deionization. *ACS Applied Energy Materials* **2019**, *2*, 1812−1822.
(890) Yu, F.; Wang, L.; Wang, Y.; Shen, X.; Cheng, Y.; Ma, J. Faradaic reactions in capacitive deionization for desalination and ion separation. *Journal of Materials Chemistry A* **2019**, *7*, 15999−16027.
(891) Sood, A.; Poletayev, A. D.; Cogswell, D. A.; Csernica, P. M.; Mefford, J. T.; Fraggedakis, D.; Toney, M. F.; Lindenberg, A. M.; Bazant, M. Z.; Chueh, W. C. Electrochemical Ion Insertion: From Atoms to Devices. *Nat. Rev. Mater.* **2021**, *6*, 847−867.
(892) Kim, S.; Lee, J.; Kim, C.; Yoon, J. $Na_2FeP_2O_7$ as a novel material for hybrid capacitive deionization. *Electrochim. Acta* **2016**, *203*, 265−271.
(893) Ferguson, T. R.; Bazant, M. Z. Nonequilibrium thermodynamics of porous electrodes. *J. Electrochem. Soc.* **2012**, *159*, A1967.
(894) Smith, R. B.; Bazant, M. Z. Multiphase porous electrode theory. *J. Electrochem. Soc.* **2017**, *164*, No. E3291.
(895) He, F.; Biesheuvel, P.; Bazant, M. Z.; Hatton, T. A. Theory of water treatment by capacitive deionization with redox active porous electrodes. *Water research* **2018**, *132*, 282−291.
(896) La Mantia, F.; Pasta, M.; Deshazer, H. D.; Logan, B. E.; Cui, Y. Batteries for Efficient Energy Extraction from a Water Salinity Difference. *Nano Lett.* **2011**, *11*, 1810−1813.
(897) Shanbhag, S.; Bootwala, Y.; Whitacre, J. F.; Mauter, M. S. Ion transport and competition effects on $NaTi_2(PO_4)_3$ and $Na_4Mn_9O_{18}$ selective insertion electrode performance. *Langmuir* **2017**, *33*, 12580−12591.
(898) Ikeshoji, T. Separation of alkali metal ions by intercalation into a prussian blue electrode. *J. Electrochem. Soc.* **1986**, *133*, 2108.
(899) Bocarsly, A. B.; Sinha, S. Effects of surface structure on electrode charge transfer properties: Induction of ion selectivity at the chemically derivatized interface. *Journal of Electroanalytical Chemistry and Interfacial Electrochemistry* **1982**, *140*, 167−172.
(900) Deakin, M. R.; Byrd, H. Prussian Blue coated quartz crystal microbalance as a detector for electroinactive cations in aqueous solution. *Anal. Chem.* **1989**, *61*, 290−295.
(901) Rassat, S. D.; Sukamto, J. H.; Orth, R. J.; Lilga, M. A.; Hallen, R. T. Development of an electrically switched ion exchange process for selective ion separations. *Sep. Purif. Technol.* **1999**, *15*, 207−222.
(902) Erinmwingbovo, C.; Palagonia, M. S.; Brogioli, D.; La Mantia, F. Intercalation into a Prussian blue derivative from solutions containing two species of cations. *ChemPhysChem* **2017**, *18*, 917−925.
(903) Singh, K.; Li, G.; Lee, J.; Zuilhof, H.; Mehdi, B. L.; Zornitta, R. L.; de Smet, L. C. Divalent Ion Selectivity in Capacitive Deionization with Vanadium Hexacyanoferrate: Experiments and Quantum-Chemical Computations. *Adv. Funct. Mater.* **2021**, *31*, 2105203.
(904) Lee, J.; Srimuk, P.; Aristizabal, K.; Kim, C.; Choudhury, S.; Nah, Y.-C.; Mücklich, F.; Presser, V. Pseudocapacitive Desalination of Brackish Water and Seawater with Vanadium-Pentoxide-Decorated Multiwalled Carbon Nanotubes. *ChemSusChem* **2017**, *10*, 3611−3623.
(905) Srimuk, P.; Lee, J.; Tolosa, A.; Kim, C.; Aslan, M.; Presser, V. Titanium Disulfide: A Promising Low-Dimensional Electrode Material for Sodium Ion Intercalation for Seawater Desalination. *Chem. Mater.* **2017**, *29*, 9964−9973.
(906) Tang, X.; Liu, H.; Su, D.; Notten, P. H.; Wang, G. Hierarchical sodium-rich Prussian blue hollow nanospheres as high-performance cathode for sodium-ion batteries. *Nano Research* **2018**, *11*, 3979−3990.
(907) Huang, Y.; Chen, F.; Guo, L.; Zhang, J.; Chen, T.; Yang, H. Y. Low energy consumption dual-ion electrochemical deionization system using NaTi2 (PO4) 3-AgNPs electrodes. *Desalination* **2019**, *451*, 241−247.
(908) Byles, B. W.; Cullen, D. A.; More, K. L.; Pomerantseva, E. Tunnel structured manganese oxide nanowires as redox active electrodes for hybrid capacitive deionization. *Nano Energy* **2018**, *44*, 476−488.
(909) Su, X.; Tan, K. J.; Elbert, J.; Ruttiger, C.; Gallei, M.; Jamison, T. F.; Hatton, T. A. Asymmetric Faradaic systems for selective electrochemical separations. *Energy Environ. Sci.* **2017**, *10*, 1272−1283.
(910) He, F.; Bazant, M. Z.; Hatton, T. A. Equivalent Circuit Model for Electrosorption with Redox Active Materials. *arXiv* **2020**, arXiv:2101.00091, .
(911) He, F.; Bazant, M. Z.; Hatton, T. A. Theory of Faradaically Modulated Redox Active Electrodes for Electrochemically Mediated Selective Adsorption Processes. *J. Electrochem. Soc.* **2021**, *168*, 053501.
(912) Ferguson, T. R.; Bazant, M. Z. Phase transformation dynamics in porous battery electrodes. *Electrochim. Acta* **2014**, *146*, 89−97.
(913) Smith, R. B.; Khoo, E.; Bazant, M. Z. Intercalation kinetics in multiphase-layered materials. *J. Phys. Chem. C* **2017**, *121*, 12505−12523.
(914) Pothanamkandathil, V.; Fortunato, J.; Gorski, C. A. Electrochemical Desalination Using Intercalating Electrode Materials: A Comparison of Energy Demands. *Environ. Sci. Technol.* **2020**, *54*, 3653−3662.
(915) Metzger, M.; Besli, M. M.; Kuppan, S.; Hellstrom, S.; Kim, S.; Sebti, E.; Subban, C. V.; Christensen, J. Techno-economic analysis of capacitive and intercalative water deionization. *Energy Environ. Sci.* **2020**, *13*, 1544−1560.
(916) Bai, P.; Bazant, M. Z. Charge transfer kinetics at the solid−solid interface in porous electrodes. *Nat. Commun.* **2014**, *5*, 3585.
(917) Marcus, R. A. Electron transfer reactions in chemistry. Theory and experiment. *Rev. Mod. Phys.* **1993**, *65*, 599.
(918) Kuznetsov, A. M.; Ulstrup, J. *Electron Transfer in Chemistry and Biology: An Introduction to the Theory*; John Wiley & Sons Ltd, 1999.
(919) Chidsey, C. E. D. Free-Energy and Temperature-Dependence of Electron-Transfer at the Metal-Electrolyte Interface. *Science* **1991**, *251*, 919−922.
(920) Zeng, Y.; Smith, R. B.; Bai, P.; Bazant, M. Z. Simple formula for Marcus−Hush−Chidsey kinetics. *J. Electroanal. Chem.* **2014**, *735*, 77−83.
(921) Fraggedakis, D.; McEldrew, M.; Smith, R. B.; Krishnan, Y.; Zhang, Y.; Bai, P.; Chueh, W. C.; Shao-Horn, Y.; Bazant, M. Z.

https://doi.org/10.1021/acs.chemrev.1c00396
Chem. Rev. 2022, 122, 13547−13635

Theory of coupled ion-electron transfer kinetics. *Electrochim. Acta* **2021**, *367*, 137432.
(922) Fraggedakis, D.; Bazant, M. Z. Tuning the stability of electrochemical interfaces by electron transfer reactions. *J. Chem. Phys.* **2020**, *152*, 184703.
(923) Park, K.-S.; Xiao, P.; Kim, S.-Y.; Dylla, A.; Choi, Y.-M.; Henkelman, G.; Stevenson, K. J.; Goodenough, J. B. Enhanced charge-transfer kinetics by anion surface modification of $LiFePO_4$. *Chem. Mater.* **2012**, *24*, 3212−3218.
(924) Trócoli, R.; Battistel, A.; Mantia, F. L. Selectivity of a Lithium-Recovery Process Based on $LiFePO_4$. *Chem.-Eur. J.* **2014**, *20*, 9888−9891.
(925) Liu, C.; Li, Y.; Lin, D.; Hsu, P.-C.; Liu, B.; Yan, G.; Wu, T.; Cui, Y.; Chu, S. Lithium Extraction from Seawater through Pulsed Electrochemical Intercalation. *Joule* **2020**, *4*, 1459−1469.
(926) He, X.; Kaur, S.; Kostecki, R. Mining Lithium from Seawater. *Joule* **2020**, *4*, 1357−1358.
(927) Hong, S.; Yoon, H.; Lee, J.; Kim, C.; Kim, S.; Lee, J.; Lee, C.; Yoon, J. Selective phosphate removal using layered double hydroxide/reduced graphene oxide (LDH/rGO) composite electrode in capacitive deionization. *J. Colloid Interface Sci.* **2020**, *564*, 1−7.
(928) Seftel, E.; Ciocarlan, R.; Michielsen, B.; Meynen, V.; Mullens, S.; Cool, P. Insights into phosphate adsorption behavior on structurally modified ZnAl layered double hydroxides. *Appl. Clay Sci.* **2018**, *165*, 234−246.
(929) He, H.; Kang, H.; Ma, S.; Bai, Y.; Yang, X. High adsorption selectivity of ZnAl layered double hydroxides and the calcined materials toward phosphate. *J. Colloid Interface Sci.* **2010**, *343*, 225−231.
(930) Park, G.; Hong, S.; Lee, C.; Lee, J.; Yoon, J. Selective fluoride removal in capacitive deionization by reduced graphene oxide/hydroxyapatite composite electrode. *J. Colloid Interface Sci.* **2021**, *581*, 396−402.
(931) Yu, X.; Tong, S.; Ge, M.; Zuo, J. Removal of fluoride from drinking water by cellulose@ hydroxyapatite nanocomposites. *Carbohydr. Polym.* **2013**, *92*, 269−275.
(932) Agartan, L.; Hayes-Oberst, B.; Byles, B. W.; Akuzum, B.; Pomerantseva, E.; Kumbur, E. C. Influence of operating conditions and cathode parameters on desalination performance of hybrid CDI systems. *Desalination* **2019**, *452*, 1−8.
(933) Sauvage, F.; Baudrin, E.; Tarascon, J.-M. Study of the potentiometric response towards sodium ions of $Na_{0.44-x}MnO_2$ for the development of selective sodium ion sensors. *Sens. Actuators, B* **2007**, *120*, 638−644.
(934) Kim, H.; Shakoor, R. A.; Park, C.; Lim, S. Y.; Kim, J.-S.; Jo, Y. N.; Cho, W.; Miyasaka, K.; Kahraman, R.; Jung, Y.; Choi, J. W. $Na_2FeP_2O_7$ As a Promising Iron-Based Pyrophosphate Cathode for Sodium Rechargeable Batteries: A Combined Experimental and Theoretical Study. *Adv. Funct. Mater.* **2013**, *23*, 1147−1155.
(935) Chang, J.; Duan, F.; Cao, H.; Tang, K.; Su, C.; Li, Y. Superiority of a novel flow-electrode capacitive deionization (FCDI) based on a battery material at high applied voltage. *Desalination* **2019**, *468*, 114080.
(936) Kim, N.; Lee, J.; Kim, S.; Hong, S. P.; Lee, C.; Yoon, J.; Kim, C. Short review of multichannel membrane capacitive deionization: Principle, current status, and future prospect. *Applied Sciences* **2020**, *10*, 683.
(937) Srimuk, P.; Husmann, S.; Presser, V. Low voltage operation of a silver/silver chloride battery with high desalination capacity in seawater. *RSC Adv.* **2019**, *9*, 14849−14858.
(938) Thu Tran, N. A.; Phuoc, N. M.; Yoon, H.; Jung, E.; Lee, Y.-W.; Kang, B.-G.; Kang, H. S.; Yoo, C.-Y.; Cho, Y. Improved Desalination Performance of Flow-and Fixed-Capacitive Deionization using Redox-Active Quinone. *ACS Sustainable Chem. Eng.* **2020**, *8*, 16701−16710.
(939) Kim, N.; Hong, S. P.; Lee, J.; Kim, C.; Yoon, J. High-desalination performance via redox couple reaction in the multi-channel capacitive deionization system. *ACS Sustainable Chem. Eng.* **2019**, *7*, 16182−16189.
(940) Dai, J.; Wang, J.; Hou, X.; Ru, Q.; He, Q.; Srimuk, P.; Presser, V.; Chen, F. Dual-Zinc Electrode Electrochemical Desalination. *ChemSusChem* **2020**, *13*, 2792.
(941) Chen, F.; Wang, J.; Feng, C.; Ma, J.; Waite, T. D. Low energy consumption and mechanism study of redox flow desalination. *Chem. Eng. J.* **2020**, *401*, 126111.
(942) Yang, S.; Choi, J.; Yeo, J.-g.; Jeon, S.-i.; Park, H.-r.; Kim, D. Flow-electrode capacitive deionization using an aqueous electrolyte with a high salt concentration. *Environ. Sci. Technol.* **2016**, *50*, 5892−5899.
(943) Ahn, J.; Kim, S.; Jeon, S.-i.; Lee, C.; Lee, J.; Yoon, J. Nafion-coated Prussian blue electrodes to enhance the stability and efficiency of battery desalination system. *Desalination* **2021**, *500*, 114778.
(944) Kim, T.; Gorski, C.; Logan, B. Low energy desalination using battery electrode deionization. *Environmental Science & Technology Letters* **2017**, *4*, 444−449.
(945) Wang, L.; Mu, C.; Li, H.; Li, F. A dual-function battery for desalination and energy storage. *Inorganic Chemistry Frontiers* **2018**, *5*, 2522−2526.
(946) Lee, J.; Lee, J.; Ahn, J.; Jo, K.; Hong, S.; Kim, C.; Lee, C.; Yoon, J. Enhancement in desalination performance of battery electrodes via improved mass transport using a multichannel flow system. *ACS Appl. Mater. Interfaces* **2019**, *11*, 36580−36588.
(947) Nam, D.-H.; Lumley, M.; Choi, K.-S. A Desalination Battery Combining $Cu_3[Fe(CN)_6]_2$as a Na-Storage Electrode and Bi as a Cl-Storage Electrode Enabling Membrane-Free Desalination. *Chem. Mater.* **2019**, *31*, 1460−1468.
(948) Kim, S.; Joo, H.; Moon, T.; Kim, S.-H.; Yoon, J. Rapid and selective lithium recovery from desalination brine using an electrochemical system. *Environ. Sci.: Proc. Impacts* **2019**, *21*, 667−676.
(949) Pasta, M.; Battistel, A.; La Mantia, F. Batteries for lithium recovery from brines. *Energy Environ. Sci.* **2012**, *5*, 9487−9491.
(950) Li, Q.; Zheng, Y.; Xiao, D.; Or, T.; Gao, R.; Li, Z.; Feng, M.; Shui, L.; Zhou, G.; Wang, X.; Chen, Z. Faradaic Electrodes Open a New Era for Capacitive Deionization. *Adv. Sci.* **2020**, *7*, 2002213.
(951) Shiiba, H.; Zettsu, N.; Nakayama, M.; Oishi, S.; Teshima, K. Defect formation energy in spinel $LiNi_0 \cdot 5Mn_1 \cdot 5O_4 - \delta$ using ab initio DFT calculations. *J. Phys. Chem. C* **2015**, *119*, 9117−9124.
(952) Lawagon, C.; Nisola, G.; Cuevas, R.; Torrejos, R.; Kim, H.; Lee, S.-P.; Chung, W.-J. $Li_{1-x}Ni_{0.5}Mn_{1.5}O_4$/Ag for electrochemical lithium recovery from brine and its optimized performance via response surface methodology. *Sep. Purif. Technol.* **2019**, *212*, 416−426.
(953) Kim, J.-S.; Lee, Y.-H.; Choi, S.; Shin, J.; Dinh, H.-C.; Choi, J. An electrochemical cell for selective lithium capture from seawater. *Environ. Sci. Technol.* **2015**, *49*, 9415−9422.
(954) Tang, W.; Liang, J.; He, D.; Gong, J.; Tang, L.; Liu, Z.; Wang, D.; Zeng, G. Various cell architectures of capacitive deionization: Recent advances and future trends. *Water research* **2019**, *150*, 225−251.
(955) Kim, N.; Lee, J.; Hong, S.; Lee, C.; Kim, C.; Yoon, J. Performance analysis of the multi-channel membrane capacitive deionization with porous carbon electrode stacks. *Desalination* **2020**, *479*, 114315.
(956) Stock, J. T.; Orna, M. V. *Electrochemistry, Past and Present*; ACS Publications, 1989; Vol. *390* DOI: 10.1021/bk-1989-0390.
(957) Zumdahl, S. S.; DeCoste, D. J. *Chemical Principles*; Nelson Education, 2012.
(958) Bard, A. J.; Faulkner, L. R. *Electrochemical Methods: Fundamentals and Applications*; John Wiley & Sons: Hoboken, NJ, 2001.
(959) Netz, R. R.; Orland, H. Beyond Poisson-Boltzmann: Fluctuation effects and correlation functions. *Eur. Phys. J. E* **2000**, *1*, 203−214.
(960) Attard, P. *Thermodynamics and Statistical Mechanics: Equilibrium by Entropy Maximisation*; Academic Press, 2002.
(961) Zhang, C. Y.; He, D.; Ma, J. X.; Tang, W. W.; Waite, T. D. Faradaic reactions in capacitive deionization (CDI) - problems and possibilities: A review. *Water Res.* **2018**, *128*, 314−330.

(962) Shukla, A.; Sampath, S.; Vijayamohanan, K. Electrochemical supercapacitors: energy storage beyond batteries. *Current Sci.* **2000**, *79*, 1656−1661.
(963) Khattak, A. M.; Ghazi, Z. A.; Liang, B.; Khan, N. A.; Iqbal, A.; Li, L.; Tang, Z. A redox-active 2D covalent organic framework with pyridine moieties capable of faradaic energy storage. *Journal of Materials Chemistry A* **2016**, *4*, 16312−16317.
(964) Armstrong, F. A.; Hill, H. A. O.; Walton, N. J. Direct electrochemistry of redox proteins. *Acc. Chem. Res.* **1988**, *21*, 407−413.
(965) Chen, P. H.; McCreery, R. L. Control of electron transfer kinetics at glassy carbon electrodes by specific surface modification. *Anal. Chem.* **1996**, *68*, 3958−3965.
(966) Drummond, T. G.; Hill, M. G.; Barton, J. K. Electrochemical DNA sensors. *Nat. Biotechnol.* **2003**, *21*, 1192−1199.
(967) Kang, X. H.; Wang, J.; Wu, H.; Aksay, I. A.; Liu, J.; Lin, Y. H. Glucose Oxidase-graphene-chitosan modified electrode for direct electrochemistry and glucose sensing. *Biosens. Bioelectron.* **2009**, *25*, 901−905.
(968) Costentin, C.; Robert, M.; Saveant, J. M. Catalysis of the electrochemical reduction of carbon dioxide. *Chem. Soc. Rev.* **2013**, *42*, 2423−2436.
(969) Solis, B. H.; Hammes-Schiffer, S. Proton-Coupled Electron Transfer in Molecular Electrocatalysis: Theoretical Methods and Design Principles. *Inorg. Chem.* **2014**, *53*, 6427−6443.
(970) Lukatskaya, M. R.; Dunn, B.; Gogotsi, Y. Multidimensional materials and device architectures for future hybrid energy storage. *Nat. Commun.* **2016**, *7*, 12647.
(971) Brousse, T.; Belanger, D.; Long, J. W. To Be or Not To Be Pseudocapacitive? *J. Electrochem. Soc.* **2015**, *162*, A5185−A5189.
(972) Gracia, R.; Mecerreyes, D. Polymers with redox properties: materials for batteries, biosensors and more. *Polym. Chem.* **2013**, *4*, 2206−2214.
(973) Lyons, M. E. Electrocatalysis using electroactive polymers, electroactive composites and microheterogeneous systems. *Analyst* **1994**, *119*, 805−826.
(974) Harris, R. D.; Auletta, J. T.; Motlagh, S. A. M.; Lawless, M. J.; Perri, N. M.; Saxena, S.; Weiland, L. M.; Waldeck, D. H.; Clark, W. W.; Meyer, T. Y. Chemical and electrochemical manipulation of mechanical properties in stimuli-responsive copper-cross-linked hydrogels. *ACS Macro Lett.* **2013**, *2*, 1095−1099.
(975) Kim, J.; Kim, J. H.; Ariga, K. Redox-active polymers for energy storage nanoarchitectonics. *Joule* **2017**, *1*, 739−768.
(976) Janoschka, T.; Martin, N.; Martin, U.; Friebe, C.; Morgenstern, S.; Hiller, H.; Hager, M. D.; Schubert, U. S. An aqueous, polymer-based redox-flow battery using non-corrosive, safe, and low-cost materials. *Nature* **2015**, *527*, 78−81.
(977) Horie, K.; Baron, M.; Fox, R. B.; He, J.; Hess, M.; Kahovec, J.; Kitayama, T.; Kubisa, P.; Marechal, E.; Mormann, W.; Stepto, R. F. T.; Tabak, D.; Vohlidal, J.; Wilks, E. S.; Work, W. J. Definitions of terms relating to reactions of polymers and to functional polymeric materials (IUPAC Recommendations 2003). *Pure Appl. Chem.* **2004**, *76*, 889−906.
(978) Heeger, A. J. Semiconducting polymers: the third generation. *Chem. Soc. Rev.* **2010**, *39*, 2354−2371.
(979) Yan, C.; Zou, L.; Short, R. Single-walled carbon nanotubes and polyaniline composites for capacitive deionization. *Desalination* **2012**, *290*, 125−129.
(980) Yan, C.; Kanaththage, Y. W.; Short, R.; Gibson, C. T.; Zou, L. Graphene/Polyaniline nanocomposite as electrode material for membrane capacitive deionization. *Desalination* **2014**, *344*, 274−279.
(981) Wang, Y.; Zhang, L.; Wu, Y.; Xu, S.; Wang, J. Polypyrrole/carbon nanotube composites as cathode material for performance enhancing of capacitive deionization technology. *Desalination* **2014**, *354*, 62−67.
(982) Gu, X.; Yang, Y.; Hu, Y.; Hu, M.; Huang, J.; Wang, C. Facile fabrication of graphene−polypyrrole−Mn composites as high-performance electrodes for capacitive deionization. *Journal of Materials Chemistry A* **2015**, *3*, 5866−5874.
(983) Zornitta, R. L.; García-Mateos, F. J.; Lado, J. J.; Rodríguez-Mirasol, J.; Cordero, T.; Hammer, P.; Ruotolo, L. A. High-performance activated carbon from polyaniline for capacitive deionization. *Carbon* **2017**, *123*, 318−333.
(984) Akhoury, A.; Bromberg, L.; Hatton, T. A. Interplay of electron hopping and bounded diffusion during charge transport in redox polymer electrodes. *J. Phys. Chem. B* **2013**, *117*, 333−342.
(985) Su, X.; Kulik, H. J.; Jamison, T. F.; Hatton, T. A. Anion-Selective Redox Electrodes: Electrochemically Mediated Separation with Heterogeneous Organometallic Interfaces. *Adv. Funct. Mater.* **2016**, *26*, 3394−3404.
(986) Bruckenstein, S.; Fensore, A. T.; Hillman, A. R. Time-resolved mono-anion, di-anion, and solvent transfers into a poly-(vinylferrocene)-modified electrode. *J. Electrochem. Soc.* **1998**, *145*, L24−L26.
(987) Jureviciute, I.; Bruckenstein, S.; Hillman, A. R. Counter-ion specific effects on charge and solvent trapping in poly(vinylferrocene) films. *J. Electroanal. Chem.* **2000**, *488*, 73−81.
(988) Schiavon, G.; Zotti, G.; Comisso, N.; Berlin, A.; Pagani, G. Ion exchange in the electrochemical switching of polypyrroles in acetonitrile by the electrochemical quartz crystal microbalance. Electrolyte incorporation by hydrogen bonding of anions to pyrrole. *J. Phys. Chem.* **1994**, *98*, 4861−4864.
(989) Arca, M.; Mirkin, M. V.; Bard, A. J. Polymer films on electrodes. 26. Study of ion transport and electron transfer at polypyrrole films by scanning electrochemical microscopy. *J. Phys. Chem.* **1995**, *99*, 5040−5050.
(990) Beer, P. D.; Gale, P. A.; Chen, G. Z. Mechanisms of electrochemical recognition of cations, anions and neutral guest species by redox-active receptor molecules. *Coord. Chem. Rev.* **1999**, *185−186*, 3−36.
(991) Beer, P. D.; Gale, P. A. Anion recognition and sensing: The state of the art and future perspectives. *Angew. Chem., Int. Ed.* **2001**, *40*, 486−516.
(992) Tan, K.-J.; Su, X.; Hatton, T. A. An Asymmetric Iron-Based Redox-Active System for Electrochemical Separation of Ions in Aqueous Media. *Adv. Funct. Mater.* **2020**, *30*, 1910363.
(993) Pickup, P. G. Conjugated metallopolymers. Redox polymers with interacting metal based redox sites. *J. Mater. Chem.* **1999**, *9*, 1641−1653.
(994) Ramanavičius, A.; Ramanavičienė, A.; Malinauskas, A. Electrochemical sensors based on conducting polymer—polypyrrole. *Electrochimica acta* **2006**, *51*, 6025−6037.
(995) Lange, U.; Roznyatovskaya, N. V.; Mirsky, V. M. Conducting polymers in chemical sensors and arrays. *Analytica chimica acta* **2008**, *614*, 1−26.
(996) Pan, L.; Yu, G.; Zhai, D.; Lee, H. R.; Zhao, W.; Liu, N.; Wang, H.; Tee, B. C.-K.; Shi, Y.; Cui, Y.; Bao, Z. Hierarchical nanostructured conducting polymer hydrogel with high electrochemical activity. *Proc. Natl. Acad. Sci. U. S. A.* **2012**, *109*, 9287−9292.
(997) Espenscheid, M. W.; Ghatakroy, A. R.; Moore, R. B.; Penner, R. M.; Szentirmay, M. N.; Martin, C. R. Sensors from polymer modified electrodes. *Journal of the Chemical Society-Faraday Transactions I* **1986**, *82*, 1051−1070.
(998) Toniolo, R.; Comisso, N.; Bontempelli, G.; Schiavon, G. Potential Shifts at Electrodes Coated with Ion-Exchange Polymeric Films. *Talanta* **1994**, *41*, 473−478.
(999) Ugo, P.; Moretto, L. M. Ion-exchange voltammetry at polymer-coated electrodes: Principles and analytical prospects. *Electroanalysis* **1995**, *7*, 1105−1113.
(1000) Espenscheid, M. W.; Martin, C. R. Electroactive ion-exchange polymers. *J. Electroanal. Chem. Interfacial Chem.* **1985**, *188*, 73−84.
(1001) Martin, C. R.; Espenscheid, M. W.; Ghatakroy, A. R. The electrochemistry of electroactive ionomers. *J. Electrochem. Soc.* **1986**, *133*, C128.
(1002) Kang, E. T.; Neoh, K. G.; Tan, K. L. Polyaniline: A polymer with many interesting intrinsic redox states. *Prog. Polym. Sci.* **1998**, *23*, 277−324.

https://doi.org/10.1021/acs.chemrev.1c00396
Chem. Rev. 2022, 122, 13547−13635

(1003) Lin, Y. H.; Cui, X. L.; Bontha, J. Electrically controlled anion exchange based on polypyrrole and carbon nanotubes nanocomposite for perchlorate removal. *Environ. Sci. Technol.* **2006**, *40*, 4004−4009.
(1004) Anson, F. C.; Ohsaka, T.; Saveant, J. M. Kinetics of Electron-Transfer Cross-Reactions within Redox Polymers - Coatings of a Protonated Polylysine Co-Polymer with Incorporated Electroactive Anions. *J. Am. Chem. Soc.* **1983**, *105*, 4883−4890.
(1005) Watanabe, M.; Longmire, M. L.; Murray, R. W. A study of ferrocene diffusion dynamics in network poly (ethylene oxide) polymer electrolyte by solid-state voltammetry. *J. Phys. Chem.* **1990**, *94*, 2614−2619.
(1006) Hillman, A. R.; Hughes, N. A.; Bruckenstein, S. Solvation phenomena in polyvinylferrocene films - effect of history and redox state. *J. Electrochem. Soc.* **1992**, *139*, 74−77.
(1007) Bruce, J. A.; Wrighton, M. S. Electrostatic Binding of Electroactive and Non-Electroactive Anions in a Surface-Confined, Electroactive Polymer - Selectivity of Binding Measured by Auger-Spectroscopy and Cyclic Voltammetry. *J. Am. Chem. Soc.* **1982**, *104*, 74−82.
(1008) Martin, C. R.; Rubinstein, I.; Bard, A. J. Polymer films on electrodes. 9. Electron and mass transfer in Nafion films containing tris (2, 2'-bipyridine) ruthenium (2+). *J. Am. Chem. Soc.* **1982**, *104*, 4817−4824.
(1009) Shi, M. L.; Anson, F. C. High sensitivity of electron transfer rates within nafion coatings saturated with Os(bpy)(3)(2+) to the extent of hydration of the coating. *J. Electrochem. Soc.* **1995**, *142*, 4205−4214.
(1010) Hardy, C. G.; Zhang, J.; Yan, Y.; Ren, L.; Tang, C. Metallopolymers with transition metals in the side-chain by living and controlled polymerization techniques. *Prog. Polym. Sci.* **2014**, *39*, 1742−1796.
(1011) Gallei, M.; Elbert, J. *Functional Metallosupramolecular Materials*; Royal Society of Chemistry, 2015; pp 120−148.
(1012) Gallei, M.; Rüttiger, C. Recent Trends in Metallopolymer Design: Redox-Controlled Surfaces, Porous Membranes, and Switchable Optical Materials Using Ferrocene-Containing Polymers. *Chem.−Eur. J.* **2018**, *24*, 10006−10021.
(1013) Mao, X.; Rutledge, G. C.; Hatton, T. A. Polyvinylferrocene for noncovalent dispersion and redox-controlled precipitation of carbon nanotubes in nonaqueous media. *Langmuir* **2013**, *29*, 9626−9634.
(1014) Mao, X.; Simeon, F.; Achilleos, D. S.; Rutledge, G. C.; Hatton, T. A. Metallocene/carbon hybrids prepared by a solution process for supercapacitor applications. *Journal of Materials Chemistry A* **2013**, *1*, 13120−13127.
(1015) Ju, H.; Leech, D. Electrochemistry of poly(vinylferrocene) formed by direct electrochemical reduction at a glassy carbon electrode. *Journal of the Chemical Society, Faraday Transactions* **1997**, *93*, 1371−1375.
(1016) Achilleos, D. S.; Hatton, T. A. Selective molecularly mediated pseudocapacitive separation of ionic species in solution. *ACS Appl. Mater. Interfaces* **2016**, *8*, 32743−32753.
(1017) Fotopoulou, K. N.; Karapanagioti, H. K. Surface properties of beached plastic pellets. *Marine environmental research* **2012**, *81*, 70−77.
(1018) Galloway, T. S.; Cole, M.; Lewis, C. Interactions of microplastic debris throughout the marine ecosystem. *Nat. Ecol. Evol.* **2017**, *1*, 0116.
(1019) Alsbaiee, A.; Smith, B. J.; Xiao, L.; Ling, Y.; Helbling, D. E.; Dichtel, W. R. Rapid removal of organic micropollutants from water by a porous β-cyclodextrin polymer. *nature* **2016**, *529*, 190−194.
(1020) Clara, M.; Strenn, B.; Gans, O.; Martinez, E.; Kreuzinger, N.; Kroiss, H. Removal of selected pharmaceuticals, fragrances and endocrine disrupting compounds in a membrane bioreactor and conventional wastewater treatment plants. *Water research* **2005**, *39*, 4797−4807.
(1021) Su, X.; Kushima, A.; Halliday, C.; Zhou, J.; Li, J.; Hatton, T. A. Electrochemically-mediated selective capture of heavy metal chromium and arsenic oxyanions from water. *Nat. Commun.* **2018**, *9*, 4701.
(1022) Hemmatifar, A.; Ozbek, N.; Halliday, C.; Hatton, T. A. Electrochemical selective recovery of heavy metal vanadium oxyanion from continuously flowing aqueous streams. *ChemSusChem* **2020**, *13*, 3865−3874.
(1023) Dimos, V.; Haralambous, K.; Malamis, S. A review on the recent studies for chromium species adsorption on raw and modified natural minerals. *Critical reviews in environmental science and technology* **2012**, *42*, 1977−2016.
(1024) Skowron, J.; Konieczko, K. Occupational exposure to chromium (VI) compounds. *Medycyna Pracy* **2015**, *66*, 407−427.
(1025) Pawełczyk, A.; Božek, F.; Grabas, K. Impact of military metallurgical plant wastes on the population's health risk. *Chemosphere* **2016**, *152*, 513−519.
(1026) Whittell, G. R.; Manners, I. Metallopolymers: New multifunctional materials. *Adv. Mater.* **2007**, *19*, 3439−3468.
(1027) Vorotyntsev, M. A.; Vasilyeva, S. V. Metallocene-containing conjugated polymers. *Adv. Colloid Interface Sci.* **2008**, *139*, 97−149.
(1028) Kim, K.; Baldaguez Medina, P.; Elbert, J.; Kayiwa, E.; Cusick, R. D.; Men, Y.; Su, X. Molecular Tuning of Redox-Copolymers for Selective Electrochemical Remediation. *Adv. Funct. Mater.* **2020**, *30*, 2004635.
(1029) Escher, B. I.; Fenner, K. Recent advances in environmental risk assessment of transformation products. *Environ. Sci. Technol.* **2011**, *45*, 3835−3847.
(1030) Thomaidi, V. S.; Stasinakis, A. S.; Borova, V. L.; Thomaidis, N. S. Is there a risk for the aquatic environment due to the existence of emerging organic contaminants in treated domestic wastewater? Greece as a case-study. *Journal of hazardous materials* **2015**, *283*, 740−747.
(1031) Tijani, J. O.; Fatoba, O. O.; Babajide, O. O.; Petrik, L. F. Pharmaceuticals, endocrine disruptors, personal care products, nanomaterials and perfluorinated pollutants: a review. *Environmental chemistry letters* **2016**, *14*, 27−49.
(1032) Xu, Y.; Liu, T.; Zhang, Y.; Ge, F.; Steel, R. M.; Sun, L. Advances in technologies for pharmaceuticals and personal care products removal. *Journal of materials chemistry A* **2017**, *5*, 12001−12014.
(1033) Alexander, J. T.; Hai, F. I.; Al-aboud, T. M. Chemical coagulation-based processes for trace organic contaminant removal: Current state and future potential. *Journal of environmental management* **2012**, *111*, 195−207.
(1034) Benner, J.; Helbling, D. E.; Kohler, H.-P. E.; Wittebol, J.; Kaiser, E.; Prasse, C.; Ternes, T. A.; Albers, C. N.; Aamand, J.; Horemans, B.; Springael, D.; Walravens, E.; Boon, N. Is biological treatment a viable alternative for micropollutant removal in drinking water treatment processes? *Water Res.* **2013**, *47*, 5955−5976.
(1035) Besha, A. T.; Gebreyohannes, A. Y.; Tufa, R. A.; Bekele, D. N.; Curcio, E.; Giorno, L. Removal of emerging micropollutants by activated sludge process and membrane bioreactors and the effects of micropollutants on membrane fouling: A review. *Journal of environmental chemical engineering* **2017**, *5*, 2395−2414.
(1036) Akhoury, A.; Bromberg, L.; Hatton, T. A. Redox-responsive gels with tunable hydrophobicity for controlled solubilization and release of organics. *ACS Appl. Mater. Interfaces* **2011**, *3*, 1167−1174.
(1037) Tian, W.; Mao, X.; Brown, P.; Rutledge, G. C.; Hatton, T. A. Electrochemically nanostructured polyvinylferrocene/polypyrrole hybrids with synergy for energy storage. *Adv. Funct. Mater.* **2015**, *25*, 4803−4813.
(1038) Shapira, B.; Avraham, E.; Aurbach, D. Side reactions in capacitive deionization (CDI) processes: the role of oxygen reduction. *Electrochim. Acta* **2016**, *220*, 285−295.
(1039) Omosebi, A.; Gao, X.; Landon, J.; Liu, K. Asymmetric electrode configuration for enhanced membrane capacitive deionization. *ACS Appl. Mater. Interfaces* **2014**, *6*, 12640−12649.
(1040) Gao, X.; Landon, J.; Neathery, J. K.; Liu, K. Modification of carbon xerogel electrodes for more efficient asymmetric capacitive deionization. *J. Electrochem. Soc.* **2013**, *160*, E106−E112.

https://doi.org/10.1021/acs.chemrev.1c00396
Chem. Rev. 2022, 122, 13547−13635

(1041) Jo, H.; Kim, K. H.; Jung, M.-J.; Park, J. H.; Lee, Y.-S. Fluorination effect of activated carbons on performance of asymmetric capacitive deionization. *Appl. Surf. Sci.* **2017**, *409*, 117−123.
(1042) Li, H.; Yu, M.; Wang, F.; Liu, P.; Liang, Y.; Xiao, J.; Wang, C.; Tong, Y.; Yang, G. Amorphous nickel hydroxide nanospheres with ultrahigh capacitance and energy density as electrochemical pseudocapacitor materials. *Nat. Commun.* **2013**, *4*, 1894.
(1043) Liu, B.; Kong, D.; Zhang, J.; Wang, Y.; Chen, T.; Cheng, C.; Yang, H. Y. 3D hierarchical Co_3O_4 @ Co_3S_4 nanoarrays as cathode materials for asymmetric pseudocapacitors. *Journal of Materials Chemistry A* **2016**, *4*, 3287−3296.
(1044) Boota, M.; Gogotsi, Y. MXene—conducting polymer asymmetric pseudocapacitors. *Adv. Energy Mater.* **2019**, *9*, 1802917.
(1045) Amatucci, G. G.; Badway, F.; Du Pasquier, A.; Zheng, T. An asymmetric hybrid nonaqueous energy storage cell. *J. Electrochem. Soc.* **2001**, *148*, A930−A939.
(1046) Qu, Q.; Zhang, P.; Wang, B.; Chen, Y.; Tian, S.; Wu, Y.; Holze, R. Electrochemical performance of MnO2 nanorods in neutral aqueous electrolytes as a cathode for asymmetric supercapacitors. *J. Phys. Chem. C* **2009**, *113*, 14020−14027.
(1047) Wang, Y.; Song, Y.; Xia, Y. Electrochemical capacitors: mechanism, materials, systems, characterization and applications. *Chem. Soc. Rev.* **2016**, *45*, 5925−5950.
(1048) Ruttiger, C.; Pfeifer, V.; Rittscher, V.; Stock, D.; Scheid, D.; Vowinkel, S.; Roth, F.; Didzoleit, H.; Stuhn, B.; Elbert, J.; Ionescu, E.; Gallei, M. One for all: cobalt-containing polymethacrylates for magnetic ceramics, block copolymerization, unexpected electrochemistry, and stimuli-responsiveness. *Polym. Chem.* **2016**, *7*, 1129−1137.
(1049) Shaw, W. D.; Walker, M.; Benson, M. Treating and drinking well water in the presence of health risks from arsenic contamination: results from a US hot spot. *Risk Analysis: An International Journal* **2005**, *25*, 1531−1543.
(1050) Pokhrel, D.; Bhandari, B.; Viraraghavan, T. Arsenic contamination of groundwater in the Terai region of Nepal: an overview of health concerns and treatment options. *Environ. Int.* **2009**, *35*, 157−161.
(1051) Camacho, L. M.; Gutiérrez, M.; Alarcón-Herrera, M. T.; Villalba, M.d L.; Deng, S. Occurrence and treatment of arsenic in groundwater and soil in northern Mexico and southwestern USA. *Chemosphere* **2011**, *83*, 211−225.
(1052) *Arsenic in Drinking Water: Background Document for Development of WHO Guidelines for Drinking Water Quality*; World Health Organization, 2011.
(1053) Song, Z.; Garg, S.; Ma, J.; Waite, T. D. Selective Arsenic Removal from Groundwaters Using Redox-Active Polyvinylferrocene-Functionalized Electrodes: Role of Oxygen. *Environ. Sci. Technol.* **2020**, *54*, 12081−12091.
(1054) Ren, Y.; Lin, Z.; Mao, X.; Tian, W.; Van Voorhis, T.; Hatton, T. A. Superhydrophobic, Surfactant-doped, Conducting Polymers for Electrochemically Reversible Adsorption of Organic Contaminants. *Adv. Funct. Mater.* **2018**, *28*, 1801466.
(1055) He, F.; Hemmatifar, A.; Bazant, M. Z.; Hatton, T. A. Selective adsorption of organic anions in a flow cell with asymmetric redox active electrodes. *Water Res.* **2020**, *182*, 115963.
(1056) Fan, H. *Theoretical and experimental study of electrochemically mediated adsorption processes*. Ph.D. Thesis. Massachusetts Institute of Technology, 2019.
(1057) Loeb, S.; Van Hessen, F.; Levi, J.; Ventura, M. The osmotic power plant. In *11th Intersociety Energy Conversion Engineering Conference*. 1976; pp 51−57.
(1058) Loeb, S. One hundred and thirty benign and renewable megawatts from Great Salt Lake? The possibilities of hydroelectric power by pressure-retarded osmosis. *Desalination* **2001**, *141*, 85−91.
(1059) Achilli, A.; Childress, A. E. Pressure retarded osmosis: from the vision of Sidney Loeb to the first prototype installation. *Desalination* **2010**, *261*, 205−211.
(1060) Logan, B. E.; Elimelech, M. Membrane-based processes for sustainable power generation using water. *Nature* **2012**, *488*, 313−319.
(1061) Helfer, F.; Lemckert, C.; Anissimov, Y. G. Osmotic power with pressure retarded osmosis: theory, performance and trends−a review. *J. Membr. Sci.* **2014**, *453*, 337−358.
(1062) Chung, T.-S.; Wan, C. F. *Membrane Technology for Osmotic Power Generation by Pressure Retarded Osmosis*; CRC Press, 2020.
(1063) Weinstein, J. N.; Leitz, F. B. Electric power from differences in salinity: the dialytic battery. *Science* **1976**, *191*, 557−559.
(1064) Yasukawa, M.; Suzuki, T.; Higa, M. *Membrane-Based Salinity Gradient Processes for Water Treatment and Power Generation*; Elsevier, 2018; pp 3−56.
(1065) Turek, M.; Bandura, B. Renewable energy by reverse electrodialysis. *Desalination* **2007**, *205*, 67−74.
(1066) Post, J. W.; Hamelers, H. V.; Buisman, C. J. Energy recovery from controlled mixing salt and fresh water with a reverse electrodialysis system. *Environ. Sci. Technol.* **2008**, *42*, 5785−5790.
(1067) Norman, R. S. Water salination: a source of energy. *Science* **1974**, *186*, 350−352.
(1068) Wick, G. L.; Schmitt, W. R. Prospects for renewable energy from the sea. *Mar. Technol. Soc. J.* **1977**, *11*, 16−21.
(1069) Forgacs, C. Recent developments in the utilization of salinity power. *Desalination* **1982**, *40*, 191−195.
(1070) Audinos, R. Electric power produced from two solutions of unequal salinity by reverse electrodialysis. *Indian J. Chem.* **1992**, *31A*, 348−354.
(1071) Jagur-Grodzinski, J.; Kramer, R. Novel process for direct conversion of free energy of mixing into electric power. *Industrial & Engineering Chemistry Process Design and Development* **1986**, *25*, 443−449.
(1072) Długołęcki, P.; Nymeijer, K.; Metz, S.; Wessling, M. Current status of ion exchange membranes for power generation from salinity gradients. *J. Membr. Sci.* **2008**, *319*, 214−222.
(1073) Veerman, J.; Saakes, M.; Metz, S. J.; Harmsen, G. Reverse electrodialysis: evaluation of suitable electrode systems. *J. Appl. Electrochem.* **2010**, *40*, 1461−1474.
(1074) Scialdone, O.; Guarisco, C.; Grispo, S.; D'Angelo, A.; Galia, A. Investigation of electrode material−redox couple systems for reverse electrodialysis processes. Part I: Iron redox couples. *J. Electroanal. Chem.* **2012**, *681*, 66−75.
(1075) Scialdone, O.; Albanese, A.; D'Angelo, A.; Galia, A.; Guarisco, C. Investigation of electrode material−redox couple systems for reverse electrodialysis processes. Part II: Experiments in a stack with 10−50 cell pairs. *Journal of electroanalytical chemistry* **2013**, *704*, 1−9.
(1076) Mei, Y.; Tang, C. Y. Recent developments and future perspectives of reverse electrodialysis technology: A review. *Desalination* **2018**, *425*, 156−174.
(1077) Veerman, J.; Post, J.; Saakes, M.; Metz, S.; Harmsen, G. Reducing power losses caused by ionic shortcut currents in reverse electrodialysis stacks by a validated model. *J. Membr. Sci.* **2008**, *310*, 418−430.
(1078) Lacey, R. Energy by reverse electrodialysis. *Ocean engineering* **1980**, *7*, 1−47.
(1079) Post, J. W.; Veerman, J.; Hamelers, H. V.; Euverink, G. J.; Metz, S. J.; Nymeijer, K.; Buisman, C. J. Salinity-gradient power: Evaluation of pressure-retarded osmosis and reverse electrodialysis. *Journal of membrane science* **2007**, *288*, 218−230.
(1080) Długołęcki, P.; Gambier, A.; Nijmeijer, K.; Wessling, M. Practical potential of reverse electrodialysis as process for sustainable energy generation. *Environ. Sci. Technol.* **2009**, *43*, 6888−6894.
(1081) Moreno, J.; Grasman, S.; Van Engelen, R.; Nijmeijer, K. Upscaling reverse electrodialysis. *Environ. Sci. Technol.* **2018**, *52*, 10856−10863.
(1082) Burheim, O. S.; Seland, F.; Pharoah, J. G.; Kjelstrup, S. Improved electrode systems for reverse electro-dialysis and electro-dialysis. *Desalination* **2012**, *285*, 147−152.

https://doi.org/10.1021/acs.chemrev.1c00396
Chem. Rev. 2022, 122, 13547−13635

(1083) Wen, T.; Solt, G.; Sun, Y. Spirally wound electrodialysis (SpED) modules. *Desalination* **1995**, *101*, 79−91.
(1084) Wright, N. C.; Winter, A. G. Design of spiral-wound electrodialysis modules. *Desalination* **2019**, *458*, 54−65.
(1085) Vermaas, D. A.; Saakes, M.; Nijmeijer, K. Power generation using profiled membranes in reverse electrodialysis. *Journal of membrane science* **2011**, *385*, 234−242.
(1086) Hong, J. G.; Chen, Y. Evaluation of electrochemical properties and reverse electrodialysis performance for porous cation exchange membranes with sulfate-functionalized iron oxide. *J. Membrane Sci.* **2015**, *473*, 210−217.
(1087) Gurreri, L.; Ciofalo, M.; Cipollina, A.; Tamburini, A.; Van Baak, W.; Micale, G. CFD modelling of profiled-membrane channels for reverse electrodialysis. *Desalination and water treatment* **2015**, *55*, 3404−3423.
(1088) Altıok, E.; Kaya, T. Z.; Güler, E.; Kabay, N.; Bryjak, M. Performance of Reverse Electrodialysis System for Salinity Gradient Energy Generation by Using a Commercial Ion Exchange Membrane Pair with Homogeneous Bulk Structure. *Water* **2021**, *13*, 814.
(1089) He, Z.; Gao, X.; Zhang, Y.; Wang, Y.; Wang, J. Revised spacer design to improve hydrodynamics and anti-fouling behavior in reverse electrodialysis processes. *Desalination and Water Treatment* **2016**, *57*, 28176−28186.
(1090) Lee, S.-Y.; Jeong, Y.-J.; Chae, S.-R.; Yeon, K.-H.; Lee, Y.; Kim, C.-S.; Jeong, N.-J.; Park, J.-S. Porous carbon-coated graphite electrodes for energy production from salinity gradient using reverse electrodialysis. *J. Phys. Chem. Solids* **2016**, *91*, 34−40.
(1091) Zhu, X.; He, W.; Logan, B. E. Influence of solution concentration and salt types on the performance of reverse electrodialysis cells. *Journal of membrane science* **2015**, *494*, 154−160.
(1092) Tedesco, M.; Brauns, E.; Cipollina, A.; Micale, G.; Modica, P.; Russo, G.; Helsen, J. Reverse electrodialysis with saline waters and concentrated brines: a laboratory investigation towards technology scale-up. *J. Membr. Sci.* **2015**, *492*, 9−20.
(1093) Winzeler, H. B.; Belfort, G. Enhanced performance for pressure-driven membrane processes: the argument for fluid instabilities. *J. Membr. Sci.* **1993**, *80*, 35−47.
(1094) Vaselbehagh, M.; Karkhanechi, H.; Takagi, R.; Matsuyama, H. Biofouling phenomena on anion exchange membranes under the reverse electrodialysis process. *J. Membr. Sci.* **2017**, *530*, 232−239.
(1095) Rijnaarts, T.; Moreno, J.; Saakes, M.; de Vos, W.; Nijmeijer, K. Role of anion exchange membrane fouling in reverse electrodialysis using natural feed waters. *Colloids and surfaces A: Physicochemical and engineering aspects* **2019**, *560*, 198−204.
(1096) Bodner, E.; Saakes, M.; Sleutels, T.; Buisman, C.; Hamelers, H. The RED Fouling Monitor: A novel tool for fouling analysis. *Journal of membrane science* **2019**, *570*, 294−302.
(1097) Luo, X.; Cao, X.; Mo, Y.; Xiao, K.; Zhang, X.; Liang, P.; Huang, X. Power generation by coupling reverse electrodialysis and ammonium bicarbonate: Implication for recovery of waste heat. *Electrochemistry communications* **2012**, *19*, 25−28.
(1098) Kim, Y.; Logan, B. E. Hydrogen production from inexhaustible supplies of fresh and salt water using microbial reverse-electrodialysis electrolysis cells. *Proc. Natl. Acad. Sci. U. S. A.* **2011**, *108*, 16176−16181.
(1099) Li, W.; Krantz, W. B.; Cornelissen, E. R.; Post, J. W.; Verliefde, A. R.; Tang, C. Y. A novel hybrid process of reverse electrodialysis and reverse osmosis for low energy seawater desalination and brine management. *Applied energy* **2013**, *104*, 592−602.
(1100) Cusick, R. D.; Kim, Y.; Logan, B. E. Energy capture from thermolytic solutions in microbial reverse-electrodialysis cells. *Science* **2012**, *335*, 1474−1477.
(1101) Chen, Q.; Liu, Y.-Y.; Xue, C.; Yang, Y.-L.; Zhang, W.-M. Energy self-sufficient desalination stack as a potential fresh water supply on small islands. *Desalination* **2015**, *359*, 52−58.
(1102) Wang, Q.; Gao, X.; Zhang, Y.; He, Z.; Ji, Z.; Wang, X.; Gao, C. Hybrid RED/ED system: Simultaneous osmotic energy recovery and desalination of high-salinity wastewater. *Desalination* **2017**, *405*, 59−67.
(1103) Van Egmond, W.; Saakes, M.; Porada, S.; Meuwissen, T.; Buisman, C.; Hamelers, H. The concentration gradient flow battery as electricity storage system: Technology potential and energy dissipation. *J. Power Sources* **2016**, *325*, 129−139.
(1104) Tufa, R. A.; Pawlowski, S.; Veerman, J.; Bouzek, K.; Fontananova, E.; di Profio, G.; Velizarov, S.; Goulão Crespo, J.; Nijmeijer, K.; Curcio, E. Progress and prospects in reverse electrodialysis for salinity gradient energy conversion and storage. *Appl. Energy* **2018**, *225*, 290−331.
(1105) Guo, W.; Cao, L.; Xia, J.; Nie, F.-Q.; Ma, W.; Xue, J.; Song, Y.; Zhu, D.; Wang, Y.; Jiang, L. Energy harvesting with single-ion-selective nanopores: a concentration-gradient-driven nanofluidic power source. *Adv. Funct. Mater.* **2010**, *20*, 1339−1344.
(1106) Cao, L.; Guo, W.; Ma, W.; Wang, L.; Xia, F.; Wang, S.; Wang, Y.; Jiang, L.; Zhu, D. Towards understanding the nanofluidic reverse electrodialysis system: well matched charge selectivity and ionic composition. *Energy Environ. Sci.* **2011**, *4*, 2259−2266.
(1107) Tedesco, M.; Scalici, C.; Vaccari, D.; Cipollina, A.; Tamburini, A.; Micale, G. Performance of the first reverse electrodialysis pilot plant for power production from saline waters and concentrated brines. *J. Membr. Sci.* **2016**, *500*, 33−45.
(1108) Tedesco, M.; Cipollina, A.; Tamburini, A.; Micale, G. Towards 1 kW power production in a reverse electrodialysis pilot plant with saline waters and concentrated brines. *J. Membr. Sci.* **2017**, *522*, 226−236.
(1109) Farrell, E.; Hassan, M. I.; Tufa, R. A.; Tuomiranta, A.; Avci, A. H.; Politano, A.; Curcio, E.; Arafat, H. A. Reverse electrodialysis powered greenhouse concept for water-and energy-self-sufficient agriculture. *Applied Energy* **2017**, *187*, 390−409.
(1110) Tamburini, A.; Tedesco, M.; Cipollina, A.; Micale, G.; Ciofalo, M.; Papapetrou, M.; Van Baak, W.; Piacentino, A. Reverse electrodialysis heat engine for sustainable power production. *Applied Energy* **2017**, *206*, 1334−1353.
(1111) Osterle, J. F. Electrokinetic Energy Conversion. *Journal of Applied Mechanics* **1964**, *31*, 161−164.
(1112) Morrison, F., Jr; Osterle, J. Electrokinetic energy conversion in ultrafine capillaries. *J. Chem. Phys.* **1965**, *43*, 2111−2115.
(1113) Yang, J.; Lu, F.; Kostiuk, L. W.; Kwok, D. Y. Electrokinetic microchannel battery by means of electrokinetic and microfluidic phenomena. *Journal of Micromechanics and Microengineering* **2003**, *13*, 963.
(1114) van der Heyden, F. H.; Stein, D.; Dekker, C. Streaming currents in a single nanofluidic channel. *Physical review letters* **2005**, *95*, 116104.
(1115) Van der Heyden, F. H.; Bonthuis, D. J.; Stein, D.; Meyer, C.; Dekker, C. Electrokinetic energy conversion efficiency in nanofluidic channels. *Nano Lett.* **2006**, *6*, 2232−2237.
(1116) van der Heyden, F. H.; Bonthuis, D. J.; Stein, D.; Meyer, C.; Dekker, C. Power generation by pressure-driven transport of ions in nanofluidic channels. *Nano Lett.* **2007**, *7*, 1022−1025.
(1117) Bocquet, L.; Charlaix, E. Nanofluidics, from bulk to interfaces. *Chem. Soc. Rev.* **2010**, *39*, 1073−1095.
(1118) Davidson, C.; Xuan, X. Effects of Stern layer conductance on electrokinetic energy conversion in nanofluidic channels. *Electrophoresis* **2008**, *29*, 1125−1130.
(1119) Zhang, J.; Zhan, K.; Wang, S.; Hou, X. Soft interface design for electrokinetic energy conversion. *Soft Matter* **2020**, *16*, 2915−2927.
(1120) Xiao, K.; Jiang, L.; Antonietti, M. Ion transport in nanofluidic devices for energy harvesting. *Joule* **2019**, *3*, 2364−2380.
(1121) Joly, L.; Ybert, C.; Trizac, E.; Bocquet, L. Hydrodynamics within the electric double layer on slipping surfaces. *Physical review letters* **2004**, *93*, 257805.
(1122) Joly, L.; Ybert, C.; Trizac, E.; Bocquet, L. Liquid friction on charged surfaces: From hydrodynamic slippage to electrokinetics. *J. Chem. Phys.* **2006**, *125*, 204716.

https://doi.org/10.1021/acs.chemrev.1c00396
Chem. Rev. 2022, 122, 13547−13635

(1123) Silkina, E. F.; Asmolov, E. S.; Vinogradova, O. I. Electro-osmotic flow in hydrophobic nanochannels. *Phys. Chem. Chem. Phys.* **2019**, *21*, 23036−23043.
(1124) Ren, Y.; Stein, D. Slip-enhanced electrokinetic energy conversion in nanofluidic channels. *Nanotechnology* **2008**, *19*, 195707.
(1125) Bahga, S. S.; Vinogradova, O. I.; Bazant, M. Z. Anisotropic electro-osmotic flow over super-hydrophobic surfaces. *Journal of fluid mechanics* **2010**, *644*, 245−255.
(1126) Belyaev, A. V.; Vinogradova, O. I. Electro-osmosis on anisotropic superhydrophobic surfaces. *Physical review letters* **2011**, *107*, 098301.
(1127) Fan, B.; Bandaru, P. Tensorial Modulation of Electrokinetic Streaming Potentials on Air and Liquid Filled Surfaces. *Langmuir* **2019**, *35*, 14812−14817.
(1128) Vinogradova, O. I.; Silkina, E. F.; Bag, N.; Asmolov, E. S. Achieving large zeta-potentials with charged porous surfaces. *Phys. Fluids* **2020**, *32*, 102105.
(1129) Mugele, F.; Baret, J.-C. Electrowetting: from basics to applications. *J. Phys.: Condens. Matter* **2005**, *17*, R705.
(1130) Mugele, F.; Heikenfeld, J. *Electrowetting: Fundamental Principles and Practical Applications*; John Wiley & Sons, 2018.
(1131) Krupenkin, T.; Taylor, J. A. Reverse electrowetting as a new approach to high-power energy harvesting. *Nat. Commun.* **2011**, *2*, 448.
(1132) Kolomeisky, A. B.; Kornyshev, A. A. Current-generating 'double layer shoe' with a porous sole. *J. Phys.: Condens. Matter* **2016**, *28*, 464009.
(1133) Haimov, E.; Chapman, A.; Bresme, F.; Holmes, A. S.; Reddyhoff, T.; Urbakh, M.; Kornyshev, A. A. Theoretical demonstration of a capacitive rotor for generation of alternating current from mechanical motion. *Nat. Commun.* **2021**, *12*, 3678.
(1134) Brogioli, D. Extracting renewable energy from a salinity difference using a capacitor. *Physical review letters* **2009**, *103*, 058501.
(1135) Aricò, A.; Bruce, P.; Scrosati, B.; Tarascon, J.; van Schalkwijk, W. Nanostructured materials for advanced energy conversion and storage devices. *Nature materials* **2005**, *4*, 366−377.
(1136) Simon, P.; Gogotsi, Y. *Nanoscience and Technology: A Collection of Reviews from Nature Journals*; World Scientific, 2010; pp 320−329.
(1137) Hunter, R. J. *Introduction to Modern Colloid Science*; Oxford University Press: Oxford, UK, 1993; Vol. 7.
(1138) Brogioli, D.; Zhao, R.; Biesheuvel, P. A prototype cell for extracting energy from a water salinity difference by means of double layer expansion in nanoporous carbon electrodes. *Energy Environ. Sci.* **2011**, *4*, 772−777.
(1139) Rica, R. A.; Brogioli, D.; Ziano, R.; Salerno, D.; Mantegazza, F. Ions transport and adsorption mechanisms in porous electrodes during capacitive-mixing double layer expansion (CDLE). *J. Phys. Chem. C* **2012**, *116*, 16934−16938.
(1140) Rica, R. A.; Ziano, R.; Salerno, D.; Mantegazza, F.; Bazant, M. Z.; Brogioli, D. Electro-diffusion of ions in porous electrodes for capacitive extraction of renewable energy from salinity differences. *Electrochim. Acta* **2013**, *92*, 304−314.
(1141) Brogioli, D.; La Mantia, F. *Interface Science and Technology*; Elsevier, 2018; Vol. *24*; pp 87−117.
(1142) Sales, B.; Saakes, M.; Post, J.; Buisman, C.; Biesheuvel, P.; Hamelers, H. Direct power production from a water salinity difference in a membrane-modified supercapacitor flow cell. *Environ. Sci. Technol.* **2010**, *44*, 5661−5665.
(1143) Burheim, O.; Sales, B.; Schaezle, O.; Liu, F.; Hamelers, H. Auto generative capacitive mixing of sea and river water by the use of membranes. *ASME 2011 International Mechanical Engineering Congress and Exposition (IMECE2011), Denver, CO*, 2011; pp 483−492.
(1144) Sales, B. B.; Liu, F.; Schaetzle, O.; Buisman, C. J.; Hamelers, H. V. Electrochemical characterization of a supercapacitor flow cell for power production from salinity gradients. *Electrochimica acta* **2012**, *86*, 298−304.
(1145) Burheim, O.; Sales, B.; Schaetzle, O.; Liu, F.; Hamelers, H. Auto generative capacitive mixing for power conversion of sea and river water by the use of membranes. *J. Energy Resour. Technol.* **2013**, *135*, 011601.
(1146) Smolinska-Kempisty, K.; Siekierka, A.; Bryjak, M. Interpolymer ion exchange membranes for CapMix process. *Desalination* **2020**, *482*, 114384.
(1147) Bijmans, M.; Burheim, O.; Bryjak, M.; Delgado, A.; Hack, P.; Mantegazza, F.; Tenisson, S.; Hamelers, H. Capmix-deploying capacitors for salt gradient power extraction. *Energy Procedia* **2012**, *20*, 108−115.
(1148) Liu, F.; Schaetzle, O.; Sales, B. B.; Saakes, M.; Buisman, C. J.; Hamelers, H. V. Effect of additional charging and current density on the performance of Capacitive energy extraction based on Donnan Potential. *Energy Environ. Sci.* **2012**, *5*, 8642−8650.
(1149) Brogioli, D.; Ziano, R.; Rica, R.; Salerno, D.; Kozynchenko, O.; Hamelers, H.; Mantegazza, F. Exploiting the spontaneous potential of the electrodes used in the capacitive mixing technique for the extraction of energy from salinity difference. *Energy Environ. Sci.* **2012**, *5*, 9870−9880.
(1150) Rica, R. A.; Ziano, R.; Salerno, D.; Mantegazza, F.; Van Roij, R.; Brogioli, D. Capacitive mixing for harvesting the free energy of solutions at different concentrations. *Entropy* **2013**, *15*, 1388−1407.
(1151) Hatzell, M. C.; Hatzell, K. B.; Logan, B. E. Using flow electrodes in multiple reactors in series for continuous energy generation from capacitive mixing. *Environmental Science & Technology Letters* **2014**, *1*, 474−478.
(1152) Iglesias, G. R.; Fernández, M. M.; Ahualli, S.; Jiménez, M. L.; Kozynchenko, O. P.; Delgado, Á. V. Materials selection for optimum energy production by double layer expansion methods. *J. Power Sources* **2014**, *261*, 371−377.
(1153) Delgado, A.; Ahualli, S.; Fernández, M.; González, M.; Iglesias, G.; Vivo-Vilches, J.; Jiménez, M. Geometrical properties of materials for energy production by salinity exchange. *Environmental Chemistry* **2017**, *14*, 279−287.
(1154) Ahualli, S.; Jimenez, M.; Fernández, M. M.; Iglesias, G.; Brogioli, D.; Delgado, A. V. Polyelectrolyte-coated carbons used in the generation of blue energy from salinity differences. *Phys. Chem. Chem. Phys.* **2014**, *16*, 25241−25246.
(1155) Fernandez, M.; Wagterveld, R.; Ahualli, S.; Liu, F.; Delgado, A.; Hamelers, H. Polyelectrolyte-versus membrane-coated electrodes for energy production by capmix salinity exchange methods. *J. Power Sources* **2016**, *302*, 387−393.
(1156) Tan, G.; Zhu, X. Polyelectrolyte-Coated Copper Hexacyanoferrate and Bismuth Oxychloride Electrodes for Efficient Salinity Gradient Energy Recovery in Capacitive Mixing. *Energy Technol.* **2019**, *8*, 1900863.
(1157) Ahualli, S.; Orozco-Barrera, S.; Fernández, M. d. M.; Delgado, Á. V.; Iglesias, G. R. Assembly of soft electrodes and ion exchange membranes for capacitive deionization. *Polymers* **2019**, *11*, 1556.
(1158) Iglesias, G.; Ahualli, S.; Delgado, A.; Arenas-Fernández, P.; Fernández, M. Combining soft electrode and ion exchange membranes for increasing salinity difference energy efficiency. *J. Power Sources* **2020**, *453*, 227840.
(1159) Ye, M.; Pasta, M.; Xie, X.; Cui, Y.; Criddle, C. S. Performance of a mixing entropy battery alternately flushed with wastewater effluent and seawater for recovery of salinity-gradient energy. *Energy Environ. Sci.* **2014**, *7*, 2295−2300.
(1160) Jia, Z.; Wang, B.; Song, S.; Fan, Y. A membrane-less Na ion battery-based CAPMIX cell for energy extraction using water salinity gradients. *RSC Adv.* **2013**, *3*, 26205−26209.
(1161) Hosein Tehrani, S. H. M.; Seyedsadjadi, S. A.; Ghaffarinejad, A. Application of electrodeposited cobalt hexacyanoferrate film to extract energy from water salinity gradients. *RSC Adv.* **2015**, *5*, 30032−30037.
(1162) Gomes, W. J.; de Oliveira, C.; Huguenin, F. Energy harvesting by nickel prussian blue analogue electrode in neutralization and mixing entropy batteries. *Langmuir* **2015**, *31*, 8710−8717.
(1163) Zhu, X.; Kim, T.; Rahimi, M.; Gorski, C. A.; Logan, B. E. Integrating Reverse-Electrodialysis Stacks with Flow Batteries for

https://doi.org/10.1021/acs.chemrev.1c00396
Chem. Rev. 2022, 122, 13547−13635

Improved Energy Recovery from Salinity Gradients and Energy Storage. *ChemSusChem* **2017**, *10*, 797−803.
(1164) Ye, M.; Pasta, M.; Xie, X.; Dubrawski, K. L.; Xu, J.; Liu, C.; Cui, Y.; Criddle, C. S. Charge-Free Mixing Entropy Battery Enabled by Low-Cost Electrode Materials. *ACS omega* **2019**, *4*, 11785−11790.
(1165) Kim, T.; Rahimi, M.; Logan, B. E.; Gorski, C. A. Evaluating battery-like reactions to harvest energy from salinity differences using ammonium bicarbonate salt solutions. *ChemSusChem* **2016**, *9*, 981−988.
(1166) Kim, T.; Rahimi, M.; Logan, B. E.; Gorski, C. A. Harvesting energy from salinity differences using battery electrodes in a concentration flow cell. *Environ. Sci. Technol.* **2016**, *50*, 9791−9797.
(1167) Kim, T.; Logan, B. E.; Gorski, C. A. High power densities created from salinity differences by combining electrode and Donnan potentials in a concentration flow cell. *Energy Environ. Sci.* **2017**, *10*, 1003−1012.
(1168) Zhang, F.; Liu, J.; Yang, W.; Logan, B. E. A thermally regenerative ammonia-based battery for efficient harvesting of low-grade thermal energy as electrical power. *Energy Environ. Sci.* **2015**, *8*, 343−349.
(1169) Zhang, F.; LaBarge, N.; Yang, W.; Liu, J.; Logan, B. E. Enhancing low-grade thermal energy recovery in a thermally regenerative ammonia battery using elevated temperatures. *ChemSusChem* **2015**, *8*, 1043−1048.
(1170) Marino, M.; Misuri, L.; Carati, A.; Brogioli, D. Proof-of-concept of a zinc-silver battery for the extraction of energy from a concentration difference. *Energies* **2014**, *7*, 3664−3683.
(1171) Marino, M.; Misuri, L.; Carati, A.; Brogioli, D. Boosting the voltage of a salinity-gradient-power electrochemical cell by means of complex-forming solutions. *Appl. Phys. Lett.* **2014**, *105*, 033901.
(1172) Cipollina, A.; Micale, G. *Sustainable Energy from Salinity Gradients*; Woodhead Publishing, 2016; pp 181−218.
(1173) Marino, M.; Misuri, L.; Ruffo, R.; Brogioli, D. Electrode kinetics in the "capacitive mixing" and "battery mixing" techniques for energy production from salinity differences. *Electrochim. Acta* **2015**, *176*, 1065−1073.
(1174) Kim, D. J.; Ponraj, R.; Kannan, A. G.; Lee, H.-W.; Fathi, R.; Ruffo, R.; Mari, C. M.; Kim, D. K. Diffusion behavior of sodium ions in $Na_{0.44}MnO_2$ in aqueous and non-aqueous electrolytes. *J. Power Sources* **2013**, *244*, 758−763.
(1175) Lee, J.; Yoon, H.; Lee, J.; Kim, T.; Yoon, J. Extraction of Salinity-Gradient Energy by a Hybrid Capacitive-Mixing System. *ChemSusChem* **2017**, *10*, 1600−1606.
(1176) Hasan, K. N. M.; Khai, T. X.; Kannan, R.; Zakaria, Z. A. Harnessing "Blue energy": A Review on Techniques and Preliminary Analysis; *MATEC Web of Conferences*. 2017; p 04013.
(1177) Pan, S. Y.; Snyder, S. W.; Lin, Y. J.; Chiang, P. C. Electrokinetic desalination of brackish water and associated challenges in the water and energy nexus. *Environ. Sci.: Water Res. Technol.* **2018**, *4*, 613−638.
(1178) Hemmatifar, A. Energy Consumption and Salt Adsorption in Capacitive Deionization. Ph.D. Thesis. Stanford University, 2018.
(1179) Suss, M. Capacitive Water Desalination with Hierarchical Porous Electrodes. Ph.D. Thesis. Stanford University, 2013.
(1180) O'Hayre, R.; Cha, S.; Colella, W.; Prinz, F. *Fuel Cell Fundamentals*; Wiley: New York, 2006; pp 59−92.
(1181) Ramachandran, A.; Hemmatifar, A.; Hawks, S. A.; Stadermann, M.; Santiago, J. G. Self similarities in desalination dynamics and performance using capacitive deionization. *Water Res.* **2018**, *140*, 323−334.
(1182) Mistry, K. H.; McGovern, R. K.; Thiel, G. P.; Summers, E. K.; Zubair, S. M.; Lienhard, J. H. Entropy generation analysis of desalination technologies. *Entropy* **2011**, *13*, 1829−1864.
(1183) Zhao, Y.; Wang, Y.; Wang, R.; Wu, Y.; Xu, S.; Wang, J. Performance comparison and energy consumption analysis of capacitive deionization and membrane capacitive deionization processes. *Desalination* **2013**, *324*, 127−133.
(1184) Choi, J.-H. Comparison of constant voltage (CV) and constant current (CC) operation in the membrane capacitive deionisation process. *Desalination and Water Treatment* **2015**, *56*, 921−928.
(1185) Ramachandran, A.; Hawks, S. A.; Stadermann, M.; Santiago, J. G. Frequency analysis and resonant operation for efficient capacitive deionization. *Water Res.* **2018**, *144*, 581−591.
(1186) Andelman, M. D.; Walker, G. S. Charge Barrier Flow-through Capacitor. U.S. US6709560B2, 2004.
(1187) Li, H.; Gao, Y.; Pan, L.; Zhang, Y.; Chen, Y.; Sun, Z. Electrosorptive desalination by carbon nanotubes and nanofibres electrodes and ion-exchange membranes. *Water Res.* **2008**, *42*, 4923−4928.
(1188) Biesheuvel, P.; Van der Wal, A. Membrane capacitive deionization. *J. Membr. Sci.* **2010**, *346*, 256−262.
(1189) Cohen-Tanugi, D.; McGovern, R. K.; Dave, S. H.; Lienhard, J. H.; Grossman, J. C. Quantifying the potential of ultra-permeable membranes for water desalination. *Energy Environ. Sci.* **2014**, *7*, 1134−1141.
(1190) Park, H. B.; Kamcev, J.; Robeson, L. M.; Elimelech, M.; Freeman, B. D. Maximizing the Right Stuff: The Trade-off between Membrane Permeability and Selectivity. *Science* **2017**, *356*, eaab0530.
(1191) Alvarado, L.; Torres, I. R.; Chen, A. Integration of ion exchange and electrodeionization as a new approach for the continuous treatment of hexavalent chromium wastewater. *Sep. Purif. Technol.* **2013**, *105*, 55−62.
(1192) Liu, Y.; Wang, J.; Xu, Y.; Wu, B. A deep desalination and anti-scaling electrodeionization (EDI) process for high purity water preparation. *Desalination* **2019**, *468*, 114075.
(1193) Ortiz, J. M.; Expósito, E.; Gallud, F.; García-García, V.; Montiel, V.; Aldaz, V. A. Desalination of underground brackish waters using an electrodialysis system powered directly by photovoltaic energy. *Sol. Energy Mater. Sol. Cells* **2008**, *92*, 1677−1688.
(1194) Wright, N. C.; Shah, S. R.; Amrose, S. E.; Winter, A. G. A robust model of brackish water electrodialysis desalination with experimental comparison at different size scales. *Desalination* **2018**, *443*, 27−43.
(1195) Doornbusch, G.; Tedesco, M.; Post, J.; Borneman, Z.; Nijmeijer, K. Experimental investigation of multistage electrodialysis for seawater desalination. *Desalination* **2019**, *464*, 105−114.
(1196) Yan, H.; Wang, Y.; Wu, L.; Shehzad, M. A.; Jiang, C.; Fu, R.; Liu, Z.; Xu, T. Multistage-batch electrodialysis to concentrate high-salinity solutions: Process optimization, water transport, and energy consumption. *J. Membr. Sci.* **2019**, *570*, 245−257.
(1197) Tong, X.; Zhang, B.; Fan, Y.; Chen, Y. Mechanism exploration of ion transport in nanocomposite cation exchange membranes. *ACS Appl. Mater. Interfaces* **2017**, *9*, 13491−13499.
(1198) Fan, H.; Huang, Y.; Yip, N. Y. Advancing the conductivity-permselectivity tradeoff of electrodialysis ion-exchange membranes with sulfonated CNT nanocomposites. *J. Membr. Sci.* **2020**, *610*, 118259.
(1199) Alabi, A.; Cseri, L.; Al Hajaj, A.; Szekely, G.; Budd, P.; Zou, L. Electrostatically-coupled graphene oxide nanocomposite cation exchange membrane. *J. Membr. Sci.* **2020**, *594*, 117457.
(1200) Fidaleo, M.; Moresi, M. Electrodialysis applications in the food industry. *Adv. Food Nutr. Res.* **2006**, *51*, 265−360.
(1201) Vera, E.; Sandeaux, J.; Persin, F.; Pourcelly, G.; Dornier, M.; Ruales, J. Deacidification of passion fruit juice by electrodialysis with bipolar membrane after different pretreatments. *Journal of food engineering* **2009**, *90*, 67−73.
(1202) Símová, H.; Kysela, V.; Černín, A. Demineralization of natural sweet whey by electrodialysis at pilot-plant scale. *Desalination and Water Treatment* **2010**, *14*, 170−173.
(1203) Bazinet, L.; Doyen, A.; Roblet, C. *Separation, Extraction and Concentration Processes in the Food, Beverage and Nutraceutical Industries*; Elsevier, 2013; pp 202−218.
(1204) Wang, Y.; Jiang, C.; Bazinet, L.; Xu, T. *Separation of Functional Molecules in Food by Membrane Technology*; Elsevier, 2019; pp 349−381.

https://doi.org/10.1021/acs.chemrev.1c00396
Chem. Rev. 2022, 122, 13547−13635

(1205) Kim, N.; Jeon, J.; Chen, R.; Su, X. Electrochemical separation of organic acids and proteins for food and biomanufacturing. *Chem. Eng. Res. Des.* **2022**, *178*, 267−288.
(1206) Lindstrand, V.; Sundström, G.; Jönsson, A.-S. Fouling of electrodialysis membranes by organic substances. *Desalination* **2000**, *128*, 91−102.
(1207) Han, L. Current Strategies for the Design of Anti-fouling Ion-Exchange Membranes. *Membrane Technology Enhancement for Environmental Protection and Sustainable Industrial Growth* **2021**, 13−25.
(1208) Vaselbehagh, M.; Karkhanechi, H.; Mulyati, S.; Takagi, R.; Matsuyama, H. Improved antifouling of anion-exchange membrane by polydopamine coating in electrodialysis process. *Desalination* **2014**, *332*, 126−133.
(1209) Wang, W.; Fu, R.; Liu, Z.; Wang, H. Low-resistance anti-fouling ion exchange membranes fouled by organic foulants in electrodialysis. *Desalination* **2017**, *417*, 1−8.
(1210) Ran, J.; Wu, L.; He, Y.; Yang, Z.; Wang, Y.; Jiang, C.; Ge, L.; Bakangura, E.; Xu, T. Ion exchange membranes: New developments and applications. *J. Membr. Sci.* **2017**, *522*, 267−291.
(1211) Tanaka, Y. *Progress in Filtration and Separation*; Elsevier, 2015; pp 207−284.
(1212) Mohammadi, R.; Tang, W.; Sillanpää, M. A systematic review and statistical analysis of nutrient recovery from municipal wastewater by electrodialysis. *Desalination* **2021**, *498*, 114626.
(1213) Brauns, E. Salinity gradient power by reverse electrodialysis: effect of model parameters on electrical power output. *Desalination* **2009**, *237*, 378−391.
(1214) Pawlowski, S.; Crespo, J. G.; Velizarov, S. Profiled ion exchange membranes: A comprehensible review. *International journal of molecular sciences* **2019**, *20*, 165.
(1215) Grabowski, A.; Zhang, G.; Strathmann, H.; Eigenberger, G. Production of high-purity water by continuous electrodeionization with bipolar membranes: influence of concentrate and protection compartment. *Sep. Purif. Technol.* **2008**, *60*, 86−95.
(1216) Wenten, I G.; Khoiruddin; Arfianto, F.; Zudiharto. Bench scale electrodeionization for high pressure boiler feed water. *Desalination* **2013**, *314*, 109−114.
(1217) Zheng, X.-Y.; Pan, S.-Y.; Tseng, P.-C.; Zheng, H.-L.; Chiang, P.-C. Optimization of resin wafer electrodeionization for brackish water desalination. *Sep. Purif. Technol.* **2018**, *194*, 346−354.
(1218) Hestekin, C. N.; Hestekin, J. A.; Paracha, S.; Morrison, G.; Pakkaner, E.; Moore, J.; Santos de Souza, L. S.; Stephens, S.; Atchley, C.; Kurtz, I. Simulating nephron ion transport function using activated wafer electrodeionization. *Commun. Mater.* **2020**, *1*, 20.
(1219) Ulusoy Erol, H. B.; Hestekin, C. N.; Hestekin, J. A. Effects of resin chemistries on the selective removal of industrially relevant metal ions using wafer-enhanced electrodeionization. *Membranes* **2021**, *11*, 45.
(1220) Mittal, D.; Jagannathan, V.; Bisht, N. S. Use of unique fractional electrodeionization in power plant applications. *Power Plant Chemistry* **2009**, *11*, 1.
(1221) Chehayeb, K. M.; Farhat, D. M.; Nayar, K. G.; Lienhard, J. H. Optimal design and operation of electrodialysis for brackish-water desalination and for high-salinity brine concentration. *Desalination* **2017**, *420*, 167−182.
(1222) Marek, J.; Čížek, J.; Tvrzník, D. Optimizing porous material in shock electrodialysis unit. *Desalin. Water Treat.* **2019**, *170*, 38−45.
(1223) Gupta, S. S.; Islam, M. R.; Pradeep, T. *Advances in Water Purification Techniques: Meeting the Needs of Developed and Developing Countries*; Elsevier, 2018.
(1224) Xing, W.; Liang, J.; Tang, W.; He, D.; Yan, M.; Wang, X.; Luo, Y.; Tang, N.; Huang, M. Versatile applications of capacitive deionization (CDI)-based technologies. *Desalination* **2020**, *482*, 114390.
(1225) He, C.; Lian, B.; Ma, J.; Zhang, C.; Wang, Y.; Mo, H.; Waite, T. D. Scale-up and Modelling of Flow-electrode CDI Using Tubular Electrodes. *Water Res.* **2021**, *203*, 117498.
(1226) Kim, C.; Srimuk, P.; Lee, J.; Aslan, M.; Presser, V. Semi-continuous capacitive deionization using multi-channel flow stream and ion exchange membranes. *Desalination* **2018**, *425*, 104−110.
(1227) Lee, J.; Lee, J.; Hong, S. W.; Kim, C.; Yoon, J. Parametric study of multichannel desalination battery for low-energy electrochemical deionization of brackish water. *Desalination* **2021**, *515*, 115188.
(1228) Hasseler, T. D.; Ramachandran, A.; Tarpeh, W. A.; Stadermann, M.; Santiago, J. G. Process design tools and techno-economic analysis for capacitive deionization. *Water Res.* **2020**, *183*, 116034.
(1229) Liu, X.; Shanbhag, S.; Bartholomew, T. V.; Whitacre, J. F.; Mauter, M. S. Cost Comparison of Capacitive Deionization and Reverse Osmosis for Brackish Water Desalination. *ACS ES&T Engineering* **2021**, *1*, 261−273.
(1230) Bales, C.; Kovalsky, P.; Fletcher, J.; Waite, T. D. Low cost desalination of brackish groundwaters by Capacitive Deionization (CDI)—Implications for irrigated agriculture. *Desalination* **2019**, *453*, 37−53.
(1231) Shen, Y.-Y.; Sun, S.-H.; Tsai, S.-W.; Chen, T.-H.; Hou, C.-H. Development of a membrane capacitive deionization stack for domestic wastewater reclamation: A pilot-scale feasibility study. *Desalination* **2021**, *500*, 114851.
(1232) Wang, Q.; Fang, K.; He, C.; Wang, K. Ammonia removal from municipal wastewater via membrane capacitive deionization (MCDI) in pilot-scale. *Sep. Purif. Technol.* **2022**, *286*, 120469.
(1233) Jeon, S.-i.; Kim, N.; Jo, K.; Ahn, J.; Joo, H.; Lee, C.; Kim, C.; Yoon, J. Improvement in the desalination performance of membrane capacitive deionization with a bipolar electrode via an energy recovery process. *Chemical Engineering Journal* **2022**, *439*, 135603.
(1234) Joo, H.; Kim, S.; Kim, S.; Choi, M.; Kim, S.-H.; Yoon, J. Pilot-scale demonstration of an electrochemical system for lithium recovery from the desalination concentrate. *Environ. Sci.: Water Res. Technol.* **2020**, *6*, 290−295.
(1235) Reale, E. R.; Regenwetter, L.; Agrawal, A.; Dardon, B.; Dicola, N.; Sanagala, S.; Smith, K. C. Low porosity, high areal-capacity Prussian blue analogue electrodes enhance salt removal and thermodynamic efficiency in symmetric Faradaic deionization with automated fluid control. *Water Research X* **2021**, *13*, 100116.
(1236) Kim, N.; Jeon, J.; Elbert, J.; Kim, C.; Su, X. Redox-mediated electrochemical desalination for waste valorization in dairy production. *Chemical Engineering Journal* **2022**, *428*, 131082.
(1237) Hand, S.; Cusick, R. D. Emerging investigator series: capacitive deionization for selective removal of nitrate and perchlorate: impacts of ion selectivity and operating constraints on treatment costs. *Environ. Sci.: Water Res. Technol.* **2020**, *6*, 925−934.
(1238) Baldea, M. From process integration to process intensification. *Comput. Chem. Eng.* **2015**, *81*, 104−114.
(1239) Keil, F. J. Process intensification. *Reviews in Chemical Engineering* **2018**, *34*, 135−200.
(1240) Kim, Y.-h.; Park, L. K.; Yiacoumi, S.; Tsouris, C. Modular chemical process intensification: a review. *Annu. Rev. Chem. Biomol. Eng.* **2017**, *8*, 359−380.
(1241) Su, X. Electrochemical Interfaces for Chemical and Biomolecular Separations. *Curr. Opin. Colloid Interface Sci.* **2020**, *46*, 77−93.
(1242) Schiffer, Z. J.; Manthiram, K. Electrification and decarbonization of the chemical industry. *Joule* **2017**, *1*, 10−14.
(1243) Verma, S.; Lu, S.; Kenis, P. J. Co-electrolysis of CO_2 and glycerol as a pathway to carbon chemicals with improved technoeconomics due to low electricity consumption. *Nature Energy* **2019**, *4*, 466−474.
(1244) Barton, J. L. Electrification of the chemical industry. *Science* **2020**, *368*, 1181−1182.
(1245) Kim, S.; Kim, J.; Kim, S.; Lee, J.; Yoon, J. Electrochemical lithium recovery and organic pollutant removal from industrial wastewater of a battery recycling plant. *Environ. Sci.: Water Res. Technol.* **2018**, *4*, 175−182.

https://doi.org/10.1021/acs.chemrev.1c00396
Chem. Rev. 2022, 122, 13547−13635

(1246) Zhao, Z.; Si, X.; Liu, X.; He, L.; Liang, X. Li extraction from high Mg/Li ratio brine with LiFePO4/FePO4 as electrode materials. *Hydrometallurgy* **2013**, *133*, 75−83.
(1247) He, L.; Xu, W.; Song, Y.; Luo, Y.; Liu, X.; Zhao, Z. New Insights into the Application of Lithium-Ion Battery Materials: Selective Extraction of Lithium from Brines via a Rocking-Chair Lithium-Ion Battery System. *Global Challenges* **2018**, *2*, 1700079.
(1248) Zhao, X.; Yang, H.; Wang, Y.; Sha, Z. Review on the electrochemical extraction of lithium from seawater/brine. *J. Electroanal. Chem.* **2019**, *850*, 113389.
(1249) Su, X.; Bromberg, L.; Tan, K.-J.; Jamison, T. F.; Padhye, L. P.; Hatton, T. A. Electrochemically mediated reduction of Nitrosamines by Hemin-Functionalized Redox electrodes. *Environmental Science & Technology Letters* **2017**, *4*, 161−167.
(1250) Vapnik, H.; Elbert, J.; Su, X. Redox-copolymers for the recovery of rare earth elements by electrochemically regenerated ion-exchange. *Journal of Materials Chemistry A* **2021**, *9*, 20068−20077.
(1251) Medina, P. B.; Cotty, S.; Kim, K.; Elbert, J.; Su, X. Emerging investigator series: electrochemically-mediated remediation of GenX using redox-copolymers. *Environ. Sci.: Water Res. Technol.* **2021**, *7*, 2231−2240.
(1252) Tan, K.-J.; Morikawa, S.; Phillips, K. R.; Ozbek, N.; Hatton, T. A. Redox-Active Magnetic Composites for Anionic Contaminant Removal from Water. *ACS Appl. Mater. Interfaces* **2022**, *14*, 8974−8983.
(1253) Chen, R.; Feng, J.; Jeon, J.; Sheehan, T.; Rüttiger, C.; Gallei, M.; Shukla, D.; Su, X. Structure and Potential-Dependent Selectivity in Redox-Metallopolymers: Electrochemically Mediated Multicomponent Metal Separations. *Adv. Funct. Mater.* **2021**, *31*, 2009307.
(1254) Alabi, A.; AlHajaj, A.; Cseri, L.; Szekely, G.; Budd, P.; Zou, L. Review of nanomaterials-assisted ion exchange membranes for electromembrane desalination. *NPJ Clean Water* **2018**, *1*, 10.
(1255) Razmjou, A.; Asadnia, M.; Hosseini, E.; Habibnejad Korayem, A.; Chen, V. Design principles of ion selective nanostructured membranes for the extraction of lithium ions. *Nat. Commun.* **2019**, *10*, 5793.
(1256) Tunuguntla, R. H.; Henley, R. Y.; Yao, Y.-C.; Pham, T. A.; Wanunu, M.; Noy, A. Enhanced water permeability and tunable ion selectivity in subnanometer carbon nanotube porins. *Science* **2017**, *357*, 792−796.
(1257) Daghrir, R.; Drogui, P.; Tshibangu, J. Efficient treatment of domestic wastewater by electrochemical oxidation process using bored doped diamond anode. *Sep. Purif. Technol.* **2014**, *131*, 79−83.
(1258) Sholl, D. S.; Lively, R. P. Exemplar Mixtures for Studying Complex Mixture Effects in Practical Chemical Separations. *JACS Au* **2022**, *2*, 322.
(1259) Mook, W.; Chakrabarti, M.; Aroua, M.; Khan, G.; Ali, B.; Islam, M.; Abu Hassan, M. A. Removal of total ammonia nitrogen (TAN), nitrate and total organic carbon (TOC) from aquaculture wastewater using electrochemical technology: a review. *Desalination* **2012**, *285*, 1−13.
(1260) Bian, Y.; Chen, X.; Ren, Z. J. pH dependence of phosphorus speciation and transport in flow-electrode capacitive deionization. *Environ. Sci. Technol.* **2020**, *54*, 9116−9123.
(1261) Kim, K.; Candeago, R.; Rim, G.; Raymond, D.; Park, A.-H. A.; Su, X. Electrochemical approaches for selective recovery of critical elements in hydrometallurgical processes of complex feedstocks. *Iscience* **2021**, *24*, 102374.
(1262) Jin, W.; Zhang, Y. Sustainable electrochemical extraction of metal resources from waste streams: from removal to recovery. *ACS Sustainable Chem. Eng.* **2020**, *8*, 4693−4707.
(1263) Kim, K.; Raymond, D.; Candeago, R.; Su, X. Selective cobalt and nickel electrodeposition for lithium-ion battery recycling through integrated electrolyte and interface control. *Nat. Commun.* **2021**, *12*, 6554.
(1264) Rodrigues, L. E. O. C.; Mansur, M. B. Hydrometallurgical separation of rare earth elements, cobalt and nickel from spent nickel−metal−hydride batteries. *J. Power Sources* **2010**, *195*, 3735−3741.
(1265) Mir, N.; Bicer, Y. Thermodynamic modeling of a combined photo-electrodialysis-chloralkali system for sustainable desalination. *Desalination* **2021**, *499*, 114822.
(1266) Mohandass, G.; Kim, T.; Krishnan, S. Continuous Solar Desalination of Brackish Water via a Monolithically Integrated Redox Flow Device. *ACS ES&T Engineering* **2021**, *1*, 1678−1687.
(1267) Chen, F.; Karthick, R.; Zhang, Q.; Wang, J.; Liang, M.; Dai, J.; Jiang, X.; Jiang, Y. Exploration of a photo-redox desalination generator. *Journal of Materials Chemistry A* **2019**, *7*, 20169−20175.
(1268) Kim, S.; Piao, G.; Han, D. S.; Shon, H. K.; Park, H. Solar desalination coupled with water remediation and molecular hydrogen production: a novel solar water-energy nexus. *Energy Environ. Sci.* **2018**, *11*, 344−353.
(1269) Santiago, A. R.; Baldaguez Medina, P. B.; Su, X. Electrochemical remediation of perfluoroalkyl substances from water. *Electrochim. Acta* **2022**, *403*, 139635.
(1270) Pan, Z.; Song, C.; Li, L.; Wang, H.; Pan, Y.; Wang, C.; Li, J.; Wang, T.; Feng, X. Membrane technology coupled with electrochemical advanced oxidation processes for organic wastewater treatment: Recent advances and future prospects. *Chemical Engineering Journal* **2019**, *376*, 120909.
(1271) Jo, K.; Baek, Y.; Kim, S.; Hong, S. P.; Yoon, J. Evaluation of long-term stability in capacitive deionization using activated carbon electrodes coated with ion exchange polymers. *Korean Journal of Chemical Engineering* **2020**, *37*, 1199−1205.
(1272) Duan, F.; Du, X.; Li, Y.; Cao, H.; Zhang, Y. Desalination stability of capacitive deionization using ordered mesoporous carbon: effect of oxygen-containing surface groups and pore properties. *Desalination* **2015**, *376*, 17−24.
(1273) Srimuk, P.; Zeiger, M.; Jackel, N.; Tolosa, A.; Kruner, B.; Fleischmann, S.; Grobelsek, I.; Aslan, M.; Shvartsev, B.; Suss, M. E.; Presser, V. Enhanced performance stability of carbon/titania hybrid electrodes during capacitive deionization of oxygen saturated saline water. *Electrochim. Acta* **2017**, *224*, 314−328.
(1274) Vineyard, D.; Hicks, A.; Karthikeyan, K.; Davidson, C.; Barak, P. Life cycle assessment of electrodialysis for sidestream nitrogen recovery in municipal wastewater treatment. *Cleaner Environmental Systems* **2021**, *2*, 100026.
(1275) Fernandez-Gonzalez, C.; Dominguez-Ramos, A.; Ibañez, R.; Irabien, A. Sustainability assessment of electrodialysis powered by photovoltaic solar energy for freshwater production. *Renewable and Sustainable Energy Reviews* **2015**, *47*, 604−615.

https://doi.org/10.1021/acs.chemrev.1c00396
Chem. Rev. 2022, 122, 13547−13635